

**Identification of the DEAD-Box Protein DDX24
as a Novel Modulator of Huntingtin Induced Caspase
Activation**

Dissertation zur Erlangung des akademischen Grades des
Doktors der Naturwissenschaften (Dr. rer. nat.)

eingereicht im Fachbereich Biologie, Chemie, Pharmazie
der Freien Universität Berlin

vorgelegt von

Katja Dorothea Welsch
aus Stuttgart

März, 2010

Die Arbeit wurde im Zeitraum von Oktober 2006 bis März 2010 unter der Leitung von Herrn Dr. Jan Bieschke und Herrn Prof. Dr. Erich E. Wanker am Max-Delbrück-Centrum für Molekulare Medizin in Berlin-Buch angefertigt.

1. Gutachter: Prof. Dr. Fritz G. Rathjen

2. Gutachter: Prof. Dr. Erich E. Wanker

Disputation am: 06.07.2010

Danksagung

Ich danke Herrn Prof. Dr. Erich Wanker für die Überlassung des Themas wie auch der Bereitstellung von finanziellen Mitteln und des Know-hows.

Vielen Dank auch an Herrn Prof. Dr. Fritz Rathjen für seine Bereitschaft die Arbeit zu begutachten.

Mein ganz besonderer Dank gilt Dr. Jan Bieschke für die Betreuung der Arbeit und die Unterstützung beim Schreiben in der Endphase. Für schwarzen Kaffee, dunkle Schokolade und die gute Freundschaft.

Bei Dr. Ralf Friedrich möchte ich mich für vor allem die Unterstützung bei den Immun-Floureszenzexperimenten sowie für die tolle Zusammenarbeit im Labor bedanken. Anup Arumughan danke ich für die Hilfe bei den LUMIER assay Untersuchungen. Dank geht auch an Raphaële Foulle, das FA-Team und Kirstin Rau für ihre Unterstützung bei den FRET Interaktionsstudien. Bei Dr. Babila Tachu bedanke ich mich für die Bereitstellung und Vorbereitung der Versuchsmäuse.

Darüber hinaus bedanke ich mich ganz herzlich bei Gerlinde Grelle und Susanne Kostka, Stephanie Plassmann sowie meinen Mit-Doktorandinnen Anne Möller und Anne Wagner für die gute Arbeitsatmosphäre und für die Hilfe bei der praktischen Arbeit. Die Arbeit mit Euch hat viel Spaß gemacht!

Außerhalb des Labors gilt mein Dank vor allem meinem Mann Andreas für seine Bereitschaft nach Berlin zu ziehen, seine unendliche Geduld und das Verständnis für die langen Arbeitszeiten. Für seine aufbauenden Worte und die selbstlose Unterstützung in allen Krisensituationen. Ohne Dich wäre ich nicht da, wo ich jetzt bin!

Schließlich danke ich meinen Eltern für die Unterstützung, die Förderung und die aufmunternden Worte und kleinen Gesten, die mir gezeigt haben, wie viel ihnen am Gelingen dieser Arbeit lag.

Table of Content

Introduction	1
1.1 Chorea Huntington (Huntington’s disease, HD)	1
1.1.1 Clinical manifestation	1
1.1.2 The huntingtin protein	2
1.1.3 Polyglutamine disorders	6
1.1.4 Amyloid hypothesis.....	7
1.1.5 Aggregation of mutant huntingtin.....	7
1.1.6 Htt inclusions may have a protective role.....	8
1.1.7 Degradation of Htt aggregates	9
1.1.8 Mutant Htt and cellular dysfunction.....	9
1.2 Cell death and apoptosis	12
1.2.1 Extrinsic apoptosis signaling via death receptor	12
1.2.2 Mitochondria-mediated (“intrinsic”) apoptosis signaling.....	13
1.2.3 Caspases: the major effectors	15
1.2.4 Cytotoxicity and apoptosis in Huntington’s disease	15
1.3 Model systems reproducing HD features	17
1.4 The DEAD-box protein family	19
1.4.1 The putative RNA helicase DEAD (Asp-Glu-Ala-Asp) box polypeptide 24 (DDX24).....	23
1.5 Genetic screens for modifiers of polyQ-induced toxicity and aggregation	24
1.6 Aim of the study	25
Results	27
2.1 RNAi screen to identify protein modulators of mutant Htt-induced cytotoxicity	27
2.1.1 Screening for modulators of Htt-induced cytotoxicity in a neuroblastoma cell line	27
2.2 Investigation of siRNA-mediated DDX24 protein knock-down in a HD PC12 cell model	37

2.2.1	Analysis of HD PC12 cell lines expressing Htt25Q-EGFP or Htt103Q-EGFP fusion proteins	37
2.2.2	Analysis of siRNA-mediated DDX24 protein knock-down in the HD PC12 cell model	40
2.2.3	Endogenous DDX24 protein silencing enhances mutant Htt-induced caspase-3/7 activity	43
2.2.4	DDX24 knock-down enhances caspase-8 and -9 activity induced by mutant Htt	45
2.3	Overexpression of human DDX24 rescues Htt-induced caspase activity	47
2.3.1	Cloning and overexpression of HA-tagged human DDX24 protein.	47
2.3.2	Knock-down of endogenous DDX24 does not affect expression of recombinant HA-DDX24 fusion protein	48
2.3.3	Overexpression of human DDX24 rescues toxic effects of DDX24 knock-down on mutant Htt-induced caspase activity	49
2.4	Expression of mutant Htt protein changes DDX24 expression in HD model systems.	51
2.4.1	DDX24 transcript levels are increased in PC12 cells expressing Htt103Q-EGFP protein	51
2.4.2	Transcript levels of DDX24 are enhanced in a HD transgenic mouse model	52
2.5	Altered levels of DDX24 do not influence Htt expression and aggregation	54
2.5.1	Expression of Htt103Q-EGFP is not affected by endogenous DDX24 protein silencing	54
2.5.2	Aggregation of Htt103Q-EGFP is not affected by knock-down of DDX24 protein	55
2.6	Interaction of DDX24 with FADD mediates apoptosis signaling	59
2.6.1	DDX24 directly binds to the apoptosis mediator FADD providing a link to the extrinsic apoptosis signaling pathway.	59
2.6.2	Overexpression of recombinant HA-FADD fusion protein increases caspase-3/7, caspase-8 and caspase-9 activity.	66
2.6.3	FADD and DDX24 synergistically modulate caspase activation by mutant Htt.	70

Discussion.73

3.1	Identification of DDX24 as a modulator of mutant Htt-induced cytotoxicity.	75
------------	---	-----------

3.2	Cellular models for mutant Htt-induced caspase activation	76
3.2.1	Mammalian cell models to monitor cellular toxicity of mutant Htt	76
3.2.2	Htt103Q-EGFP increases caspase-3/7, caspase-8 and caspase-9 activity in PC12 cells	77
3.3	DDX24 mediates mutant Htt-induced caspase activation	79
3.3.1	Knock-down of DDX24 increases mutant Htt-induced caspase-3 activity	79
3.3.2	Htt-induced caspase-8 and -9 activity is increased by DDX24 silencing.	79
3.4	Overexpression of human DDX24 inhibits mutant Htt-induced caspase activation	80
3.5	Mutant Htt expression and aggregation induces DDX24 transcription . .	81
3.5.1	Mutant Htt expression leads to dysregulated gene expression	81
3.5.2	Expression of mutant Htt increases DDX24 mRNA levels in PC12 cells	83
3.5.3	Transgenic HD mice exhibit enhanced DDX24 transcription.	83
3.5.4	Transgenic N171-82Q mice show reduced DDX24 protein levels	84
3.6	DDX24 does not affect mutant Htt expression and aggregation	85
3.6.1	DDX24 does not influence mRNA transcription of mutant Htt	86
3.6.2	Protein expression of mutant Htt is not affected by DDX24	86
3.6.3	DDX24 does not interact with mutant Htt aggregates	87
3.6.4	Aggregation of mutant Htt is independent of DDX24 function	87
3.7	Interaction of DDX24 with the apoptosis mediator FADD	88
3.7.1	The role of death receptors in neurodegenerative disorders	90
3.8	Co-regulation of caspases by DDX24 and FADD	91
3.9	A model for the influence of DDX24 on Htt-induced caspase activation	92
3.10	Outlook and further directions	95
	Materials and Methods	97
4.1	Materials	97
4.1.1	Bacterial stains	97
4.1.2	Cell lines	97
4.1.3	Expression vectors	98

4.1.4 Microbiological media and buffers	99
4.1.5 Media and supplements for mammalian cell culture	100
4.1.6 Oligonucleotides	100
4.1.7 Antibodies.	101
4.1.8 Enzymes, proteins, markers and DNA	102
4.1.9 Kits.	102
4.1.10 Chemicals and consumables.	103
4.1.11 Laboratory equipment.	104
4.2 Methods.	105
4.2.1 Molecular biology	105
4.2.2 Protein biochemistry.	109
4.2.3 Methods in cell biology.	112
Literature	119
Abstract.	151
Zusammenfassung.	152
Appendix A: List of abbreviations.	153
Appendix B: “p200” onthology list	156
Appendix C: Result of “p200 screen”	167
Appendix D: Plasmid maps	173

Table of Figures

Figure 1.1: Domain structure of huntingtin	3
Figure 1.2: Schematic representation of a polar zipper structure	8
Figure 1.3: Intrinsic and extrinsic pathways of caspase activation in mammals.....	14
Figure 1.4: Intranuclear neuronal inclusions in multiple neuron populations of endstage N171-82Q mice	18
Figure 1.5: A schematic presentation of conserved motifs in DEAD-box protein family members	19
Figure 1.6: Schematic representation of the conserved motifs found in human DDX24 and rat DDX24.....	24
Figure 2.1: Functional analysis of the target proteins selected for the “p200”- RNAi screening	28
Figure 2.2: Expression of the HD320_Q68 protein induces caspase-3/7 activity in Neuro2a cells	29
Figure 2.3: Expression of the protein HD320_Q68 in Neuro2a cells	29
Figure 2.4: Proof of concept experiments for the RNAi screening assay	30
Figure 2.5: Definition of toxicity suppressors and toxicity enhancers.....	31
Figure 2.6: Schematic overview of the recombinant proteins Htt25Q-EGFP and Htt103Q-EGFP.....	37
Figure 2.7: Expression of the Htt25Q-EGFP and Htt103Q-EGFP proteins after induction with 2.5 μ M muristerone for 48 hours	37
Figure 2.8: Detection of the proteins Htt103Q-EGFP and Htt25Q-EGFP in PC12 cells	38
Figure 2.9: Fluorescence microscopy analysis of Htt25Q-EGFP and Htt103Q-EGFP expression in PC12 cells.....	39
Figure 2.10: Quantification of caspase-3/7 and -8 activities in PC12 cells expressing the proteins Htt103Q-EGFP or Htt25Q-EGFP	40
Figure 2.11: Treatment of PC12 cells with DDX24 siRNA pools reduces endogenous DDX24 mRNA levels	41
Figure 2.12: DDX24 knock-down efficiency of different DDX24 specific siRNAs	42
Figure 2.13: Quantification of the DDX24 knock-down by real-time PCR analysis	43

Figure 2.14: Silencing of endogenous DDX24 protein enhances mutant Htt-induced caspase-3/7 activation.....	44
Figure 2.15: PC12 cell expressing Htt25Q-EGFP do not show increased caspase-3/7 activity after DDX24 protein knock-down	45
Figure 2.16: Expression of Htt103Q-EGFP protein activates caspase-8 and caspase-9 in PC12 cells.....	46
Figure 2.17: DDX24 protein knock-down increases caspase-8 and -9 activity in PC12 cells expressing Htt103Q-EGFP	47
Figure 2.18: Expression of HA-DDX24 fusion protein in PC12 cells	48
Figure 2.19: Representative Western blot demonstrating silencing of rat endogenous DDX24 protein using siDDX24_1, _2, _3 and _4 as well as the pool of siDDX24_1 to _4 in the presence or absence of overexpressed HA-DDX24 fusion protein.....	49
Figure 2.20: Overexpression of human HA-DDX24 fusion protein rescues caspase activity induced by DDX24 knock-down and simultaneous expression of Htt103Q-EGFP	50
Figure 2.21: Overexpression of HttQ103-EGFP protein results in increased DDX24 mRNA in mammalian cells.....	52
Figure 2.22: DDX24 transcription is changed in the striatal brain region of 15 weeks old transgenic HD mice.....	53
Figure 2.23: Representative Western blot of DDX24 protein levels in striatal tissue of 15 weeks old mice and PC12 cells	54
Figure 2.24: Expression of Htt103Q-EGFP is not influenced by DDX24 knock-down	55
Figure 2.25: Endogenous DDX24 protein does not colocalize with mutant Htt aggregates.....	56
Figure 2.26: Reduction of intracellular DDX24 protein levels does not influence Htt103Q-EGFP aggregate formation	57
Figure 2.27: Knock-down of endogenous DDX24 protein does not affect the formation of Htt103Q-EGFP aggregates visible in the fluorescence microscope.....	58
Figure 2.28: Protein-protein interaction network linking DDX24 to Htt as well as caspase-3 and -8, which are key players of apoptosis	59
Figure 2.29: Co-immunoprecipitation of Fire-V5-DDX24 with PA-Reni-FADD.....	60
Figure 2.30: Analysis of DDX24 binding to FADD using a LUMIER assay	61
Figure 2.31: Expression of the fusion proteins ECFP-DDX24 and EYFP-FADD in HEK293 cells	62

Figure 2.32: Confirmation of the DDX24 interaction with FADD using a FRET assay.....	63
Figure 2.33: Colocalization of DDX24 and FADD in PC12 cells.....	65
Figure 2.34: Western blot analysis of the overexpression of recombinant HA-FADD fusion protein in PC12 cells.....	67
Figure 2.35: FADD overexpression increases Htt103Q-EGFP-induced caspase activity.....	69
Figure 2.36: Overexpression of HA-FADD protein with simultaneous DDX24 protein knock-down results in additive enhancement of caspase activity in mammalian cells.....	71
Figure 3.1: Suggested model for the function of DDX24 in mutant Htt-induced caspase activation.....	94

Tables

Table 1.1: Human DEAD-box proteins	20
Table 2.1: Target proteins identified as toxicity suppressors.....	34
Table 2.2: Target proteins identified as toxicity enhancers	35
Table 4.1: Primer/probe quantitative real-time PCR.....	100
Table 4.2: DDX24 targeting siRNA sequences	101
Table 4.3a: Components of a multiplexed real-time PCR reaction using purchased TaqMan Gene Expression Assays.....	108
Table 4.3b: Components of a multiplexed real-time PCR reaction using self designed primer/probe set	108

Chapter 1

Introduction

1.1 Chorea Huntington (Huntington's disease, HD)

Chorea Huntington or Huntington's disease (HD) is an autosomal dominant inherited, progressive neurodegenerative disorder. It has a prevalence of 3-10 cases per 100,000 individuals. The age of the disease onset is around 30-50 years and the patients die within 10 to 20 years. Besides the late onset of the disease rare juvenile cases have also been reported. The disorder was first described in 1872 by George Huntington who identified: "1. *Its hereditary nature.* 2. *A tendency to insanity and suicide.* 3. *Its manifesting itself as a grave disease only in adult life.*" (Huntington, 1872)

1.1.1 Clinical manifestation

The first signs of Huntington's chorea (Chorea: Greek for "dance") are subtle motor disturbances, clumsiness, mild personality changes and slowing of the intellectual processes. These symptoms progress slowly to more severe involuntary movements, hypokinesia, rigidity (Thompson et al., 1988) and eventually a loss of the capacity to move (Brandt et al., 1984; Folstein et al., 1987; Penney et al., 1990). The progression of the disease also manifests in speech impairment, and later the loss of speech, as well as in muscle wasting and weight loss (Sanberg et al., 1981). Moreover, the cognitive impairments get worse over time and in the last stage of the disease patients show severe dementia (Folstein et al., 1983). Besides the physical and cognitive symptoms, also personality changes like irritability and aggression, loss of motivation and depressed moods as well as anxiety emerge (Dewhurst et al., 1970; Jensen et al., 1993). Death of the patients generally occurs as a consequence of heart failure or aspiration pneumonia (Chiu and Alexander, 1982).

The neuropathological hallmark of HD is the gradual atrophy of the striatum (caudate nucleus and putamen; Vonsattel et al., 1985). The severity of the striatal degeneration is assessed by a grading system which classifies the HD stages into five severity grades depending on the degree of striatal atrophy. Starting with Grade 0, characterized by a 30-40% neuronal loss in the caudate nucleus, the system ascends to Grade 4 which includes cases with gross striatal atrophy and up to 95% neuronal loss (Vonsattel et al., 1985). In contrast to the lower grades in which only a slight atrophy in the striatal structures is observed, the more fatal grades also show degeneration of non-striatal structures like the cerebral cortex. As a consequence of the cerebral atrophy the weight of the total

Introduction

brain decreases by approximately 10-40% in HD patients (Vonsattel et al., 1985; Vonsattel and DiFiglia, 1989).

The major part of the striatal neuronal cell population is represented by medium-sized projection spiny neurons - neurons that send projections to other nuclei - which are partly regulated by dopaminergic inputs, using the inhibitory transmitter GABA (γ -aminobutyric acid). Since these neurons have an inhibitory function, their degeneration results in an enhanced stimulation of the motor cortex which provokes the HD characteristics and uncontrolled movements (Joel, 2001).

At present there is no therapy which is able to cure HD, prevent the onset of the disease or impede its progression. However, there are treatments available to reduce the severity of some of the HD symptoms. For the symptomatic treatment to reduce the severity of chorea in HD, tetrabenazine was developed, which attenuates hypokinesia by promoting degradation of dopamine (Walker, 2007). It was approved in 2008 for this use in the US. Rigidity can be treated with antiparkinsonian drugs like pramipexole (Bonelli et al., 2002) and psychiatric symptoms can be treated with antidepressant drugs such as fluoxetine (Bates et al., 2002; De Marchi et al., 2001).

Although there have been relatively few studies of exercises and therapies that help rehabilitate cognitive symptoms of HD, there is some evidence for the usefulness of physical therapy and speech therapy (Bilney et al., 2003). So far, only the transplantation of fetal tissue into the caudate nucleus and putamen of HD patients has led to improvement of cognitive function (Bachoud-Levi et al., 2000). However, the practicability of this approach is restricted by the availability of fetal neuronal tissue. Nevertheless, the fast progressing stem cell research might solve this problem and could provide the required tissue material in larger amounts (Snyder et al., 2010).

1.1.2 The huntingtin protein

Huntingtin (Htt) is a protein consisting of 3,144 amino acids with a molecular mass of ~ 349 kDa. The wild-type protein is expressed throughout all tissues of the human body, in both neuronal and non-neuronal cells. Although, in the brain it is mainly expressed in the two most affected regions in HD, the striatum and the cerebral cortex (Strong et al., 1993). Intracellularly Htt is localized in nuclei, cell bodies as well as in dendrites and nerve terminals (Trottier et al., 1995; DiFiglia et al., 1995). Subcellular fractionations show that it is predominantly found in the membrane-containing fractions and associated with microtubules (Gutekunst et al., 1995). The mutant form of Htt shows an altered intracellular localization. Perinuclear accumulation of mutant Htt can be observed as well as the formation of neuronal intranuclear inclusions (NIIs, DiFiglia et al., 1997). Although Htt is a large protein it contains only three characteristic protein domains (Figure 1.1). The polyglutamine (polyQ) domain is located 17 amino acids downstream of the N-terminus of the protein, and is followed by a polymorphic proline-rich sequence (HDCRG, 1993) and the HEAT-repeat region. 37 HEAT-repeats can be clustered into three subdomains at positions 205-329, 745-942 and 534-1710 in the protein (Andrade and Bork, 1995). The HEAT-domains are

Introduction

involved in cytoplasmic and nuclear transport processes, microtubule dynamics and chromosome segregation (Andrade and Bork, 1995; Andrade et al., 2001). Moreover, a nuclear export signal (NES) is located at C-terminus of the Htt protein (Xia et al., 2003; Figure 1.1).

Both, wild-type and mutant Htt can undergo four types of post-translational modification such as phosphorylation, ubiquitination, SUMOylation and palmitoylation. Phosphorylation can take place at S421 by Akt or protein kinase B, at S434 by cyclin-dependent kinase 5 and at S536 (Humbert et al., 2002; Luo et al., 2005; Schilling et al., 2006). Ubiquitination and SUMOylation, the reversible binding of small ubiquitin-related protein modifiers, take place at the lysine residues K6, K9 and K15 (Steffan et al., 2004; Kalchman et al., 1996). Palmitoylation on C215 by HIP14 (huntingtin-interacting protein 14) was observed in cell model systems (Yanai et al., 2006). Furthermore, Htt is cleaved by caspases at the aspartate residues D513, D552 and D586 (Wellington et al., 2002) and by calpain (Gafni and Ellerby, 2002). Cleavage of mutant Htt by caspase-3 and calpain results in the formation of N-terminal fragments which are more toxic and aggregation prone than the full-length protein (Kim et al., 2001). These fragments are suggested to diffuse into the nucleus (Gafni et al., 2004; Sun et al., 2002) or to be actively translocated (Ona et al., 1999).



Figure 1.1: Domain structure of huntingtin (modified from Cattaneo et al., 2005). Htt contains a N-terminal polyglutamine tract Q(n) and a polyproline region P(n). The yellow bars indicate the three main HEAT repeat clusters at aa positions 205-329, 745-942 and 534-1710. The blue bar refers to the nuclear export signal (NES). Red arrowheads indicate caspase cleavage sites located at D513 (caspase-3), D552 (caspase-2/-3) and D586. Ubiquitination/SUMOylation occurs at K6, K9 and K15 (green circle). Phosphorylation sites are located at S421, S434 and S536 indicated by blue circles.

Genetics

HD is caused by an expanded CAG trinucleotide repeat located in the exon 1 of the IT15 gene (HDCRG, 1993). The CAG-repeat is translated into a polyglutamine (polyQ) sequence located at the N-terminus in the Htt protein. The CAG-repeat expansion results in an increased number of glutamine residues within the polyQ stretch (HDCRG, 1993). The longer the polyQ sequence in Htt the more severe are the symptoms in HD. Normally, unaffected individuals have 35 or less CAG repeats, whereas in patients suffering from HD the number of CAG trinucleotides exceeds 40 up to 182 repeats (Rubinsztein et al., 1996; Sathasivam et al., 1997). There is an inverse correlation between the number of CAG-repeats and the age of disease onset. Alleles with 35-39 repeats are only very sporadic associated with onset of the disease, whereas individuals with alleles in the

Introduction

range of 40-50 repeats will develop the disease in an age of around 30-50 years. Consequently, very long CAG-repeats (> 70) are responsible for the juvenile and infantile cases of HD (HDCRG, 1993). Besides the inverse correlation between the number of CAG repeats and the age of onset a direct correlation exists for the number of repeats and the Vonsattel grades of neuropathological severity (see Chapter 1.1.1.). The longer the CAG-repeat the higher will be the Vonsattel grade of the affected brain.

Functions of normal Htt

The normal function of Htt is still unclear, although many different possible functions are being discussed. Knock-out of the mouse HD gene *Hdh* resulted in embryonic lethality, which implicates an essential role of Htt in embryonic development (Duyao et al., 1995; Nasir et al., 1995; Zeitlin et al., 1995).

Yeast two-hybrid screenings, affinity pull-down assays as well as immunoprecipitation studies have identified numerous Htt interaction partners. The cellular functions of these proteins suggest that Htt might be involved in processes such as protein trafficking and vesicle transport, endocytosis, postsynaptic signaling, transcriptional regulation and anti-apoptotic processes.

Protein trafficking and vesicle transport

Htt interacts with HAP1 (Huntingtin associated protein 1), a protein expressed in many tissues including the brain. HAP1 interacts with dynactin and is involved in the dynein/dynactin complex-mediated transport of vesicles and endosomes along microtubules in axons. Htt is suggested to be associated to this complex via HAP1 (Block-Galarza et al., 1997; Engelender et al., 1997) and might play a role as a bridging protein between the dynein/dynactin complex and the cargo (Harjes and Wanker, 2003; Li and Li, 2004).

Endocytosis

The interactions of Htt with HIP1, PACSIN1, SH3GL3 and α -Adaptin C give evidence that Htt has a function in clathrin-mediated endocytosis (Kalchman et al., 1997; Sittler et al., 1998; Modregger et al., 2002). HIP1 interacts with α -Adaptin C, α -Adaptin A and clathrin and is involved in clathrin-mediated endocytosis. In this process Htt might promote the association of HIP1 and α -Adaptin C via direct interaction with both proteins and consequently influence the vesicle formation (Metzler et al., 2001; Waelter et al., 2001a). SH3GL3 represents another interaction partner of Htt that is involved in endocytosis. Its rat homologue SH3p13 interacts with dynamin I and synaptojanin, which are both essential factors of the receptor-mediated endocytosis and the synaptic vesicle recycling (Ringstad et al., 1997). Htt was also found to interact with PACSIN1, which is a neuronal phosphoprotein located in synaptic bouton and is involved in recycling of synaptic vesicles. In HD brains the levels of PACSIN1 are reduced and the protein is translocated in the cytoplasm which suggests an impairment of vesicle recycling in HD (Modregger et al., 2002).

Introduction

Postsynaptic signaling

A common interaction partner of Htt and HAP1 is the protein FIP-2 which links both to the Rab8 signaling cascade. The Rab8 cascade regulates the polarized membrane transport via reorganization of actin filaments and microtubules, which is linked to modification processes of the dendritic spines shape (Li et al., 2000; Hattula and Peranen, 2000; Tang et al., 2003).

Another protein critical for the spine morphology and synapse formation is GIT1 (Zhang et al., 2003), which was found to interact with Htt (Goehler et al., 2004). In addition, Htt interacts with PSD-95 (postsynaptic density protein 95) mediating the anchoring of NMDA and kainate receptors to the postsynaptic membrane (Garcia et al., 1998; Sun et al., 2001). PSD-95 interacts with SynGAP which influences synapse plasticity via the RAS/MAPK signaling cascade (Kim et al., 1998). Thus, Htt might play an important role in synaptic signaling processes as well as in the organization of the postsynaptic membrane.

Transcriptional regulation

Htt interacts with several transcription factors and expression profiles of various genes are altered in the presence of mutant Htt (Sugars and Rubinsztein, 2003; Cha, 2007). One example represents the CRE-(cAMP response element)-mediated transcription regulation. Under normal conditions CREB (CRE-binding protein) binds to the DNA as well as to CBP (a co-factor of the CRE-mediated transcription pathway) which links CREB to the basal transcriptional machinery to initiate expression of genes responsible for neuronal survival. The presence of mutant Htt impairs the transcription initiation as described in Chapter 1.1.8 (Cong et al., 2005; Jiang et al., 2006). Another example is the expression of the neurotrophic factor BDNF (brain derived neurotrophic factor), an important survival factor for striatal neurons. Its expression is negatively regulated by the REST/NRST complex. Htt binds to this complex thereby preventing translocation of REST/NRST into the nucleus (Zuccato et al., 2003). Mutant Htt is no longer able to bind the REST/NRST complex resulting in translocation of the complex into the nucleus where it initiates BDNF transcription (Zuccato et al., 2003). Moreover, Htt interacts with various other transcription factors, like CA150, CTBP, HYPA, HYPB, HYPC, NCOP, NF- κ B or TBP (Li and Li, 2004), which points to an important role of Htt in the regulation of gene expression.

Anti-apoptotic function

Importantly, wild-type Htt is assumed to have an anti-apoptotic function in cells. Several studies have demonstrated that expression of wild-type Htt protects striatal-derived cells against apoptotic stimuli (Rigamonti et al., 2001; 2000; Zhang et al., 2006). By interaction with HIP1 (huntingtin-interacting protein 1) wild-type Htt prevents the formation of the apoptosis-activating HIP1/HIPPI (HIP1-protein inductor) complex (Kalchman et al., 1997; Wanker et al., 1997; Gervais et al., 2002) and inhibits the activation of caspase-8. However, mutant Htt has a much lower affinity to bind

HIP1 than the wild-type protein. The influence of Htt on the formation of the HIP1/HIPPI complex is suggested to be important in the loss-of-function toxicity in HD (Chapter 1.1.8)

Htt is also a substrate for Akt, a serine/threonine kinase which is known to activate survival pathways in cells (Humbert et al., 2002). In addition, wild-type Htt seems to act downstream of the cytochrome c release by mitochondria, inhibiting the formation of the apoptosome complex and thereby preventing the activation of caspase-9 and consequently of caspase-3 (Rigamonti et al., 2000; 2001) Moreover, wild-type Htt was found to directly interact with active caspase-3 inhibiting its proteolytic activity (Zhang et al., 2006). The mutant form of Htt can also bind to caspase-3, but with a lower affinity, enhancing caspase-3 activity and cell death (Zhang et al., 2006). Several studies have shown that expression pattern of apoptosis related proteins are dysregulated as a consequence of mutant Htt expression. Among these proteins are caspases (Apostol et al., 2006), targets of the pro-apoptotic tumor suppressor p53 (Sipione et al., 2002) and members of death receptor superfamily such as FAS (Anderson et al., 2008) and TNF-receptors (Borovecki et al., 2005).

1.1.3 Polyglutamine disorders

Besides HD nine further neurodegenerative disorders are caused by an abnormal expansion of a CAG-repeat. Among these are dentatorubral and pallidolusian atrophy (DRPLA), spinocerebellar ataxias (SCA) 1, 2, 3, 6, 7 and 17 as well as spinal and bulbar muscular atrophy (SBMA; „Kennedy-Disease“). Each of these disorders shows similar symptoms of motor impairment but different degrees of cognitive decline. The elongated polyQ region leads to the formation of large intranuclear and cytoplasmic aggregates and a selective loss of specific neuronal cells (Orr and Zoghbi, 2007; Bates et al., 2002). Although neurodegeneration is a general characteristic of these disorders (Yuan and Yankner, 2000), the mode of cell death is still unclear. Neuronal cell death can occur as a result of various intra- and extracellular signals which might lead to necrosis, excitotoxicity, autophagic cell death or apoptosis (see below). It is likely that these processes develop in parallel during disease progression and orchestra neurodegeneration by promoting each other ultimately resulting in neuronal loss.

Necrosis is an acute form of cell death induced by cellular stress, such as injury or high levels of toxins. It does not follow the well defined cascade of chemical reactions like it is the case for apoptosis but there are some typical characteristics such as cell swelling, chromatin digestion, disruption of the plasma membrane and the organelle membranes. In late necrosis DNA is hydrolysed, vacuolation of the endoplasmic reticulum and organelle breakdown occurs, finally followed by cell lysis (Martin, 2001; Kerr et al., 1972). *Excitotoxicity* is caused by excessive stimulation of NMDA receptor resulting in enhanced Ca^{2+} influx in neurons, which in turn activates mitochondrial mediated apoptosis (Nicholls and Budd, 1998) (see Chapter 1.2.4). *Autophagic cell death* usually occurs under starvation conditions. However, it can be also triggered by apoptotic signals such as growth

factor deprivation (Maiuri et al., 2007). In cells that undergo autophagic cell death large vacuoles are formed degrading organelles, prior to the nucleus being destroyed (Maiuri et al., 2007).

Apoptosis (programmed cell death) is regarded as the predominant form of neuronal death in chronic neurodegenerative disorders such as AD, amyotrophic lateral sclerosis (ALS) and HD (Thomas et al., 1995; Troost et al., 1995; Smale et al., 1995). It is a highly regulated intracellular degradation process characterized by the activation of various caspases organized in a sequential fashion which will be described in detail in Chapter 1.2.

1.1.4 Amyloid hypothesis

In all polyQ diseases, the expansion of the polyQ tract leads to destabilization of the protein fold. The protein undergoes conformational changes either before or coincident with the formation of highly ordered β -sheet rich aggregates, referred to as amyloid fibrils.

In vitro studies have demonstrated that the process of amyloid formation proceeds in a time and concentration dependent fashion, starting with an initial lag-phase in which microaggregates/spherical oligomers are formed. This lag-phase can be bypassed by addition of fibrillar seeds (Scherzinger et al., 1999). Once formed, the oligomeric structures can proceed to protofibrils and finally self-assemble into mature fibrils (Poirier et al., 2002).

Amyloid fibrils are typically deposited in the brain and/or in peripheral tissues and have been linked to neurodegeneration and diseases of organ dysfunction such as cardiomyopathy (Cornwell et al., 1988). However, it has been proposed that early formed oligomeric structures might be the main toxic species rather than mature amyloid fibrils (Bucciantini et al., 2002; 2004). *In vitro* studies showed that protein aggregates with an oligomeric morphology for mammalian cells (Bucciantini et al., 2002; 2004). Nevertheless, the mechanisms by which amyloid fibril formation causes neurodegeneration in patients and the identity of the pathogenic species have not been determined yet.

1.1.5 Aggregation of mutant huntingtin

The fibrillar aggregates formed by mutant Htt exon1 protein are extremely stable, protease- and SDS-resistant *in vitro* and *in vivo* (Scherzinger et al., 1997). Protein aggregates consisting of N-terminal fragments of mutant Htt are found in intranuclear inclusion bodies as well as dystrophic neurites in brains of HD patients (DiFiglia et al., 1997; Sieradzan et al., 1999).

There are two suggested ways for the formation of mutant Htt aggregates, the polar zipper model and the transglutaminase hypothesis. The polar zipper model suggests that the presence of an expanded polyQ tract leads to the destabilization of the tertiary Htt protein conformation which promotes abnormal protein-protein interactions between wild-type and mutant Htt as well as other polyQ containing proteins. This results in the formation of β -sheets that form polar zippers

via hydrogen bonds between the molecules (Perutz et al., 1994; Stott et al., 1995; Figure 1.2). These polar zippers can either form oligomeric intermediates or align directly to form stable β -sheet protofibrils which assemble into mature fibrils (Perutz et al., 1994). This zipper structures would be similar to amyloid cross-beta structures found in disease-associated aggregates from AD, PD or prion diseases.

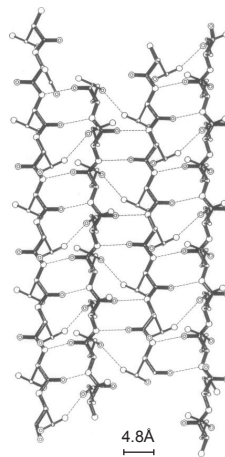


Figure 1.2: Schematic representation of a polar zipper structure (Perutz et al., 1994). Structure of two paired antiparallel polyQ β -strands which are linked by hydrogen bonds between main and side chains.

Another hypothesized way of fibril formation proposes an enzymatically mediated crosslinking. According to this theory, transglutaminases, enzymes which mediate the crosslinking of glutamine residues, play a role in the formation of aggregates by linking polyQ-rich protein sequences. It was shown that Htt serves as a substrate for transglutaminases (Kahlem et al., 1998) and that the transglutaminase activity is increased in HD brains (Karpuij et al., 1999). According to this hypothesis the presence of an elongated polyQ tract in the disease protein will result in an enhanced transglutaminase-mediated crosslinking.

1.1.6 Htt inclusions may have a protective role

Since Htt aggregates in intranuclear inclusions (Chapter 1.1.4) are a hallmark of HD it has been hypothesized that the formation of aggregates may be the trigger for the neuronal degeneration. However, it is still under debate whether inclusions found in HD brains represent a toxic or protective structure. In human brains the density of inclusions in the cortex correlates with the CAG-repeat length (DiFiglia et al. 1997; Becher et al., 1998). However, only little correlation between the number of inclusions and cell death in the most affected areas of HD brains has been observed (Gutekunst et al., 1999; Kuemmerle et al., 1999). Furthermore, promotion of inclusion formation was found to rescue Htt-induced proteasome dysfunction in a cell culture model (Bodner et al., 2006).

It seems possible that the sequestration of misfolded proteins into inclusions and the formation of aggregates represent a way to protect cells against misfolded proteins being more toxic in a soluble than in an aggregated form (Ciechanover and Brundin, 2003; Gunawardena and Goldstein, 2005). When striatal neurons were transfected with mutant Htt under conditions suppressing the formation of inclusions an increase in neuronal cell death was observed, supporting the hypothesis of a protective role of Htt inclusions (Saudou et al., 1998). Moreover, it was demonstrated that cells containing Htt inclusions survive better than cells without such structures (Arrasante et al., 2004). This suggests that large inclusions with Htt aggregates might be less toxic than soluble mutant Htt. Moreover, cells with mutant Htt in a soluble form are likely to contain oligomeric structures. Such oligomeric forms and protofibrils may be highly reactive because of their larger surface area which may correlate with toxicity.

1.1.7 Degradation of Htt aggregates

Under normal conditions misfolded proteins are degraded in the cell via two pathways. In the ubiquitin-proteasome system (UPS) proteins are tagged for degradation by conjugation of ubiquitin, followed by their destruction in the 26S proteasome (Ciechanover and Brundin, 2003). In neurodegenerative disorders accumulation of ubiquitinated proteins is often found in protein aggregates (Lennox et al., 1988; Lowe et al., 1988). In many cases these proteins are furthermore associated with subunits of the proteasome (Bence et al., 2001, Waelter et al., 2001b). This may reflect the failure of the UPS to remove the abnormal proteins. A possible explanation for this phenomenon in polyQ disorders is the inability of eukaryotic proteasomes to cut peptides with glutamine chains of 9-29 Qs and the occasional failure of protein fragments of more than 35 Qs to exit the proteasome (Holmberg et al., 2004; Venkatraman et al., 2004).

Autophagy represents another pathway for protein degradation, particularly for protein complexes or aggregates which are too big to be degraded in the narrow pore of the proteasome. In the process of macroautophagy intracellular components are sequestered into an autophagic vacuole (autophagosome) which subsequently fuses with lysosomes to degrade the contents (Levine and Kroemer, 2008). Kegel and colleagues found an increase in autophagosomes in striatal cells expressing mutant Htt (Kegel et al., 2000). The sequestration of misfolded proteins and their degradation may prevent their toxicity. Thus, increased autophagy may be a consequence of the accumulation of misfolded and aggregated proteins.

1.1.8 Mutant Htt and cellular dysfunction

The elongation of the polyQ tract in Htt is believed to affect the function of the protein in two ways: on the one hand the expansion mutation leads to new functions of the protein which are toxic (“toxic gain-of-function”). On the other hand a toxic loss-of-function of wild-type Htt might

Introduction

take place. Both alterations in Htt may contribute to the disruption of intracellular processes, eventually resulting in neuronal dysfunction and cell death.

Gain-of-function

The primary consequence of the expansion mutation in the HD gene is a toxic gain-of-function of the Htt protein. Proteolytic cleavage of the mutant Htt protein leads to formation of N-terminal fragments (Kim et al., 2001), which then are translocated to the nucleus where they form aggregate structures (Ona et al., 1999; Chapter 1.1.2.). The nuclear localization of mutant Htt was shown to enhance its toxicity in cell culture and mouse models (Saudou et al., 1998; Ross and Poirier, 2004; Schilling et al., 2004). Toxicity of Htt in the nucleus may be caused by interference of mutant Htt with physiological gene transcription.

Many transcriptional regulators contain glutamine-rich activating domains which are necessary for the interaction with transcription factors. Proteins carrying polyQ stretches like Htt could bind to these domains leading to changes in transcriptional activity of the binding partner (Schaffar et al., 2004; Gerber et al., 1994).

CBP (CREB-binding protein) and Sp1 (Specificity protein 1) are two major transcriptional regulators shown to interact with mutant Htt. CBP is an important transcription co-activator and mediator of neuronal cell survival. It contains a C-terminal glutamine-rich domain which can interact with mutant Htt. It was demonstrated that this interaction induces cellular toxicity (Steffan et al., 2000). Furthermore, sequestration of CBP into Htt aggregates was observed in cell and mouse model systems (Kazantsev et al., 1999; Steffan et al., 2000; Nucifora et al., 2001).

Similar to CBP, the transcription activator Sp1 also contains a glutamine-rich activation domain, which binds and regulates the basal transcriptional machinery including (TAF)II130 (Tanese and Tjian, 1993). Sp1 can specifically bind to the N-terminus of mutant Htt (Yu et al., 2002). This disturbs Sp1-mediated gene regulation by disrupting the Sp1-TAFII130 protein complex and altering the expression of certain Sp1 neuronal target genes such as the dopamine D2 receptor (Dunah et al., 2002).

Another important transcription factor, p53, has been found to interact with mutant Htt (Steffan et al., 2000). It regulates expression of several mitochondrial proteins such as the apoptosis mediator BAX (Miyashita and Reed, 1995; Polyak et al., 1997). Expression levels of p53 and its activity have been found to be increased in cellular systems expressing mutant Htt as well as in HD transgenic mice and HD patients (Bae et al., 2005). This suggests that mitochondrial functions and apoptosis are altered in HD.

The toxic gain-of-function of mutant Htt is also believed to interfere with mitochondrial mediated calcium homeostasis and apoptosis. The elongation of the polyQ stretch in Htt was shown to decrease mitochondrial ATP/ADP production (Seong et al., 2005). Impaired energy metabolism of mitochondria may lead to this reduction in ATP production. This may also be accompanied by

Introduction

a reduction of mitochondrial membrane potential which results in a higher sensitivity to NMDA-mediated calcium influx and excitotoxicity (Novelli et al., 1988; Fagni et al., 1994). Moreover, it was shown that mutant Htt has a potentiating effect on NMDA receptor activity leading to increased calcium influx (Zeron et al., 2004; 2002), impairment of mitochondrial function and increased oxidative stress (Lafon-Cazal et al., 1993; Reynolds and Hastings, 1995), eventually resulting in excitotoxicity.

Loss-of-function

Htt misfolding is thought to indirectly lead to loss-of-function toxicity by sequestering other proteins into Htt aggregates. Like other misfolded proteins Htt is bound by heat-shock proteins (HSPs) such as Hsp40 and Hsp70 as a cellular attempt to refold the mutant protein (Jana et al., 2000). However, these chaperones are sequestered into Htt aggregates, which prevent them to exert their normal functions (Sakahira et al., 2002). This may lead to accumulation of other misfolded proteins in addition to aggregated Htt (Hay et al., 2004). Besides heat shock proteins, several components of the proteasome like catalytic and regulatory subunits as well as ubiquitin conjugating enzymes are sequestered into the aggregates (Wytenbach et al., 2000; Jana et al., 2001). This results in the impairment of the ubiquitin-proteasome system (Bence et al., 2001). The presence of ubiquitin residues in Htt aggregates indicates that the cell tags the protein for degradation by the proteasome. The expansion mutation however, prevents the proteasomal degradation (Jana et al., 2001). This leads to a progressive accumulation of misfolded proteins within the cell which eventually can induce cell death by apoptosis or autophagy (Jana et al., 2001; Iwata et al., 2005).

The formation of mutant Htt aggregates is assumed to impair axonal transport. As described in Chapter 1.1.2, wild-type Htt acts in axonal transport via interaction with HAP1. The mutant form of Htt alters the formation of the HAP1/p150 complex leading to an impaired association of motor proteins and microtubules. This may result in the loss of BDNF transport and of neurotrophic support in neurons (Gauthier et al., 2004). Another hypothesis suggests that mutant Htt aggregates physically block axons on their narrow terminals (Gunawardena and Goldstein, 2005). The impairment of axonal transport may directly lead to disruption of postsynaptic signal transmission by either reducing the concentration of synaptic vesicles or by altering the availability of synaptic proteins. This may happen as a result of protein sequestration into Htt aggregates by interaction with mutant Htt or as a consequence of transcriptional dysregulation triggered by Htt (Li et al., 2003).

As further described in Chapter 1.1.2, wild-type Htt has a protective effect through its interaction with HIP1, which prevents the formation of the HIP1/HIPPI complex and activation of caspase-8 (Gervais et al., 2002). The mutant form of Htt binds with lower affinity to HIP1 than the wild-type protein. Under disease conditions mutant Htt aggregates sequester wild-type Htt into neuronal inclusions and thereby deplete it from the cytoplasm. As a consequence less amounts of free normal

Htt are present in the cell leading to enhanced liberation of HIP1, formation of the HIP1/HIPPI complex and activation of caspase-8 (Gervais et al., 2002).

1.2 Cell death and apoptosis

In general, cell death occurs in response to a variety of stimuli by either necrosis or apoptosis. In case of necrosis death stimuli such as acute ischemia or injury (Linnik et al., 1993; Emery et al., 1998) lead directly to cell death. Necrotic cell death is characterized by mitochondrial and nuclear swelling, condensation of chromatin followed by disruption of organelle and plasma membranes, DNA degradation by random enzymatic cleavage and eventually cell lysis (Martin, 2001; Kerr et al., 1972).

Apoptosis, also known as programmed cell death, is a normal event in the life cycle of multicellular organisms. Apoptotic cells die in response to several stimuli in a controlled and regulated process, in which the cell itself plays an active role, which is why apoptosis is often termed “cellular suicide”. The process is characterized by the induction of a caspase protease activation cascade that destroys cell survival factors by cleavage and activates pro-apoptotic molecules. This process is accompanied by condensation of the cytoplasm, aggregation of mitochondria and ribosomes, nucleus condensation and aggregation of the chromatin. In the end stage of cell death the chromosomal DNA is cleaved to 180 bp internucleosomal fragments and small vesicles - so called “apoptotic bodies” - are formed (Hengartner, 2000; Wyllie et al., 1980; Kerr et al., 1972; Wyllie, 1980; Liu et al., 1997). Two major pathways for activation of the apoptotic cascade can be distinguished. On the one hand the cascade is activated by extrinsic death receptor-mediated signaling triggered by extracellular signals that induce intracellular interactions that lead to cell death. On the other hand the caspase cascade is activated by intrinsic signaling as a result of intracellular stress like radiation, growth factor deprivation or oxidative stress (Elmore, 2007).

1.2.1 Extrinsic apoptosis signaling via death receptor

The death receptor pathway (Figure 1.3) is triggered by extracellular signaling molecules which bind to members of the death receptor superfamily such as Fas/CD95 or TNFR1 (tumor necrosis factor receptor 1). Binding of ligands like FasL or TNF-alpha to the receptor results in a clustering of death receptors that facilitates signal amplification. Following the binding of the ligand and receptor clustering, conformational changes in the intracellular domains lead to the presentation of a death-domain. Binding of TNF-alpha to the TNFR1 receptor results in binding of the intracellular adaptor molecule TRADD (TNFR-associated death domain) to the receptor death domain and recruitment of other proteins like FADD (Fas-associated via death domain) (Hsu et al., 1995). Interaction of FasL with the receptor leads to the binding of FADD to the receptor via its death domain (DD) (Boldin et al., 1995; Chinnaiyan et al., 1995), and the formation of a protein complex termed DISC (death inducing signaling complex) (Kischkel et al., 1995). The binding of FADD enables

the complex to recruit and bind numerous pro-caspase-8 molecules by homotypic interactions via their “death effector domains” (DED) (Boldin et al., 1996; Muzio et al., 1996).

Caspase-8 activation in the DISC is a two step process. First, procaspase-8 molecules dimerize and undergo conformational changes resulting in the gain of full enzymatic activity. In the second step the activated caspase is autoproteolytically processed to allow the dissociation of caspase-8 from the DISC complex (Boatright et al., 2003). Caspase-8 proteolytically activates effector (or “executioner”) caspases such as caspase-3 and caspase-7 (Cryns and Yuan, 1998). These proteins subsequently process their apoptotic substrates such as ICAD (inhibitor of caspase-activated DNase), whose cleavage leads to CAD (caspase-activated DNase) mediated DNA fragmentation (Liu et al., 1997; Enari et al., 1998; Sakahira et al., 1998). Activation of caspase-8 can be blocked by the enzymatically inactive caspase homologue c-FLIP (Irmeler et al., 1997).

Besides caspases -3 and -7, BID, a pro-apoptotic Bcl-2 family member, represents another critical substrate of caspase-8. Proteolytic cleavage of BID to the truncated form tBID results in its translocation from the cytosol to the outer mitochondrial membrane where it initiates membrane permeabilisation by oligomerisation of BAX and BAK (Esposti, 2002). This promotes pore formation and cytochrome c release. The molecules BID and tBID integrate the death receptor and the mitochondrial pathway and serve as the linker between the two pathways (Esposti, 2002).

1.2.2 Mitochondria-mediated (“intrinsic”) apoptosis signaling

In contrast to the receptor-mediated pathway in which apoptosis signaling is induced by ligand binding to a receptor, the intrinsic or mitochondrial mediated pathway is activated by non-receptor-mediated stimuli. The stimuli initiating this pathway can be the withdrawal of growth factors, cytokines or hormones which lead to a failure of apoptosis suppression (Elmore, 2007). Alternatively, the direct insults such as ischaemia, oxidative stress excitotoxicity or radiation can activate the intrinsic pathway. In neurodegenerative disorders injurious signals can include toxic proteins or lipids such as ceramides (Pettus et al., 2002).

All these intrinsic stimuli cause changes in the mitochondrial membrane resulting in membrane permeabilization, loss of mitochondrial membrane potential and release of pro-apoptotic proteins (Saelens et al., 2004; Birbes et al., 2002). One group of released proteins is involved in the caspase-dependent mitochondrial pathway. It consists of cytochrome c, Smac/DIABLO and HtrA2/Omi (Du et al., 2000; van Loo et al., 2002a; Garrido et al., 2006). After release from the mitochondria cytochrome c associates with Apaf-1 (apoptosis protease activating factor-1) which leads to the recruitment of pro-caspase-9 molecules into a multiprotein complex. This complex, consisting of oligomerized Apaf-1, cytochrome c and pro-caspase-9 is termed the “apoptosome” (Chinnaiyan, 1999; Hill et al., 2004). The formation of the apoptosome results in autoactivation of caspase-9 and initiates the downstream activation of the caspase cascade leading to cleavage of effector caspases -3 and -7. Smac/DIABLO and HtrA2/Omi release results in the sequestration

Introduction

of IAPs (inhibitors of apoptosis proteins) which prevent the activation of downstream caspases (van Loo et al., 2002b; Schimmer, 2004).

A second group of pro-apoptotic proteins released by mitochondria contains AIF (apoptosis inducing factor), endonuclease G and ICAD. After release from the mitochondria all three factors translocate to the nucleus and cause DNA fragmentation (Joza et al., 2001; Li et al., 2001; Enari et al., 1998). Whereat AIF and endonuclease G act independently of caspase activation, however ICAD is proteolytically activated by caspase-3 to generate active CAD (Enari et al., 1998).

Members of the Bcl-2 family are important factors which control key events in the mitochondrial mediated apoptosis pathway (Cory and Adams, 2002). They can be classified into pro- and anti-apoptotic proteins. Bcl-2 proteins are localized at the surface of mitochondria influencing mitochondrial membrane permeability and cytochrome c release. Bcl-10, BAX, BAK, BID, BAD, BIM, BIK and BLK serve as pro-apoptotic proteins, whereas Bcl-2, Bcl-x, Bcl-XL, Bcl-XS, Bcl-w and BAG have anti-apoptotic functions. The relative abundance of pro- and anti-apoptotic factors determines the fate of a cell to undergo apoptosis. However, the exact mechanism for cell death is still unclear.

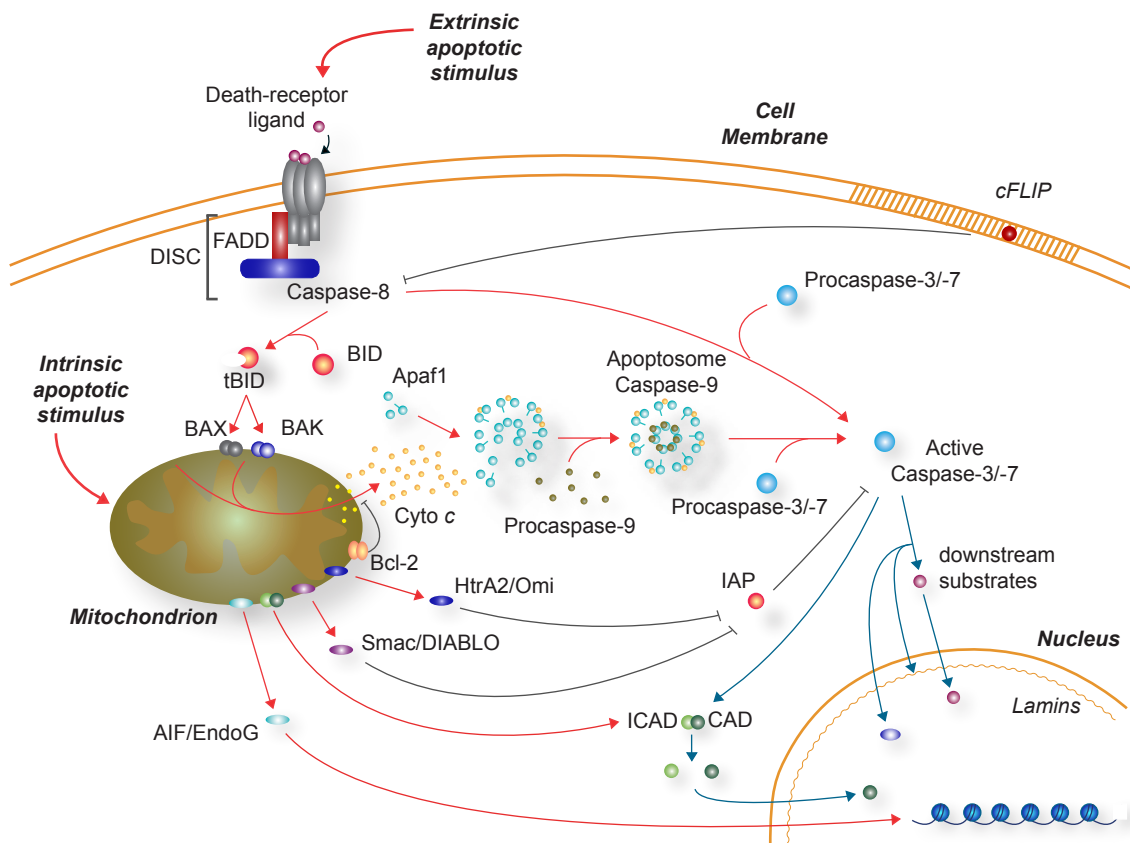


Figure 1.3: Intrinsic and extrinsic pathways of caspase activation in mammals (modified from D'Amelio et al., 2009).

1.2.3 Caspases: the major effectors

Both apoptotic pathways described above end in the final execution phase, in which caspases play major roles. Caspases are cysteine proteases which are homologous to each other and are highly conserved through evolution (Alnemri et al., 1996). All caspases have an active-site cysteine and cleave their substrates after aspartic acid residues. Their respective specificities are determined by the composition of four amino-terminal residues next to the cleavage site (Thornberry et al., 1997). Inhibition of caspase activity results in reduction or even prevention of apoptosis (Earnshaw et al., 1999). In proliferating cells caspases exist as enzymatically inactive zymogens, composed of an N-terminal prodomain and the two domains p10 and p20, which represent the mature enzyme after activation. Activated caspases are heterotetramers composed of two p20/p10 heterodimers (Earnshaw et al., 1999). The members of the caspase protease family are classified according to their function in the apoptotic caspase cascade into upstream initiators and downstream effectors (executioners). Upstream caspases such as caspase-2, -8, -9 and -10 are activated by an apoptosis signal as described in Chapter 1.2.1 and 1.2.2. Effector caspases such as caspase-3, -6 and -7 act downstream of the initiator caspases. They are activated by proteolytic cleavage by the upstream caspases. After activation, effector caspases mediate cell death either by destruction of survival promoting proteins or by activation of pro-apoptotic factors, eventually leading to the characteristic morphological and biochemical changes (Slee et al., 2001). Various intracellular components are targets for activated caspases. Cleavage of nuclear lamins (filaments forming the nuclear lamina), which are involved in chromatin condensation and nuclear shrinkage, is often observed. As described in Chapter 1.2.2 cleavage of ICAD causes the release of an endonuclease (CAD) and its translocation into the nucleus to fragment DNA (Sakahira et al., 1998). Cleavage of cytoskeletal proteins such as actin, plectin, Rho kinase 1 (ROCK1) and gelsolin leads to cell fragmentation, blebbing (formation of “*bulges in the plasma membrane caused by localized decoupling of the cytoskeleton from the plasma membrane*”; <http://en.wikipedia.org/wiki/Blebbing>) and the formation of apoptotic bodies (Kothakota et al., 1997).

1.2.4 Cytotoxicity and apoptosis in Huntington's disease

In the brain of HD patients several caspases have been shown to be activated (Vis et al., 2005; Kiechle et al., 2002). Caspase activity was found to be connected to Htt in two ways. On the one hand the expression and aggregation of mutant Htt causes activation of caspases by its altered function as described in Chapter 1.1.8. On the other hand it serves as a caspase substrate itself.

Activation of caspases by mutant Htt

Overexpression and aggregation of mutant Htt induces intracellular stress like mitochondrial or ER stress which results in activation of several caspases such as caspase-3/7, -9 and -8 (Hackam et al., 2000; Rigamonti et al., 2001; 2000; Zeron et al., 2004; Apostol et al., 2006; Zhang et al., 2006). Mitochondrial abnormalities such as alterations of membrane potentials and

Introduction

depolarization at lower calcium levels have been observed in several HD models (Sawa et al., 1999; Panov et al., 2002). Mutant Htt was demonstrated to directly bind to the mitochondrial membrane (Choo et al., 2004; Panov et al., 2002) leading to membrane depolarization. Moreover, mitochondrial proteins such as death signaling factors and proteins of the respiratory chain are transcriptionally dysregulated in the presence of mutant Htt (Bae et al., 2005; Cui et al., 2006). This increases susceptibility of the mitochondrial membrane to depolarization and results in release of cytochrome c or AIF (Green and Reed, 1998; van Loo et al., 2002a). These events activate the intrinsic apoptosis signaling cascade in which the apoptosome complex is formed and caspase-9 and -3 are activated. Additionally, induction of apoptosis signaling is associated with endoplasmic reticulum (ER) stress as a consequence of misfolded protein accumulation and aggregation which also activates mitochondrial apoptosis signaling (Smith and Deshmukh, 2007; Puthalakath et al., 2007). Furthermore, caspase-9 is activated independently of the apoptosome via the misfolded protein response (Morishima et al., 2002; Rao et al., 2002). As described in Chapter 1.1.8 mutant Htt overexpression furthermore influences caspase activation of caspase-8 and -3 via its interaction with HIP1.

Cleavage of Htt by caspases

The Htt protein has been demonstrated to be a substrate for several caspases (Goldberg et al., 1996; Wellington et al., 1998, 2000), since it contains cleavage sites for caspase-3 at amino acids D513 and D552, for caspase-2 at D552 and for caspase-6 at D586 (Figure 1.1; Wellington et al., 1998, 2000). Two additional caspase-3 cleavage sites located at amino acids D530 and D589 were shown to be silent (Wellington et al., 2000). The cleavage of mutant and wild-type Htt at the active sites generates N-terminal protein fragments. Studies using transgenic HD mouse models demonstrated that effector caspase-1 gene transcription is upregulated in early stages of the disease (Ona et al., 1999). During disease progression the transcription of the gene encoding caspase-3 is upregulated and the protein becomes activated (Chen et al., 2000; Apostol et al., 2006). During progression of disease activities of caspase-1 and -3 are increased which results in an enhanced generation of Htt fragments (Wellington et al., 2000).

The enhanced cleavage of wild-type Htt eventually results in the depletion of the normal protein (Ona et al., 1999), which plays an important role in transcription regulation of the neurotrophic factor BDNF, a pro-survival factor (Zuccato et al., 2001). BDNF was shown to protect cells from apoptosis by inhibition of caspase-9 and caspase-3 mediated apoptosis signaling (Rigamonti et al. 2000; 2001). Recent studies support the hypothesis that caspase-3-mediated cleavage of mutant Htt is crucial for induction of neuronal cell death. Inhibition of caspase-3 resulted in a significant reduction in neuronal cell death after striatal lesions induced by malonate (inhibitor of the mitochondrial enzyme succinate dehydrogenase) in adult rats (Toulmond et al., 2004). Proteolytical cleavage of Htt results in nuclear translocation of the cleavage products which leads to further upregulation of caspase-1 transcription (Ona et al., 1999). N-terminal Htt fragments generated by caspase cleavage are translocated from the cytosol into the nucleus where they form intranuclear

inclusions, which links activation of caspases to aggregate formation. The nuclear translocation then results in abnormal protein interactions altering transcriptional regulation of pro- or anti-apoptotic genes closing the circle of caspase-mediated Htt cleavage and induction of caspase activation.

1.3 Model systems reproducing HD features

Within the last years several model systems for polyQ-repeat diseases have been developed in mouse, rat, *C. elegans*, *Drosophila*, yeast and numerous cell-culture systems (Bates et al., 2002; Ross, 2002, Rubinsztein, 2002) to model different aspects of disease. Within this study I used two mammalian cell culture systems and a transgenic mouse model to investigate mutant Htt-induced cytotoxicity and its modulation.

Transiently transfected Neuro2a cells

The expression of mutant Htt results in the formation of amyloid fibrils and cytotoxicity (Zoghbi and Orr, 2000; Scherzinger et al., 1999). To identify new potential modifiers of Htt-induced cytotoxicity in RNAi knock-down assays I used a mouse neuroblastoma cell line (Neuro2a) as a model system. The cell line was developed in 1970 by K. N. Prasad (Prasad et al., 1970) and is commonly used as a model system to study polyQ disorders such as HD and SCA (Omi et al., 2008; Wang et al. 1999; Yoshida et al., 2002). In addition it was utilized to investigate protein misfolding diseases like PD or AD (Uney et al., 1993; Zhou et al., 2008; Filiz et al., 2008; Dumanchin-Njock et al., 2001). To perform a toxicity modifier screen I transfected the cells with an expression vector (pcDNA1-HD320_Q68) encoding an N-terminal human Htt fragment with 320 aa and a polyQ stretch of 68 glutamines. The expression of this Htt protein leads to the formation of SDS-resistant aggregates detectable by filter retardation assay (Scherzinger et al., 1997) and causes cytotoxicity which can be monitored by caspase activation assays (Filiz et al., 2008; Dumanchin-Njock et al., 2001).

Inducible expression of Htt in PC12 cells

To study the pathogenic mechanisms leading to cytotoxicity in detail an inducible rat pheochromocytoma (PC12) cell model system was used. Originally, this cell line was derived from a pheochromocytoma of the rat adrenal medulla (Greene and Tischler, 1976). It can be reversibly differentiated into neurons by addition of nerve growth factor (NGF). The HD PC12 cell lines used in this study were generated by B. Apostol and colleagues (2003). They contain a stably integrated sequence for the expression of a human N-terminal Htt fragment, which can be induced by addition of ponasterone A or muristerone A to the cells. Two different truncated Htt exon1 proteins with either 25 or 103 glutamine residues and a carboxy-terminal EGFP epitope tag are produced in the PC12 cell lines (Apostol et al., 2003). A schematic representation of the expression constructs is shown in Figure 2.6. Cells expressing the Htt protein with a wild-type polyQ tract (Htt25Q-EGFP)

Introduction

show a diffuse distribution of the EGFP fusion protein (Figure 2.9), whereas expression of Htt with an expanded polyQ stretch of 103 glutamines (Htt103Q-EGFP) results in the formation of cytosolic aggregates (Apostol et al., 2003; Figure 2.8 and 2.9) and cytotoxicity, which can be monitored by caspase-3/7 assays (Apostol et al., 2006; this study).

The transgenic HD mouse model TgHD82Q

The transgenic mouse model I used in this study was generated by G. Schilling and colleagues in 1999 (Schilling et al., 1999). The animals contain a cDNA construct expressing an N-terminal Htt fragment of 171 aa and a polyQ tract of 82 glutamines (N171-82Q) (Schilling et al., 1999). The mice expressing N171-82Q develop behavioral abnormalities such as tremor, loss of coordination, hypokinesia and abnormal gait. The first symptoms appear at 2 months of age with the failure to gain weight and in the last 4 – 6 weeks of the lifespan the animals lose weight. Impairment of motor function is visible at the age of 3 months followed by progressive behavioral symptoms, including tremor, uncoordination, hypokinesia and hindlimb claspings. In the endstage of the disease transgenic mice are smaller and less responsive to stimuli than healthy control animals (Schilling et al., 1999). Moreover, intranuclear inclusions and neuritic aggregates of Htt were found in multiple populations of neurons in these mice (Figure 1.4; Schilling et al., 1999).

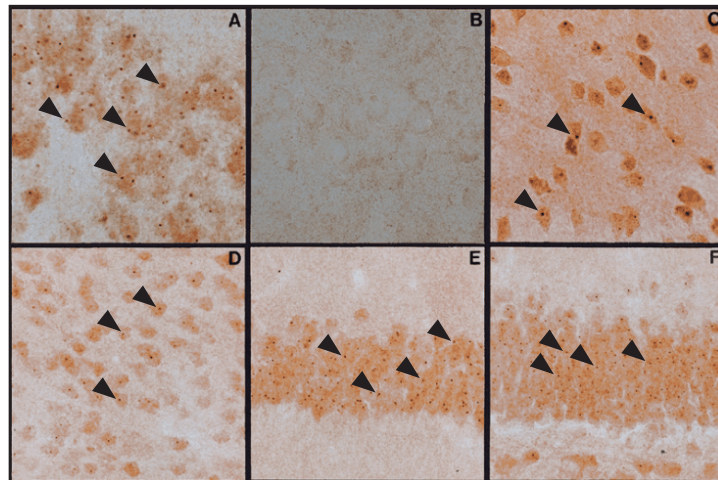


Figure 1.4: Intranuclear neuronal inclusions in multiple neuron populations of endstage N171-82Q mice (modified from Schilling et al., 1999). Inclusions are stained with a polyclonal antibody AP194 recognizing Htt N-terminal amino acids 1-17 in sections of (A) pyriform cortex of transgenic and (B) control animals; inclusions in (C) striatum, (D) cortex, (E) hippocampus and (F) dentate gyrus are shown (inclusions are indicated by arrowheads).

1.4 The DEAD-box protein family

DEAD-box proteins are a large group of 38 putative RNA helicases which have been shown to be involved in every aspect of RNA metabolism such as transcription, pre-mRNA splicing, rRNA processing, in RNA transport, translational initiation, ribosomal biogenesis and RNA decay (de la Cruz et al., 1999; Luking et al., 1998). Members of this protein family are found in most organisms from prokaryotes to humans. The protein family was first defined as a group of NTPases sharing common sequence elements (Gorbalenya et al., 1989). Today, DEAD-box proteins are characterized by sharing nine conserved sequence motifs with very little variation (Linder et al., 1989; Tanner et al., 2003). The presence of these motifs is a criterion for classification of a protein within the family of helicases, but an enzymatic activity has been demonstrated only for a limited number of these proteins.

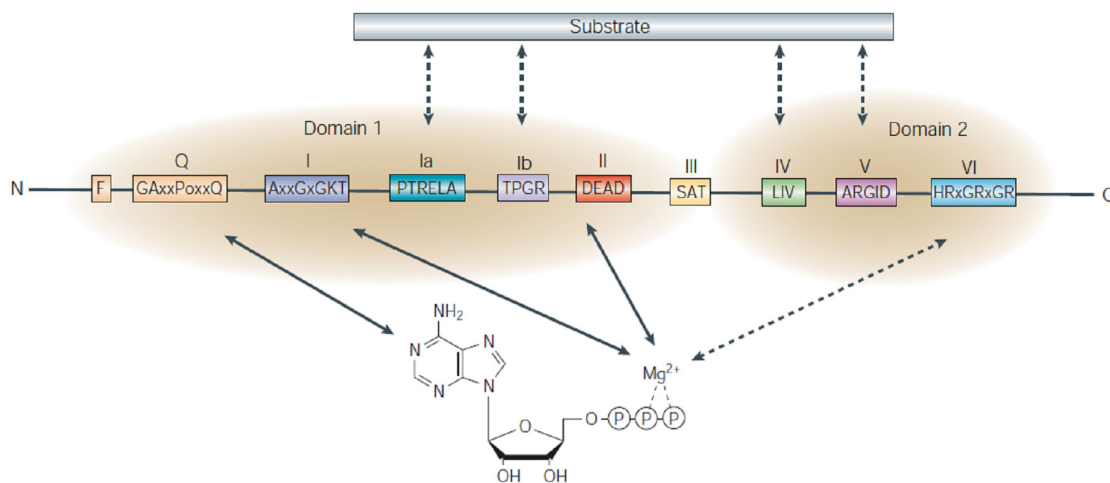


Figure 1.5: A schematic presentation of conserved motifs in DEAD-box protein family members (from Rocak and Linder, 2004). The Q-motif, motifs I, II (Walker motif A and B) and Motif VI bind ATP and are required for its hydrolysis. Motifs Ia, Ib, IV and V are supposed to be involved in RNA binding.

The nine conserved motifs are as follows: Q-motif, motif I, motif Ia, motif Ib, motif II, motif III, motif IV, motif V, and motif VI (Figure 1.5.) Motif II is also known as the “Walker B motif” and contains the name giving amino acid sequence D-E-A-D (Asp-Glu-Ala-Asp). This motif, as well as motif I (“Walker A motif”), Q-motif and motif VI, is required for ATP binding and hydrolysis (Tanner et al., 2003; Blum et al., 1992; Pause et al., 1994; 1992), whereas motifs Ia and Ib, III, IV and V are supposed to be involved in the interaction with RNA (Svitkin et al., 2001).

Table 1.1 gives an overview about the members of the DEAD-box protein family and their intracellular function if known. Several DEAD-box proteins were found to influence *transcription* by interacting with components of the transcription machinery (Yan et al., 2003; Rajendran et al., 2003; Rossow and Janknecht, 2003). In addition they were shown to act as co-activators/-suppressors (Yan et al., 2003; Rajendran et al., 2003). In *pre-mRNA splicing* members

Introduction

of the DEAD-box protein family are believed to promote the remodeling and dissociation of the RNA-protein complex by their ATPase activity (Kistler and Guthrie, 2001; Chen et al., 2001). *Ribosome biogenesis* is a multistep process in which several RNA species, numerous ribosomal proteins, and many trans-acting factors are involved. DEAD-box proteins were demonstrated to be critical for rRNA maturation (de la Cruz et al., 1999; 2003; Kressler et al., 1999). In *S. cerevisiae*, 14 out of the 24 known DEAD-box proteins are required for ribosomal subunit formation (Kressler et al., 1999). *Export of mRNA* from the nucleus into the cytosol through the nuclear pore also requires binding of DEAD-box proteins (Linder and Stutz, 2001; Keene, 2003). To facilitate translocation the protein-RNA complex the DEAD-box proteins interact with components of the nuclear pore (Zhao et al., 2002; Weirich et al., 2004). Two members of the DEAD-box family eIF4A and Ded1 have been shown to be essential for translation initiation in yeast (Linder, 2003). Within this process they are supposed to unwind secondary RNA structures and to remove other proteins bound to the mRNA (Svitkin et al., 2001; Berthelot et al., 2004). Eventually, DEAD-box proteins are required for RNA degradation, the so called *RNA decay*. RNA degradation occurs in the exosome, a complex of several exonucleases that degrade RNAs in the nucleus and in the cytoplasm (Raijmakers et al., 2004).

Interestingly, two members of the DEAD-box protein family were found to be involved in apoptosis signaling. In 2005, the DEAD-box family member DDX47 was identified as an interaction partner of GABAA receptor-associated protein (GABARAP), a molecular chaperone for the GABAA receptor in cortical neurons (Lee et al., 2005). Lee and colleagues could demonstrate that the co-transfection of GABARAP and DDX47 cDNA in a tumor cell line induces apoptosis.

Furthermore, a very recent study by Sun and colleagues identified DDX3 as a component of an anti-apoptotic protein complex (Sun et al., 2008). This complex is associated with death receptors and contains glycogen synthase kinase-3 (GSK3), DDX3 and the cellular inhibitor of apoptosis protein-1 (cIAP-1). In this study DDX3 was shown to act in a protective manner blocking the induction of death receptor-mediated apoptosis signaling (Chapter 1.2.1) which results in activation of caspase-3 (Sun et al. 2008).

Table 1.1: Human DEAD-box proteins (modified from Linder, 2006)

Gene Symbol	Alias	Function	Reference
DDX1	DBP-RB; UKVH5d; DDX1	Amplified in retinoblastoma; cellular co-factor of HIV-1 Rev, nucleolar	Andersen et al., 2005 Godbout and Squire, 1993 Fang et al., 2004
DDX2A	eIF4A I	Translation initiation	Rogers et al., 2002
DDX2B	eIF4A II	Translation initiation	Rogers et al., 2002

Introduction

Gene Symbol	Alias	Function	Reference
DDX3Y	DBY	Role in spermatogenesis	Sekiguchi et al., 2004 Ditton et al., 2004
DDX3X	DBX; DDX3; HLP2; DDX14; DDX3X	Role in spermatogenesis; transcription activator; potential tumor suppressor	Andersen et al., 2005 Chung et al., 1995 Yedavalli et al., 2004
DDX4	VASA; MGC111074; DDX4	Translation initiation; similar to Drosophila Vasa that interacts with eIF5B	Castrillon et al., 2000 Johnstone et al., 2004
DDX5	p68; HLR1; G17P1; HUMP68	Transcription; pre-mRNA splicing; mRNA stability and ribosome biogenesis; nucleolar; co-activator of p53 mediated stress re- sponse (anti-apoptotic function)	Andersen et al., 2005 Hloch et al., 1990 Ford et al., 1988 Bates et al., 2005
DDX6	p54; RCK; HLR2	Oncogene RCK; translation initiation of c-myc mRNA; nuclear; assembly of stored mRNP particles; mRNA masking in analogy to clam homologue	Minshall et al., 2001 Smillie et al., 2002 Akao et al., 2003 Akao et al., 1992 Lu and Yunis, 1992
DDX10	HRH-J8	Nucleolar	Andersen et al., 2005 Fischer and Weis, 2002
DDX17	p72; RH70	Nucleolar; transcription regulation	Andersen et al., 2005 Lamm et al., 1996 Wilson et al., 2004
DDX18	MrDb	Mcy-regulated; nucleolar	Andersen et al., 2005 Grandori et al., 1996
DDX19A	DDX19L		Schmitt et al., 1999
DDX19B	DBP5; RNAh; DDX19	mRNA export	Schmitt et al., 1999
DDX20	DP103; GEMIN3	Spliceosomal snRNP biogenesis	Charroux et al., 1999 Grundhoff et al., 1999
DDX21	GUA; GURDB; RH-II/ GU; RH-II/GuA	Ribosomal RNA production; co-factor for c-Jun-activated transcription	Andersen et al., 2005 Valdez et al., 1996 Henning et al., 2003 Yang et al., 2003
DDX23	prp28; PRPF28; MGC8416; U5-100K; U5-100KD	Pre-mRNA splicing	Teigelkamp et al., 1997

Introduction

Gene Symbol	Alias	Function	Reference
DDX24		Nucleolar	Andersen et al., 2005 Zhao et al., 2000
DDX25	GRTH	Gonadotropin-regulated testicular RNA helicase; component of mRNP particle; regulator of the tumor necrosis factor receptor 1 and caspase pathways and promotes NF- κ B function to control apoptosis in spermatocytes	Tang et al., 1999 Gutti et al., 2008
DDX27	RHLP; Rrp3p; PP3241; HSPC259	Nucleolar	Andersen et al., 2005
DDX28	MDDX28	Mitochondrial and nuclear localization	Valgardsdottir et al., 2001
DDX31		Nucleolar	Andersen et al., 2005
DDX39	BAT1; DDXL; BAT1L; URH49	Pre-mRNA splicing and export	Pryor et al., 2004
BAT1	UAP56; DDX39B	Pre-mRNA splicing and export	Peelman et al., 1995 Fleckner et al., 1997 Lehner et al., 2004
DDX41	ABS		Irion et al., 2004 Irion and Leptin, 1999
DDX42	SF3b125; RHELP; RNAHP	Pre-mRNA splicing; splicing	Will et al., 2002
DDX43	CT13; HAGE	Displays tumor-specific expression	Martelange et al., 2000
DDX46	Prp5; PRPF5	Pre-mRNA splicing	Will et al., 2002
DDX47	E4-DBP	Co-transfection of GABARAP and DDX47 cDNA into a tumor cell line induces apoptosis, nucleolar	Andersen et al., 2005 Scherl et al., 2002
DDX48	EIF4A3	Component of the EJC (Exon-Junction-Complex); has also been found in proteomic studies of the nucleolus	Ferraiuolo et al., 2004 Andersen et al., 2005 Chan et al., 2004
DDX49		Nucleolar	Andersen et al., 2005

Introduction

Gene Symbol	Alias	Function	Reference
DDX50	GU2; GUB; MGC3199; RH-II/GuB	Localizes to nuclear speckles containing splicing factor SC35; co-factor for c-Jun-activated transcription, nucleolar	Andersen et al., 2005 Valdez et al., 2002a Valdez et al., 2002b Westermarck et al., 2002
DDX51		Nucleolar	Andersen et al., 2005
DDX52	ROK1; HUSSY19	Nucleolar	Andersen et al., 2005
DDX53	CAGE; CT26	CAGE is expressed in a variety of cancers but not in normal tissues except testis	Cho et al., 2002
DDX54	DP97	Nucleolar	Andersen et al., 2005 Scherl et al., 2002 Rajendran et al., 2003
DDX55		Nucleolar	Andersen et al., 2005
DDX56	DDX21; DDX26; NOH61	Associates with nucleoplasmic 65S pre-ribosomal particles; nucleolar	Andersen et al., 2005 Zirwes et al., 2000
DDX59	ZNHIT5		

1.4.1 The putative RNA helicase DEAD (Asp-Glu-Ala-Asp) box polypeptide 24 (DDX24)

DDX24 is a member of the DEAD-box protein family with a size of 96.3 kDa. It is supposed to act as an RNA helicase. Its amino acid sequence shows the characteristic domains of its protein family namely the RNA binding domain as well as an ATPase domain (Zhao et al., 2000). A yeast two-hybrid screen performed in our group identified DDX24 as an interaction partner of GIT1. GIT1 was found to directly interact with mutant Htt and modulates its aggregation (Goehler et al., 2004), which suggests a link between DDX24 and Htt aggregation and toxicity. The yeast homologue of DDX24, Mak5, was found to be involved in the biosynthesis of the 60S ribosome subunit (Zagulski et al., 2003). However, the cellular function of DDX24 in mammals is still unclear. Previous studies were predominantly limited to structural analysis of the protein. Figure 1.6 schematically shows the human DDX24 protein (total length 859 aa) compared to rat DDX24 (total length 851 aa) and highlights the conserved domains of the DEAD-box protein family. The sequence of the human DDX24 gene shares only little similarity to other members of the human DEAD-box protein family, but it has a high similarity to mouse DDX24 at the amino acid level (Zhao et al., 2000) as well as to the amino acid sequence of rat specific DDX24. The protein is ubiquitously expressed but most abundant in heart and brain tissue (Zhao et al., 2000). The

lowest levels were detected in thymus and small intestine. A study published in 2008 demonstrated DDX24 functioning in packaging of HIV-1 (Human immunodeficiency virus type 1) (Ma et al., 2008), but its normal cellular function still remains an open question.

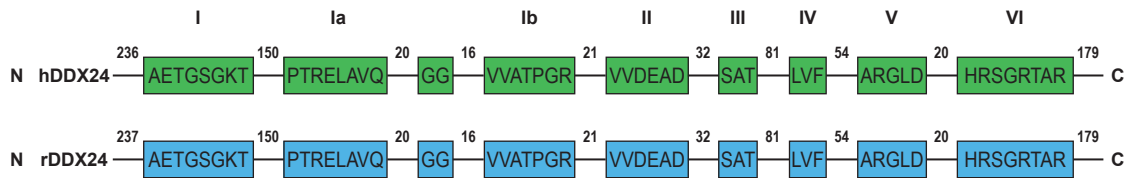


Figure 1.6: Schematic representation of the conserved motifs found in human DDX24 and rat DDX24 (hDDX24; rDDX24). The numbers show the number of amino acids in the N- and C-terminals and the intervals between adjacent motifs (modified from Zhao et al. 2000).

1.5 Genetic screens for modifiers of polyQ-induced toxicity and aggregation

Within the last years various genetic screening studies have been performed to identify modifiers of polyQ-induced aggregation and toxicity in several model systems such as yeast, *Drosophila* or *C. elegans* (Willingham et al., 2003; Giorgini et al., 2005; Bilen and Bonini, 2007; Kaltenbach et al., 2007; Kazemi-Esfarjani and Benzer, 2000; Nollen et al., 2004; Doumanis et al., 2009). Within these studies several different methods were used to identify modulator proteins such as protein over-expression or RNAi. A recent study by L. Kaltenbach (2007) identified modulators of Htt-induced toxicity using a combination of several approaches (Kaltenbach et al., 2007). First, they screened for interaction partners of mutant Htt by yeast two-hybrid screening and second by an affinity pull-down assay using Htt exon 1 protein constructs with elongated polyQ stretches (48Q, 55Q, 75Q and 97Q) (Kaltenbach et al., 2007). The proteins which were identified to interact with mutant Htt were then tested on their effect on a Htt-fragment-induced retina degeneration phenotype in *Drosophila*. The proteins that were found to influence the phenotype were clustered according to their physiological function. The authors found proteins which influence Htt toxicity in *Drosophila* in processes such as synaptic transmission, cytoskeletal organisation/biogenesis, signal transduction, transcription and protein degradation such as proteolysis and ubiquitin cycle (Kaltenbach et al., 2007).

In an earlier study S. Willingham and colleagues performed a genome-wide screen for Htt toxicity enhancers in yeast (Willingham et al., 2003). For the screen they used yeast deletion strains which were transformed with a cDNA construct encoding a Htt exon 1 fragment with 53 glutamines. The screen was quantified by assaying growth of the particular yeast strains. The authors clustered the identified toxicity enhancers in three functionally related categories such as a) stress response,

including oxidative, osmotic and nitrosative stress, b) protein folding and c) ubiquitin-dependent protein catabolism (Willingham et al., 2003).

In 2004 E. Nollen and colleagues performed a genome wide RNA screen to identify genes that - when suppressed - prevent aggregate formation of a YFP-fusion protein containing an elongated polyQ region in *C. elegans*. The effect of the silencing was analyzed using fluorescence microscopy and FRAP (fluorescence recovery after photo bleaching) analysis (Nollen et al. 2004). The modifiers which were identified to suppress aggregation were categorized by the authors into five major classes: modifiers which are involved in a) RNA metabolism, such as RNA synthesis and splicing, b) protein synthesis, including transcription initiation, elongation and ribosomal organisation, c) protein folding, in which proteins like chaperonins, Hsp70 and DnaJ were found, d) protein degradation, represented by members of the ubiquitin-proteasome system and e) trafficking processes such as vesicle and nuclear import and cytoskeletal dynamics (Nollen et al. 2004).

Some of the functional processes identified to influence toxicity and aggregation of polyQ proteins overlap between the several screens such as protein folding and degradation, including members of the chaperone system and the ubiquitin-proteasome pathway (Nollen et al., 2004; Willingham et al., 2003; Kaltenbach et al., 2007; Bilen and Bonini 2007; Giorgini et al., 2005; Kazemi-Esfarjani and Benzer, 2000; Doumanis et al., 2009). Modifiers are often involved in transcriptional processes and protein biosynthesis (Giorgini et al., 2005; Nollen et al., 2004; Kaltenbach et al., 2007) as well as in protein transport (Kaltenbach et al., 2007; Kazemi-Esfarjani and Benzer, 2000; Nollen et al., 2004; Giorgini et al., 2005). Moreover, proteins which act in RNA metabolism processes such as splicing or RNA synthesis have been identified as modifiers of polyQ toxicity and aggregation (Doumanis et al., 2009; Nollen et al., 2004; Bilen and Bonini, 2007).

1.6 Aim of the study

The aim of my project is to find proteins that influence Htt-induced cytotoxicity and to link the identified modifiers to the intracellular processes which are affected by mutant Htt expression. By analyzing these processes additional insight in the molecular pathways being influenced by mutant Htt can be gained. This should reveal a deeper understanding of the mechanisms by which mutant Htt-induced toxicity develops.

First, an RNAi screening assay will be developed and optimized in a mammalian cell culture system. Second, a set of 200 suggested modifier proteins will be tested on their influence on mutant Htt-induced caspase activation.

Following the RNAi screen the main focus of my study will be to investigate both, the mechanical effect of DDX24, identified as a novel modulator of mutant Htt-induced cytotoxicity, as well as the relation between DDX24 and its interaction partners to understand the functional role of DDX24 in cytotoxicity and apoptosis in HD.

Chapter 2

Results

2.1 RNAi screen to identify protein modulators of mutant Htt-induced cytotoxicity

2.1.1 Screening for modulators of Htt-induced cytotoxicity in a neuroblastoma cell line

The expression of mutant Htt with a pathogenic polyQ sequence leads to cellular dysfunction, cytotoxicity and neurodegeneration, mainly as a consequence of a toxic gain-of-function of the Htt protein (Landles and Bates, 2004). This has been demonstrated in a variety of HD models such as yeast, mammalian cells, *Caenorhabditis elegans*, *Drosophila* and transgenic mice (Hickey and Chesselet, 2003; Zoghbi and Botas, 2002; Driscoll and Gerstbrein, 2003). Previous studies have shown that the expression of mutant Htt interferes with a variety of intracellular pathways such as transcriptional activation and co-activation (Boutell et al., 1999; Steffan et al., 2000; Dunah et al., 2002), mitochondrial energy metabolism (Browne et al., 1997; Panov et al., 2002), axonal transport (Gunawardena et al., 2003), receptor-mediated signaling pathways such as JUN, ERK, MAPK or AKT (Perrin et al., 2009; Apostol et al., 2006; Colin et al., 2005; Ribeiro et al., 2010; Liévens et al., 2008), vesicle trafficking (Velier et al., 1998; Qin et al., 2004) and neurotransmitter secretion (Kaltenbach et al., 2007). In addition, it was demonstrated that proteins involved in protein degradation (Venkatraman et al., 2004; Holmberg et al., 2004), folding, metabolism (Willingham et al., 2003; Giorgini et al., 2003; Nollen et al., 2004) and apoptosis (Aiken et al., 2004; Kaltenbach et al., 2007) modulate the toxicity of mutant Htt.

To find proteins that modulate mutant Htt-induced cytotoxicity 200 proteins (“p200”) were selected based on literature information about biological processes that influence HD pathogenesis (for a recent review see van Ham et al., 2009). A gene ontology (GO) analysis of the target protein selection is presented in Figure 2.1. The potential modifiers are involved in cellular processes such as apoptosis and cell death, cell cycle/cell division, cell development, extracellular communication, intracellular signaling, stress response, protein degradation, transport, to mention some examples (Figure 2.1). The complete list of target proteins can be found in the Appendix.

Results

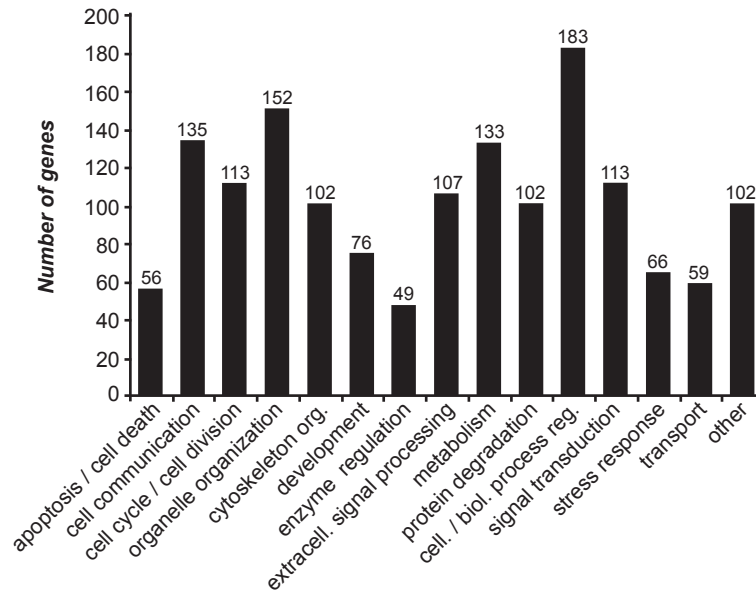


Figure 2.1: Functional analysis of the target proteins selected for the “p200”- RNAi screening

To identify modifiers of mutant Htt-induced cytotoxicity, I established an RNAi screening assay in a neuroblastoma cell line (Neuro2a). First, I tested the induction of cytotoxicity by expression of a truncated Htt protein with a pathogenic polyQ stretch. To do so, Neuro2a cells were transfected with the expression plasmid pcDNA1-HD320_Q68 coding for the protein HD320_Q68, a toxic 320 aa Htt protein containing a polyQ stretch of 68 glutamines. After incubation for 48 hours cellular toxicity was detected using a caspase-3/7 activity assay (Chapter 4.2.3). Neuro2a cells expressing the mutant Htt protein HD320_Q68 showed a significantly higher caspase-3/7 activity than cells which were not transfected with pcDNA1-HD320_Q68 plasmid (Figure 2.2).

Results

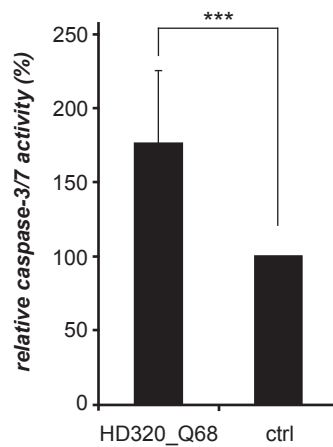


Figure 2.2: Expression of the HD320_Q68 protein induces caspase-3/7 activity in Neuro2a cells. Cells were transfected with pcDNAI-HD320_Q68 and incubated for 48 hours. Non-transfected Neuro2a cells were analyzed as controls. Caspase-3/7 activity was detected by the standard caspase assay and the activity values were normalized to the values measured in the non-transfected controls. Neuro2a cells overexpressing HD320_68Q protein show induced caspase-3/7 activation compared to the non-transfected controls ($p < 0.001$, $n = 8$).

The expression of the HD320_Q68 protein was confirmed by SDS-PAGE and immunoblotting (Figure 2.3). Neuro2a cells were transfected with the expression plasmid pcDNAI-HD320_Q68 and after 48 hours total cell lysates were analyzed. The overexpressed HD320_Q68 protein migrating at ~ 65 kDa was detected by Western blotting using an anti-Htt CAG53b antibody.

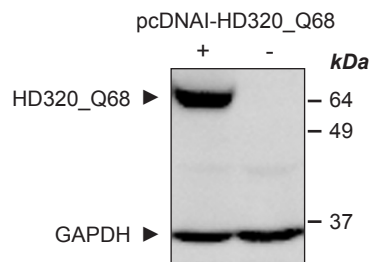


Figure 2.3: Expression of the protein HD320_Q68 in Neuro2a cells. The HD320_Q68 protein expression was analyzed 48 hours after transfection of Neuro2a cells with pcDNAI-HD320_Q68 by separating 30 μ g total protein on SDS-PAGE and detection of HD320_Q68 by Western blotting. The mutant Htt protein was detected with the CAG53b antibody.

In the next step, I performed siRNA-mediated knock-down experiments for selected target proteins as a proof of concept. Therefore, Neuro2a cells were transfected with 0.2 μ g pcDNAI-HD320_Q68 and 2.5 pmol of specific siRNA pools targeting p53 (siTP53) selected as an activator of caspase-3/7 and profilin1 (siPFN1) serving as a repressor of caspase-3/7 activity. Controls were transfected with the non-targeting siRNA siGLOred. The cells were incubated for 48 hours, followed by detection of the caspase-3/7 activity using the standard caspase assay. The relative caspase activity

Results

was quantified by normalizing the activity values of the HD320_Q68 expressing cells transfected with the specific siRNA pools to the control cells expressing HD320_Q68 and transfected with siGLOred control RNA. Figure 2.4 A demonstrates that in Neuro2a cells transfected with p53 specific siRNA pools the caspase-3/7 activity is increased, whereas in cells treated with siRNA pools targeting profilin1 a reduction of HD320_Q68 induced caspase-3/7 activity was observed. The silencing of the target proteins in Neuro2a cells was confirmed by analysis of the protein levels in total cell extracts of cells transfected with siRNA pools specifically targeting p53 and profilin1 mRNAs. Total extracts of Neuro2a cells were prepared 48 hours after transfection, and 30 μ g protein were separated by 12.5% SDS-PAGE and blotted on nitrocellulose. Intracellular levels of target proteins were detected using anti-p53 and anti-profilin1 antibodies (Figure 2.4 B).

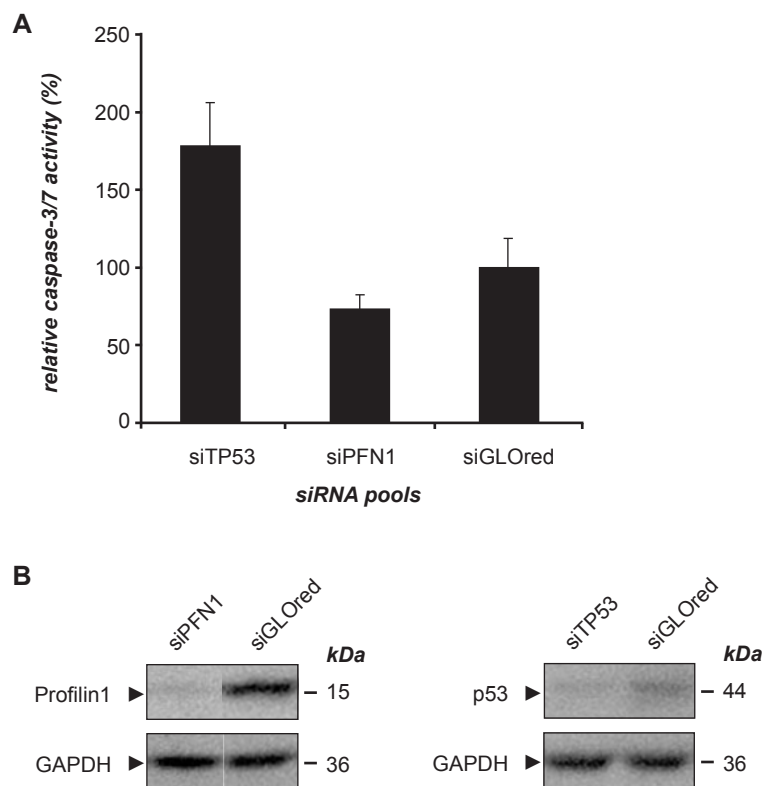


Figure 2.4: Proof of concept experiments for the RNAi screening assay. Neuro2a cells were transfected with pcDNAI-HD320_Q68 and specific siRNA pools targeting p53 or profilin1 mRNA and incubated for 48 hours. (A) Caspase-3/7 activity levels were monitored using the standard caspase-3/7 assay. The relative activity values were normalized to cells transfected with pcDNAI-HD320_Q68 and control siRNA siGLOred. Protein knock-down of the positive control p53 resulted in an increased caspase-3/7 activity, while the silencing of profilin1 resulted in a reduced caspase-3/7 activity. (B) Analysis of the siRNA-mediated knock-down of p53 and profilin1 in 30 μ g total protein from Neuro2a cell extracts containing HD320_Q68 after incubation for 48 hours. Total lysates were analyzed by SDS-PAGE and Western blotting. Endogenous proteins were detected using anti-p53 and anti-profilin1 antibodies.

Next, I performed the RNAi screening in order to identify target proteins which modulate mutant Htt-induced toxicity by either acting as toxicity suppressors or as toxicity enhancers. The definition

Results

of the target proteins depends on their effect on HD320_Q68 induced caspase-3/7 activity. siRNA down-regulated proteins, which increased HD320_Q68 induced caspase-3/7 activity by a factor of more than 1.3 were defined as toxicity suppressors, while down-regulated proteins which had the opposite effect and reduced caspase-3/7 activity by more than a factor of 0.8 were defined as toxicity enhancers. Figure 2.5 schematically shows how potential toxicity suppressors and enhancers are defined by RNAi screening.

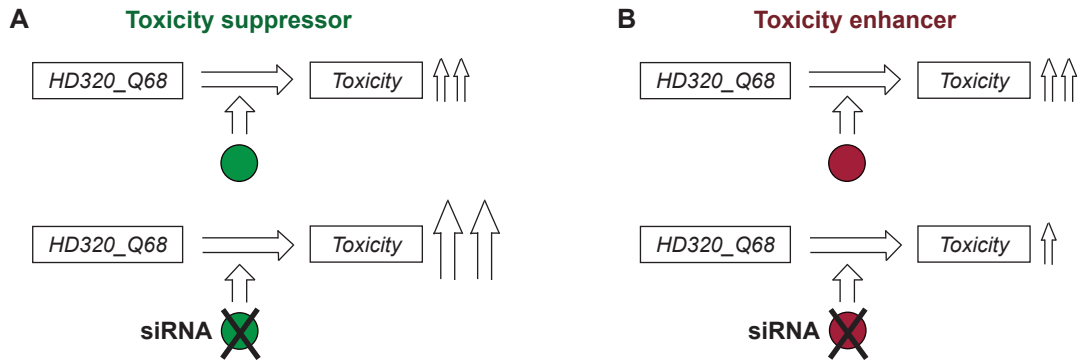


Figure 2.5: Definition of toxicity suppressors and toxicity enhancers. (A) A target protein is defined as a toxicity suppressor when its knock-down increases mutant Htt-induced toxicity. (B) A target protein is regarded as a toxicity enhancer when its knock-down reduces mutant Htt-induced toxicity.

For the screening, Neuro2a cells seeded in 96 well microtiter plates were co-transfected with 0.2 μ g of pcDNAI-HD320_Q68 and 2.5 pmol of target specific siRNA pools according to the protocol described in Chapter 4.2.3. The samples were incubated for 48 hours allowing silencing of the target protein and expression of HD320_Q68 protein which induces cytotoxicity. The effect of the siRNA treatment on HD320_Q68 induced toxicity then was detected using the standard caspase-3/7 activity assay. Screening data were evaluated using two types of controls, 1) cells transfected with siRNA pools without Htt expression (control 1) and 2) cells expressing HD320_Q68 but were not transfected with siRNA pools (control 2, Diagram 2.1). In all samples caspase-3/7 activity was monitored in an 1 hour kinetic measurement recording caspase-3/7 activity signals every 5 min. For quantification of the relative caspase-3/7 activity the slopes of the kinetic curves were determined between 20 - 60 min of the kinetic and the slope value was regarded as a measure for the relative caspase-3/7 activity in the cells. The analytical process by which target proteins were analyzed and classified into toxicity suppressors and toxicity enhancers is explained in Diagram 2.1.

Results

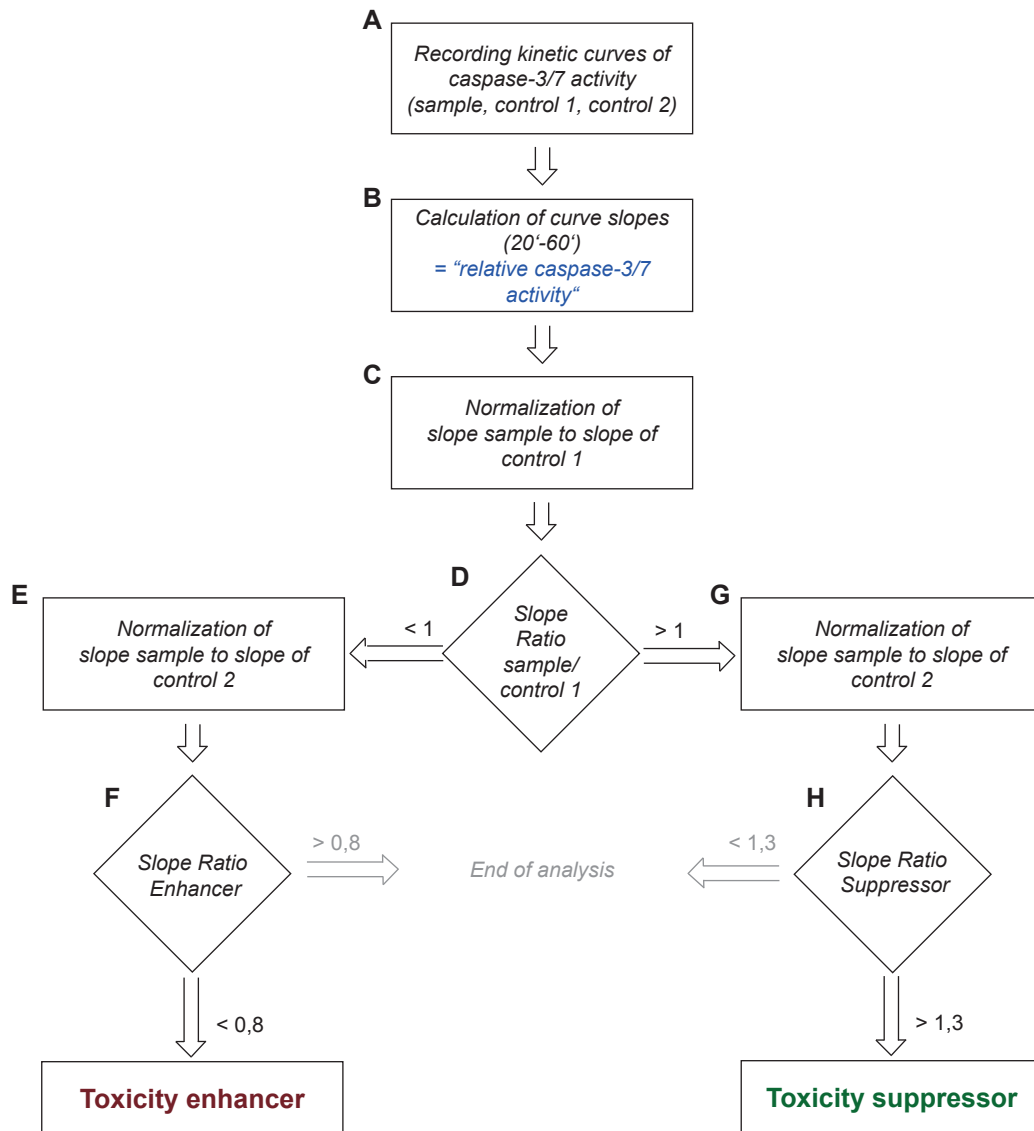


Diagram 2.1: Analysis of the screening results - classification procedure for the identification of toxicity suppressors and toxicity enhancers. (A) Detection of the absolute caspase-3/7 activity signals in a kinetic measurement. The fluorescence representing caspase activity was recorded every 5 min over a time of 1 hour in samples treated with pcDNAI-HD320_Q68 and siRNA pools (referred to as "sample") as well as in the control only transfected with siRNA pools (referred to as "control 1") and the control only treated with pcDNAI-HD320_Q68 (referred to as "control 2"). (B) Calculation of the activity curve slopes between time points 20 min and 60 min. The slopes of the kinetic curves are regarded as a measurement of the relative caspase-3/7 activity within the particular sample or control. (C) Normalization of the sample slopes to the slopes of control 1. This step compares the effect of the target protein knock-down on caspase-3/7 activity in the presence of mutant Htt with the effect of the siRNA-mediated protein silencing alone. This first normalization step reveals the slope ratio of the particular sample and its corresponding control 1. (D) Based on the values of the "slope ratio sample/control 1" target proteins are divided into two groups. Samples that show higher caspase-3/7 activity than the corresponding control 1 reveal a slope ratio > 1.0 and are regarded as potential toxicity suppressors. Samples that have a lower slope than their control 1 reveal a slope ratio of < 1.0 and are classified as potential toxicity enhancer. In the next step, a second normalization is made. (E) & (G) This normalization step

Results

compares the relative caspase-3/7 activity of the sample ("sample slope") with the relative activity obtained in control 2 ("slope of control 2") to determine whether the target protein enhances or reduces the mutant Htt-induced toxicity. (F) Specification of "toxicity enhancers": the slope of samples that revealed a slope ratio (sample/control 1) < 1 is normalized to the slope of control 2 revealing a value termed "slope ratio enhancer". If this value (sample/control 2) is < 0.8 the target protein silenced in the sample is defined as a "toxicity enhancer". If the value is > 0.8 the sample is excluded from the group of potential toxicity enhancers. (H) Specification of toxicity suppressors: the sample slope of samples which revealed a slope ratio (sample/control 1) > 1 in step (D) is normalized to the slope of the control 2. If the obtained value ("slope ratio suppressor") is > 1.3 the target protein silenced in the sample is defined as a "toxicity suppressor". Target proteins whose slope ratio suppressor value is < 1.3 are not followed up.

The modulator screen was repeated twice revealing 66 toxicity suppressors and 9 toxicity enhancers in the first and 18 toxicity suppressors and 24 toxicity enhancers in the second round. Two additional subset screens were performed, the first one silencing a set of 45 target proteins revealing 10 toxicity enhancers and 2 suppressors. The second subset screen consisting of 23 targets resulted in 2 toxicity enhancers and 3 toxicity suppressors. A general overview of the screenings showing the hit target proteins identified in the particular screens can be found in the Appendix. 18 target proteins were found as hits in at least two of the screens. For these targets I calculated the average fold-change of HD320_Q68 induced toxicity and classified them according to the standard definitions. Target proteins whose knock-down revealed a change in mutant Htt-induced caspase-3/7 activity > 1.3 were defined as toxicity suppressors, while knock-down of target proteins reducing toxicity to < 0.8 were referred to as toxicity enhancers as described in Diagram 2.1. After this calculation step 13 proteins remained as final set of toxicity modifiers, which were identified in at least two separate screens. Seven of the modifiers were defined as toxicity suppressors, whereas six modifiers were classified as toxicity enhancers. These modifiers can be clustered into several functional groups such as cell cycle and cell division, cytoskeletal organization and biogenesis, signal transduction, synaptic transmission, RNA-metabolism and regulation of transcription (Tables 2.1 and 2.2).

Results

Table 2.1: Target proteins identified as toxicity suppressors

Toxicity suppressors

Symbol Gene-ID	Protein name	Biological process	Functional information	Avg (Stdev)	Number of Posi- tives
MAD2L1 4085	Mitotic spindle as- sembly checkpoint protein MAD2A	Cell cycle, cell division, mitosis	Component of the spindle-assembly checkpoint; required for the execution of the mitotic checkpoint; inhibits the activity of the anaphase promoting complex	1.59 (0.22)	3
IMMT 10989	Mitochondrial inner membrane protein	Mitochondria maintenance	Component of the mitochondrial inner membrane; suggested to play a role in protein import related to maintenance of mitochondrial structure, regulation of mitochondrial morphology	1.71 (0.27)	3
TARBP1 6894	TAR (HIV-1) RNA binding protein 1	RNA processing, transcription regulation	Probable S-adenosyl-L-methionine-de- pendent methyltransferase; methylates RNA molecules such as tRNAs	2,58 (0,47)	3
SQSTM1 8878	Sequestosome-1	Apoptosis, differentiation, immune response	Binds ubiquitin as an adapter protein binding, regulates activation of NFKB1 by TNF-alpha, nerve growth factor (NGF) and interleukin-1; involved in titin/TTN downstream signaling in muscle cells; regulates signaling cascades through ubiquitination; in- volved in cell differentiation, apoptosis (anti-apoptotic), immune response and regulation of K+ channels	1.43 (0.09)	2
TARBP2 6895	RISC-loading complex subunit TARBP2 (TAR (HIV-1) RNA binding protein 2)	RNA-mediated gene silencing, translation regula- tion	Required for formation of the RNA induced silencing complex (RISC)	1.83 (0.29)	2
ARPC1B 10095	Actin-related pro- tein 2/3 complex subunit 1B	Cellular compo- nent movement, regulation of actin filament polymerization	Regulates actin polymerization; mediates the formation of branched actin networks	2.18 (0.06)	2
NR4A1 3164	Nuclear receptor subfamily 4 group A member 1	Transcription regulation, signal transduction	Member steroid-thyroid hormone-reti- noid receptor superfamily; orphan receptor	3,29 (0.42)	2

Results

Table 2.2: Target proteins identified as toxicity enhancers

Toxicity enhancers

Symbol Gene-ID	Protein name	Biological process	Functional information	Avg (Stdev)	Number of Posi- tives
PFN2 5217	Profilin-2	Regulation of actin polymerization/depolymerization, actin cytoskeleton organization	Binds to actin and affects the structure of the cytoskeleton; prevents the polymerization of actin at high concentrations and enhances it at low concentrations	0.36 (0.12)	3
RNF146 81847	RING finger protein 146	Unknown	Suggested to function early in the progression of Alzheimer's disease (v. Rotz et al., 2005)	0.58 (0.07)	3
CEP1 11064	Centriolin (Centrosomal protein 110 kDa)	Cell cycle, cell division	Acts in cell cycle progression and cytokinesis; anchors exocyst and SNARE complexes at the midbody, allowing secretory vesicle-mediated abscission	0.60 (0.05)	3
DDX24 57062	DEAD-box protein 24	Unknown, putative RNA helicase	- not available -	0.72 (0.07)	3
MAP3K11 4296	Mitogen-activated protein kinase kinase kinase 11	G1 phase of mitotic cell cycle, activation of JUN kinase activity, cell proliferation, cell death, protein amino acid autophosphorylation, protein oligomerization	Activates the JUN N-terminal pathway; required for serum-stimulated cell proliferation and for mitogen and cytokine activation of MAPK14 (p38), MAPK3 (ERK) and MAPK8 (JNK1) (MAP kinase pathway); influences microtubule organization during the cell cycle	0.61 (0.05)	2
SH3GL1 6455	Endophilin-A2	Central nervous system development, endocytosis Signal transduction	Implicated in endocytosis	0.70 (0.03)	2

Interestingly, I found modifiers involved in all functional groups acting as toxicity suppressors as well as toxicity enhancers. The mitochondrial inner membrane protein (IMMT) which I identified as a toxicity suppressor was previously found in pull-down screens as an interactor of Htt (Kaltenbach et al., 2007). Two modifiers, the mitotic spindle assembly checkpoint protein MAD2A (MAD2L1) and centriolin (CEP1) are involved in cell cycle and cell division (Li and Benezra, 1996;

Results

Gromley et al., 2003). The MAD2L1 gene product was identified as a toxicity suppressor, while centriolin was defined as an enhancer of toxicity. Besides its function in the cell cycle the centriolin protein was demonstrated to be involved in vesicle secretion modulating SNARE-mediated vesicle fusion (Gromley et al., 2005). A study published by L. Kaltenbach and colleagues demonstrated SNARE components to influence mutant Htt toxicity (Kaltenbach et al., 2007). The protein ARPC1B (actin-related protein 2/3 complex subunit 1B), which was defined as a toxicity suppressor and PFN2 (profilin-2), a toxicity enhancer, both play a role in cytoskeletal organization by regulating actin polymerization (Welch et al., 1997; Gieselmann et al., 1995). Profilin-2 was recently demonstrated to directly interact with Htt and to inhibit aggregate formation, suggesting a role in HD pathogenesis (Shao et al., 2008). Other modifier proteins found in the screen are involved in signal transduction such as SQSTM1 (sequestosome-1), NR4A1 (nuclear receptor subfamily 4 group A member 1), MAP3K11 (mitogen-activated protein kinase kinase kinase 11) and SH3GL1 (endophilin-A2). Sequestosome-1 is a ubiquitin binding protein involved in NF-kappaB signaling (Table 2.1) and was found to accumulate in neurofibrillary tangles and Lewy bodies in neurons of patients with Alzheimer's and Parkinson's disease, respectively (Zatloukal et al., 2002). NR4A1 is a member of the steroid receptor family and recent studies have demonstrated functional impaired of steroid receptors in HD (Hoon, 2006; Schiffer et al., 2008; Chandra et al., 2008). Endophilin-A2 and MAP3K11 were both identified as toxicity enhancers. A study by M. Ralser and colleagues has demonstrated that members of the endophilin family directly interact with Htt modulating its cellular toxicity in yeast (Ralser et al., 2005). MAP3K11 can be linked to HD pathogenesis via its function in the JUN N-terminal pathway that is implicated in Htt toxicity (Liu et al., 2000; Merienne et al., 2003; Perrin et al., 2009; Table 2.2).

One interesting subset of modifiers DDX24, TARBP1 and TARBP2 are proteins involved in RNA-metabolism. The two TARBP proteins regulate transcriptional processes on RNA level by regulation of RNA polymerase II function and siRNA-mediated gene silencing (Wu-Baer et al., 1995; Gatignol et al., 1991; Haase et al., 2005). TARBP2 regulates PKR (translation initiation factor 2-alpha kinase 2) activation which is increased in HD and other neurodegenerative disorders contributing to transcriptional dysregulation and extrastriatal degeneration (Peel et al., 2001; Peel, 2004; Bando et al., 2005). Two proteins of the identified modulators, DDX24 and RING finger protein 146 (RNF146), have unknown functions. RNF146 has been found to be upregulated in brains of AD patients (von Rotz et al., 2005). However, only little is known about DDX24, a member of the DEAD-box protein family and a putative RNA helicase (Zhao et al., 2000). The cellular function of DDX24 is still undetermined and previous studies were predominantly limited to structural analysis of the protein (see Chapter 1.4.1). The limited knowledge about DDX24 prompted me to examine its role in Htt-induced apoptosis signaling in more detail.

2.2 Investigation of siRNA-mediated DDX24 protein knock-down in a HD PC12 cell model

2.2.1 Analysis of HD PC12 cell lines expressing Htt25Q-EGFP or Htt103Q-EGFP fusion proteins

To confirm and expand the results obtained in the Neuro2a cells siRNA knock-down experiments for DDX24 were performed in inducible PC12 cell lines expressing EGFP-tagged Htt exon 1 fusion proteins with either 25 or 103 glutamines (Apostol et al. 2003; Figure 2.6) after induction with muristerone. Previous studies have demonstrated that Htt103Q-EGFP forms insoluble aggregates and induces caspase-3/7 activity in PC12 cells, while the protein Htt25Q-EGFP is soluble and does not induce cellular toxicity (Apostol et al., 2003; 2006).

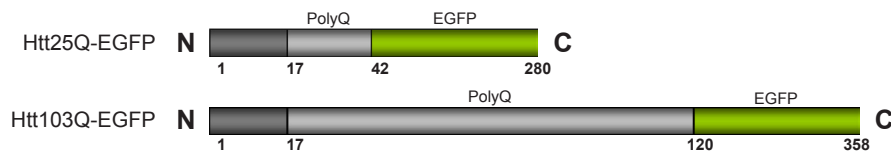


Figure 2.6: Schematic overview of the recombinant proteins Htt25Q-EGFP and Htt103Q-EGFP. The proteins consist of a truncated exon 1 containing the first 17 aa of the Htt protein and either 25 or 103 glutamines. Both Htt proteins are fused to a C-terminal EGFP epitope tag.

First, I investigated whether the expression of the recombinant proteins Htt25Q-EGFP and Htt103Q-EGFP was induced by addition of 2.5 μ M muristerone to the medium. Cell lysates were prepared 48 hours after induction and 30 μ g protein were analyzed by SDS-PAGE followed by Western blotting. The expression of the fusion proteins was detected on the blot by incubation with the CAG53b antibody. I found that the proteins Htt25Q-EGFP and Htt103Q-EGFP migrating at \sim 35 and 65 kDa, respectively, are produced in PC12 cells under the conditions used (Figure 2.7).

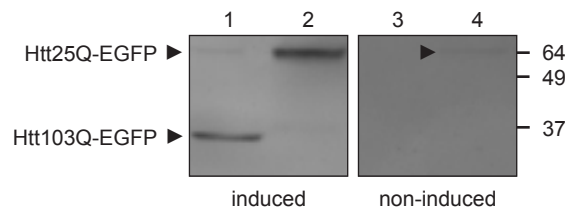


Figure 2.7: Expression of the Htt25Q-EGFP and Htt103Q-EGFP proteins after induction with 2.5 μ M muristerone for 48 hours. Cell extracts were prepared and 30 μ g of total protein were separated by 12.5% SDS-PAGE and analyzed by Western blotting. The Htt protein variants were detected using the CAG53b antibody.

Next, I analyzed whether the Htt103Q-EGFP protein expressed in PC12 cells forms insoluble aggregates, while Htt25Q-EGFP remains soluble as described before in the literature (Apostol et al., 2003) by performing a filter retardation assay (Scherzinger et al., 1997). PC12 cells were

Results

induced for the expression of the recombinant proteins Htt25Q-EGFP and Htt103Q-EGFP and incubated for 72 hours. Cell samples were harvested at time points of 24, 48 and 72 hours. Cells were lysed in standard lysis buffer and increasing amounts of total cell extracts were filtered through a cellulose acetate membrane. To detect Htt103Q-EGFP aggregates on the membrane surface, the filter was exposed to UV light (460 nm), which is able to excite the fluorescent EGFP-tag of the Htt fusion proteins (Figure 2.8 A). The fluorescence signal was detected in a photo imager and subsequently analyzed with the AIDA quantification software (Figure 2.8 B). In PC12 cells expressing Htt103Q-EGFP aggregate formation was detected after 24 hours. However, such structures were not detected in cells expressing the Htt25Q-EGFP protein. Besides the detection by their fluorescent EGFP-tag Htt103Q-EGFP aggregates can also be detected on the filter by incubation of the membrane with the CAG53b antibody as shown in Figure 2.8 C for PC12 cells, which were incubated with muristerone for 48 hours expressing Htt25Q-EGFP or Htt103Q-EGFP.

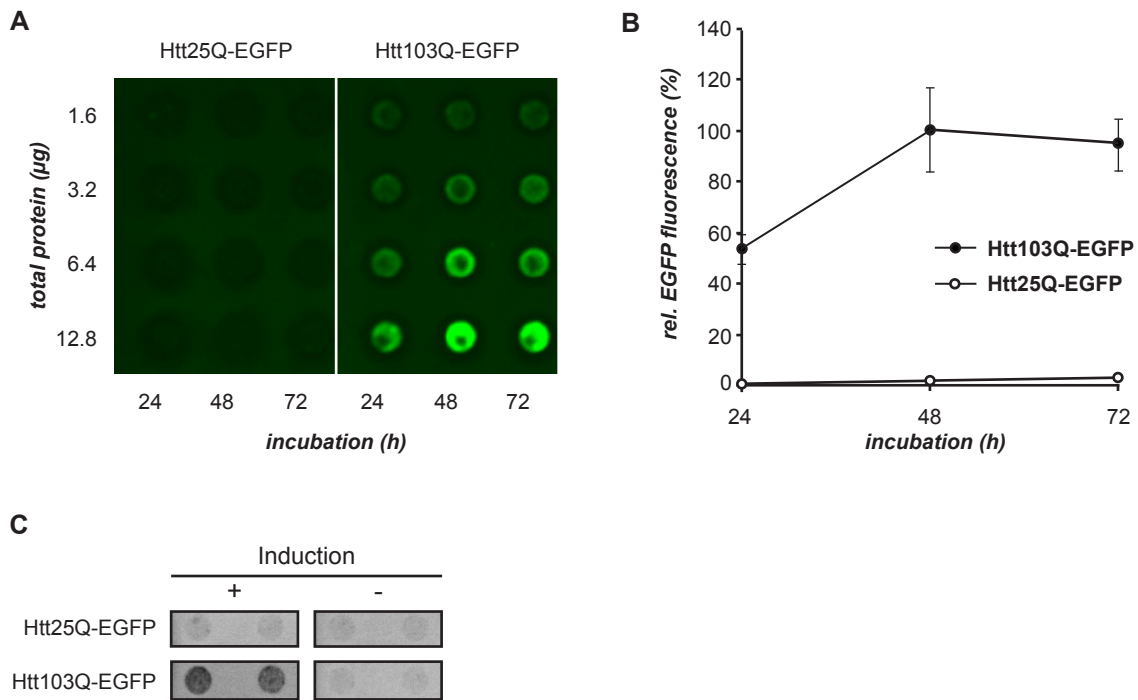


Figure 2.8: Detection of the proteins Htt103Q-EGFP and Htt25Q-EGFP in PC12 cells. (A) Analysis of aggregates in total cell lysates (1% NP-40 in standard lysis buffer) from PC12 cells expressing Htt103Q-EGFP or Htt25Q-EGFP by native filter retardation assay after induction with 2.5 μM muristerone for 24, 48 and 72 hours. Aggregates formed by Htt103Q-EGFP were detected by exposure of the membrane to 460 nm UV light. Cell extracts from PC12 cells expressing Htt25Q-EGFP revealed no aggregates on the filter membrane. (B) Quantification of the native filter retardation assay shown in (A). (C) Detection of Htt aggregates in cell lysates of Htt25Q-EGFP and Htt103Q-EGFP expressing PC12 cells by immunostaining. Cells were induced with muristerone for 48 hours, lysed and 7.5 μg of total protein was filtered through a cellulose acetate membrane. The recombinant Htt fusion proteins were detected by incubation of the membrane with the CAG53b antibody.

Results

Furthermore, the recombinant Htt fusion proteins are visible under the fluorescence microscope (Figure 2.9). To detect overexpressed Htt25Q-EGFP and Htt103Q-EGFP proteins PC12 cells were induced with 2.5 μ M muristerone. After 72 hours cells were fixed with 4% paraformaldehyde and cell nuclei were stained with DAPI. I found that PC12 cells expressing Htt25Q-EGFP showed a diffuse green fluorescence in the cytoplasm, while in cells expressing Htt103Q-EGFP bright green inclusions with aggregates were visible (left panels). As a control both cell lines were analyzed without addition of muristerone. In these cells no green fluorescence was observed (right panels).

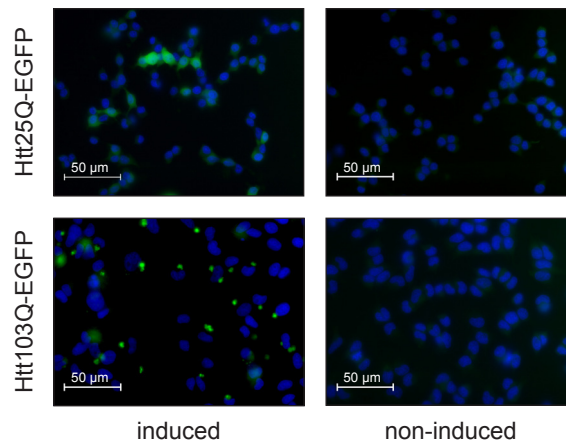


Figure 2.9: Fluorescence microscopy analysis of Htt25Q-EGFP and Htt103Q-EGFP expression in PC12 cells. PC12 cells were induced for expression of the Htt fusion proteins for 72 hours (induction by 2.5 μ M muristerone) and fixed with paraformaldehyde. Cell nuclei were stained with DAPI; the proteins Htt25Q-EGFP and Htt103Q-EGFP are visualized by their fluorescent EGFP-tag (Ex470 nm/Em525nm) Exposure times: Htt25Q-EGFP induced 25 ms, Htt25Q-EGFP non-induced 968 ms, Htt103Q-EGFP induced 14 ms, Htt103Q-EGFP non-induced 2324 ms.

To investigate the effect of the overexpression of Htt25Q-EGFP and Htt103Q-EGFP on activation of caspase-3/7, PC12 cells were induced with 2.5 μ M muristerone to allow expression of the Htt fusion proteins. After 48 hours of induction the activity of intracellular caspase-3/7 was determined using a standard assay (Figure 2.10 A). PC12 cells expressing the Htt103Q-EGFP protein showed a significant increase in caspase-3/7 activity compared to the non-induced control cells which do not express Htt103Q-EGFP. In PC12 cells which express Htt25Q-EGFP the caspase-3/7 activity levels do not differ from the non-induced control cells.

In the same experiment I further tested whether Htt103Q-EGFP and Htt25Q-EGFP protein expression in PC12 cells induces activation of caspase-8. To detect caspase-8 activity the standard caspase-8 assay was performed (Chapter 4.2.3). PC12 cells expressing Htt103Q-EGFP showed increased activity of caspase-8 compared to the non-induced controls, while in cells expressing Htt25Q-EGFP the activity is comparable to the non-induced cells and very low (Figure 2.10 B).

Results

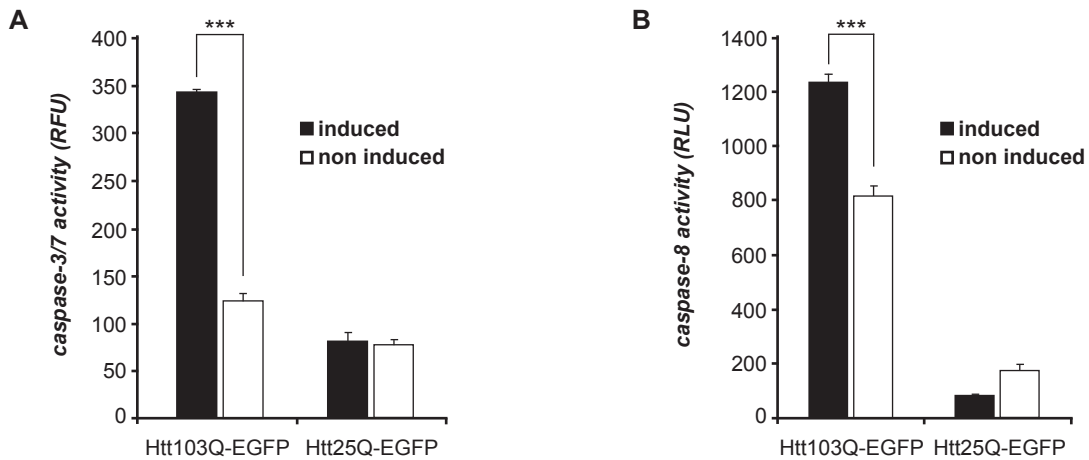


Figure 2.10: Quantification of caspase-3/7 and -8 activities in PC12 cells expressing the proteins Htt103Q-EGFP or Htt25Q-EGFP. PC12 cells were induced with 2.5 μ M muristerone for 48 hours followed by determination of the relative caspase activity using the standard caspase-3/7 and caspase-8 assays. (A) PC12 cells expressing Htt103Q-EGFP show increased activity of caspase-3/7 compared to non-induced cells ($p < 0.001$, $n = 3$). Expression of the Htt25Q-EGFP protein did not show an effect on caspase-3/7 activation. (B) Activity of caspase-8 is increased in PC12 cells expressing Htt103Q-EGFP compared to the non-induced controls ($p < 0.001$, $n = 3$). In PC12 cells expressing Htt25Q-EGFP the caspase-8 activity levels are comparable with the corresponding negative controls which do not express Htt25Q-EGFP and are much lower than the activity detected in Htt103Q-EGFP expressing cells.

Taken together, I could show that the recombinant proteins Htt25Q-EGFP and Htt103Q-EGFP are produced in PC12 cells after induction with 2.5 μ M muristerone (Figure 2.7). Further, I confirmed the formation of Htt aggregates in cells expressing Htt103Q-EGFP protein (Apostol et al., 2003) and demonstrated that Htt25Q-EGFP is present as a soluble protein in PC12 cells (Figure 2.8 and 2.9). Additionally, the previously described activation of caspase-3/7 in cells expressing Htt103Q-EGFP was confirmed (Apostol et al., 2006) and the expression of the protein Htt25Q-EGFP was shown to not induce caspase-3/7 activity (Figure 2.10 A). I also could demonstrate the activation of caspase-8 by Htt103Q-EGFP expression in PC12 cells which has not been shown before in this HD model (Figure 2.10 B).

2.2.2 Analysis of siRNA-mediated DDX24 protein knock-down in the HD PC12 cell model

The screening on modulators of Htt-induced cytotoxicity was performed in Neuro2a cells using pools of four siRNAs targeting the mRNA of interest. In order to analyze the effects of RNAi-mediated DDX24 protein knock-down on Htt103Q-EGFP induced caspase activation I first established the optimal DDX24 protein knock-down conditions in the PC12 cell system and then verified the specificity of the siRNA-mediated DDX24 silencing. To find the optimal amount of siRNA for the knock-down in large scale cell assays I performed an siRNA titration experiment.

Results

Increasing amounts of an siRNA pool containing four types of siRNAs all targeting DDX24 mRNA were tested for their knock-down efficiency in PC12 Htt103Q-EGFP cells which did not express the Htt fusion protein. The cells were treated with 0 to 200 pmol of the siRNA pool in 6 cm cell culture dishes and incubated for 48 hours. The total RNA was isolated from the cell extracts, transcribed into cDNA as described in Chapter 4.2.1 and analyzed by quantitative real-time PCR. In two separate reactions the DDX24 mRNA levels were quantified in relation to the transcription levels of either ACTB or GAPD serving as endogenous controls. For a detailed description of the quantification procedure see Chapter 4.2.1. DDX24 mRNA levels were significantly ($p < 0.0001$) decreased in PC12 cells transfected with 50 pmol of the DDX24 siRNA pool compared to the non-transfected control cells (Figure 2.11). Similar effects were obtained with higher siRNA amounts (100 pmol and 200 pmol). The normalization of DDX24 mRNA levels to the mRNA levels of ACTB or GAPD both revealed similar results (Figure 2.11 A and B).

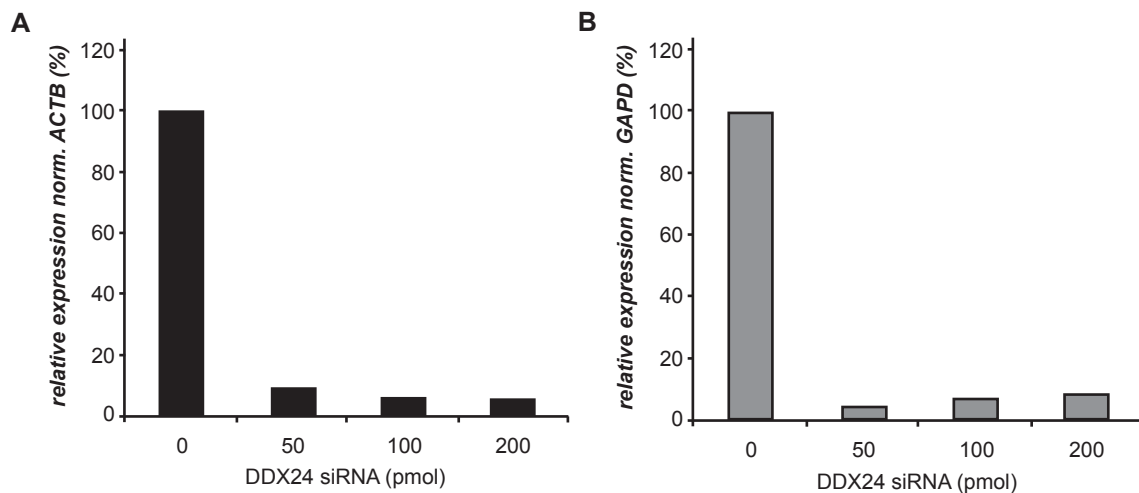


Figure 2.11: Treatment of PC12 cells with DDX24 siRNA pools reduces endogenous DDX24 mRNA levels. PC12 Htt103Q-EGFP cells were transfected with increasing amounts of siDDX24 pools and incubated for 48 h. The mRNA levels of DDX24 were analyzed by quantitative real-time PCR (qRT-PCR) normalized to (A) ACTB mRNA levels or (B) GAPD mRNA levels. All tested amounts of siRNA pools revealed a significant reduction of DDX24 mRNA levels. The most efficient reduction of mRNA levels was obtained with 50 - 100 pmol siRNA.

In the next step, I investigated the efficiency of the DDX24 protein knock-down in PC12 cells by the different siRNAs contained in the pool targeting DDX24 mRNA (siDDX24_1, siDDX24_2, siDDX24_3 and siDDX24_4). The target sequences of the particular siRNAs on the DDX24 mRNA can be found in Chapter 4.1.6. Hence, it was tested in the following experiment whether all siRNAs represented in the pool account for the DDX24 protein knock-down and how efficient the particular siRNAs reduce DDX24 protein expression. The experiments were performed in the PC12 cell lines expressing the proteins Htt103Q-EGFP or Htt25Q-EGFP, respectively. 100 pmol of each type of siRNA were used for transfection and the cells were then induced for 48 hours with 2.5 μ M muristerone. As a negative control cells transfected with 100 pmol non-targeting siGLOred siRNA were analyzed. In case of Htt103Q-EGFP expressing PC12 cells also 100 pmol of the siRNA pool

Results

containing all four types of siRNAs were transfected. After cell lysis the amount of DDX24 protein in cell extracts was analyzed by SDS-PAGE and Western blotting using an anti-DDX24 antiserum. Furthermore, the expression of the proteins Htt103Q-EGFP and Htt25Q-EGFP was confirmed with the anti-Htt CAG53b antibody; actin served as loading control (Figure 2.12 A and B). The DDX24 protein expression levels were subsequently analyzed using the AIDA quantification software (Figure 2.12 C and D). In both PC12 cell lines all four siRNAs reduced DDX24 protein levels. Transfection of cells with siDDX24_1 or siDDX24_4 revealed the most efficient reduction of DDX24 protein levels. The reduction of the DDX24 protein was less efficient in cells treated with siDDX24_2 and siDDX24_3.

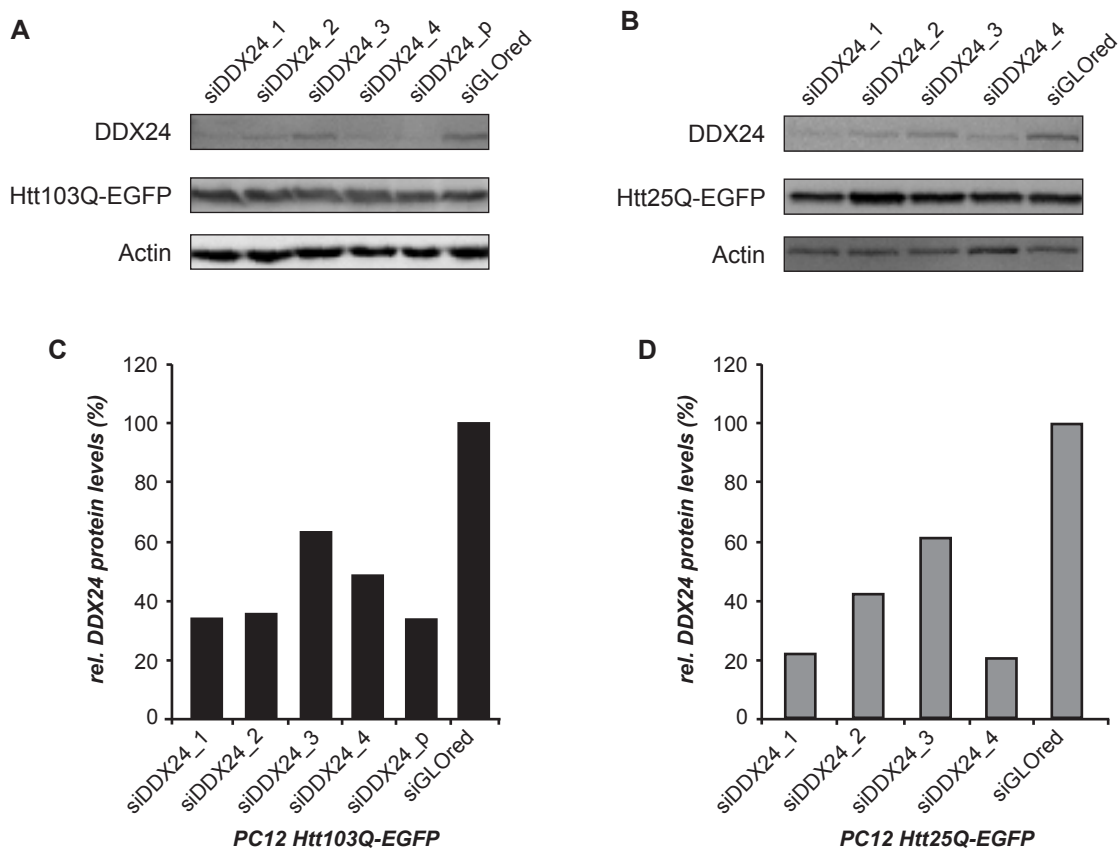


Figure 2.12: DDX24 knock-down efficiency of different DDX24 specific siRNAs. PC12 cells expressing Htt103Q-EGFP or Htt25Q-EGFP were individually transfected with 100 pmol of one type of DDX24 targeting siRNAs and incubated for 48 hours. (A) The reduction of endogenous DDX24 protein then was analyzed by SDS-PAGE and Western blotting. DDX24 was detected with an anti-DDX24 antiserum, the expression of (A) Htt103Q-EGFP and (B) Htt25Q-EGFP was visualized with the CAG53b antibody; detection of the actin protein with an anti-actin antibody served as loading control. (C) & (D) Quantification of the DDX24 protein levels by AIDA software. All tested siRNAs reduce DDX24 protein levels. The strongest reduction was detected in cells transfected with siDDX24_1 or siDDX24_4.

Next, the knock-down efficiency of the different siRNAs was quantified using real-time PCR. PC12 cells derived from the knock-down experiment described above were lysed, the total RNA

Results

was isolated as described in Chapter 4.2.1 and the amount of DDX24 mRNA was determined. The obtained DDX24 levels were related to the ACTB mRNA levels serving as an endogenous control. The relative DDX24 mRNA levels then were normalized to DDX24 mRNA levels obtained in cells transfected with siGLOred (Figure 2.13). DDX24 mRNA levels were reduced by all four DDX24-specific siRNAs. Cells transfected with the siRNAs siDDX24_1 or siDDX24_4 showed the most efficient reduction of DDX24 mRNA. The transfection with siDDX24_2 or siDDX24_3 resulted in a moderate reduction of DDX24 mRNA levels (Figure 2.13).

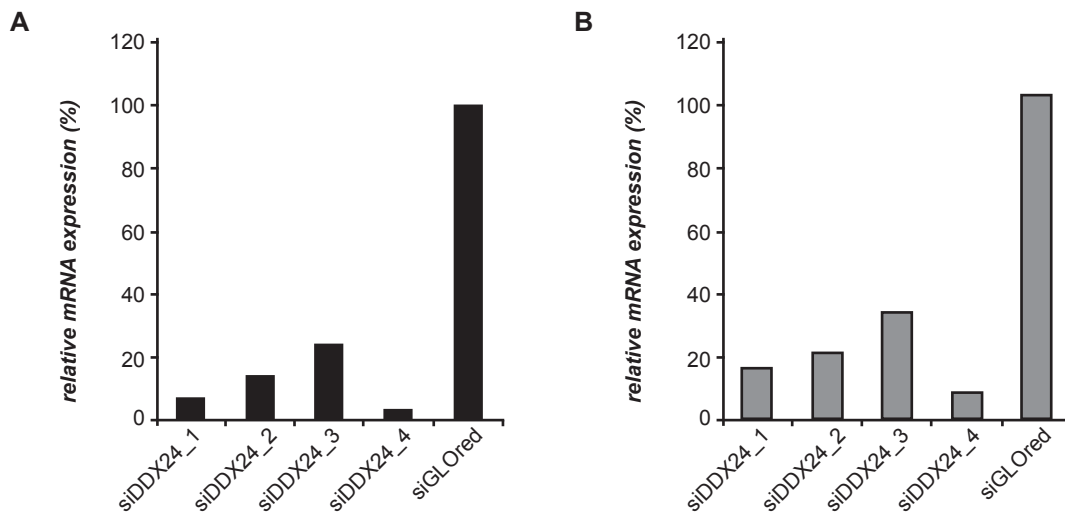


Figure 2.13: Quantification of the DDX24 knock-down by real-time PCR analysis. PC12 cells expressing (A) Htt103Q-EGFP or (B) Htt25Q-EGFP were treated with 100 pmol of DDX24-specific siRNAs. After incubation for 48 hours total RNA was isolated and the amount of endogenous DDX24 mRNA was analyzed by quantitative real-time PCR using ACTB for normalization. All siRNAs tested were able to reduce DDX24 mRNA levels. However, the most efficient reduction was obtained in cells transfected with siDDX24_1 or siDDX24_4.

2.2.3 Endogenous DDX24 protein silencing enhances mutant Htt-induced caspase-3/7 activity

To investigate whether DDX24 knock-down in PC12 cells reduces mutant Htt-induced toxicity similar to Neuro2a cells (Chapter 2.1.1), I performed additional RNAi experiments. PC12 cells overexpressing Htt103Q-EGFP protein (induction by 2.5 μ M muristerone) were transfected with a mix of siDDX24_1 and siDDX24_4 or with non-targeting siRNA siGLOred. As a second negative control cells were treated with carrier DNA only. Following 48 hours of incubation caspase-3/7 activity was monitored using the standard assay (Chapter 4.2.3). In addition, for each sample the number of cells was quantified. Non-induced cells, which only express very low amounts of Htt103Q-EGFP protein, were also assayed for their caspase-3/7 activity. Caspase activity signals were normalized to the signals detected in Htt103Q-EGFP expressing cells treated with siGLOred

Results

siRNA. Interestingly, I found that endogenous DDX24 silencing dramatically increased (~3-fold) the caspase-3/7 activity in Htt103Q-EGFP expressing cells, but not in non-induced cells expressing low levels of the Htt protein (Figure 2.14).

This finding is conflicting with the result obtained with the Neuro2a cells where DDX24 appeared to be a toxicity enhancer (Chapter 2.1.1). Likely, the discrepancy can be attributed to normalization of the caspase activity to total cell numbers. In the screen the caspase activity was not normalized to cell numbers, harboring the danger that modulators whose protein knock-down itself is very toxic are wrongly identified as toxicity enhancers. This occurs if the knock-down of a toxicity suppressor is extremely toxic to the cells resulting in high rates of apoptosis and a reduction in the number of cells in the particular well. The loss of cells results in a low overall activity signal, although each cell may have drastically enhanced caspase activity. To circumvent this problem all larger scale knock-down experiments performed in PC12 cells were carefully controlled for cell density. These experiments revealed the induction of caspase activity by DDX24 knock-down. This indicates that DDX24 indeed is a potential modulator of mutant Htt-induced cytotoxicity. However, it functions as a toxicity suppressor rather than as a toxicity enhancer as assumed from the Neuro2a screen.

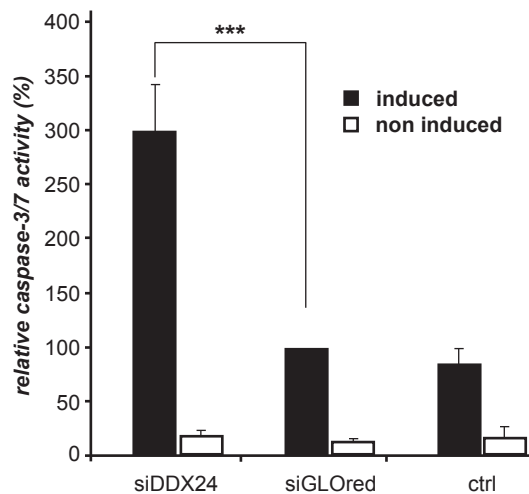


Figure 2.14: Silencing of endogenous DDX24 protein enhances mutant Htt-induced caspase-3/7 activation. PC12 cells were transfected with siDDX24_1 and siDDX24_4 or with siGLOred control siRNA; as a second negative control cells were treated with carrier DNA only. Expression of Htt103Q-EGFP protein was induced by addition of 2.5 μ M muristerone; non-induced controls were treated with equal amounts of ethanol. The cells were incubated for 48 hours and caspase-3/7 activity was quantified using the standard assay. The relative caspase activity values were normalized to the values of induced cells transfected with siGLOred. In PC12 cells expressing large amounts of Htt103Q-EGFP protein the DDX24 knock-down resulted in a ~3-fold increased caspase-3/7 activity ($p < 0.001$, $n = 4$) compared to the activity observed in the controls treated with siGLOred. Caspase-3/7 activity levels in cells treated with siGLOred control siRNA were similar to those detected in cells treated with carrier DNA. No change in caspase-3/7 activity was detected in non-induced cells expressing very low amounts of Htt103Q-EGFP protein.

Results

To test whether the DDX24 knock-down-mediated increase in caspase-3/7 activity is dependent on Htt103Q-EGFP overexpression in PC12 cells, I also silenced DDX24 expression in PC12 cells expressing the protein Htt25Q-EGFP which does not induce caspase-3/7 activity (Figure 2.10). PC12 cells overexpressing the proteins Htt25Q-EGFP or Htt103Q-EGFP (induction with 2.5 μ M muristerone) were transfected with siDDX24_1 and _4 or the control siRNA siGLOred. As negative controls cells were treated with carrier DNA. After incubation for 48 hours caspase-3/7 activity was analyzed using the standard assay. For quantification of the caspase activity signals, I normalized the relative activity values detected in the samples to the activity values obtained in the siGLOred transfected controls. As shown in Figure 2.15, I found that in cells expressing Htt25Q-EGFP in contrast to Htt103Q-EGFP expressing cells the activity of caspase-3/7 was not increased upon DDX24 protein knock-down. This indicates that the effect of DDX24 protein knock-down on caspase-3/7 activity is dependent on the expression of a toxic mutant Htt protein.

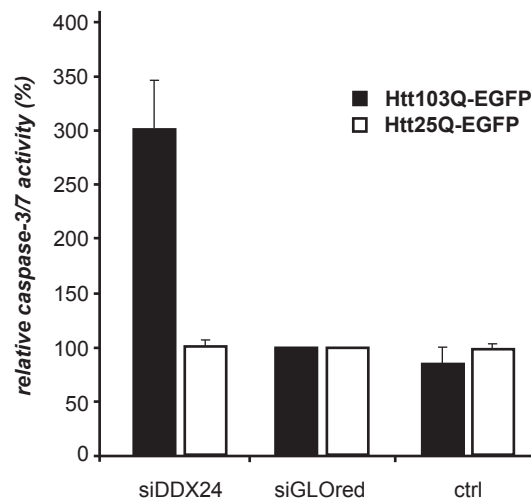


Figure 2.15: PC12 cell expressing Htt25Q-EGFP do not show increased caspase-3/7 activity after DDX24 protein knock-down. PC12 cells transfected with siDDX24_1 and _4 or siGLOred as well as non-transfected cells were analyzed. Expression of the proteins Htt25Q-EGFP and Htt103Q-EGFP was induced with 2.5 μ M muristerone. After incubation for 48 hours the activity of caspase-3/7 was analyzed using the standard caspase assay. The relative caspase-3/7 activity signals were normalized to the signals in cells transfected with siGLOred. In PC12 cells expressing Htt103Q-EGFP caspase-3/7 activity is increased upon endogenous DDX24 silencing, while in Htt25Q-EGFP expressing cells the activity levels do not change.

2.2.4 DDX24 knock-down enhances caspase-8 and -9 activity induced by mutant Htt

Within the caspase activation cascade caspase-3 acts as a downstream effector of caspase-8 and -9 (Chapter 1.2.3). With regard to this I next investigated the effect of siRNA mediated DDX24 silencing on the activation of caspase-8 and -9. First, I determined the effect of Htt103Q-EGFP protein expression on the activation of caspase-8 and -9 in PC12 cells. PC12 cells were induced with muristerone for 48 hours to allow Htt103Q-EGFP expression. As a control non-induced cells

Results

were analyzed. The activities of caspase-8 and -9 were subsequently detected by using the standard caspase-8 and caspase-9 activity assays. I found that overexpression of the Htt103Q-EGFP protein leads to a significantly increased activity of caspase-8 ($p < 0.001$) and caspase-9 ($p < 0.005$) in PC12 cells (Figure 2.16).

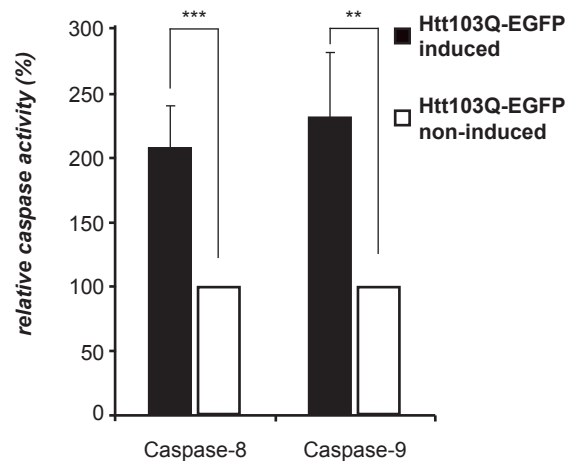


Figure 2.16: Expression of Htt103Q-EGFP protein activates caspase-8 and caspase-9 in PC12 cells. PC12 Htt103Q-EGFP cells were induced 48 hours with 2.5 μ M muristerone for the expression of Htt103Q-EGFP protein. Caspase-8 and -9 activities were detected using the standard caspase assays; the activity values were quantified by normalizing the relative activity signals in induced cells to the signals measured in the non-induced controls. The expression of Htt103Q-EGFP results in a significantly increased caspase-8 ($p < 0.001$, $n=4$) and caspase-9 ($p < 0.005$, $n=4$) activity.

In the next step, I investigated whether the DDX24 protein knock-down similar to caspase-3/7 increases the activity of caspase-8 and -9 in PC12 cells expressing Htt103Q-EGFP. PC12 Htt103Q-EGFP cells were transfected with an siRNA mix of siDDX24_1 and _4 or non-targeting siGLOred control siRNA and induced for 48 hours by addition of 2.5 μ M muristerone. Non-induced PC12 Htt103Q-EGFP cells were analyzed as controls. Caspase-8 and -9 activities were detected with the respective standard assays (Chapter 4.2.3). As described before, the relative activity values were normalized to the values detected in the siGLOred treated samples expressing Htt103Q-EGFP. As shown in Figure 2.17 A, the knock-down of endogenous DDX24 in PC12 cells expressing Htt103Q-EGFP significantly increased caspase-8 activity ($p < 0.001$), while in non-induced control cells no significant change of caspase-8 activity was observed.

The quantification of caspase-9 activity revealed a similar result. PC12 cells expressing Htt103Q-EGFP showed a two-fold increase in caspase-9 activity ($p < 0.001$) after transfection with siDDX24_1 and _4 compared to the caspase-9 activity in cells treated with non-targeting siRNA siGLOred or in non-transfected cells (Figure 2.17 B). However, knock-down of the DDX24 protein does not significantly influence caspase-9 activity in non-induced PC12 cells. This indicates that DDX24 is not only able to influence caspase-3/7 activity in Htt103Q-EGFP expressing cells. It also regulates the activities of caspase-8 and -9.

Results

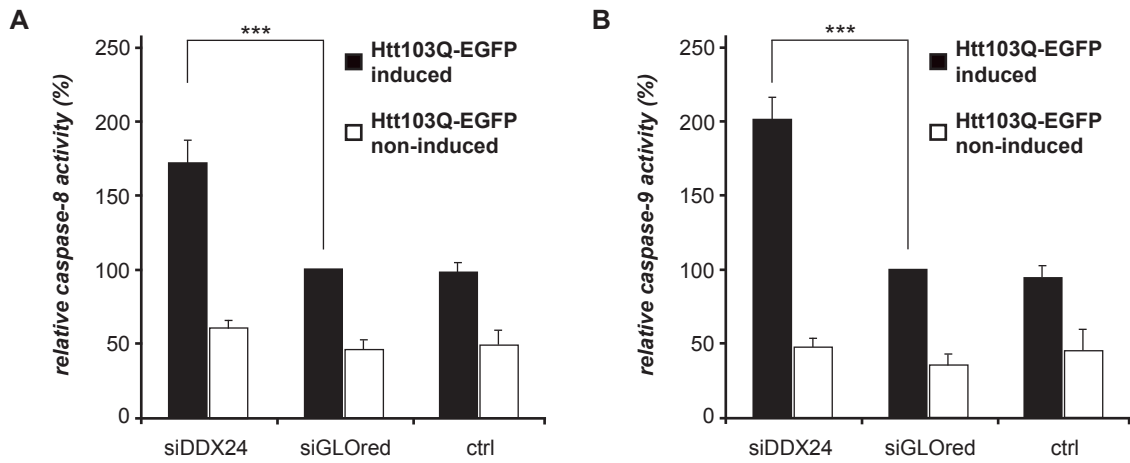


Figure 2.17: DDX24 protein knock-down increases caspase-8 and -9 activity in PC12 cells expressing Htt103Q-EGFP. PC12 cells were transfected with a mix of siDDX24_1 and _4 siRNA and induced with 2.5 μ M muristerone for 48 hours. Non-induced cells were analyzed as controls. The activity levels of caspase-8 and -9 were detected using the standard caspase assays. (A) In cells expressing toxic Htt103Q-EGFP the DDX24 knock-down significantly increases caspase-8 activity ($p < 0.001$, $n = 4$), while caspase-8 activity in non-induced PC12 cells is not affected by siRNA mediated DDX24 knock-down. (B) Endogenous DDX24 silencing also enhances Htt103Q-EGFP induced activation of caspase-9 revealing a 2-fold increase in activity ($p < 0.001$, $n = 4$). Samples not treated with muristerone do not show changes in caspase-9 activity after knock-down of DDX24 protein.

2.3 Overexpression of human DDX24 rescues Htt-induced caspase activity

2.3.1 Cloning and overexpression of HA-tagged human DDX24 protein

The enhanced activity of caspases following endogenous DDX24 silencing suggests a potential protective role of DDX24 in PC12 cells. To substantiate this hypothesis, the effect of DDX24 overexpression on Htt-induced cytotoxicity was analyzed. To allow overexpression of DDX24 in the PC12 cell culture model, a DNA expression construct was generated. cDNA with a length of 2850 bp coding for human DDX24 was shuttled into the pTL1-HA-D48 expression vector using the Gateway[®] Cloning strategy (Invitrogen). The resulting plasmid produces full length DDX24 protein, with an N-terminal hemagglutinin (HA) epitope tag (HA-DDX24; Figure 2.18). The human DDX24 protein shares 79 % sequence identity with the rat protein and 78 % with the mouse protein.

For expression of the HA-DDX24 fusion protein, PC12 cells were transfected with 2 μ g of pTL1-HA-DDX24 plasmid according to the protocol described in Chapter 4.2.3. Cells were incubated at 37 $^{\circ}$ C and after 48 hours lysed under native conditions. The cell extract containing HA-DDX24 fusion protein was subsequently separated by SDS-PAGE (30 μ g loaded) and

Results

transferred onto a nitrocellulose membrane for Western blotting. For detection of the HA-DDX24 fusion protein and the endogenous rat DDX24 protein the membrane was incubated with anti-DDX24 antiserum. Additionally, the expression of the HA-DDX24 fusion protein was confirmed by incubation of the membrane with anti-HA antibody (Figure 2.18).

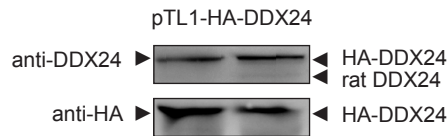


Figure 2.18: Expression of HA-DDX24 fusion protein in PC12 cells. Total lysates of PC12 cells expressing HA-DDX24 protein were denatured and 30 μ g of total protein was separated on a 12.5 % acrylamide SDS gel. The expression of HA-DDX24 was confirmed by Western blotting and incubation of the membrane with an anti-DDX24 antiserum (upper panel) and anti-HA antibody (lower panel). A weak protein band referring to the rat endogenous DDX24 protein (rDDX24) is detected with the anti-DDX24 antiserum.

2.3.2 Knock-down of endogenous DDX24 does not affect expression of recombinant HA-DDX24 fusion protein

As described in Chapter 2.2, the silencing of endogenous DDX24 in PC12 cells expressing Htt103Q-EGFP enhances the activity of caspases induced by the toxic Htt protein. If DDX24 has a protective function and reduces Htt-induced cytotoxicity, its overexpression should rescue Htt-induced caspase activity. In previous experiments it was found that the overexpression of HA-tagged proteins alone leads to an enhanced level of cytotoxicity, regardless whether HA-DDX24 or a control protein was expressed. To avoid this problem an RNAi rescue experiment was performed.

First, I tested whether the human HA-DDX24 protein can be overexpressed in PC12 cells under conditions when the endogenous DDX24 protein is silenced by RNAi. PC12 cells expressing Htt103Q-EGFP (induced with 2.5 μ M muristerone) were co-transfected with the expression vector pTL1-HA-DDX24 for expression of HA-DDX24 fusion protein and with siRNAs targeting rat DDX24 (siDDX24_1, _2, _3 and _4). PC12 cell were either treated with 100 pmol of one type of siDDX24_1 to _4 or with the pool containing all four siRNAs (siDDX24_p). In control samples siDDX24_1, _2, _3 and _4 or the pool were co-transfected with 2 μ g carrier DNA. The cells were incubated at 37 $^{\circ}$ C and harvested after 48 hours. PC12 cells were lysed under native conditions and 60 μ g of total protein were heat-denatured and analyzed by SDS-PAGE and Western blotting. The Western blot membrane was immunostained with the anti-DDX24 antiserum to detect the overexpressed HA-DDX24 fusion protein as well as the rat endogenous DDX24 protein. In addition, the blot was incubated with the CAG53b antibody to visualize Htt103Q-EGFP protein; actin was detected as loading control with the anti-actin antibody. Figure 2.19 shows a representative Western blot analysis. siDDX24_1 reduced endogenous levels of rat DDX24 but did not affect

Results

the expression of human HA-DDX24 fusion protein. The siRNAs siDDX24_2 and siDDX24_3 also reduced the rat DDX24 protein levels and showed no effect on the expression of HA-DDX24 fusion protein. However, these siRNAs have been shown previously to silence endogenous rat DDX24 less efficiently than the siRNAs siDDX24_1 and siDDX24_4 (Chapter 2.2.2; Figure 2.12). Interestingly, I found that the siRNA siDDX24_4, which is able to silence rat endogenous DDX24 very efficiently (Chapter 2.2.2), also reduces the expression of human HA-DDX24 fusion protein. This was also confirmed when cell extracts of PC12 cells transfected with the siDDX24 siRNA pool were analyzed. Hence, only siDDX24_1 was used in the subsequent rescue experiment to avoid silencing of human HA-DDX24 by RNAi.

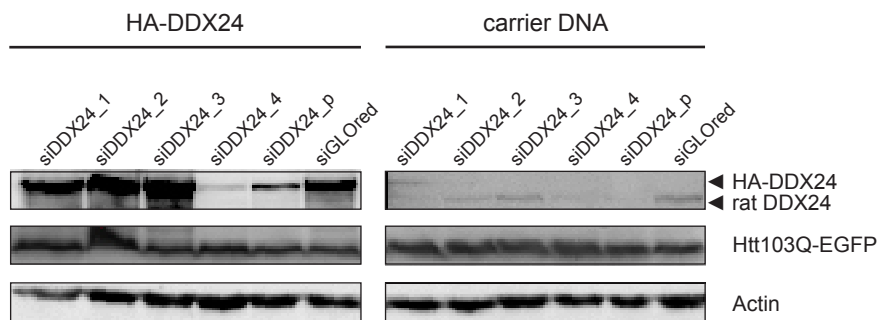


Figure 2.19: Representative Western blot demonstrating silencing of rat endogenous DDX24 protein using siDDX24_1, _2, _3 and _4 as well as the pool of siDDX24_1 to _4 in the presence or absence of overexpressed HA-DDX24 fusion protein. PC12 cells induced for Htt103Q-EGFP expression were co-transfected with 2 μ g pTL1-HA-DDX24 and 100 pmol of either one type of siDDX24 siRNA or the pool of all four siRNAs (siDDX24_p). In the control cells the pTL1-HA-DDX24 plasmid was substituted by carrier DNA. After incubation for 48 hours PC12 cells were harvested and lysed under native conditions. 60 μ g of total protein were denatured and separated on a 12.5 % acrylamide SDS gel. The expression of HA-DDX24 fusion protein and of endogenous rat DDX24 protein was detected on a Western blot by incubation with anti-DDX24 antiserum. For detection of Htt103Q-EGFP protein the membrane was incubated with the CAG53b antibody; actin serving as loading control was detected by the anti-actin antibody. The expression of endogenous DDX24 protein is efficiently reduced by siDDX24_1 and siDDX24_4 as described before, as well as by the siDDX24 pool. Besides this, transfection of HA-DDX24 expressing PC12 cells with siDDX24_4 or the siDDX24 pool resulted in a reduction of HA-DDX24 protein expression.

2.3.3 Overexpression of human DDX24 rescues toxic effects of DDX24 knock-down on mutant Htt-induced caspase activity

In the next step, I tested whether the overexpression of human HA-DDX24 fusion protein can rescue the effect of endogenous DDX24 protein silencing on Htt103Q-EGFP induced caspase activity. PC12 cells were induced for the expression of Htt103Q-EGFP protein using 2.5 μ M muristerone and transfected with 100 pmol siDDX24_1 siRNA and 2 μ g of pTL1-HA-DDX24 expression plasmid. In the control cells siDDX24_1 was transfected with 2 μ g carrier DNA. After 48 hours cell numbers were determined by counting and a standardized number of cells was re-seeded as triplicates in a 96 well plate. After 1 hour the activities of caspase-3/7 and caspase-8 were

Results

determined using standard assays and were monitored in a multiplexed reaction (Chapter 4.2.3). Figure 2.20 shows caspase-3/7 and -8 activities of PC12 cells in which endogenous DDX24 was silenced and human HA-DDX24 was simultaneously expressed (siDDX24/HA-DDX24) relative to cells in which DDX24 was silenced but which did not express the HA-DDX24 fusion protein (siDDX24 /-). As shown in Figure 2.20 A, the activity of caspase-3/7 induced by Htt103Q-EGFP expression and endogenous DDX24 protein silencing was significantly ($p < 0.001$) reduced by the overexpression of HA-DDX24 fusion protein. Moreover, caspase-8 activity was significantly ($p < 0.005$) suppressed when the HA-DDX24 fusion protein was overexpressed (Figure 2.20 B).

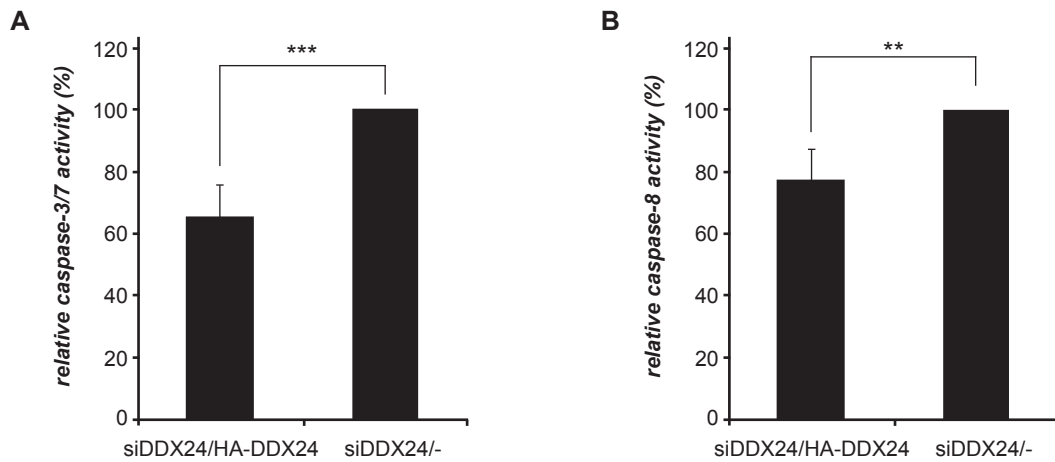


Figure 2.20: Overexpression of human HA-DDX24 fusion protein rescues caspase activity induced by DDX24 knock-down and simultaneous expression of Htt103Q-EGFP. In PC12 cells expressing Htt103Q-EGFP endogenous DDX24 expression levels were reduced by RNAi using siDDX24_1 simultaneously to the overexpression of HA-DDX24 fusion protein. In the control samples only the DDX24 knock-down was performed. Cells were transfected with siDDX24_1 and either the expression plasmid pTL1-HA-DDX24 or carrier DNA. Cells were incubated for 48 hours at 37 °C. After harvesting the activities of caspase-3/7 and -8 were determined using standard assays. The relative caspase activities were normalized to the signals detected in cells that did not overexpress the HA-DDX24 protein. (A) Htt103Q-EGFP expressing PC12 cells treated with siDDX24_1 and overexpressing HA-DDX24 fusion protein showed a significantly reduced activity of caspase-3/7 compared to controls ($p < 0.001$, $n=5$). (B) Overexpression of HA-DDX24 fusion protein significantly reduces the toxic effect of endogenous DDX24 silencing on caspase-8 activity ($p < 0.005$, $n=4$).

2.4 Expression of mutant Htt protein changes DDX24 expression in HD model systems

2.4.1 DDX24 transcript levels are increased in PC12 cells expressing Htt103Q-EGFP protein

In the next part of the study, the effect of mutant Htt overexpression on DDX24 mRNA levels was analyzed.

Previously, I could show that the reduction of endogenous DDX24 protein by RNAi increases caspase-3/7 and caspase-8 activity in PC12 cells overexpressing Htt103Q-EGFP (Chapter 2.2.3 and 2.2.4). This indicates that DDX24 has a protective effect on mutant Htt-induced toxicity in mammalian cells. Thus, mutant Htt expression might also influence the transcript and protein levels of DDX24 in PC12 cells. I therefore investigated whether DDX24 transcript levels are altered in PC12 cells overexpressing Htt103Q-EGFP or Htt25Q-EGFP protein.

Expression of the recombinant proteins was induced for 48 hours by 2.5 μ M muristerone and endogenous DDX24 mRNA levels were quantified by real-time PCR analysis (Chapter 4.2.1). As a control non-induced PC12 cells which do not express the proteins Htt103Q-EGFP or Htt25Q-EGFP were analyzed. I observed that the DDX24 mRNA levels are significantly increased by ~150 % ($p < 0.02$) in PC12 cells overexpressing Htt103Q-EGFP in comparison to the non-induced controls. However, such effect was not observed in cells overexpressing the protein Htt25Q-EGFP (Figure 2.21). This indicates that overexpression of mutant Htt protein stimulates the transcription of DDX24 mRNA in mammalian cells.

Results

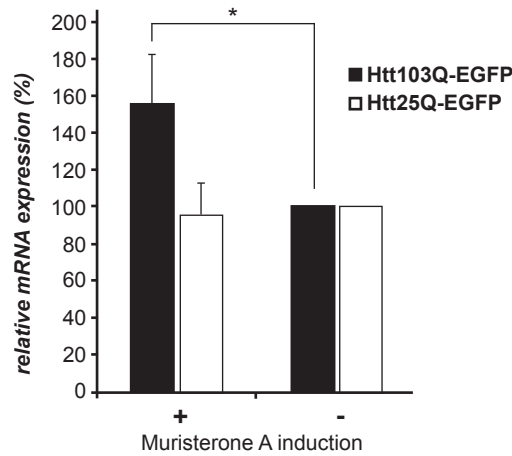


Figure 2.21: Overexpression of HttQ103-EGFP protein results in increased DDX24 mRNA in mammalian cells. PC12 cells were induced for overexpression of the recombinant proteins Htt103Q-EGFP or Htt25Q-EGFP by 2.5 μ M muristerone for 48 hours. DDX24 transcript levels were quantified in the total RNA isolates of the PC12 cells by two-step real-time PCR. The DDX24 mRNA levels were normalized to the amount of total RNA, and the relative expression of DDX24 transcript was determined by normalizing DDX24 mRNA levels to the levels of the controls which do not express Htt103Q-EGFP or Htt25Q-EGFP protein. The expression of Htt103Q-EGFP protein leads to a significant increase in DDX24 mRNA levels ($p < 0.02$, $n = 5$), whereas the levels do not change in PC12 cells expressing Htt25Q-EGFP protein.

2.4.2 Transcript levels of DDX24 are enhanced in a HD transgenic mouse model

In order to verify the results obtained in the PC12 cell culture system and to evaluate the importance of this finding regarding the pathogenesis of Huntington's disease, DDX24 mRNA levels were assayed in the transgenic mouse model TgHD82Q (Chapter 1.3). For this experiment groups of male animals with either 6 weeks or 15 weeks of age were tested for their DDX24 transcript levels in the striatum compared to the levels in the rest brain. Mice at the age of 6 weeks not yet begin to show the phenotypic abnormalities like inability to gain weight and impaired motor performance on the rotor rod (Schilling et al., 1999). In contrast, transgenic mice with an age of 15 weeks represent the end stage of the disease and show all the behavioral characteristics such as tremor, abnormal gait, hypokinesia and weight loss as well as nuclear inclusions and neuritic aggregates (see Figure 1.4). For each age a number of 3, respectively 4 male transgenic (tg) and wild-type (wt) animals were analyzed. From the isolated brains the striata were dissected and analyzed for their DDX24 specific mRNA content. Tissue samples were homogenized and the total RNA was isolated as described in Chapter 4.2.1. The DDX24 mRNA levels in the preparations then were quantified by real-time PCR. A significantly ($p < 0.02$) enhanced expression of the DDX24 mRNA by 130 % was observed in the striatum of 15 weeks old transgenic mice, whereas transgenic animals with an age of 6 weeks

Results

did not show any changes in their striatal DDX24 mRNA levels compared to the corresponding wt controls (Figure 2.22).

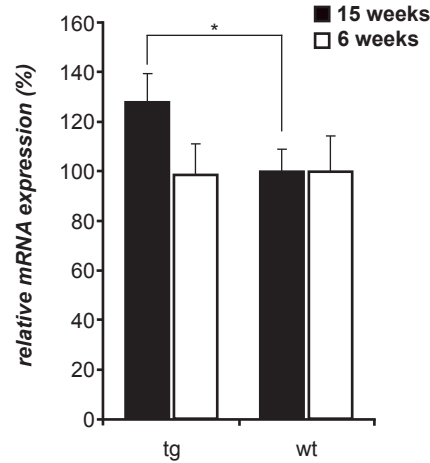


Figure 2.22: DDX24 transcription is changed in the striatal brain region of 15 weeks old transgenic HD mice. DDX24 mRNA levels were determined via two-step real-time PCR using total RNA isolates from striatal tissue of 6 and 15 weeks old wild-type and transgenic N171-82Q expressing mice. In the initial phase of the disease at the age of 6 weeks no change in DDX24 mRNA levels between wild-type and transgenic mice is visible. By contrast, at the age of 15 weeks - the end stage of the disease - transgenic animals show significantly enhanced DDX24 transcript levels compared to the wild-type mice ($p < 0.02$, $n = 3$).

To test whether the results obtained for the transcript levels of DDX24 correlate with the levels of DDX24 protein in the striatum of 15 weeks old animals, a Western blot analysis was performed. Proteins from the striatal section were isolated from the organic- and interphase which remained after chloroform separation in the RNA isolation procedure by acetone precipitation (Chapter 4.2.2). 300 μ g of total protein were mixed with SDS-loading buffer, denatured by heat and separated by SDS-PAGE. Following protein transfer to the nitrocellulose membrane the endogenous DDX24 protein was visualized by incubation of the membrane with the anti-DDX24 antiserum, GAPDH was used as loading control. Surprisingly, samples of transgenic 15 weeks old animals showed decreased DDX24 protein levels in striatal tissue compared to the protein levels detected in wild-type littermates (Figure 2.23 A). This result is unexpected since DDX24 transcript levels are enhanced in the striatum of transgenic HD mice (Figure 2.22), suggesting an accelerated degradation of DDX24 in HD mice. In contrast, PC12 cells overexpressing Htt103Q-EGFP did not show changes in the protein levels of endogenous DDX24 (Figure 2.23 B).

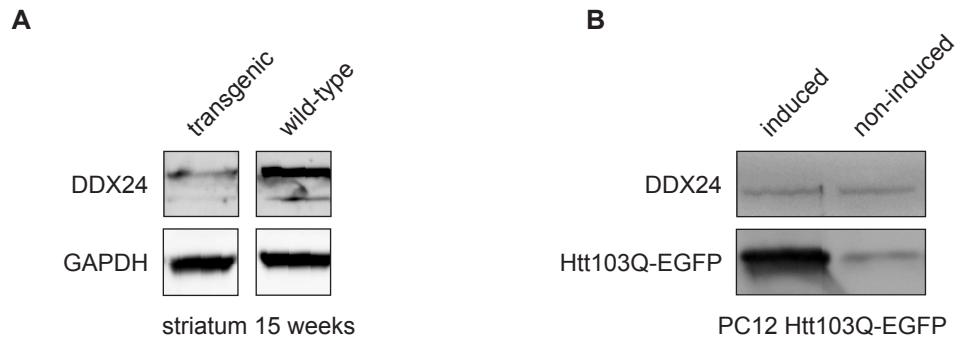


Figure 2.23: Representative Western blot of DDX24 protein levels in striatal tissue of 15 weeks old mice and PC12 cells. (A) 300 μ g of total protein derived from the striatal tissue of transgenic and wild-type animals were separated by SDS-PAGE and the proteins were transferred to nitrocellulose by Western blotting. For detection of the DDX24 protein the membrane was incubated with an anti-DDX24 antiserum; the loading control GAPDH was visualized with an anti-GAPDH antibody. In 15 weeks old transgenic animals the levels of endogenous DDX24 protein in the striatum are decreased compared to age-matched wild-type controls. (B) Total cell extracts of PC12 cells expressing Htt103Q-EGFP and of non-induced cells were analyzed by SDS-PAGE using anti-DDX24 antiserum for the detection of endogenous DDX24 levels. The Htt103Q-EGFP protein was detected with the CAG53b-antibody. No changes in the expression levels of DDX24 between induced and non-induced cells were detectable on the Western blot.

2.5 Altered levels of DDX24 do not influence Htt expression and aggregation

2.5.1 Expression of Htt103Q-EGFP is not affected by endogenous DDX24 protein silencing

In the next part of the study I investigated whether the reduction of endogenous DDX24 protein levels by RNAi influences the expression of mutant Htt or its ability to form aggregates. I have shown before that the expression of Htt103Q-EGFP in PC12 cells leads to the activation of several caspases and induces the transcription of DDX24.

In order to analyze the effect of DDX24 knock-down on the expression of mutant Htt103Q-EGFP PC12 cells were induced with muristerone and transfected with DDX24 mRNA specific siRNA (siDDX24_1 or siDDX24_4). Controls were transfected with non-targeting siGLOred siRNA. After incubation for 48 hours PC12 cells were harvested and the total RNA was isolated. To quantify the transcript levels of Htt103Q-EGFP a real-time PCR analysis was performed using a FAM-labeled TaqMan probe which was specifically designed to detect the Htt103Q-EGFP transcript (Chapter 4.1.6). I observed no differences in the transcript levels of Htt103Q-EGFP in samples treated with siDDX24_1 or _4 compared to the controls, indicating that the reduction

Results

of endogenous DDX24 levels in PC12 cells does not affect the levels of Htt103Q-EGFP mRNA (Figure 2.24 A).

In addition to the real-time PCR analysis, the expression of Htt103Q-EGFP protein in PC12 cells was monitored. PC12 cells transfected with siDDX24_1 or siDDX24_4 were induced for 48 hours with muristerone, lysed under native conditions and 60 μ g of total protein were analyzed by SDS-PAGE and immunoblotting (Figure 2.24 B). To detect overexpressed Htt103Q-EGFP protein the membrane was incubated with CAG53b antibody. Endogenous DDX24 protein was detected with anti-DDX24 antiserum; the loading control actin was detected with anti-actin antibody.

In agreement with the results obtained in the real-time PCR experiment knock-down of DDX24 did not influence the Htt103Q-EGFP protein levels (Figure 2.24 B). Thus, endogenous DDX24 silencing does neither affect the expression of Htt103Q-EGFP on the mRNA level nor on the protein level. Consequently, the increase in Htt103Q-EGFP induced caspase activity by DDX24 knock-down cannot be the result of changes in Htt103Q-EGFP protein expression.

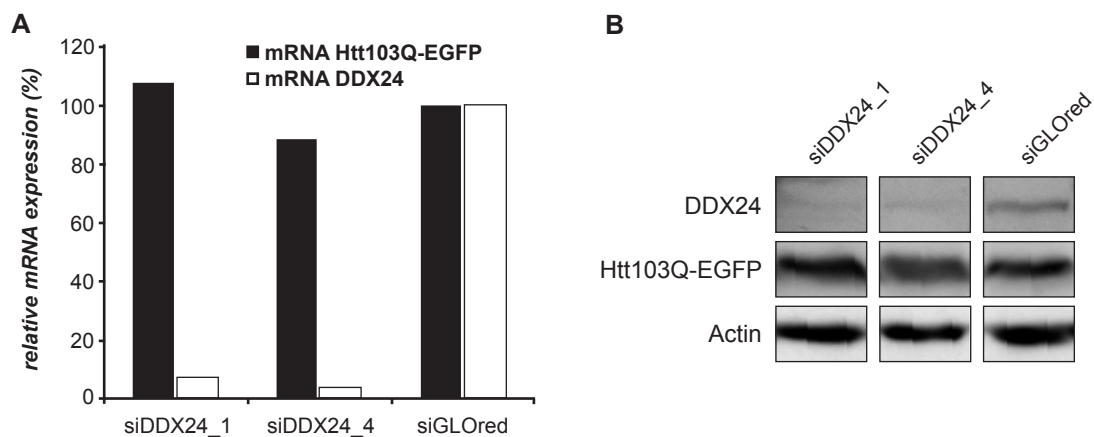


Figure 2.24: Expression of Htt103Q-EGFP is not influenced by DDX24 knock-down. (A) mRNA levels of DDX24 and Htt103Q-EGFP were analyzed by quantitative real-time PCR using specific primers and TaqMan probes. The degradation of mRNA coding for DDX24 protein does not result in changes of Htt103Q-EGFP mRNA transcription. (B) Western blot analysis of the Htt103Q-EGFP protein levels in cell extracts of PC12 cells induced for Htt103Q-EGFP expression and transfected with siDDX24_1 or siDDX24_4. 60 μ g of total protein in the cell extracts were separated on a 12.5 % acrylamide gel and analyzed by Western blotting. To detect DDX24 protein an anti-DDX24 antiserum was used, for detection of Htt103Q-EGFP the membrane was incubated with the CAG53b antibody. Actin served as a loading control. No changes in the expression levels of Htt103Q-EGFP protein were observed.

2.5.2 Aggregation of Htt103Q-EGFP is not affected by knock-down of DDX24 protein

Next, I visualized the endogenous DDX24 protein using immunofluorescence microscopy to detect the intracellular distribution of DDX24 and of Htt103Q-EGFP. Moreover, this method was utilized to investigate whether DDX24 colocalizes with insoluble Htt103Q-EGFP aggregates. PC12 cells were treated with 2.5 μ M muristerone to induce the expression of Htt103Q-EGFP protein for

Results

72 hours. Non-induced PC12 cells, which do not express the protein Htt103Q-EGFP, were used as controls. Cells were fixed with 4 % paraformaldehyde and stained against the endogenous DDX24 protein with the anti-DDX24 antiserum followed by incubation with a Cy3-fluorescence labeled secondary antibody. The cell nuclei were stained with DAPI. In all cells the endogenous DDX24 protein labeled with the red fluorescent Cy3 was found to be diffusely distributed in the cell body. Nuclear foci of DDX24 were found in part in cells that expressed Htt103Q-EGFP (Figure 2.25, indicated by arrowhead). Aggregates of the Htt103Q-EGFP protein were detected by their green fluorescent EGFP-tag (Ex470nm/Em525). I could not observe a colocalization of DDX24 with Htt103Q-EGFP aggregates in PC12 cells.

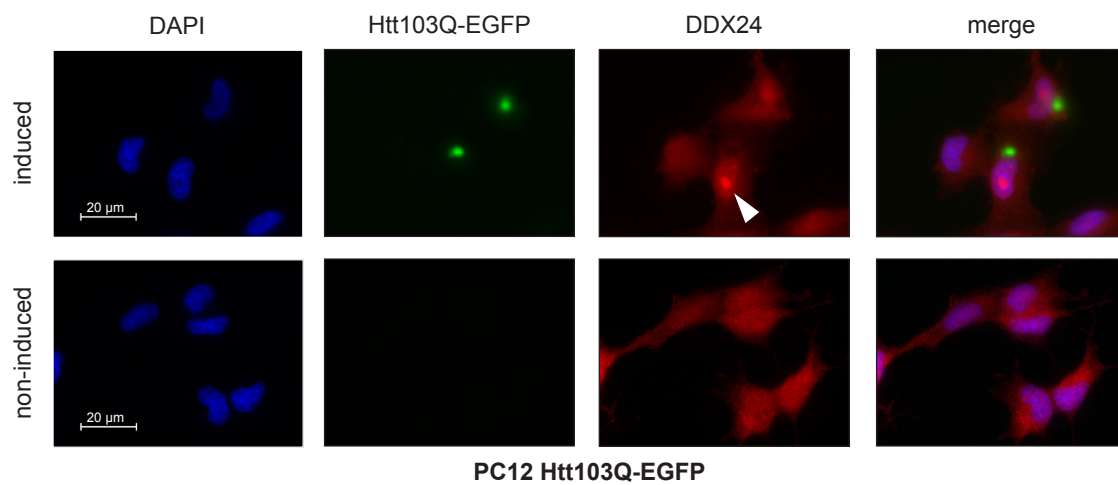


Figure 2.25: Endogenous DDX24 protein does not colocalize with mutant Htt aggregates. PC12 cells expressing Htt103Q-EGFP were induced with muristerone for 72 hours. For immunofluorescence analysis cells were fixed with 4 % paraformaldehyde and the endogenous DDX24 protein was stained with anti-DDX24 antiserum followed by incubation with a Cy3-labeled anti-rabbit secondary antibody. The cell nuclei were visualized by DAPI staining (blue). All cells show a diffuse staining indicating the DDX24 protein (red), the arrowhead indicates a nuclear focus of DDX24. Exposure times induced/non-induced: DAPI 209/294 ms, Htt103Q-EGFP 36/69 ms, DDX24-Cy3 86/244 ms. A colocalization of DDX24 and the Htt103Q-EGFP inclusions (green) was not observed.

In order to evaluate whether the observed effects of endogenous DDX24 silencing on Htt-induced caspase activity are linked to the formation of Htt103Q-EGFP aggregates, a filter retardation assay was performed. PC12 cells were induced for 72 hours to express Htt103Q-EGFP protein and simultaneously transfected with the siRNAs siDDX24_1 and siDDX24_4. Control samples either were transfected with non-targeting siRNA siGLOred or treated with carrier DNA. PC12 cells were harvested at time points of 24, 48 and 72 hours and subsequently lysed under native conditions. To monitor the amount of aggregates formed in the particular samples increasing amounts of total cell extract were filtered through a cellulose acetate membrane (Scherzinger et al., 1997). The Htt103Q-EGFP aggregates, which were retained on the membrane surface, were detected by exposure of the membrane to blue UV light (460nm; Figure 2.26 A). If the knock-down of DDX24 protein inhibits aggregation, less Htt103Q-EGFP aggregates should be detected on the membrane

Results

surface compared to the controls treated with siGLOred or carrier DNA. In case of an increase in aggregation the EGFP signal should be strengthened. However, I found that the amount of aggregates formed in PC12 cells transfected with a combination of siDDX24_1 and _4 was not different than in control cells (Figure 2.26). This indicates that DDX24 does not influence the formation of endogenous Htt103Q-EGFP aggregates and that the effect of DDX24 protein knock-down on HttQ103-EGFP-induced caspase activity is not influenced by changes in aggregate formation.

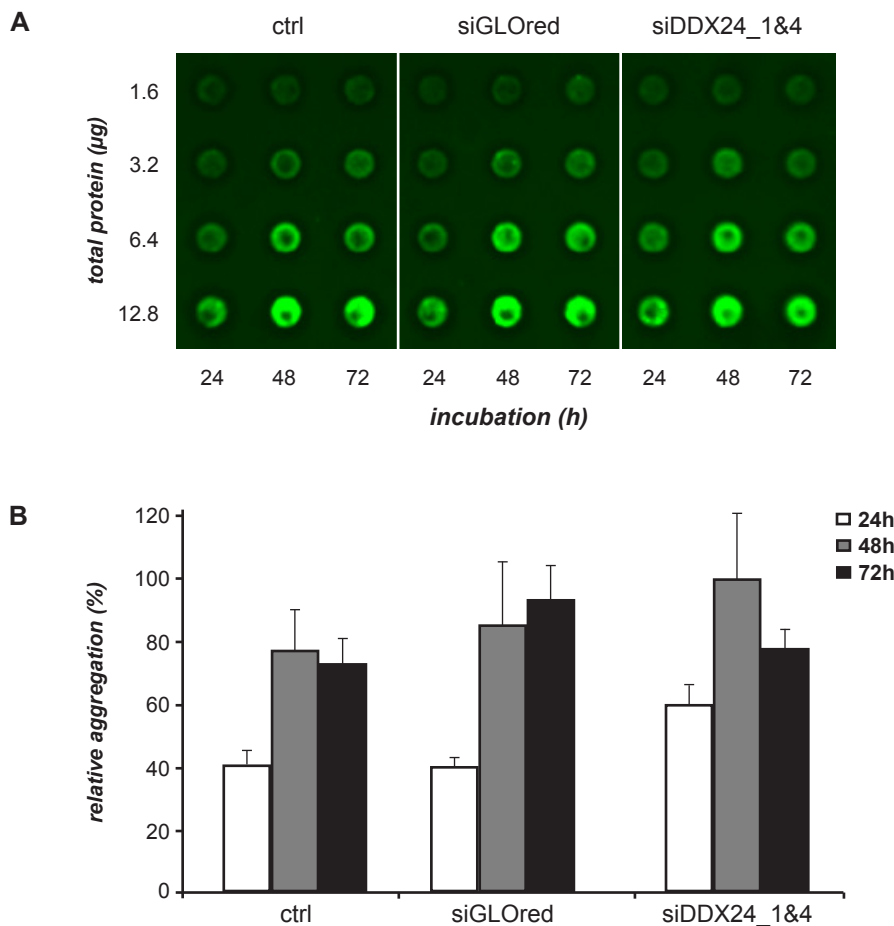


Figure 2.26: Reduction of intracellular DDX24 protein levels does not influence Htt103Q-EGFP aggregate formation. PC12 cells expressing Htt103Q-EGFP were transfected with either DDX24 targeting siRNAs (siDDX24_1 and _4) or non-targeting siRNA siGLOred. (A) Samples were incubated for 24 to 72 hours allowing aggregate formation. After lysis in 1 % NP-40 standard lysis buffer under native conditions total cell extracts were subjected to the filter retardation assay and aggregates on the membrane were detected by their fluorescent EGFP-tag (exposure to UV light, 460nm). (B) Quantification of the native filter retardation assay. The amounts of aggregates in the knock-down samples do not significantly differ from the controls.

To corroborate this observation, I performed an immunofluorescence microscopy experiment detecting intracellular Htt103Q-EGFP aggregates and endogenous DDX24 protein. PC12 cells were transfected with siDDX24_1 and _4 and induced for expression of the recombinant protein

Results

Htt103Q-EGFP. As controls PC12 cells were transfected with siGLOred non-targeting siRNA. 72 hours after induction and transfection the cells were fixed with 4% paraformaldehyde and immunostained against endogenous DDX24 protein using the anti-DDX24 antiserum in combination with a Cy5-labeled anti-rabbit antibody. Cell nuclei were stained with DAPI. In the fluorescence microscope the Htt103Q-EGFP protein was detected by its green fluorescence. Figure 2.27 shows the reduction of endogenous DDX24 protein levels in PC12 cells transfected with a combination of siDDX24_1 and _4 compared to the controls transfected with siGLOred. I found that the number of Htt103Q-EGFP aggregates does not significantly change upon DDX24 silencing in PC12 cells. This result is consistent with the data from the filter retardation assay.

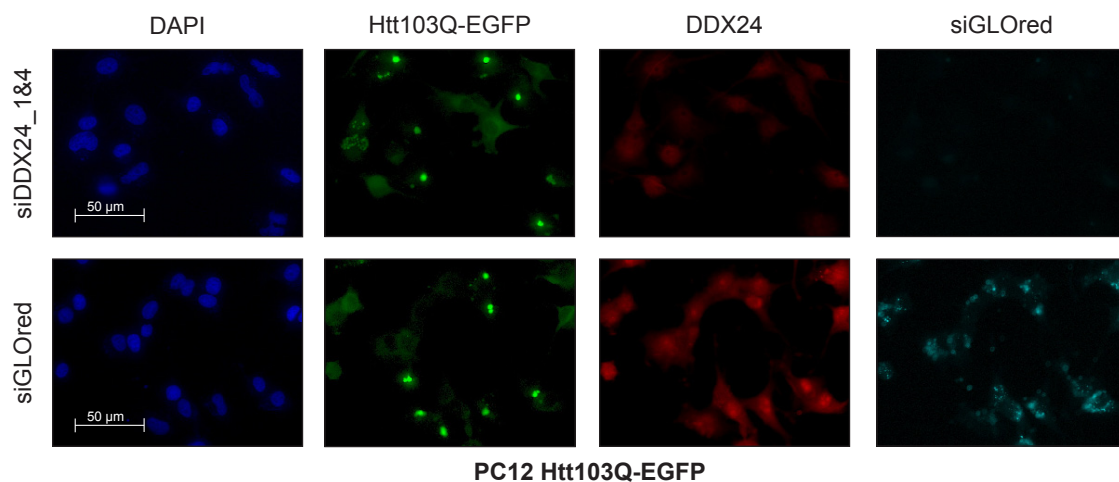


Figure 2.27: Knock-down of endogenous DDX24 protein does not affect the formation of Htt103Q-EGFP aggregates visible in the fluorescence microscope. PC12 cells were induced for Htt103Q-EGFP expression and transfected with a combination of siDDX24_1&_4 for DDX24 protein knock-down. Control cells were treated with non-targeting siGLOred siRNA. After 72 hours PC12 cells were fixed in 4% paraformaldehyde and incubated with anti-DDX24 antiserum as well as with Cy5-labeled secondary antibody for the detection of the endogenous DDX24 protein (red). Cell nuclei were stained with DAPI (blue), EGFP-labeled Htt and aggregates are shown in green. The red fluorescent control siRNA siGLOred is displayed in cyan (color manually changed). Exposure times siDDX24_1&4/siGLOred: DAPI 25/26ms, Htt103Q-EGFP 48/48 ms, DDX24-Cy3 17/17ms, siGLOred 488/488ms. PC12 cells transfected with siDDX24_1&_4 show reduced amounts of endogenous DDX24 protein (upper panel). The amount of Htt103Q-EGFP aggregates is comparable in both samples.

2.6 Interaction of DDX24 with FADD mediates apoptosis signaling

2.6.1 DDX24 directly binds to the apoptosis mediator FADD providing a link to the extrinsic apoptosis signaling pathway

The results of the first part of the study established that DDX24 exerts a protective function in Htt103Q-EGFP induced caspase activity, but does not directly influence Htt103Q-EGFP overexpression or aggregation. In the next part of the study I focused on the question how the protective effect of DDX24 protein is linked to the apoptosis network. For this purpose a database search for all potential interaction partners was performed using the Unified Human Interactome Database “UniHI” (Chaurasia et al., 2007; 2009). The resulting list was screened for DDX24 interaction partners which are either linked to Htt or caspase-3 and caspase-8 in order to obtain a protein-protein interaction network for the apoptosis signaling pathway (Figure 2.28).

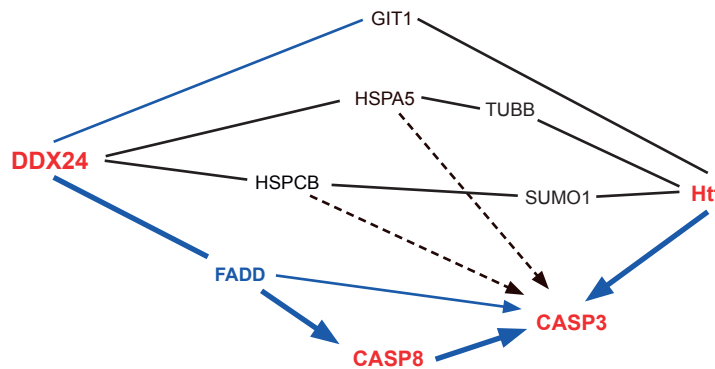


Figure 2.28: Protein-protein interaction network linking DDX24 to Htt as well as caspase-3 and -8, which are key players of apoptosis (modified from the outcome of the blast in the Unified Human Interactome Database).

The network analysis suggests that FADD (Fas-associated via death domain) represents a direct link between DDX24 and caspase-8 and caspase-3 and thus the caspase activation pathway (Figure 2.28). As described extensively in Chapter 1.2.1 FADD plays a crucial role in the signal transduction of the receptor-mediated apoptosis pathway. Thus, I next investigated the interaction between DDX24 and FADD using binding assays such as co-immunoprecipitation (Co-IP), luminescence-based mammalian interactome mapping (LUMIER) and Förster resonance energy transfer (FRET).

First, a co-immunoprecipitation (Co-IP) experiment was performed in a mammalian cell culture system (Chapter 4.2.2). HEK293 cells were co-transfected with expression plasmids for the two recombinant proteins. The first one (pFireV5-DDX24) is coding for a V5-tagged DDX24 fusion protein with a firefly luciferase (F-luc, see below) and the other one (pPAREni-FADD) codes for the postulated interaction partner FADD, fused to a protein A (PA)-tag and the renilla luciferase (R-luc).

Results

As a control HEK293 cells were transfected with pFireV5-DDX24 and the empty expression vector pPAReni-DM, which codes only for the PA-Renilla luciferase fusion protein (PA-Reni).

After incubation for 24 hours cells were lysed and the whole cell extracts were incubated with magnetic IgG coated Dynabeads® (Invitrogen) which bind the PA-tag of the PA-Reni fusion proteins. After several washing steps the magnetic beads potentially binding the co-precipitated Fire-V5-DDX24 protein were heat-denatured in SDS-containing buffer. Next, the samples were separated by SDS-PAGE, followed by Western blotting. To detect the Fire-V5-DDX24 fusion protein that was co-immunoprecipitated by PA-Reni-FADD, the membrane was incubated with a V5-specific antibody. Furthermore, a PA-recognizing antibody was used to detect PA-Reni-FADD fusion protein and PA-Reni control protein. Figure 2.29 shows that the Fire-V5-DDX24 fusion protein can be co-immunoprecipitated with the protein PA-Reni-FADD, but not with the control protein PA-Reni, confirming the interaction predicted by the UniHI database.

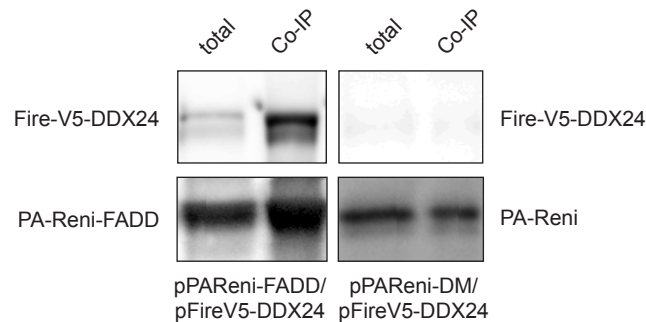


Figure 2.29: Co-immunoprecipitation of Fire-V5-DDX24 with PA-Reni-FADD. HEK293 cells were transfected with pPAReni-FADD and pFireV5-DDX24, whereas control cells were transfected with the empty vector pPAReni-DM and pFireV5-DDX24. After an incubation for 24 hours, protein complexes were precipitated using IgG coated Dynabeads® binding the PA-Reni-FADD fusion protein, separated by SDS-PAGE and transferred to nitrocellulose for Western blotting. The co-immunoprecipitated Fire-V5-DDX24 fusion protein was detected by anti-V5 antibody and PA-Reni-FADD was visualized with an anti-PA antibody. In HEK293 cells expressing the fusion proteins PA-Reni-FADD and Fire-V5-DDX24 a co-precipitation of Fire-V5-DDX24 with PA-Reni-FADD is observed. In contrast, the PA-Reni protein alone is not able to bind and precipitate Fire-V5-DDX24.

In addition, a modified version of the LUMIER method (Barrios-Rodiles et al., 2005; Palidwor et al., 2009; Chapter 4.2.2) was used for the validation of the interaction. As in the Co-IP experiment HEK293 cells were transfected with the expression vectors pPAReni-FADD/pFireV5-DDX24. Additionally, cells were transfected vice versa with pPAReni-DDX24/pFireV5-FADD. As controls HEK293 cells were treated with combinations of pPAReni-FADD/pFireV5-DM (empty vector), pPAReni-DM/pFireV5-DDX24, pPAReni-DDX24/pFireV5-DM and pPAReni-DM/pFireV5-FADD. Double-negative controls were transfected with pPAReni-DM and pFireV5-DM. To isolate PA-renilla-tagged fusion proteins PA-Reni-FADD, PA-Reni-DDX24 and PA-Reni, the cell extracts were incubated in IgG coated plates. After several washing steps, the binding (co-immunoprecipitation) of the firefly-V5-tagged fusion proteins Fire-V5-DDX24, Fire-V5-FADD

Results

and Fire-V5 to the PA-renilla-tagged fusion proteins were quantified by measuring the firefly luciferase activity in a luminescence plate reader using the Dual-Glo™ Luciferase Assay System (Promega). As expressional control the renilla luciferase activity was also measured for PA-renilla luciferase binding to the IgG-coated magnetic plates. Samples containing both fusion proteins showed a ~ 5-fold higher luminescence signal than the controls (Figure 2.30). This confirms the results of the co-immunoprecipitation experiment and thus, the interaction between DDX24 and FADD.

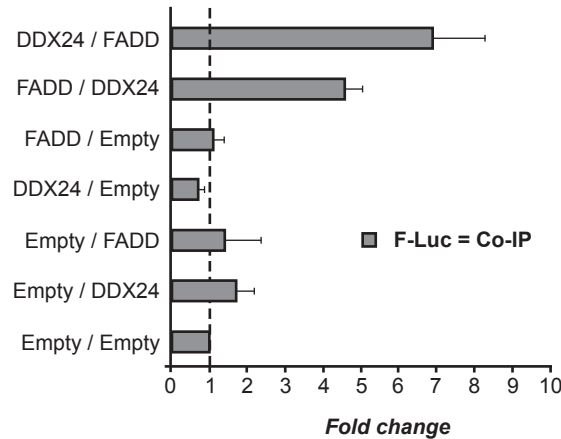


Figure 2.30: Analysis of DDX24 binding to FADD using a LUMIER assay. HEK293 cells were co-transfected with expression plasmids pPAREni-FADD and pFireV5-DDX24 for expression of PA-Reni-FADD and Fire-V5-DDX24. Vice versa, cells were transfected with pPAREni-DDX24 and pFireV5-FADD allowing expression of PA-Reni-DDX24 and Fire-V5-FADD. As controls served cells transfected with combinations of pPAREni-FADD/pFireV5-DM, pPAREni-DDX24/pFireV5-DM as well as pPAREni-DM/pFireV5-FADD, pPAREni-DM/pFireV5-DDX24 and pPAREni-DM/ pFireV5-DM (double-negative control). HEK293 cells were incubated for 24 hours, lysed and the fusion protein complexes were isolated from the cell extracts by incubation of the lysates in IgG coated plates binding the PA-fusion proteins. Subsequently, the firefly luciferase activity of the V5-F-Luc fusion proteins that were co-immunoprecipitated were quantified by measuring the relative luminescence signals detected as relative luminescence units (RLU). The relative luminescence signals were subsequently normalized to the signals obtained in the double-negative control transfected with both empty vectors (Empty/Empty=1).

Furthermore, the interaction between DDX24 and FADD was confirmed using a FRET-based interaction assay (for detailed description see Chapter 4.2.3). Plasmids encoding ECFP-DDX24 (pdECFP-DDX24) and EYFP-FADD (pdEYFP-FADD) fusion proteins were co-transfected into HEK293 cells. Cells co-transfected either with pdECFP-DDX24/pdEYFP-Amp (empty expression vector) or with pdEYFP-FADD/pdECFP-Amp were used as negative controls. Moreover, HEK293 cells were either transfected with pdECFP-DDX24/pcDNA3.1- β -Gal or pdEYFP-FADD/pcDNA3.1- β -Gal serving as controls for calculation of the ECFP- and EYFP-correction factors as described in Chapter 4.2.3. The samples were incubated for 24 hours at 37°C. To prove the interaction between the fusion proteins, cells were excited with a wavelength of 436 nm and the FRET signal was detected by measuring the fluorescence emitted at 530 nm. In order to quantify

Results

FRET signals, fluorescence signals of ECFP- and EYFP-labeled interaction partners must be quantified independently.

To detect ECFP fluorescence the samples were excited with UV light with a wavelength of 436 nm and the fluorescence emission was detected at 485 nm. For EYFP detection an excitation wavelength of 485 nm was used and the emission was detected at 530 nm. Figure 2.31 shows the relative fluorescence signals of the various samples after subtraction of the background signal. The fluorescence signals vary between samples due to different protein expression levels. The highest expression levels of ECFP and EYFP fluorescence are observed in cells expressing both fusion proteins ECFP-DDX24 and EYFP-FADD or one of the fusion proteins in addition to β -Gal. In contrast, the fluorescence signals in cells transfected with pdECFP-DDX24 and pdEYFP-Amp or with pdEYFP-FADD and pdECFP-Amp were 5- to 10-fold lower.

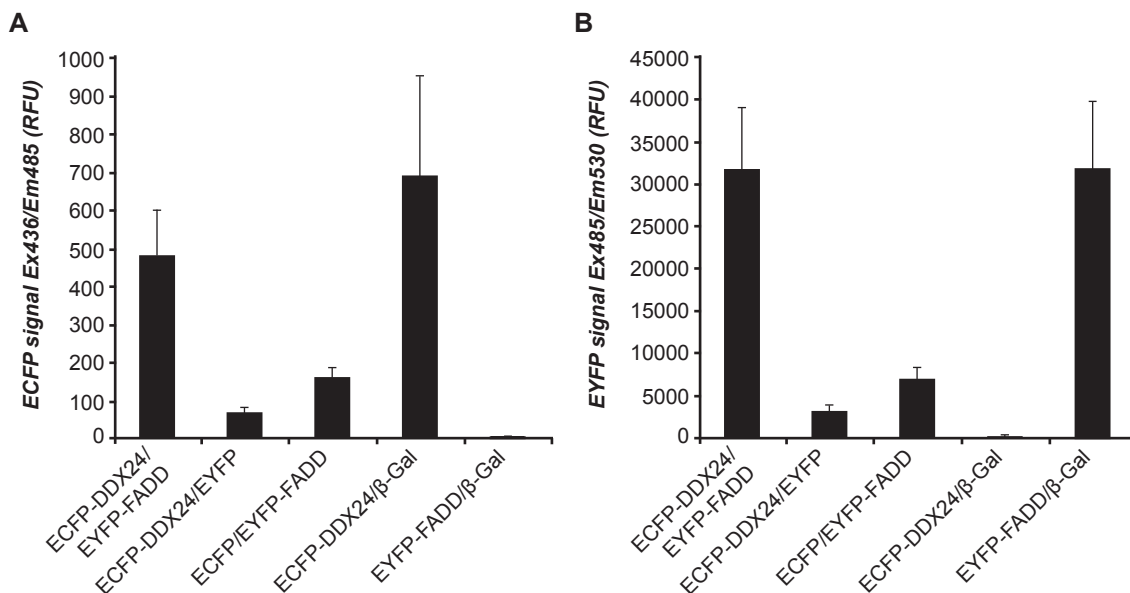


Figure 2.31: Expression of the fusion proteins ECFP-DDX24 and EYFP-FADD in HEK293 cells. For expression of the proteins HEK293 cells were transfected with the expression vectors pdECFP-DDX24 and pdEYFP-FADD. FRET controls were transfected with either pdECFP-DDX24 and pdEYFP-Amp or with pdEYFP-FADD and pdECFP-Amp. As controls for calculation of the correction-factors cells were transfected with pcDNA3.1- β -Gal and either pdECFP-DDX24 or pdEYFP-FADD. (A) After incubation for 24 hours the ECFP fluorescence signals were detected by excitation of the samples at 436 nm and fluorescence detection at 485 nm. (B) EYFP fluorescence signals were determined by excitation with UV light in a wavelength of 485nm and detection of the fluorescence emission at 530nm.

The fluorescence signals were then used to normalize the FRET signals to the protein expression levels and to calculate the netto FRET signals (netFRET; Chapter 4.2.3). In Figure 2.32 A, the netFRET signals of the samples expressing ECFP-DDX24 and EYFP-FADD fusion proteins as well as those of the controls containing either ECFP-DDX24 and EYFP protein or EYFP-FADD fusion protein and ECFP are shown. For validation the netFRET signals of the interaction between DDX24 and FADD were compared to the signals obtained for the protein pair LSM1/LSM2 serving

Results

as positive control (Figure 2.32 B). Both proteins are U6 small nuclear RNA associated proteins, which were demonstrated to interact in the human mRNA degradation framework (Lehner and Sanderson, 2004). The protein pair PSMD5/SLC22A15 served as a negative control (Figure 2.32 C). PSMD5 is a component of the proteasome protein complex (Gevaert et al., 2003), while SLC22A15 is integrated into the membrane, where it acts as an ion transporter (Eraly and Nigam, 2002). Since PSMD5 and SLC22A15 are located in different cellular compartments, an interaction between these proteins is very unlikely.

The netFRET signal in cells overexpressing ECFP-DDX24/EYFP-FADD is ~ 6.2-fold higher than the signal in control cells expressing ECFP-DDX24/EYFP protein. The signal obtained in cells overexpressing ECFP-DDX24/EYFP-FADD was 3-fold higher than the signal detected in the control cells overexpressing EYFP-FADD/ECFP. This finding confirms the interaction between DDX24 and FADD and corroborates the interaction demonstrated in the Co-IP experiment and the LUMIER assay.

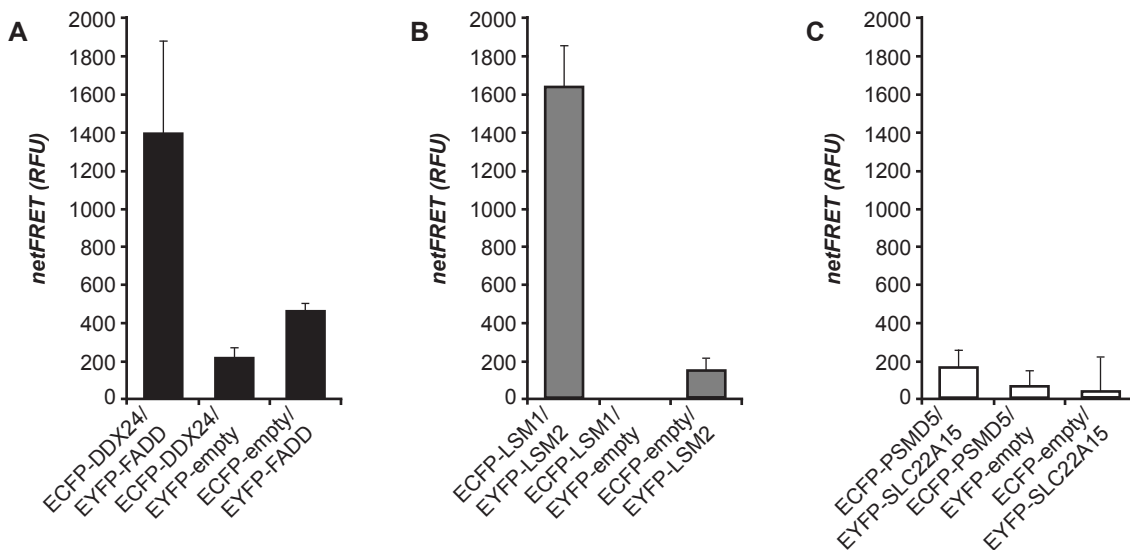


Figure 2.32: Confirmation of the DDX24 interaction with FADD using a FRET assay. (A) HEK293 cells were transfected with pdECFP-DDX24 and pdEYFP-FADD, controls were transfected with either pdECFP-DDX24 and pdEYFP-Amp or with pdEYFP-FADD and pdECFP-Amp. 24 hours after transfection the samples were analyzed for their ECFP-EYFP FRET signal by excitation with UV light using a wavelength of 436 nm for ECFP excitation. FRET signals were detected at a wavelength of 530 nm corresponding to the emission wavelength of EYFP. The FRET signals then were correlated to the ECFP and EYFP fluorescence in order to obtain the netFRET signals (Chapter 4.2.3). The netFRET signals in cells expressing the fusion proteins ECFP-DDX24 and EYFP-FADD were found to be 3- to 6.2-fold higher than the signals observed in the control cells, indicating an interaction between DDX24 and FADD. (B) netFRET signals of the positive control protein pair LSM1/LSM2. (C) Negative control proteins PSMD5 and SLC22A15 do not interact. Thus, their co-expression results in very low netFRET signals.

Moreover, a fluorescence microscopy experiment was performed to verify the interaction between DDX24 and FADD. PC12 cells co-transfected with combinations of the expression vectors

Results

pc-myc-FADD/pTL1-HA-DDX24 coding for Myc-FADD and HA-DDX24 fusion proteins or with pc-myc-DDX24/pTL1-HA-FADD for expression of Myc-DDX24 and HA-FADD were grown on glass slides. As a negative control pTL1-HA-FADD was transfected with carrier DNA. The cells then were either induced with 2.5 μ M muristerone for Htt103Q-EGFP expression or treated with ethanol as a solvent control. After an incubation period of 72 hours the PC12 cells were fixed with 4% paraformaldehyde and incubated with an anti-HA antibody (rabbit) in combination with an anti-Myc antibody (mouse). Subsequently, the samples were incubated with fluorescence labeled secondary antibodies. For detection of HA-fusion proteins a Cy3-labeled donkey anti-rabbit antibody was used, for visualization of the Myc-tagged proteins I used a Cy5-labeled goat anti-mouse antibody. The cell nuclei were stained with DAPI. The distribution of the overexpressed fusion proteins then was determined by fluorescence microscopy. Figure 2.33 shows that a colocalization of DDX24 and FADD occurs in PC12 cells expressing both combinations of the fusion proteins Myc-FADD/HA-DDX24 and Myc-DDX24/HA-FADD, respectively (Figure 2.33 A and C). The colocalization was observed independently of the expression of Htt103Q-EGFP (Figure 2.33 A and B). The colocalization of HA-DDX24/Myc-FADD and Myc-DDX24/HA-FADD detected by fluorescence microscopy confirms the results from the other interaction studies and verifies the interaction between DDX24 and FADD.

Results

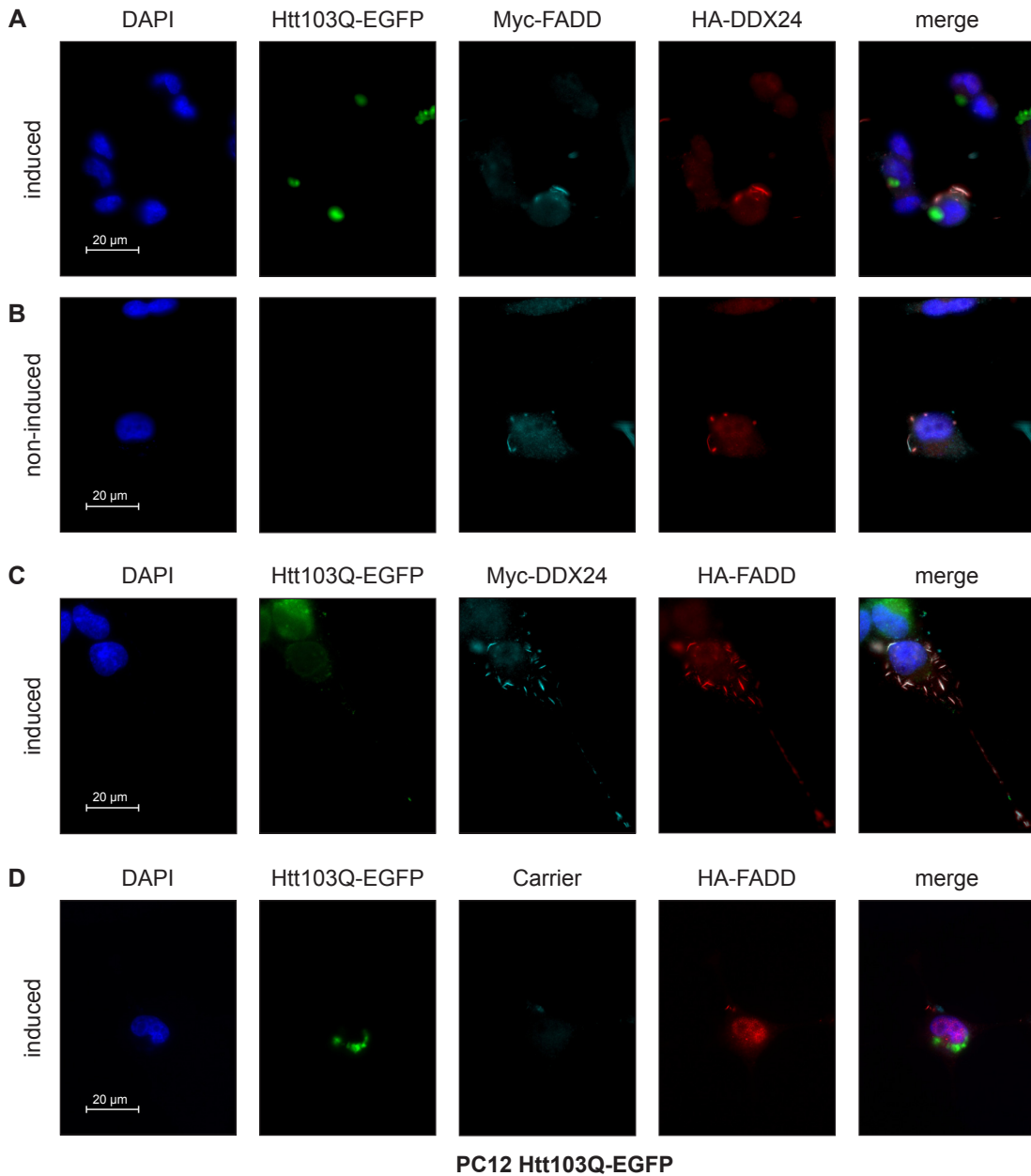


Figure 2.33: Colocalization of DDX24 and FADD in PC12 cells. (A) & (B) PC12 cells were transfected with pTL1-HA-DDX24 and pc-myc-FADD expression plasmids. (A) Htt103Q-EGFP expression was induced with 2.5 μM muristerone, (B) non-induced controls were treated with ethanol. Cells were fixed with 4% paraformaldehyde 72 hours post transfection and immunostained for Myc-FADD and HA-DDX24 with anti-Myc (mouse) and anti-HA (rabbit) antibodies. To analyze the colocalization under the fluorescence microscope the PC12 cells were incubated with an anti-mouse Cy5-antibody for visualization of Myc-FADD (cyan) and a Cy3-labeled anti-rabbit antibody for the detection of HA-DDX24 (red). Cell nuclei were stained with DAPI (blue); Htt103Q-EGFP was detected by its EGFP-tag (green). (C) PC12 cells transfected with pc-myc-DDX24 and pTL1-HA-FADD and induced for 72 h by muristerone. Cells are stained with anti-Myc/anti-mouse-Cy5 and anti-HA/anti-rabbit-Cy3 antibodies to

detect Myc-DDX24 (cyan) and HA-FADD (red). (D) PC12 cells were transfected with pTL1-HA-FADD and carrier DNA and induced with muristerone for 72 hours. HA-FADD is visualized with anti-HA/anti-rabbit-Cy3. Cells were additionally incubated with anti-Myc/anti-mouse-Cy5 for analysis of the background Cy5-signal. Color code in all panels: DAPI: blue; Htt103Q-EGFP: green; Myc-FADD/Myc-DDX24: Cy5, cyan; HA-DDX24/HA-FADD: Cy3, red. Exposure times (A)/(B): DAPI 120/110 ms, Htt103Q-EGFP 67/147 ms, Myc-FADD-Cy5 22/28 ms, HA-DDX24-Cy3 754/457 ms. Exposure times (C)/(D): DAPI 66/98 ms, Htt103Q-EGFP 1499/41 ms, Myc-DDX24-Cy5/carrier 5/176 ms, HA-FADD-Cy3 2412/1409 ms. DDX24 colocalizes with FADD in both combinations with a minimal background signal. The DDX24/FADD colocalization is independent of Htt103Q-EGFP protein expression.

2.6.2 Overexpression of recombinant HA-FADD fusion protein increases caspase-3/7, caspase-8 and caspase-9 activity

In the last paragraph, I described the protein-protein interaction between the recombinant proteins DDX24 and FADD, which I was able to confirm in a series of different experiments. To investigate whether the interaction between DDX24 and FADD plays a role in the caspase activation cascade recombinant FADD protein was overexpressed in the mammalian PC12 cell system. First, I generated an expression plasmid (pTL1-HA-FADD) allowing expression of the full length human FADD protein fused to an N-terminal HA-tag. To do so, I inserted a cDNA fragment coding for the human FADD protein into the pTL1-HA-D48 expression vector using the Gateway® shuttling system (Chapter 4.2.1). To demonstrate the overexpression of the recombinant HA-FADD protein PC12 cells were transfected with 2 µg of the pTL1-HA-FADD plasmid. Following incubation for 48 hours PC12 cells were lysed under native conditions and the total cell extract was analyzed for the expression of HA-FADD by SDS-PAGE and Western blotting. For detection of the recombinant HA-FADD fusion protein the anti-HA antibody was used (Figure 2.34). The HA-FADD fusion protein is well expressed in the PC12 cells, although it shows many smaller bands, which might indicate incomplete translation or degradation of the protein.

Results

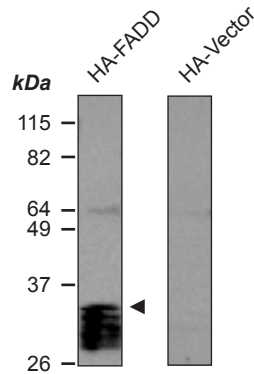


Figure 2.34: Western blot analysis of the overexpression of recombinant HA-FADD fusion protein in PC12 cells. Cells were transfected with 2 μg of the expression plasmid pTL1-HA-FADD or with empty HA-vector in control samples. The samples were incubated for 48 hours and subsequently analyzed by SDS-PAGE (12.5 % gel) followed by Western blotting. The overexpressed recombinant HA-FADD fusion protein was detected on the membrane with the anti-HA antibody. Besides the protein band referring to the full length HA-FADD fusion protein (~29 kDa) many smaller bands were detected which may indicate incomplete protein translation or protein degradation.

Next, it was tested whether HA-FADD protein expression influences the activity of caspase-3/7, -8 and -9 in Htt103Q-EGFP protein expressing cells. PC12 cells were transfected with 2 μg of pTL1-HA-FADD to achieve expression of the recombinant HA-FADD fusion protein and control cells were transfected with 2 μg of the empty pTL1-HA-D48 vector. The expression of Htt103Q-EGFP was induced for 48 hours by muristerone addition. As a control non-induced PC12 cells were also transfected with the pTL1-HA-FADD expression plasmid or the pTL1-HA-D48 empty vector. The effect of HA-FADD protein overexpression on the activity of caspase-3/7, caspase-8 and caspase-9 was analyzed using the standard assays (Chapter 4.2.3). The obtained caspase activities were normalized using the viability rates monitored in the same samples by the resazurin conversion assay (Chapter 4.2.3). The relative caspase activity signals were subsequently normalized to the signals detected in PC12 cells that were transfected with pTL1-HA-D48 but did not express recombinant Htt103Q-EGFP fusion protein (Figure 2.35).

I observed that the activity of caspase-3/7 was increased by the overexpression of recombinant HA-FADD fusion protein compared to the activity detected in the controls that were transfected with the empty vector pTL1-HA-D48. This effect was observed in PC12 cells overexpressing Htt103Q-EGFP as well as in cells that did not express the Htt protein, although the caspase-3/7 signals detected in non-induced cells were much lower than those of Htt103Q-EGFP protein expressing cells (Figure 2.35 A). As caspase-8 is the initiator for caspase-3/7, the overexpression of the HA-FADD fusion protein should also increase the activity of caspase-8. PC12 cells expressing recombinant HA-FADD indeed showed increased caspase-8 activity compared to cells transfected with the empty expression vector pTL1-HA-D48 both in the presence (250 %) and absence (130 %) of Htt103Q-EGFP expression (Figure 2.35 B). The caspase activity obtained in the control cells that did not express Htt103Q-EGFP was however lower than those in Htt103Q-EGFP expressing cells. Next, the effect of recombinant HA-FADD protein expression on the activity of caspase-9

Results

was analyzed. Caspase-9 acts downstream of caspase-8 within the caspase cascade and can be indirectly modulated by the protein FADD. Similar to the activity of caspase-8, the overexpression of the HA-FADD fusion protein resulted in an enhanced caspase-9 activity in comparison to the control cells which were transfected with pTL1-HA-D48. As seen for caspase-3/7 and caspase-8 the activity of caspase-9 was higher in PC12 cells expressing Htt103Q-EGFP than in non-induced control cells (Figure 2.35 C).

In summary, overexpression of recombinant HA-FADD fusion protein results in an overall increase of caspase activity in both, presence and absence of Htt103Q-EGFP. The highest caspase activities were detected in PC12 cells expressing both proteins HA-FADD and Htt103Q-EGFP. This indicates that overexpression of HA-FADD increases caspase-mediated apoptosis synergistically with mutant Htt expression.

Results

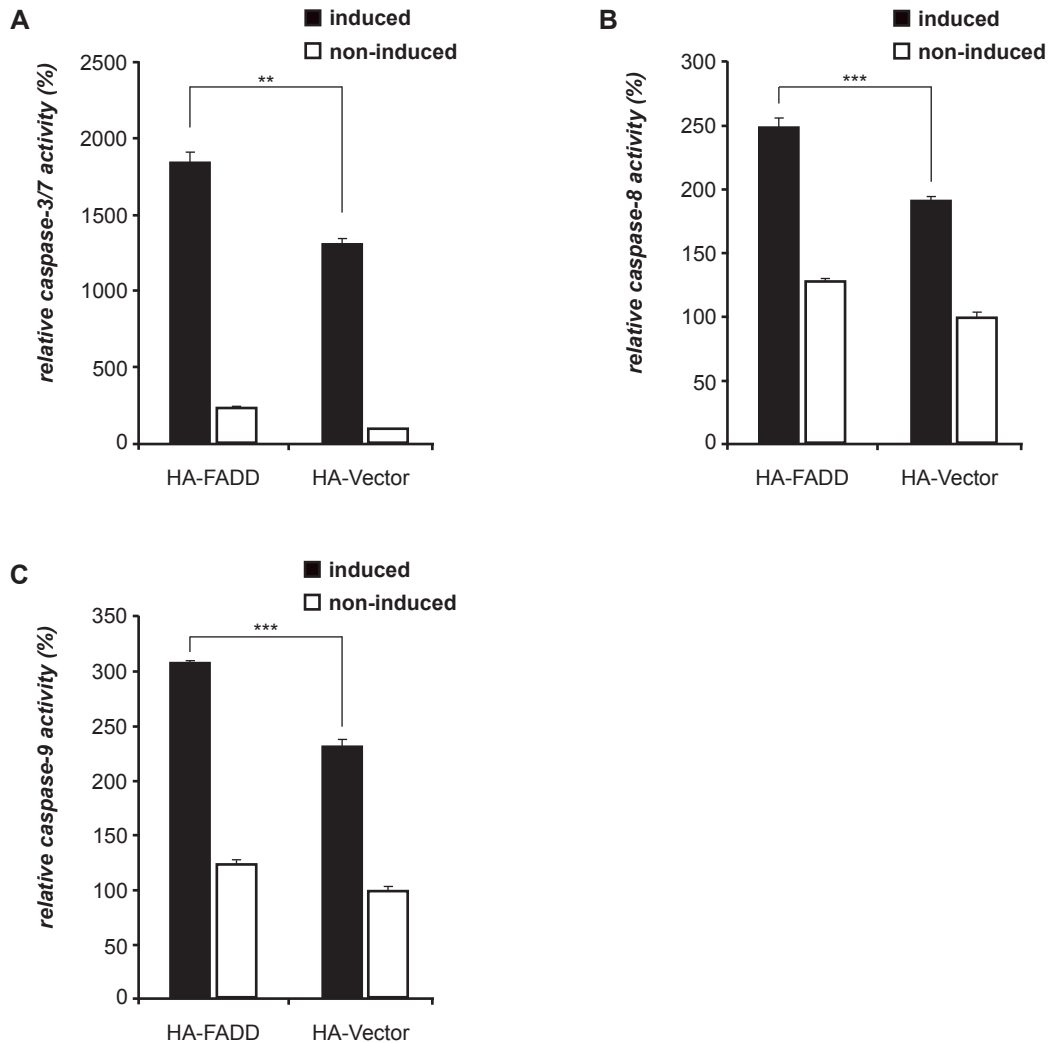


Figure 2.35: FADD overexpression increases *Htt103Q-EGFP*-induced caspase activity. PC12 cells were transfected with either *pTL1-HA-FADD* for the expression of recombinant HA-FADD fusion protein or with the empty expression vector *pTL1-HA-D48*. After induction of *Htt103Q-EGFP* protein overexpression for 48 hours the activities of caspase-3/7, -8 and -9 were analyzed. As controls non-induced cells transfected with *pTL1-HA-FADD* or *pTL1-HA-D48* were analyzed. The relative caspase activities were normalized to the activities detected in non-transfected cells which do not express *Htt103Q-EGFP*. (A) Overexpression of recombinant HA-FADD fusion protein leads to increased caspase-3/7 activity (induced :1800 % vs. 1300%, $p < 0.005$, $n = 3$; non-induced: 240 % vs. 100 %). (B) Increased caspase-8 activity (induced: 250 % vs. 190 %, $p < 0.001$, $n = 3$; non-induced: 130 % vs. 100 %) was also detected when the proteins HA-FADD and *Htt103Q-EGFP* were coexpressed. (C) Expression of *Htt103Q-EGFP* leads to an increase in caspase-9 activity (induced 300% vs. 230 %, $p < 0.001$, $n = 3$; non-induced 120 % vs. 100 %) which is additionally enhanced by the coexpression of recombinant HA-FADD fusion protein.

2.6.3 FADD and DDX24 synergistically modulate caspase activation by mutant Htt

I could show that the overexpression of the HA-FADD fusion protein as well as the silencing of endogenous DDX24 protein increased the caspase activity induced by the expression of Htt103Q-EGFP protein. Moreover, the interaction between DDX24 and FADD could be confirmed by expression of the fusion proteins in mammalian cells using various detection methods (see Chapter 2.6.1). With regard to these findings it is plausible to assume that DDX24 mediates caspase activation via interaction with FADD.

In order to further characterize the relation of DDX24 and FADD concerning the activation of the caspase cascade an experiment was performed in which PC12 cells were co-transfected with siDDX24_1&_4 for DDX24 protein knock-down and pTL1-HA-FADD plasmid for overexpression of the HA-FADD fusion protein. As controls PC12 cells were either transfected with siDDX24_1&_4 and pTL1-HA-D48 to achieve protein knock-down in the absence of HA-FADD overexpression or with siGLOred and pTL1-HA-FADD to study the effect of HA-FADD overexpression in the absence of DDX24 knock-down. Additionally, the cells were induced for 48 hours by muristerone addition for expression of Htt103Q-EGFP protein. Cells co-transfected with non-targeting siGLOred siRNA and the empty vector pTL1-HA-D48 were analyzed as double-negative controls. Caspase-3, -8 and -9 activities were normalized to cell numbers using the resazurin viability assay (Chapter 4.2.3). The relative caspase activities were normalized to those in control cells transfected with siGLOred and pTL1-HA-D48. In accordance with the previously described experiments both, the overexpression of recombinant HA-FADD as well as the protein knock-down of endogenous DDX24, enhanced the activity of caspase-3/7 and caspase-8 in Htt103Q-EGFP expressing cells (Figure 2.36 A & B). Simultaneous overexpression of HA-FADD and DDX24 knock-down in the same cells resulted in an amplification of caspase-3/7 and caspase-8 activity compared to cells either overexpressing HA-FADD or only containing reduced DDX24 protein levels (Figure 2.36 A & B). The activity of caspase-9 was increased in PC12 cells overexpressing the HA-FADD fusion protein and in cells with reduced DDX24 protein levels. However, compared to untreated controls no further activation was observed in cells which express the recombinant HA-FADD protein and have reduced levels of the DDX24 protein (Figure 2.36 C). This indicates that FADD and DDX24 synergistically modulate mutant Htt-induced toxicity and supports the hypothesis that DDX24 influences mutant Htt-induced toxicity via the caspase-8 mediated apoptosis pathway through its interaction with FADD.

Results

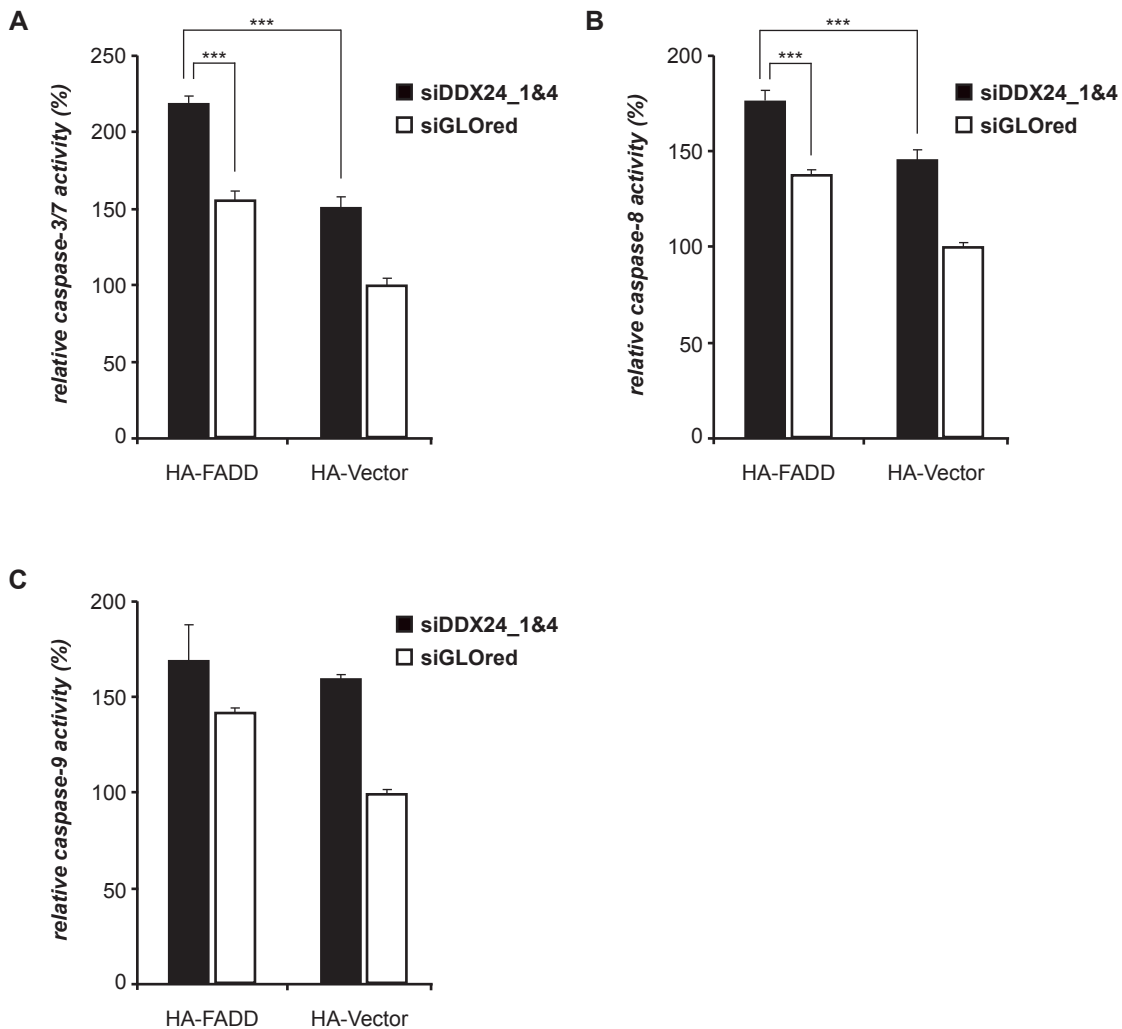


Figure 2.36: Overexpression of HA-FADD protein with simultaneous DDX24 protein knock-down results in additive enhancement of caspase activity in mammalian cells. PC12 cells were induced for Htt103Q-EGFP expression and transfected with siDDX24_1&_4 and pTL1-HA-FADD for endogenous DDX24 protein silencing with overexpression of HA-FADD protein. The corresponding controls were transfected with siDDX24_1&_4 and the empty vector pTL1-HA-D48. Other samples were treated with siGLOred and pTL1-HA-FADD to express recombinant HA-FADD protein or with pTL1-HA-D48 serving as double-negative control. Caspase activation was determined using the standard activity assays and the relative activities were normalized to the signals obtained in the negative control. (A) & (B) The simultaneous protein knock-down of DDX24 with the overexpression of recombinant HA-FADD results in an amplified activation of caspase-3/7 ($p < 0.001$, $n = 3$) and caspase-8 ($p < 0.001$, $n = 3$) compared to samples either treated with DDX24 specific siRNA siDDX24_1&_4 or the expression plasmid pTL1-HA-FADD ($p < 0.001$, $n = 3$). Cells either expressing the HA-FADD fusion protein or containing reduced DDX24 protein levels show enhanced caspase activation compared to the negative control. Lower signals were observed in cells co-transfected with pTL1-HA-FADD and siDDX24_1&_4. (C) Analysis of caspase-9 revealed an activity increase in cells expressing recombinant HA-FADD protein and having reduced DDX24 protein levels. However, the simultaneous expression of HA-FADD and knock-down of DDX24 did not further increase caspase-9 activity.

Results

Chapter 3

Discussion

Huntington's disease is like other neurodegenerative disorders such as Alzheimer's disease (AD) or Parkinson's disease (PD) characterized by severe neuronal death resulting in atrophy in the striatal region and the cerebral cortex (Vonstattel et al., 1985). Cell death in striatal neurons is a consequence of cytotoxicity and enhanced apoptosis induced by mutant Htt protein. A main focus of drug development research therefore is the ambition to find treatments to impede neuronal degradation preferably before onset of the disease and manifestation of symptoms. One possible strategy to address this aim is to inhibit the aggregation of neurotoxic mutant Htt. Many studies published within the last years focused on aggregate formation since cytotoxicity is regarded as a secondary effect resulting as a consequence of aggregation. Recent studies mostly used small molecule screening approaches to identify molecules which are able to modulate aggregation or clearance pathways (Sarkar et al., 2007; Desai et al., 2006; Coufal et al., 2007). An alternative strategy is to inhibit signaling pathways by which mutant Htt confers toxicity. This could be attained by activation or inactivation of molecular modulators of apoptosis and/or survival pathways.

Protein misfolding and the resulting aggregation of proteins causes toxicity by the activation of cellular signaling pathways. Previous studies demonstrated the interaction of mutant Htt with a wide range of proteins involved in many different cellular processes (Goehler et al., 2006; Kaltenbach et al., 2007). As a consequence of mutant Htt expression numerous genes are transcriptionally dysregulated, which has been shown in cell and animal models of HD as well as in HD patients (Kita et al., 2002; Sipione et al., 2002; Wyttenbach et al., 2001; Apostol et al., 2006; Lee et al., 2007; Runne et al., 2008; Luthi-Carter et al., 2000; Crocker et al., 2006; Kuhn et al., 2007; Brochier et al., 2008; Lorincz and Zawistowski, 2009; Lovrecic et al., 2009; Anderson et al., 2008; Hodge et al., 2006; Borovecki et al., 2005). This implicates an important role of genetic modifiers in the pathogenesis of HD. Identification of these modifiers and their particular mechanism of action can shed light on the disease mechanisms offering new opportunities for therapeutic interventions.

Within the past years several groups focused on genome wide aggregation and toxicity modifier screens using various model systems (Willingham et al., 2003; Nollen et al., 2004; Kaltenbach et al., 2007). In these models mutant Htt is expressed with a simultaneous down-regulation or an overexpression of the genetic modifier orthologue in the respective model organism in order to investigate their effect on aggregation and toxicity. Some of the functional classes and biological mechanisms identified in these screens were consistent for different polyQ disorders, including genes involved in protein folding and degradation, transcriptional regulation, translation and RNA metabolism (Kazemi-Esfarjani and Benzer, 2000; Nollen et al., 2004; Bilen and Bonini, 2007). Interestingly,

Discussion

many modifiers involved in RNA-metabolism were found in polyQ toxicity and aggregation screens, but hardly in screens focusing on other (non-polyQ) neurodegenerative disorders, e. g. Parkinson's disease (van Ham et al., 2009) which allows the conclusion that a polyQ specific toxicity mechanism exists. Furthermore, a very recent study revealed that some modifiers are particularly specific for certain polyQ proteins (Branco et al., 2008). Within this study J. Branco and colleagues compared the effect of modifiers on Htt and Ataxin-1 induced toxicity. They found several proteins exclusively modulating Ataxin-1 toxicity, such as heat-shock RNA ω (Hsr ω) or Nucleoporin-44A (Nup44A). Moreover, they identified other proteins which modulate Htt and Ataxin-1 toxicity but in opposite ways such as AKT1. They demonstrated e.g. that AKT1 enhances Ataxin-1 induced toxicity but suppresses the toxicity of mutant Htt (Branco et al., 2008).

To put the results of Htt toxicity and aggregation modulator screens into context, the identified protein "hits" can be linked to other types of screening experiments such as disease related changes of gene expression patterns. The identified modifier proteins can then be linked with each other and with known components of disease-related protein signaling pathways via protein-protein network analysis. Such approaches allow a very detailed insight into signaling networks and cellular mechanisms contributing to a particular disease, such as HD (van Ham et al., 2009). In the future, the detailed knowledge of the cellular processes which are affected in the disease might offer a way for therapeutic interventions to specifically target mechanisms in distinct stages of the disease development and progression.

Against the background of this systems biology approach which connects the whole network of intracellular processes to the pathogenesis of a distinct disease, the present study employs a small scale protein modifier screen on Htt-induced cytotoxicity. From the modifiers identified in the screen DDX24 was selected to analyze its effect as a toxicity suppressor or enhancer, in detail. The study investigated the influence of mutant Htt on intracellular DDX24 expression and, vice versa, the influence of DDX24 on the expression and aggregation of mutant Htt. An apoptosis-specific protein-protein interaction network analysis linked DDX24 to FADD, a mediator of caspase activity. Focusing on a potential role in the caspase-mediated apoptosis, the interplay between DDX24 and its interaction partner FADD was elucidated with regard to Htt-induced caspase activity. Finally, a model is proposed, suggesting a protective role of DDX24 on mutant Htt-induced caspase activity by inhibiting the death receptor-mediated apoptosis pathway.

The identification of DDX24 as a modulator of mutant Htt-induced toxicity, its characterization as a toxicity suppressor and the suggested mechanism by which it mediates the extrinsic apoptosis pathway shall be discussed in detail.

3.1 Identification of DDX24 as a modulator of mutant Htt-induced cytotoxicity

In the present study I performed an RNAi screen on 200 proteins suggested to be modifiers of mutant Htt-induced toxicity. The potential modifiers were selected according to their intracellular function and their potential involvement in HD pathogenesis. A gene ontology analysis (Figure 2.1) revealed that the selected modifiers are active in cellular pathways such as protein misfolding and degradation, transport, signaling, mitochondrial and RNA metabolism, cellular stress response, cell cycle control and apoptosis. The complete list of the selected 200 protein targets including annotations can be found in the Appendix. The RNAi screen was performed using a Neuro2a cell line which transiently expressed a truncated version of the mutant Htt protein HD320_Q68 containing a polyQ stretch with a length of 68 glutamines. Expression of the protein results in induction of caspase-3/7 activity (Figure 2.2), which was used as a read-out for mutant Htt-induced cytotoxicity. Simultaneously to the expression of the mutant Htt protein the particular target modifiers were silenced by RNAi using specific siRNA pools. The screen identified a total number of 13 reproducible genetic modifiers, which influenced mutant Htt-induced caspase activity. The screening hits were classified into toxicity suppressors (Table 2.1) and toxicity enhancers (Table 2.2), depending on whether their downregulation increased or lowered Htt-induced caspase activity (Chapter 2.1.1., Figure 2.5). Seven targets were identified as toxicity suppressors (MAD2L1, IMMT, TARBP1, TARBP2, SQSTM1, ARPC1B, NR4A1), while six were found to be toxicity enhancers (PFN2, RNF146, CEP1, DDX24, MAP3K11, SH3GL1).

The majority of these toxicity modifiers are involved in cellular processes which were previously shown to be directly or indirectly affected in HD. Two of the modifiers are linked to HD by direct interaction with Htt. The inner mitochondrial membrane protein IMMT was found to interact with Htt in a pull-down screen by L. Kaltenbach and colleagues (Kaltenbach et al., 2007). In a very recent study PFN2 was identified as an inhibitor of Htt aggregation by directly binding to Htt (Shao et al., 2008). The CEP1 gene product is involved in SNARE mediated vesicle fusion (Gromley et al., 2005) and other proteins acting in this process have been demonstrated to influence mutant Htt toxicity in *Drosophila* (Kaltenbach et al., 2007).

Several identified modifiers might exert an indirect influence on mutant Htt. The protein coded by SQSTM1 acts in NF-kappaB signaling as a ubiquitin binding protein. It was found to colocalize with neurofibrillary tangles and Lewy bodies in neurons from Alzheimer's and Parkinson's disease patients (Zatloukal et al., 2002). NR4A1 acts as steroid receptor and recent studies have demonstrated steroid receptors to be impaired in HD (Hoon et al., 2006; Schiffer et al., 2008; Chandra et al., 2008). The signaling proteins endophilin-A2 (SH3GL1) and MAP3K11 are linked to HD as well. Members of the Endophilin family were found to interact with Htt modulating its toxicity in yeast (Ralser et al., 2005). MAP3K11 acts in the JUN N-terminal pathway, which

is implicated to be important for Htt toxicity (Liu et al., 2000; Merienne et al., 2003; Perrin et al., 2008). The transcription regulator TARBP2 regulates PKR activation which is increased in HD and other neurodegenerative disorders contributing to transcriptional dysregulation and extrastriatal degeneration (Peel et al., 2001; Peel, 2004; Bando et al., 2005).

One interesting group of modifiers (TARBP1, TARBP2 and DDX24) is involved in RNA-metabolism including regulation of transcription/translation (Wu-Baer et al., 1995; Gatignol et al., 1991; Haase et al., 2005). mRNA-metabolism was found to be a molecular process, which is specifically involved in polyQ disorders (van Ham et al., 2009). Unlike TARBP1 and TARBP2, the intracellular function of DDX24 is not clearly determined yet. In the RNAi screens performed in the present study DDX24 was reproducibly identified as a toxicity modifier (three positives; Table 2.2). The protein belongs to the DEAD-box protein family which facilitates cellular RNA-metabolism processes such as transcription, translation, RNA transport and RNA decay, just to mention a few (Linder, 2006). The DEAD-box protein family is characterized by a highly conserved domain structure which is required for RNA-binding and ATP hydrolysis. Only little is known about the role of this protein family in the context of neurodegenerative disorders (Crockner et al., 2006), but some family members such as DDX5 (p68) and DDX3 have been previously demonstrated to be involved in apoptosis and survival signaling (Rossow et al., 2003; Wilson et al., 2004; Bates et al., 2005; Li et al., 2006).

RNA binding proteins were previously identified as an important group of toxicity modulators in HD (Wytenbach et al., 2001; Kita et al., 2002) as discussed above. Furthermore, DEAD-box proteins were found to be involved in apoptosis regulation (Rossow et al., 2003; Wilson et al., 2004; Bates et al., 2005; Li et al., 2006). These findings accompanied by the highly reproducible outcome of DDX24 as a toxicity modulator and the limited knowledge about the role of DEAD-box protein family members in neurodegenerative disorders prompted me to further investigate DDX24. For this purpose I used HD model systems such as a transiently transfected Neuro2a cell line, two stably transfected PC12 cell lines and a transgenic HD mouse model.

3.2 Cellular models for mutant Htt-induced caspase activation

3.2.1 Mammalian cell models to monitor cellular toxicity of mutant Htt

While a Neuro2a cell line was used to perform the RNAi screens to identify protein modulators of Htt-induced toxicity (Chapter 2.1), variations in the experimental reproducibility were observed during the screening process. These were likely caused by differing transfection efficiencies in the experiments. Thus, I decided to use a PC12 cell model in which Htt is stably transfected to verify

the results I obtained in the Neuro2a cells regarding the identification of DDX24 as a Htt toxicity modulator and to investigate its role in mutant Htt-induced caspase activity in detail.

The PC12 cells express a truncated N-terminal fragment of Htt exon1 (Htt25Q-EGFP or Htt103Q-EGFP) after induction with muristerone. Both proteins consist of the amino acids 1 to 17, the polyQ-repeat region with 25 or 103 glutamines, respectively, and are fused to a C-terminal EGFP-tag (Apostol et al., 2003; Figure 2.6). Htt103Q-EGFP expressed in these cells was previously demonstrated to form aggregates which can be detected by a filter retardation assay (Figure 2.8) and by fluorescence microscopy (Figure 2.9). By contrast, Htt25Q-EGFP does not aggregate and is diffusely distributed in the cell body (Figure 2.8 and 2.9).

3.2.2 Htt103Q-EGFP increases caspase-3/7, caspase-8 and caspase-9 activity in PC12 cells

The PC12 cell line was created by B. Apostol and colleagues in 2003. In their study they demonstrated that the expression of Htt103-EGFP does not affect the cell viability determined by trypan-blue staining, a DNA-fragmentation assay and a metabolic viability test (Apostol et al., 2003). In a later study, however, they found that caspase-3 is upregulated and activated in Htt103Q-EGFP expressing cells (Apostol et al., 2006). In my study three members of the caspase family were tested for their activation in cells expressing Htt103Q-EGFP, namely caspase-3/7, caspase-8 and caspase-9. In agreement with the findings by Apostol and colleagues I could demonstrate that Htt103Q-EGFP expression indeed induces caspase-3/7 activity, while the expression of Htt25Q-EGFP has no effect (Figure 2.10 A). A similar result could be obtained for caspase-8 which is activated in cells expressing Htt103Q-EGFP (Figure 2.10 B and 2.16), but not in Htt25Q-EGFP expressing cells (Figure 2.10 B). In addition, I could demonstrate that caspase-9 activity is induced by recombinant Htt103Q-EGFP expression (Figure 2.16).

Caspase-8 activation

Several studies have demonstrated that caspases are activated in the brain of HD patients (Vis et al., 2005; Kiechle et al., 2002) such as caspase-3, -8 and -9, which were analyzed in the present study. Htt was found to induce the activity of these proteases via various mechanisms. In 2000, A. Hackam and colleagues demonstrated that Htt influences the activity of caspase-8 and subsequently of caspase-3 via its interaction with HIP1 (huntingtin interacting protein 1) in cell culture models (Hackam et al., 2000). Free HIP1 was found to interact with HIPPI (HIP1 interacting protein) resulting in a complex formation followed by recruitment and activation of caspase-8 (Chapter 1.1.8). This leads to activation of the downstream effector caspase-3, eventually resulting in apoptosis via the extrinsic pathway. In the non-disease state HIP1 is bound by wild-type Htt which prevents the formation of the caspase-8 activating HIP1/HIPPI complex. Mutant Htt can also bind HIP1 but with lower binding affinity than the wild-type protein facilitating the liberation

Discussion

of free HIP1 and the formation of the HIP1/HIPPI complex (Gervais et al., 2002). Moreover, the HIP1/HIPPI complex is assumed to translocate into the nucleus where it interacts with the putative promoters of caspase-1, caspase-8 and caspase-10, increasing the expression of the caspase genes (Majumder et al., 2007a; 2007b). Free HIP1 also acts as a pro-apoptotic factor by itself, triggering apoptosis following the intrinsic pathway (Hackam et al., 2000; Choi et al., 2006), which might result in the activation of caspase-3.

Caspase-9 activation

Besides the induction of caspase-8 activity mutant Htt was demonstrated to influence the activity of caspase-9. In 2001, it was shown that overexpression of wild-type Htt results in reduced caspase-9 and caspase-3 activation after apoptotic stimulation in cell culture models (Rigamonti et al., 2001). Wild-type Htt supposedly blocks the formation of the apoptosome complex (see Chapter 1.2.2; Rigamonti et al., 2001). In contrast, overexpression of mutant Htt resulted in an increased activation of caspase-9 and -3 (Rigamonti et al., 2001). Moreover, mutant Htt was found to impair the mitochondrial function by direct binding to the mitochondrial membrane (Choo et al., 2004; Panov et al., 2002), triggering membrane depolarization. It also indirectly induces membrane depolarization by transcriptional dysregulation of proteins involved in the respiratory chain and mitochondrial death signaling (Bae et al., 2005; Cui et al., 2006). All three mechanisms lead to a release of cytochrome c, formation of the apoptosome complex and activation of caspase-9, and subsequently of caspase-3 (Zeron et al., 2004; Green and Reed, 1998). In an apoptosome independent pathway cytosolic caspase-9 (caspase-3) is activated in the misfolded protein response pathway as a result of ER stress, which is induced by mutant Htt accumulation (Morishima et al., 2002; Rao et al., 2002).

Caspase-3 activation

In addition to its influence on the initiator caspases (caspase-8 and -9) which indirectly leads to caspase-3 activation, Htt was also demonstrated to directly modulate the activity of the effector caspase-3. A recent study by Y. Zhang and colleagues demonstrated that wild-type Htt binds to active caspase-3 and inhibits its proteolytic activity. Mutant Htt was found to bind caspase-3 as well, but with a much lower affinity, resulting in higher levels of active caspase-3 and cell death (Zhang et al., 2006). Moreover, caspase-3 expression was demonstrated to be upregulated and activated in the PC12 cell model which was applied in this present study (Apostol et al., 2006).

My findings that the caspases-3/7, -8 and -9 are activated in PC12 cells expressing Htt103Q-EGFP are in agreement with the observations presented in the literature. The PC12 cells thus model the key aspects of mutant Htt-induced activation of caspase-8 and -9 as well as caspase-3. It should thus be an appropriate system to study the mechanism of DDX24-mediated Htt toxicity.

3.3 DDX24 mediates mutant Htt-induced caspase activation

3.3.1 Knock-down of DDX24 increases mutant Htt-induced caspase-3 activity

In the apoptotic signaling cascade caspases are activated as a result of particular stimuli (Earnshaw et al., 1999). Mutant Htt directly influences the activation of caspases and some of the apoptotic stimuli as described in the previous paragraph (Apostol et al, 2006; Gervais et al., 2002; Rigamonti et al., 2001; 2000; Zhang et al., 2006; Chapter 3.2.2). In this study I first focused on the activation of caspase-3 which serves as an effector caspase mediating cell death in both, the extrinsic and the intrinsic apoptosis pathway (Cryns and Yuan, 1998; Chapter 1.2.3). I discovered an enhancing effect of DDX24 silencing on Htt-induced caspase-3 activation in an RNAi experiment. When endogenous DDX24 was silenced in PC12 cells expressing Htt103Q-EGFP, an increase in caspase-3 activity was obtained in comparison to the controls without DDX24 silencing (Figure 2.14). A possible problem in this experiment could be a nonspecific caspase activation as a result of an RNAi off-target effect. Off-target effects are a central problem in using RNAi techniques and might occur as a result of the two following mechanisms. On the one hand the double stranded siRNAs can activate non-specific cellular innate immune responses, such as the interferon response (Bridge et al., 2003; Sledz et al., 2003). On the other hand synthetically produced siRNAs may inadvertently show complementarity to other mRNAs of non-target genes (Jackson et al., 2003; 2006). Thus, RNAi is not always entirely specific and confirmation of the specificity, and hence the validity, of the results is an essential part of RNAi experiments. Considering this, I first demonstrated the efficiency (Figure 2.11) and specificity of the RNAi-mediated DDX24 knock-down (Figure 2.12). As shown in Figure 2.15, I could demonstrate that the effect of DDX24 on Htt-induced caspase activity is specific for the expression of the Htt103Q-EGFP protein, since the knock-down of DDX24 in cells expressing Htt25Q-EGFP did not affect caspase-3 activity. From this result I conclude that DDX24 specifically suppresses mutant Htt-induced caspase-3/7 activity.

3.3.2 Htt-induced caspase-8 and -9 activity is increased by DDX24 silencing

In order to verify whether the activation of caspase-3 is triggered via the extrinsic (caspase-8 mediated) or intrinsic (caspase-9 mediated) apoptosis pathway additional RNAi experiments were performed. In PC12 cells expressing Htt103Q-EGFP the effect of DDX24 protein knock-down on the activities of caspase-8 and caspase-9 was investigated. Caspase-8 plays a major role in receptor-mediated apoptosis signaling (extrinsic pathway) and I could demonstrate that PC12 cells express-

ing Htt103Q-EGFP show significantly increased caspase-8 activity if DDX24 is silenced by RNAi (Figure 2.17 A) compared to the controls in which DDX24 protein levels were not reduced.

A similar effect was obtained for the activation of caspase-9 (Figure 2.17 B) which is a component of the apoptosome complex. Caspase-9 is known to be a key player of the mitochondrial (intrinsic) apoptosis pathway activating caspase-3 (Chinnaiyan, 1999; Hill et al. 2004; Chapter 1.2.2). In PC12 cells expressing Htt103Q-EGFP caspase-9 activity was increased by endogenous DDX24 protein silencing. These results suggest that activation of caspase-3 by DDX24 is not exclusively mediated through the extrinsic or the intrinsic pathway but that both contribute to caspase-3 activation. A crosstalk between extrinsic and intrinsic apoptosis signaling is mediated by cytosolic BID, which is proteolytically cleaved into tBID by active caspase-8. Activated tBID subsequently translocates to the mitochondrial membrane and initiates the intrinsic pathway (Esposti, 2002; Chapter 1.2.1).

Silencing of DDX24 led to increased caspase activity in the presence of mutant Htt, but the toxicity did not increase in the absence of Htt expression nor in the presence of Htt25Q-EGFP. This finding suggests that DDX24 does not act as a direct activator of caspases. Thus, DDX24 may rather be related to signal transmission than directly activate the caspase cascade. From the literature other members of the DEAD-box protein family have been found to play a role in the caspase activation cascades. Recent studies suggested RIG-1 (retinoic acid-inducible gene I) also termed DDX58 and MDA-5 (melanoma differentiation-associated antigen 5), to be directly involved in the activation of caspase-1 and caspase-3 (Rintahaka et al., 2008). Both act via the mitochondrial antiviral signaling protein pathway which induces activation of caspase-9 and Apaf1 (Besch et al., 2009). The studies of J. Rintahaka and R. Besch applied protein overexpression or activation of RIG-1/MDA-5 to induce the apoptotic pathway, postulating an activating function of both proteins (Rintahaka et al. 2008; Besch et al., 2009). In contrast to the activation of caspases by overexpression of RIG-1/MDA-5, the present study suggests an inhibitory function for the DEAD-box protein DDX24 whose downregulation resulted in an enhanced activity of the caspases.

3.4 Overexpression of human DDX24 inhibits mutant Htt-induced caspase activation

Since RNAi-mediated DDX24 knock-down increased mutant Htt-induced caspase activity, it was next investigated whether overexpression of human DDX24 is able to rescue the effect of protein silencing. DDX24 was reduced by RNAi in Htt103Q-EGFP expressing cells which were transfected with an expression plasmid encoding a human HA-DDX24 fusion protein. Rat and human DDX24 sequences are sufficiently dissimilar that one of the four siRNAs used in my experiments efficiently targeted endogenous rat DDX24 but not the human DDX24 mRNA (Figure 2.19). Samples only treated with DDX24 specific siRNA which were used as controls showed high activities of caspase-3 and caspase-8 (Figure 2.20). However, in cells additionally expressing HA-DDX24 the toxicity-

increasing effect of the knock-down was reduced significantly (Figure 2.20). The observation that HA-DDX24 overexpression is able to rescue caspase-3/7 and caspase-8 activity strengthens the hypothesis that DDX24 influences Htt-induced caspase activity in an inhibitory manner. Furthermore, the observations allow the conclusion that DDX24 might primarily mediate Htt-induced caspase activity via the extrinsic pathway by acting upstream of caspase-8.

It has been reported in the literature, that DEAD-box proteins can indeed act as negative regulators in receptor-mediated apoptosis signaling. Very recently the DEAD-box protein DDX3 was found to fulfill an inhibitory function in the extrinsic apoptosis signaling pathway by forming an anti-apoptotic protein complex at the death receptor (Sun et al., 2008). The formation of this complex was demonstrated to prevent activation of caspase-8 (Sun et al., 2008). In a second study GRTH (Gonadotropin-regulated testicular helicase; DDX25) was shown to act as a negative regulator of the TNFR1 (tumor necrosis factor receptor 1) mediated caspase pathway (Gutti et al., 2008). This protein was found to promote NF-kappaB function to control apoptosis in spermatocytes of adult mice via transcriptional regulation (Gutti et al., 2008). It seems possible that DDX24 might influence caspase activation either directly by interactions with other proteins of the caspase signaling cascade or indirectly by regulating gene expression of pro- or anti-apoptotic factors.

3.5 Mutant Htt expression and aggregation induces DDX24 transcription

The findings discussed in Chapter 3.3 and 3.4 reveal the possibility that DDX24 might act protectively in mutant Htt-induced apoptosis signaling. Htt expression and aggregation may thus affect the expression of DDX24.

3.5.1 Mutant Htt expression leads to dysregulated gene expression

Wild-type Htt is known to influence the transcriptional regulation of other genes. The presence of mutant Htt leads to transcriptional dysregulation, which is regarded as one of the characteristics in HD (Sugars and Rubinsztein, 2003; Cha, 2007; Chapter 1.1.8). Within the past years numerous studies concentrated on the characterization of mutant Htt-induced changes in gene expression using various HD models such as cell culture systems (Kita et al., 2002; Sipione et al., 2002; Wyttenbach et al., 2001; Apostol et al., 2006; Lee et al., 2007; Runne et al., 2008) and transgenic HD mice (Luthi-Carter et al., 2000; Crocker et al., 2006; Kuhn et al., 2006; Brochier et al., 2008; Lorincz and Zawistowski, 2009). Other groups studied the expression profiles in blood or brain material derived from HD patients (Lovrecic et al., 2009; Anderson et al., 2008; Hodge et al., 2006; Borovecki et al., 2005). Taken together these studies identified many genes involved with various cellular functions that are dysregulated in HD (Cha, 2007).

Discussion

The affected physiological functions include changes in genes encoding *neurotransmitters and receptors* such as the dopamine receptors D1 and D2, whose mRNA levels were found to be altered in the caudate nucleus of HD brains (Augood et al., 1997; Runne et al., 2008). Moreover, subunits of the NMDA glutamate receptors were found to be decreased in the caudate and putamen of HD patients (Arzberger et al., 1997) and in HD cell models (Apostol et al., 2006). Other dysregulated genes are involved in *transcription regulation* such as ARIX (Arix1 homeodomain protein) or TP53 (p53) (Apostol et al., 2006; Kita et al., 2002); p53 itself regulates expression of genes in apoptosis/survival. Another group of genes which expression is altered in HD is coding for proteins of the *ribosomal protein* family (Crocker et al., 2006; Kita et al., 2002). Moreover, genes have been identified to be dysregulated which encode proteins which are involved in *signal transmission*. For example G-protein signaling proteins (Hodge et al., 2006; Runne et al., 2008; Luthi-Carter et al., 2000) or protein kinases such as PKC (protein kinase c) family members were identified (Wytttenbach et al., 2001; Sipione et al., 2002). Furthermore, expression changes have been found for genes encoding proteins involved in *intracellular transport* and *vesicle trafficking* such as sortilin1 (SORT1), sirpa (SHPS-1) or mitochondrial import receptor subunit TOM70 (TOMM70A) (Wytttenbach et al., 2001; Sipione et al., 2002).

In addition, altered gene expression was observed for well known *cell death* regulators. This includes proteins of the inflammatory response signaling like I κ B-alpha or NF-kappaB binding subunit (Apostol et al., 2006; Luthi-Carter et al., 2000). Moreover, the expression of transcription factors such as ID1 and p53 which regulate genes of apoptosis/survival pathways like LGADD34, GADD45, p21 and 14-3-3 Bcl-2 and BAX have been demonstrated to be altered in HD cell models (Wytttenbach et al. 2001; Sipione et al. 2002; Apostol 2006 Kim et al., 2007). Furthermore, genes encoding proteins which are involved in the apoptotic caspase cascade such as caspase-3 and caspase-2 have been found to be dysregulated in cell culture models (Apostol et al., 2006). Interestingly, the DEAD-box protein DDX5 (p68) was identified to be upregulated as a consequence of mutant Htt expression in mouse striatal tissue (Crocker et al., 2006). DDX5 acts as a co-activator of p53 and is involved in the cellular response to DNA damage (Bates et al., 2005; Chapter 3.5.3).

Importantly, cells were shown to specifically upregulate proteins involved in defense mechanisms protecting the cell against Htt-induced cytotoxicity. This includes genes of the cellular stress response pathways such as genes of heat-shock response and the unfolded protein response. Several molecular chaperones and heat-shock factors such as HSF1, Hsp70, Hsp27, Hsp40 and BiP/GRP78 (Westerheide and Morimoto, 2005; Morely et al., 2002; Mu et al., 2008; Apostol et al., 2006; Runne et al., 2008) have been demonstrated to be upregulated as a result of intracellular protein aggregation. The increased expression of chaperones confers protection against polyQ toxicity (Morley et al., 2002).

3.5.2 Expression of mutant Htt increases DDX24 mRNA levels in PC12 cells

The results obtained from the previously discussed RNAi and toxicity rescue experiments suggest that DDX24 might act as a protective factor attenuating Htt-induced cytotoxicity. Following this idea, a possible intracellular defense mechanism could be the upregulation of DDX24 to strengthen its protective influence. In order to observe the effect of mutant Htt expression and aggregation on DDX24 transcription, the DDX24 mRNA levels were quantified in the PC12 cell system as well as in a HD mouse model. PC12 cells were induced to express Htt103Q-EGFP or Htt25Q-EGFP protein, respectively, for 48 hours. Relative quantities of endogenous DDX24 transcript were determined by real-time PCR analysis. As shown in Figure 2.21, cells expressing Htt103Q-EGFP possessed ~ 50 % higher DDX24 mRNA levels than the solvent treated controls. In contrast, Htt25Q-EGFP expressing cells did not show changes in DDX24 transcription compared to the corresponding control (Figure 2.21).

A gene expression study using a rat genome microarray analysis has been performed previously in the same Htt103Q-EGFP expressing PC12 cell line (Apostol et al., 2006). In contrast to the present study, B. Apostol and colleagues were not able to identify DDX24 to be upregulated in the presence of Htt103Q-EGFP, which can be explained by the lack of DDX24 specific oligonucleotide probes on the microarray used in their study. However, they showed changes in genes involved in apoptosis signaling, including enhanced expression of the gene coding for caspase-3 which fits to my observation that caspase-3 is highly activated in PC12 cells expressing the Htt103Q-EGFP protein.

Additionally to DDX24 and DDX5/p68 (Chapter 3.5.3), another RNA binding protein - Rmb3 (RNA binding motif 3) - has been identified to be dysregulated in PC12 cell culture models of HD (Wytttenbach et al., 2001; Kita et al., 2002). Contrary to DDX24 and DDX5, Rmb3 expression was found to be downregulated as a result of mutant Htt expression (Wytttenbach et al., 2001; Kita et al., 2002). Overexpression of Rmb3 was also shown to reduce Htt-induced apoptosis (Kita et al., 2002) and the authors therefore conclude a protective function for Rmb3 (Kita et al., 2002). Just like DDX24, Rmb3 is assumed to be involved in RNA metabolism, but its intracellular function is still unknown.

3.5.3 Transgenic HD mice exhibit enhanced DDX24 transcription

The striatal brain region is severely affected by neuronal cell death in HD (Vonsattel et al., 1985). Thus, potential changes in DDX24 mRNA were investigated in striatal tissue samples from transgenic N171-82Q HD mice by quantitative real-time PCR analysis. In 15 weeks old transgenic mice DDX24 mRNA levels were found to be increased by a factor of 1.3 compared to the wild-type controls, while the transcript levels did not differ in animals with 6 weeks of age (Figure 2.22).

In the year 2000 a comparative study was performed by R. Luthi-Carter and colleagues identifying transcriptional changes in the transgenic R6/2 and N171-82Q HD mouse models (Luthi-Carter et al., 2000). In their work mRNA levels of 6000 genes were screened suggesting altered levels of proteins involved in signaling pathways such as neurotransmitter release or calcium and retinoid signaling (Luthi-Carter et al., 2000). Another study by S. Crocker and colleagues investigated Htt-induced changes in gene expression patterns in the striatal region of 10 weeks old R6/2 transgenic HD mice (Crocker et al., 2006). The study revealed that genes involved in transcription, translation, protein synthesis, calcium homeostasis, ATP metabolism and DNA/RNA binding are differently expressed in HD mice compared to the wild-type controls (Crocker et al., 2006). Interestingly, the study identified the DEAD-box protein DDX5 (p68), which is upregulated in the striatal region of R6/2 transgenic mice.

One year before, DDX5/p68 had been discovered to be indirectly involved in apoptosis induction by acting as a co-activator of the p53 tumor suppressor (Bates et al., 2005) which in turn induces transcription of pro-apoptotic genes such as BAX (see Chapter 1.2.1 and 1.2.2; Vogelstein et al., 2000). In contrast to the observed effects of DDX24 on the induction of apoptosis shown in the present study, RNAi depletion of DDX5/p68 caused a reduction of p53-dependent apoptosis. This suggests that DDX5 influences apoptosis by a different mechanism than DDX24.

Thus, DDX24 represents the second member of the DEAD-box protein family whose expression is upregulated in the striatum of a transgenic HD mouse model. The gene expression studies performed in PC12 cell culture and HD mouse striatal tissue have demonstrated the upregulation of DDX24 transcription as a result of mutant Htt expression. Combined with the findings from the knock-down experiments and the results obtained in the toxicity rescue experiments, I conclude that DDX24 might have a protective function in HD pathogenesis.

No correlation between stress conditions and the expression of other DEAD-box protein family members has been found in animals or humans yet. However, in plants upregulation of stress responsive DEAD-box helicases has been shown to play an important role in facilitating antibiotic stress tolerance by regulating transcription and expression of stress response genes (Vashisht and Tuteja, 2006).

3.5.4 Transgenic N171-82Q mice show reduced DDX24 protein levels

Contrary to the enhanced expression levels of DDX24 transcript in Htt103Q-EGFP expressing PC12 cells and in striatal tissues of transgenic N171-82Q mice, no effect on the DDX24 protein levels in cells expressing Htt103Q-EGFP could be detected by Western blotting. In brain tissues derived from HD transgenic mice even a reduction in the DDX24 protein levels was observed by Western blot analysis (Figure 2.23). The reduction of endogenous DDX24 protein levels although mRNA levels are increased may have the following reasons.

On the one hand, the increased amount of DDX24 protein could be degraded by the ubiquitin-proteasome system (UPS) which is activated as a result of mutant Htt expression (Díaz-Hernández et al., 2003; Bett et al., 2006). However, the activation of the UPS in HD is controversially discussed, since conflicting results have been obtained in studies using different HD model systems. The studies of M. Díaz-Hernández and J. S. Bett demonstrated increased proteasomal peptidase activities in brain extracts of HD mouse models. By contrast, other groups have shown no change in UPS activity by demonstrating that the proteasomal peptidase activities do not differ in cells expressing protein fragments of mutant or wild-type Htt (Ding et al., 2002). A similar lack of UPS upregulation was demonstrated in vulnerable neurons of a HD mouse model (Bowman et al., 2005). Other groups have found a decrease in proteasome activity in response to mutant Htt expression giving evidence for an impairment of the UPS in HD. Studies in the labs of R. Kopito and N. Nukina showed that transiently expressed mutant Htt caused inhibition of the ubiquitin-proteasome system in cell culture (Bence et al., 2001; Jana et al., 2001; Chapter 1.1.7).

Another explanation for the reduced amounts of DDX24 protein detected by Western blotting is an increase in the proteolytical cleavage of DDX24 resulting in reduced levels of full size DDX24 protein. This hypothesis might be supported by the fact that DDX24 contains a potential caspase-3 cleavage site. Caspase-3 is able to cleave substrates at a DXXD-like amino acid sequence and was shown to cleave the RB (retinoblastoma) protein at a sequence DEAD (Asp-Glu-Ala-Asp) (Jänicke et al., 1996) which corresponds to the name giving ATP binding motif II in the DEAD-box protein family members (Chapter 1.4; Figure 1.5 and 1.6). Two studies addressing the function of DEAD-box protein 3 (DDX3) obtained a cleavage product as a result of apoptosis activation (Li et al., 2006; Sun et al. 2008). Thus, one can speculate that this might also apply to other DEAD-box proteins acting in caspase activation pathways. Following this hypothesis DDX24 could be a substrate for activated caspase-3 and might be cleaved and degraded under stress conditions such as the expression of mutant Htt. However, I did not detect additional cleavage bands on the immuno blot of PC12 cells expressing mutant Htt, thus this hypothesis can currently only be regarded as speculation.

3.6 DDX24 does not affect mutant Htt expression and aggregation

The experiments discussed before suggest DDX24 to play a protective role in Htt-induced caspase activation. In this context DDX24 might affect two different processes which are implicated in Htt-induced toxicity. On the one hand DDX24 could play a role as an activator or inhibitor of apoptosis pathways induced by mutant Htt. On the other hand, it may exert influence on mutant Htt itself by either modulating the expression of the protein, its aggregation propensities or its degradation.

In Chapter 3.6.1 I will discuss the properties of DDX24 regarding Htt expression, aggregation and degradation.

3.6.1 DDX24 does not influence mRNA transcription of mutant Htt

In a genome-wide RNAi screen for enhancers of protein aggregation in a *C. elegans* model of polyQ disease E. Nollen and colleagues identified modulator proteins which belong to many different cellular pathways such as RNA metabolism, protein synthesis, protein folding and protein degradation (Nollen et al., 2006). As DDX24 is a member of the DEAD-box family it is possible that it plays a role in regulatory processes of mRNA transcription or translation and protein biosynthesis in the ribosome. Acting in one of these processes DDX24 might be able to influence the gene expression of mutant Htt.

Following the process of protein biosynthesis from gene transcription to protein translation I first focused on the transcription of the Htt103Q-EGFP mRNA. The regulation of Htt gene expression has not been well studied yet. However, a study by Z. Feng and colleagues demonstrated that the tumor suppressor p53 activates Htt mRNA transcription under stress conditions (Feng et al., 2006). The tumor suppressor p53 itself has been demonstrated to be activated by the DEAD-box protein DDX5 (Bates et al., 2005), which was further identified as a protein upregulated in the striatum of HD mice (Crocker et al., 2006). This suggests a possible function of DEAD-box proteins in the transcriptional regulation of Htt.

To address the question whether DDX24 influences Htt-induced cytotoxicity by acting as a component of the *IT15* gene transcription machinery, PC12 cells were induced for Htt103Q-EGFP expression and DDX24 was silenced by RNAi. The relative quantities of Htt and DDX24 transcripts were determined by real-time PCR analysis. As displayed in Figure 2.24 A, endogenous silencing of DDX24 did not reveal significant changes in relative Htt mRNA levels. This result contradicts the hypothesis that DDX24 regulates Htt expression by influencing its mRNA transcription.

3.6.2 Protein expression of mutant Htt is not affected by DDX24

As a second possibility DDX24 might play a role in translation or protein synthesis, thus influencing intracellular Htt protein levels. The DDX24 protein contains a RNA binding domain (Zhao et al., 2000; Chapter 1.4.1) which is characteristic for its protein family (Svitkin et al., 2001; Chapter 1.4). Via this domain DDX24 could theoretically bind to mRNA molecules and modulate the translation process resulting in altered Htt protein levels. The yeast homologue of DDX24, Mak5, was found to be a component of a multiprotein complex facilitating biosynthesis of the 60S ribosome subunit (Zagulski et al., 2003), which is in turn obligatory for the biosynthesis of proteins. According to

the current state of knowledge modulators of Htt protein biosynthesis are not known from the literature.

In order to investigate whether DDX24 influences Htt protein biosynthesis in mammalian systems, similar to its homologue Mak5 in yeast, DDX24 was silenced in Htt103Q-EGFP expressing PC12 cells by RNAi. The Htt103Q-EGFP protein levels were detected by Western blot analysis. As shown in Figure 2.24 B, the Htt protein levels in cells silenced for DDX24 expression do not differ from those obtained in control cells. From this result can be concluded that DDX24 silencing does not affect Htt protein biosynthesis. Thus, DDX24 most likely does not influence the translation Htt mRNA.

3.6.3 DDX24 does not interact with mutant Htt aggregates

As a third possibility, DDX24 might directly modulate Htt-induced toxicity by influencing its aggregation state. In a study by H. Goehler in 2004, GIT1 (G-protein-coupled receptor kinase-interacting protein 1) was identified as a direct interaction partner of DDX24. Within the same study GIT1 was identified as a genetic modifier stimulating Htt aggregation. Moreover, it was demonstrated that GIT1 associates with wild-type Htt, colocalizes to mutant Htt aggregates and accumulates in inclusion bodies in the brains of a HD mouse model as well as HD patient brains (Goehler et al., 2004). Thus, GIT1 might provide a link between Htt and the DEAD-box protein and all three proteins might be part of a protein complex modulating mutant Htt aggregation.

An immunofluorescence experiment was performed in PC12 cells in order to investigate the possible intracellular interaction of DDX24 with aggregated Htt103Q-EGFP (Figure 2.25). For the analysis of the intracellular distribution of DDX24 cells were immunostained for DDX24 and Htt inclusions were visualized by excitation of the EGFP-tag of the fusion protein. However, DDX24 did not colocalize to the Htt103Q-EGFP inclusions (Figure 2.25 upper panel). This result indicates that DDX24 does not interact with insoluble mutant Htt aggregates.

3.6.4 Aggregation of mutant Htt is independent of DDX24 function

A direct protein-protein interaction represents only one possible way for DDX24 to modulate mutant Htt aggregation. From the literature many proteins have been identified to modulate aggregation without direct binding to Htt. For example heat-shock-factor 1 (HSF1) which regulates heat-shock protein expression was found to act as a suppressor of polyQ aggregation (Nollen et al., 2004). Besides the inhibition of Htt aggregate formation a second way to modulate Htt aggregation would be by increasing the clearance and degradation of accumulated Htt from the cell. This can be accomplished by proteasomal protein degradation as it was demonstrated for the overexpression of the E3-ubiquitin ligase parkin which was found to promote clearance of expanded polyQ

proteins by activating the proteasomal degradation machinery (Tsai et al., 2003). An additional mechanism to remove accumulated proteins from the cell is the autophagy-mediated clearance. In 2006, A. Yamamoto and colleagues identified several proteins in a cell-based functional genetic screen which are required for the clearance of mutant Htt aggregates and which are upregulated by mutant Htt expression (Yamamoto et al., 2006). In their study they focused on the effect of IRS-2 (insulin receptor substrate 2), a mediator of the insulin signaling pathway which was identified to activate autophagy-mediated clearance resulting in reduction of aggregated Htt without directly binding to mutant Htt (Yamamoto et al., 2006).

In order to investigate whether DDX24 influences mutant Htt aggregation, a time course experiment was performed monitoring the progression of aggregate formation in cells endogenously silenced for DDX24. PC12 cells were induced for Htt103Q-EGFP expression and aggregate formation was monitored over an incubation time of 72 hours. Simultaneously, endogenous DDX24 protein levels were reduced by RNAi. Figure 2.26 shows the amount of Htt aggregates in the cell lysates from DDX24 knock-down cells and controls. The amount of aggregates detected was found to be similar in all samples independently of the endogenous DDX24 silencing. This result was confirmed by analysis of intracellular Htt103Q-EGFP aggregates using fluorescence microscopy (Figure 2.27).

Summarizing these observations, I can conclude that DDX24 neither affects the expression of the Htt103Q-EGFP protein, nor the formation or degradation of aggregates which are detected by filter retardation assay or visible under the fluorescence microscope. Thus, the findings suggest that DDX24 does not participate in cellular protein degradation processes such as autophagy-mediated clearance or protein degradation via the UPS pathway. With regard to the colocalization study I can further exclude an influence of DDX24 on aggregation (and subsequently on Htt-induced cytotoxicity) via a direct interaction with Htt103Q-EGFP.

From this I assume that DDX24 influences Htt-induced caspase activity by a process which is independent of Htt expression and the formation of aggregates or their degradation. Thus, I subsequently investigated the hypothesis that DDX24 influences mutant Htt-induced cytotoxicity downstream of Htt expression and aggregation by mediating the signaling pathways that lead to caspase activation and apoptosis.

3.7 Interaction of DDX24 with the apoptosis mediator FADD

To better understand the function of uncharacterized proteins it is often useful to identify interaction partners which may provide a link between the protein of interest and cellular processes and pathways. In this study, I performed a search for DDX24 interaction partners using the *UniHI* database (Chaurasia et al., 2007; 2009; Figure 2.28). I found a direct interaction between DDX24 and the apoptosis mediator FADD, which acts as an adaptor protein at the death receptor, mediating apoptosis via activation of caspase-8 in the extrinsic apoptosis signaling pathway (Chapter 1.2.1;

Discussion

Figure 1.3). Since DDX24 was found to influence Htt-induced caspase-8 and caspase-3 activation, I hypothesized that the modulating effect might be mediated via the interaction with FADD. To confirm the interaction between DDX24 and FADD several independent methods were applied. First, I performed a co-immunoprecipitation (Co-IP) experiment in HEK293 cells (Chapter 2.6.1; Figure 2.29). The postulated interaction between DDX24 and FADD was confirmed by immunoblotting. Next, I used the LUMIER method (description see Chapter 4.2.2) to validate the binding of DDX24 and FADD (Figure 2.30). Furthermore, I analyzed the interaction by FRET assay (Figure 2.32; Chapter 4.2.3) using DDX24 and FADD ECFP- and EYFP-fusion proteins. Finally, I confirmed the interaction between DDX24 and FADD by overexpression of both proteins as HA- and Myc-fusions in PC12 Htt103-EGFP cells and immunofluorescence staining. The staining revealed a colocalization of the proteins in presence and absence of Htt103Q-EGFP protein (Figure 2.33). I found that all methods confirmed the interaction between DDX24 and FADD, supporting the hypothesis that DDX24 might mediate caspase activation via an interaction with FADD.

FADD is known to be a key player in death receptor-mediated apoptosis signaling as described in Chapter 1.2.1. After activation of the death receptor, FADD is bound as an adaptor protein to the intracellular death domain of the receptor and thereby mediates the formation of the death inducing signaling complex DISC and activation of caspase-8 (Figure 1.3). The interaction between DDX24 and FADD suggests that DDX24 might influence the formation of the DISC complex. With regard to the finding that endogenous DDX24 silencing induces activity of caspase-8 in the presence of mutant Htt, I hypothesize an inhibitory function of DDX24 on the transmission of the apoptosis signal from the death receptor via binding to FADD. A competitive binding of DDX24 to FADD could either prevent the recruitment and binding of FADD to the death domains or impede binding and activation of caspase-8.

A similar function has been reported in the literature for the DEAD-box protein DDX3. DDX3 impedes TRAILR2 receptor-mediated apoptosis in resistant cancer cells by direct association with the death receptor, preventing the recruitment of FADD and caspase-8 (Li et al., 2006). However, when caspase-8 is activated DDX3 gets cleaved and dissociates from the receptor. Cleavage of DDX3 then further induces the caspase cascade, leading to a positive feedback loop in apoptosis regulation (Li et al., 2006). In a very recent study M. Sun and colleagues could demonstrate that the inhibitory effect of DDX3 can be extended to each of the four major death-inducing receptors (TRAILR1, TRAILR2, TNFR1 and FAS). Furthermore, they found that DDX3 forms an anti-apoptotic complex at the death receptor including GSK3 (Glycogen synthase kinase-3) and cIAP-1 (cellular inhibitor of apoptosis protein-1). This complex is assumed to inhibit formation of the DISC complex and activation of caspase-8 (Sun et al., 2008). In their study M. Sun and colleagues demonstrate that the stimulation of the death receptor abrogates the anti-apoptotic complex by inactivation of GSK3 and cleavage of DDX3 and cIAP-1, allowing the apoptotic signaling cas-

cade to proceed. Moreover, they show siRNA-mediated DDX3 knock-down to enhance caspase-3 activity.

In my study caspase activation was initiated by the expression of mutant Htt. This is different to the study of M. Sun in which caspase-8 activity was triggered by stimulation of the death receptors. However, the effects of DDX24 on caspase activity are similar between DDX24 and DDX3. Endogenous DDX24 silencing resulted in increased caspase-8 and caspase-3/7 activity (Figure 2.17 and 2.14) which can be partially rescued by overexpression of the human DDX24 protein (Figure 2.20). Furthermore, DDX24 interacts with the apoptosis mediator FADD (Figure 2.29/2.30 and 2.32/2.33), which suggests that it may influence its function in mediating apoptosis.

3.7.1 The role of death receptors in neurodegenerative disorders

The DDX24 interaction partner FADD is crucial for death receptor-mediated apoptosis (Figure 1.3; Chapter 1.2.1). The role of death receptor-mediated apoptosis in HD is not well studied yet, but there are some findings which might elucidate the connection between mutant Htt expression and receptor-mediated apoptosis.

Several studies have shown that expression and aggregation of mutant Htt changes the expression pattern of apoptosis related proteins (Apostol et al., 2006; Sipione et al., 2002; Wyttenbach et al., 2001). Interestingly, this group includes proteins which are related to receptor-mediated apoptosis signaling. In a study published in 2000 I. Ferrer and colleagues demonstrate reduced protein levels of FAS and FasL in caudate nucleus and putamen of HD patients (Ferrer et al., 2000). However, in a very recent study upregulation of the death receptor FAS was detected in blood and brain samples of HD patients (Anderson et al., 2008). Furthermore, a study published in 2005 revealed the upregulation of other members of the tumor necrosis factor receptor (TNFR) superfamily in HD patients blood (Borovecki et al., 2005). This points to a role of death receptor-mediated apoptosis signaling in HD pathogenesis. Additionally, changes in the gene expression levels of the FAS receptor ligand FasL have been demonstrated to occur in other neurodegenerative disorders such as Alzheimer's and Parkinson's disease. Two studies have demonstrated an increased expression of FasL in cultured neurons as well as in brains of AD patients (Morishima et al., 2001; Su et al., 2003). In addition, the study of Y. Morishima and colleagues demonstrated that the upregulation of FasL results in activation of the receptor-mediated apoptosis pathway which contributes to neuronal cell death in AD (Morishima et al., 2001). However, contrary observations have been made in studies investigating the expression of FAS/FasL in the context of Parkinson's disease. In 1996 M. Mogi and colleagues discovered an increase in the expression levels of the soluble FAS receptor in the nigro-striatal regions of PD brains (Mogi et al., 1996), but in a later study decreased expression levels of FAS and FasL were detected in brain material of PD patients (Ferrer et al., 2000).

The dysregulation in gene expression of death receptor superfamily members in HD and other neurodegenerative disorders suggests a role of the death receptor-mediated apoptosis signaling in the pathogenesis leading to cytotoxicity and neuronal cell death. However, it is unclear today whether receptor-mediated apoptosis is activated as a consequence of a primary activation of the intrinsic apoptosis signaling or whether it is activated independently.

3.8 Co-regulation of caspases by DDX24 and FADD

I found that DDX24 inhibits Htt-induced caspase activity in PC12 cells (Chapter 2.2. and 2.3). Furthermore, I was able to demonstrate the interaction of DDX24 with the apoptosis mediator FADD. Based on these findings, I hypothesize that DDX24 may counteract FADD in maintaining an activation/repression balance regulating apoptosis signaling. In order to investigate this hypothesis, simultaneous FADD overexpression and DDX24 RNAi studies were performed in the HD PC12 cell system. First of all I tested the effect of FADD overexpression on Htt-induced caspase activity. As shown in Figure 2.35, overexpression of the HA-FADD fusion protein results in increased activity of caspase-3, caspase-8 and caspase-9. This effect is independent of the expression of Htt103Q-EGFP. However, the caspase activities in cells expressing high amounts of mutant Htt are much higher than in control cells which were not induced for Htt103Q-EGFP expression. The result obtained in this experiment is consistent with the expectations from available literature information since FADD is known to act in a pro-apoptotic fashion facilitating caspase-8 autoactivation (Chapter 1.2.1).

To further investigate the hypothesis that DDX24 and FADD interact in order to balance receptor-mediated caspase activation, HA-FADD was overexpressed in PC12 cells in which the DDX24 protein levels were reduced by RNAi. Figure 2.36 displays the synergistical effect on Htt-induced cytotoxicity which results from the HA-FADD overexpression and the reduced intracellular DDX24 protein levels. A gain-of-toxicity was observed for the activities of caspase-3 and caspase-8 which were induced by Htt103Q-EGFP. Both activities were increased in samples treated with the HA-FADD expression plasmid and DDX24 specific siRNA in comparison to the controls either overexpressing HA-FADD or being silenced for DDX24. Interestingly, such a synergistic effect was not detected for caspase-9, although, the overexpression of HA-FADD and the DDX24 knock-down alone increased Htt-induced caspase-9 activity (Figure 2.36 C). These observations provide evidence that DDX24 indeed might influence caspase-8 and -3 activities via the extrinsic apoptosis pathway through its interaction with FADD.

3.9 A model for the influence of DDX24 on Htt-induced caspase activation

In the following I will combine the results from my study with mechanistic models of Htt-induced toxicity drawn from the literature. Based on these data I will propose a role of DDX24 in mutant Htt-induced caspase activation and apoptosis.

Mutant Htt expressed in the cell is cleaved by caspase-6 generating N-terminal Htt fragments (Graham et al., 2006) which accumulate in intranuclear inclusions and lead to neuronal dysfunction (Davies et al., 1997; DiFiglia et al., 1997). However, whether these intranuclear inclusions or soluble forms of mutant Htt trigger toxicity, is still under debate. Several chains of evidence suggest the activation of the intrinsic apoptosis pathway by mutant Htt. Mutant Htt aggregation has been demonstrated to induce expression of proteins involved in the mitochondrial-mediated apoptosis pathway and to reduce expression of proteins of the respiratory chain (Bae et al., 2005; Cui et al., 2006). Both processes result in mitochondrial impairment as well as enhanced vulnerability of the mitochondria (Fan and Raymond, 2007) and lead to the release of apoptotic factors such as cytochrome c. This finally results in initiation of the intrinsic apoptosis pathway (Zeron et al., 2004; Green and Reed, 1998; Chapter 1.2.2).

Moreover, mutant Htt directly binds to mitochondria which triggers membrane depolarization as well as release of Ca^{2+} and cytochrome c (Choo et al., 2004; Panov et al., 2002). Cytochrome c assembles with Apaf-1 and procaspase-9 forming the apoptosome complex which activates caspase-3 finally leading to cell death (Green and Reed, 1998). Under stress conditions caspase-9 and -3 are also activated independently of the apoptosome via the misfolded protein response pathway as a result of ER stress (Morishima et al., 2002; Rao et al., 2002).

Furthermore, stress factors including death receptors ligands, IL-1 β and free radicals are produced as a consequence of mutant Htt-induced stress and released from the cell (Yuan and Yankner, 2000; Friedlander, 2003). Consequently, the released death receptor ligands bind to their corresponding death receptors on the surface of neighboring cells activating the extrinsic apoptosis signaling cascade inducing caspase-8 and subsequently caspase-3 (Elmore, 2007; Cryns and Yuan, 1998). All this evidence suggests that mutant Htt triggers apoptosis primarily via the intrinsic mitochondrial pathway.

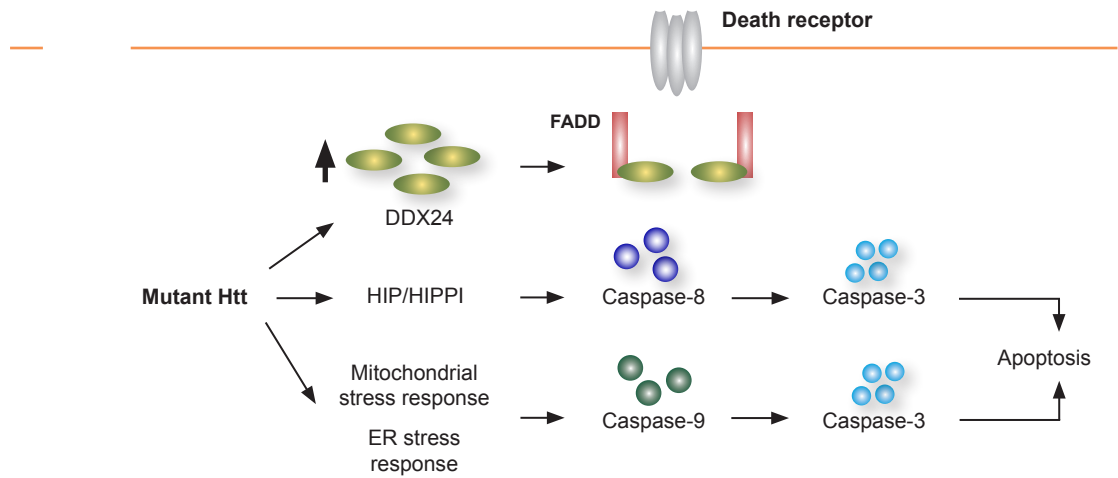
Moreover, these findings suggest a two stage process (Figure 3.1) in which mutant Htt expression leads to a chain reaction initiating cell death by first inducing the intrinsic mitochondrial apoptosis pathway which subsequently results in the activation of receptor-mediated apoptosis. In parallel, receptor-mediated apoptosis is directly activated by mutant Htt via the HIP/HIPPI complex which activates caspase-8 (Gervais et al., 2002; Chapter 1.1.8).

Discussion

My results indicate a regulatory role of DDX24 in the receptor-mediated apoptosis pathway. In the model I postulate that DDX24 expression is upregulated in cells as an intracellular stress response to mutant Htt expression. The upregulation of DDX24 might occur at a stage in HD pathogenesis in which Htt inclusions already have formed and transcriptional changes occur as a result of the mutant protein expression. My data indicate that DDX24 directly binds to the apoptosis mediator FADD, which may prevent the formation of the DISC protein complex at the death receptor. The inhibition of DISC formation might then reduce receptor-mediated apoptosis as well as activation of the caspase cascade. This might be a general mechanism of cellular stress response.

When the cells pass into a later stage of the cell death process increased amounts of intercellular caspase-3 are available in cells. The protease may cleave the DDX24 protein at its DEAD sequence which results in liberation of FADD and the formation of DISC at the death receptor. Alternatively, the degradation of DDX24 might also be a result of enhanced ubiquitin-proteasome system (UPS) activation induced by the protein misfolding response (Díaz-Hernández et al., 2003; Bett et al., 2006). The degradation of DDX24 and the liberation of FADD enhance the susceptibility of the death receptor to external death signals which are released from cells already in the stage of dying. Due to the reduced DDX24 levels, the external apoptosis signals can be transmitted smoothly through the extrinsic signaling cascade. DDX24 degradation would thus result in additional activation of caspase-8 and caspase-3, ultimately leading to rapid apoptosis. This process would represent a positive feedback-loop in caspase activation.

Early stage



Late stage

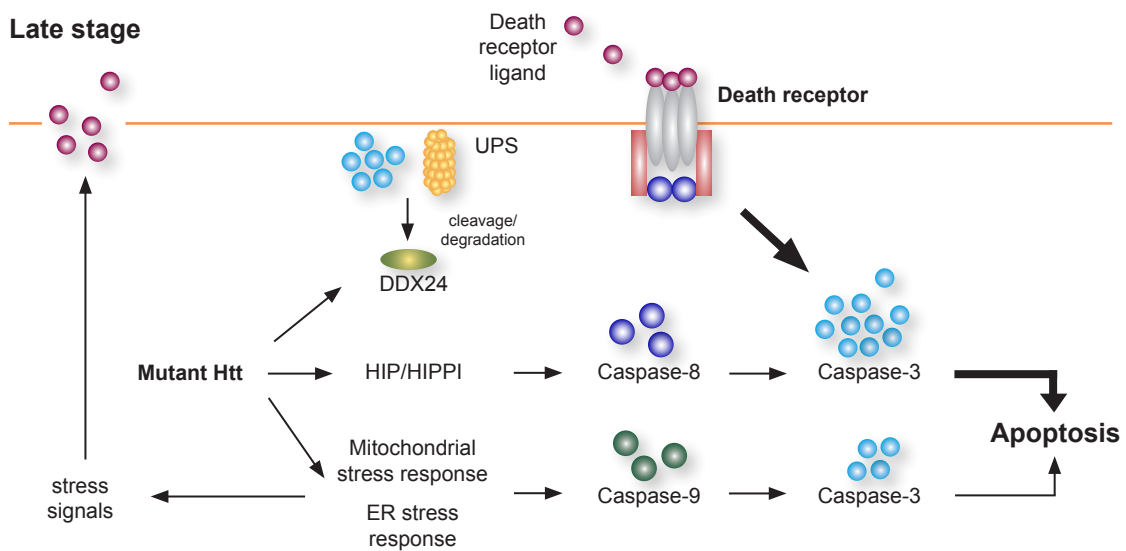


Figure 3.1: Suggested model for the function of DDX24 in mutant Htt-induced caspase activation. Aggregation of mutant Htt activates caspase-3 through mitochondrial- and HIP1-mediated pathways. It also leads to upregulation of DDX24. DDX24 binds to FADD potentially inhibiting recruitment of FADD to the death receptor and/or formation of the DISC protecting the cell against additional extracellular stress signaling. Activation of caspase-3 and/or upregulation of the UPS is assumed to result in degradation of DDX24 and liberation of FADD. This leads to enhanced susceptibility of the death receptors to external death stimuli. Death receptor ligands released by apoptotic cells bind to death receptors on other cells and induce the receptor-mediated extrinsic apoptosis signaling cascade additionally activating caspase-8 and caspase-3, which results in cell death.

3.10 Outlook and further directions

In order to better understand the role of DDX24 in receptor-mediated apoptosis, the interaction between DDX24 and FADD and the functional consequences of this protein interaction need to be further investigated. If DDX24 binding inhibits FADD activation, it should be possible to rescue caspase activity induced by DDX24 knock-down/FADD overexpression by co-expressing the proteins DDX24 and FADD. A second possibility to show a rescuing effect on caspase activation would be the endogenous silencing of DDX24 as well as of FADD. Third, an experiment in which the binding of DDX24 to FADD is impaired by mutation of possible binding sites or blocking of the interaction with small molecules should result in an enhanced activation of caspases, strengthening the hypothesis of an inhibitory DDX24/FADD protein complex.

My model proposes that DDX24 might be degraded by increased UPS activity in the late stage of apoptosis, which might facilitate extrinsic caspase activation. While the induction of the UPS by misfolded proteins has been well demonstrated in transgenic HD mice (Díaz-Hernández et al., 2003; Bett et al., 2006), the degradation of DDX24 by the UPS still needs to be demonstrated. To prove the hypothesis that DDX24 is degraded by the UPS it should be investigated, whether DDX24 in the striatum of transgenic HD mice is ubiquitinated. Furthermore, inhibition of the proteasomal activity should increase DDX24 protein levels which should have consequences for the activation of caspases.

I hypothesize that in the late stage of apoptosis DDX24 is cleaved by caspase-3, which might accelerate cell death. Experiments demonstrating that DDX24 is indeed a substrate of caspase-3 need to be performed. A similar experiment was shown by M. Sun (2008) demonstrating that DDX3 is cleaved by caspase-3 and that this influences death receptor signaling (Sun et al., 2008).

Moreover, it would be interesting to investigate whether the effect of DDX24 on caspase activation is exclusively mediated by caspase-8 activating caspase-3 or whether other pathways involving DDX24 influence caspase-3 activation. To address this question intracellular levels of caspase-8 could be reduced by RNAi in addition to DDX24 silencing in PC12 cells overexpressing mutant Htt protein. Alternatively caspase-8 could specifically be inhibited by caspase-8 inhibitors such as Z-IETD-FMK.

Discussion

Chapter 4

Materials and Methods

4.1 Materials

4.1.1 Bacterial stains

Mach1™ T1R *E. coli*/ F- Φ 80lacZ Δ M15 Δ lacX74 *hsdR*(rK-, mK+) Δ recA1398 *endA1 tonA* (Invitrogen), recommended strain for use with the Gateway® Cloning System.

DH10B *E. coli*/ F' *mcrA* Δ -(*mrr hsd RMS-mcr BC*) ϕ 80dlacZ Δ M15 Δ lacX74 *deoR recA1 araD139* Δ (*ara leu*)7697 *galU galK* λ - *rpsL endA1 nupG* (Invitrogen).

4.1.2 Cell lines

Neuro2a Mouse neuroblastoma cell line, about 30% of the cells grow like neuronal cells; 70% are round, loosely attached cells (DKMZ, Deutsche Sammlung für Mikroorganismen und Zellkulturen GmbH)

PC12 Htt25Q
-EGFP

PC12 Htt103Q
-EGFP

Rat adrenal pheochromocytoma cell line; expressing a Htt exon 1 protein fragment containing either 25Q or 103Q fused to an EGFP-epitope tag after induction with Muristerone A or Ponasterone A. Grow on collagene coated plates. Differentiation by growing in starvation medium (1 % horse serum) supplemented with 50 ng/ml NGF (Apostol et al., 2003).

HEK293 Human embryonal kidney cell line; adherent fibroblastoid cells growing as monolayer (DKMZ, Deutsche Sammlung für Mikroorganismen und Zellkulturen GmbH).

4.1.3 Expression vectors

pcDNAI/Amp

-HD320_Q68 Expression vector for expression for the HD320_Q68 protein in mammalian cells under the control of the CMV promoter. The vector contains an ampicillin resistance.

pcDNA3.1- β -Gal Expression vector for the β -Galactosidase protein in mammalian cells under the control of the CMV promoter. Vector based on pcDNA3.1. The vector contains an ampicillin resistance.

pTL1-HA1-D48 Expression vector for HA-fusion proteins. Upstream of the multiple cloning site of pTL (1, 2, 3) the coding sequence for the HA-epitope has been introduced in all three reading frames (HA 1, 2, 3), and a Kozak-sequence has been inserted (Sittler et al., 1998) (Vector map: Appendix).

pc-myc-CMV-D12

Expression vector for the expression of fusion proteins containing an N-terminal Myc-epitope tag in mammalian cells under the control of the CMV promoter. Vector contains an ampicillin resistance (RZPD) (Vector map: Appendix).

pPAReni-DM

pFireV5-DM

Vectors are based on pcDNA3.1(+) (Clontech). For the pPAReni-DM the following cassette was cloned between the BamHI and XbaI sites: Kozak sequence, a double protein A epitope, renilla luciferase and the ccdB cassette with flanking R1 and R2 att-sites. For the pFireV5-DM vector the following cassette was cloned between the BamHI and XbaI sites: firefly luciferase, V5 epitope and the ccdB cassette with flanking R1 and R2 att-sites (Vector maps: Appendix).

pdECFP-Amp

pdEYFP-Amp

Expression vectors for ECFP- and EYFP-fusion proteins based on pcDNA3.1 (+) (Clontec). Both vectors are Gateway-adapted destination vectors, containing the ccdB gene flanked by the attR recombination sites. pdEYFP/pdECFP are designed for fusing a gene of interest to an N-terminal EYFP/ECFP-tag according to the Gateway Cloning Technology (Invitrogen) and for expression of this gene in mammalian cells under control of the human CMV-IE promoter and enhancer (Vector maps: Appendix).

Materials and Methods

4.1.4 Microbiological media and buffers

1000x Ampicillin stock	100 mg/ml dissolved in 50% ethanol, stored at -20°C
AttoPhos™ buffer	50 mM Tris-HCl pH 9.0, 500mM NaCl, 1mM MgCl ₂
AttoPhos™ reagent	10 mM AttoPhos reagent dissolved in 100mM Tris pH9.0
1% BSA	Bovine serum albumin was dissolved in 1x PBS to a final concentration of 1 % (w/v)
Co-IP washing buffer	20mM Tris-HCl pH 7.5, 150mM NaCl, 0.1 % NP-40, freshly added protease inhibitors (Complete™ final concentration: 1x; 1mM PMSF)
10x DNA sample buffer	0.42% bromophenol blue, 0.42% xylene cyanol, 25% ficoll type 400, dissolved in distilled water, stored at -20°C
1000x Kanamycin stock	25mg/ml dissolved in distilled water, stored at -20°C
Lysis buffer for mammalian cells (native)	50mM Tris-HCl pH 8.8, 100 mM NaCl, 5mM MgCl ₂ , 1%, NP-40 1mM EDTA, stored at 4°C, add protease inhibitors (Complete™ final concentration: 1x; 1mM PMSF) and 25U/ml benzonase straight before use
LB-(Luria Bertani) medium	10g/l Bacto Pepton, 5g/l yeast-extract, 10g/l NaCl, pH7.2
25x Protease inhibitors	One tablet of Complete™ protease inhibitor (Roche) dissolved in 2ml distilled water, stored at -20°C
10x PBS	80g NaCl, 2g KCl, 14.4g Na ₂ HPO ₄ , 2.4g KH ₂ PO ₄ , to 1l with distilled water
4% PFA	4 g of paraformaldehyde dissolved in 100 ml PBS and heated at 50°C for 5 minutes to reach a clear solution, stored at -20°C
PMSF	100mM PMSF dissolved in isopropanol, stored at -20.
12.5 % resolving gel	3.125ml of 40% Bisacrylamide, 2.5ml of 1.5 M Tris-HCl (pH8.8), 100µl of 10% SDS, 4.2ml ddH ₂ O, 100µl of 10% APS, and 10µl TEMED
5% stacking gel	0.75ml of 40% acrylamide, 1.5ml of 0.5M Tris-HCl (pH6.8), 60µl of 10% SDS, 3.6ml ddH ₂ O, 60µl of 10% APS, and 6µl TEMED
4x SDS loading buffer	200mM Tris-HCl pH6.8, 400mM DTT, 8% SDS, 4mg/ml bromophenol blue, 40% glycerol, store at -20°C
1 x SDS running buffer	1 x WB-buffer, 0.1% SDS
3% skim milk	skim milk powder was dissolved in TBS-T to a final concentration of 3% (w/v)

Materials and Methods

Stripping buffer pH 2.2	200mM Glycin, 1% Tween20, 0.1% SDS
S.O.C. Medium	2% Tryptone, 0.5% Yeast Extract, 10mM NaCl, 2.5mM KCl, 10mM MgCl ₂ , 10mM MgSO ₄ , 20mM glucose
1x TBE	1x TBE 1mM EDTA, 45mM Tris-Borate pH 8.0
TBS	20mM Tris-HCl pH 7.5, 150mM NaCl
TBS-T	20mM Tris-HCl pH 7.5, 150mM NaCl, 0.05% Triton X-100
10 x WB-buffer	30g/l Tris, 144g/l Glycin
Western blot buffer	1 x WB-buffer, 10 % Ethanol

4.1.5 Media and supplements for mammalian cell culture

Dulbecco's modified Eagle medium (DMEM) with 4.5 g/L D-Glucose, Sodium Pyruvate, without L-Glutamine	Gibco
Dulbecco's modified Eagle medium (DMEM) with L-Glutamine, 1000 mg/L D-Glucose, Sodium Pyruvate	Gibco
0.5% Trypsin and 0.53mM Na-EDTA in Hanks' B.S.S.	Gibco
Fetal calf serum (FBS) from E.G. approved countries	Gibco
Dulbecco's phosphate buffered saline (D-PBS) without calcium, magnesium	Gibco
L-Glutamine	Gibco
Penicillin G (10000 units/ml) and Streptomycin sulfate (10000µg/ml) in 0.85% saline	Gibco
MEM Non Essential Amino Acids (100X)	Gibco
Geneticin (G418, 50mg/ml)	Gibco
Zeocin (100µg/ml)	Invitrogen
Muristerone A (1mM in ethanol)	Invitrogen/Sigma

4.1.6 Oligonucleotides

Table 4.1: Primer/probe quantitative real-time PCR

Name	Sequence 5' -> 3'
PC12LT_EGFP fw	TGG TGA GCA AGG GCG AGG A
PC12LT_EGFP rev	TGG TGC AGA TAG ACT TCA G
Sonde PC12LT_EGFP	6-FAM - CAG CCT GGT CGA GCT GGA - BHQ1

Materials and Methods

Oligonucleotides have HPLC purification grade and were synthesized by BioTeZ Berlin-Buch GmbH in a quantity of 10 nmol. Primers and probe have been resolved in nuclease-free water and diluted to a concentration of 10 pmol/ μ l.

siRNAs

siGENOME siRNAs were purchased from Dharmacon siRNA Technologies (Thermo Scientific). siGENOME smart pool siRNAs targeting genes of the p200 list were a kind gift of Dr. Steffan Wiemann (DKFZ; Heidelberg).

siGENOME siRNA set of 4 and single siRNAs were purchased in a quantity of 5 nmol and have been resolved to a concentration of 20 μ M in 1x siRNA buffer (Dharmacon; diluted from 5x siRNA buffer in RNase-free H₂O).

Table 4.2: DDX24 targeting siRNA sequences

Name	Target sequence
siDDX24_1 (D-097043-01)	GGAAGCAAGUGACGAUCGA
siDDX24_2 (D-097043-02)	ACUGACAGAUUACCGCUUA
siDDX24_3 (D-097043-03)	GGUCGUAGCCUGGUAUUUG
siDDX24_4 (D-097043-04)	ACGAAUCCUUCAUAAAGAAA

4.1.7 Antibodies

Primary antibody	Species	Dilution	Supplier
Anti-Actin	mouse	1:2000	Abcam
Anti-CAG53b	rabbit	1:5000	own production by E. Scherzinger
Anti-DDX24	rabbit	1:500 (WB) 1:100 (IF)	own production by M. Lalowski (antiserum)
Anti-GAPDH	rabbit	1:2000	Sigma
Anti-HA (WB)	mouse	1:2000	Babco
Anti-HA (IF)	rabbit	1:100	Sigma
Anti-Myc	mouse	1:100	Santa Cruz
Anti-PA	rabbit	1:2000	Sigma
Anti-p53	rabbit	1:1000	Cell Signaling
Anti-V5	mouse	1:5000	Invitrogen

Secondary antibody	Conjugate	Species	Dilution	Supplier
Anti-rabbit IgG	Alkaline Phosphatase	goat	1:10000	Sigma
Anti-mouse IgG	Alkaline Phosphatase	goat	1:10000	Sigma
Anti-rabbit IgG	Peroxidase	goat	1:2000	Chemicon

Materials and Methods

Anti-mouse IgG	Peroxidase	goat	1:2000	Chemicon Jackson Immuno
Anti-rabbit IgG	Cy3	donkey	1:200	Research
Anti-mouse IgG	Cy5	goat	1:200	Dianova

4.1.8 Enzymes, proteins, markers and DNA

Benchmark pre-stained protein ladder	Invitrogen
Benzonase purity grade II	Merck
BSA 10 mg/ml	NEB
Herrings Sperm Carrier DNA	Clontech
LR Clonase enzyme mix	Invitrogen
Proteinase K	Sigma

4.1.9 Kits

Apo-ONE® homogenous caspase-3/7 assay	Promega
BCA Protein assay reagent	Pierce
Caspase-Glo® 8 Assay	Promega
Caspase-Glo® 9 Assay	Promega
Dual-Glo™ Luciferase Assay System	Promega
Lipofectamin 2000	Invitrogen
Plasmid Mini Kit	Qiagen
Plasmid Midi Kit	Qiagen
RNeasy Mini Kit	Qiagen
RNeasy Lipid Tissue Mini Kit	Qiagen
RNase free DNase Set	Qiagen
RevertAid H Minus First Strand cDNA Synthesis Kit	Fermentas
TaqMan Gene Expression Assay DDX24 (rat)	AppliedBiosystems
TaqMan Gene Expression Assay DDX24 (mouse)	AppliedBiosystems
TaqMan Rat GAPD (GAPDH) Endogenous Control	AppliedBiosystems
TaqMan Mouse GAPD (GAPDH) Endogenous Control	AppliedBiosystems
TaqMan Rat ACTB Endogenous Control	AppliedBiosystems
TaqMan® Universal PCR Master Mix	AppliedBiosystems
Western Lightning ECL	Perkin Elmer

4.1.10 Chemicals and consumables

3MM Whatman filter paper	Whatman
Agarose	Invitrogen
Ammoniumpersulfate (APS)	BioRad
Ampicillin-trihydrate	Sigma-Aldrich
Blot absorbent filter paper	BioRad
Bromophenol blue	Merck Eurolab GmbH
Cell culture dishes	DB Falcon
Cell scrapers (COSTAR)	Corning Inc.
Cellulose acetate membrane 0.2 µm	Schleicher and Schuell
Collagen solution Type I from calf skin	Sigma-Aldrich
Complete protease inhibitor cocktail	Roche
Dithiothreitol (DTT)	Serva
Dimethylsulfoxide (DMSO)	Sigma-Aldrich
Ethidium bromide solution 10mg/ml	Sigma-Aldrich
Filter paper GB005	Schleicher and Schuell
Fluoronunc 96-well plates	Nunc
Glycerol	Merck Eurolab GmbH
IgG-coated Dynabeads	Invitrogen
MicroAmp Optical 8-Tube Strip	AppliedBiosystems
MicroAmp Optical 8-Cap Strip	AppliedBiosystems
MicroAmp Optical 96-well reaction plate	AppliedBiosystems
MicroAmp Optical Adhesive film	AppliedBiosystems
Muristerone A 1mg lyophilized	Sigma
NP-40 (IGEPAL CA 630)	Sigma-Aldrich
Protran BA 83 nitrocellulose membrane	Schleicher and Schuell
Phenylmethylsulfonylfluoride (PMSF)	Sigma-Aldrich
Polyoxyethylensorbitan-Monolaureat Tween20	Sigma-Aldrich
P-t-Octylphenyl-polyoxyethylen Triton X-100	Sigma-Aldrich
ProLong® Gold antifade reagent	Invitrogen
Resazurin	Sigma-Aldrich
RNAse Zap	Carl Roth
Sodium	Sigma-Aldrich

Materials and Methods

TEMED	Life Technologies
TrypanBlue solution (0.4 %)	Sigma-Aldrich

All other chemicals, salts, buffer substances, solvents, acids and bases were purchased from Carl Roth GmbH. Used chemicals had the purification grade per analysis (p.a.).

4.1.11 Laboratory equipment

7500 Real-time PCR system	AppliedBiosystems
Cryo 1C freezing container	Nalgene
Electroporator	BioRad
Electroporation cuvettes	BioRad
Image reader LAS-3000	Fujifilm
NanoDrop 8000 Photometer	Peqlab
Infinite M200 plate reader	Tecan
Polyacrylamide gel electrophoresis apparatus, Criterion system	BioRad
Semi-dry Western blotting apparatus	BioRad
PTC-200 gradient cyler	MJ Research
Tissue Homogenizer	VWR
Zeiss Imager.Z1 Microscope	Zeiss

4.2 Methods

4.2.1 Molecular biology

Shuttling of cDNA constructs into appropriate expression vectors

cDNA construct from the RZPD clone library were integrated into expression vectors using commercially available Gateway® technology (Invitrogen). The entry clones of FADD (RZPDo839C12160) and DDX24 (RZPDo839H0780) were shuttled into the destination vectors pTL-HA1-D48, pc-myc-CMV-D12, pPAREni-DM and pFireV5-DM as well as in pdEYFP-Amp and pdECFP-Amp according to the shuttling protocol of the Gateway® system (Invitrogen; www.invitrogen.com).

Chemical transformation of *E. coli*

Plasmid DNA was transformed into chemically competent *E. coli* Mach1-T1R. 5µl of plasmid DNA was added to 50 µl of competent Mach1-T1R cells and incubated on ice for 30 min followed by heat-shock for 30 sec at 42°C. Subsequently, the cells were put back on ice for 1 min to cool down, mixed with 250µl S.O.C. medium without antibiotics and then incubated at 37°C under shaking for 1 hour. Aliquots were then plated onto antibiotics treated LB-agar plates and grown at 37°C over night.

Plasmid preparation from *E. coli*

For amplification of plasmid DNA, LB medium supplemented with the appropriate antibiotics was inoculated with *E. coli* colonies carrying the desired plasmid and grown over night at 37°C in an incubator-shaker, and subsequently harvested by centrifugation. Depending on the DNA quantities plasmid DNA was purified using the Qiagen Plasmid Mini or Midi Kit according to manufacturer's instructions.

Determination of DNA and RNA concentration

To determine the concentration of nucleic acids, the absorbance of the purified DNA or RNA in aqueous solution was measured at 260 and 280 nm in a NanoDrop spectrophotometer (PqLab). An A₂₆₀ reading of 1.0 is equivalent to ~50 µg/ml double-stranded DNA or ~40 µg/ml single-stranded RNA. The A₂₆₀/A₂₈₀ ratio is used to assess DNA/RNA purity. An A₂₆₀/A₂₈₀ ratio of 1.8 - 2.1 is indicative of highly purified DNA or RNA.

Materials and Methods

Restriction digest of DNA

Restriction digests were performed in the restriction buffers and according to the protocols supplied by the manufacturer. For restriction digestion ca. 1 µg of the plasmid preparation were incubated at 37°C for 1-2 h. The reactions were stopped by adding 10x DNA sample buffer and the products were separated by electrophoresis on an agarose gel.

DNA electrophoresis

To separate DNA fragments the samples mixed with loading buffer were loaded to a 1 % (w/v) agarose gel, which contained 0.5 g/ml ethidium bromide to visualize the DNA after separation under UV-light, as a running buffer 1x TBE was used.

RNA isolation from mammalian cell culture and mouse brain tissue

Total RNA from mammalian cells was extracted and purified using RNeasy Mini Kit (Qiagen) following the manufacturer's instructions. For disruption of the cells the cell pellets were resuspended in lysis buffer provided in the kit and spin through QIAshredder homogenizer columns (Qiagen). To avoid contamination of the RNA preparation with chromosomal DNA samples were incubated with DNaseI after binding to the RNeasy spin column using the RNase free DNase Kit (Qiagen). The purified total RNA was eluted from the columns using 30 µl RNase-free water.

To isolate total RNA from mouse brain I used the RNeasy Lipid Tissue Mini Kit (Qiagen) according to the manufacturer's protocol. Samples derived from mouse striatal tissue were mechanically homogenized in QIAzol Lysis Reagent (Qiagen) and mixed with chloroform. After addition of chloroform, the homogenate was separated into an aqueous and an organic phase by centrifugation. RNA partitions to the upper, aqueous phase, while DNA partitions to the interphase and proteins to the lower, organic phase or the interphase.

The upper, aqueous phase was extracted and ethanol was added to provide appropriate binding conditions. The samples were then applied to the RNeasy spin column, where the total RNA binds to the membrane and phenol and other contaminants are efficiently washed away. Total RNA was finally eluted in 60 µl RNase-free water.

The concentration of the total RNA preparations was determined using a spectrophotometer (NanoDrop8000; Peqlab) as described above.

cDNA synthesis via reverse transcription

Using the retroviral enzyme reverse transcriptase one can transcribe RNA into complementary cDNA. Such as other polymerases this specific RNA dependent DNA polymerase needs an oligonucleotide bound to the RNA and serving as the starting point of the strand complementation. For transcription of the total RNA isolate unspecific Oligo-dT primers were used. These primers consist of 10 – 15 thymine bases and recognize the poly-A-tail of eukaryotic mRNA. For

Materials and Methods

the cDNA synthesis from cellular total RNA the RevertAid™ H minus first strand cDNA synthesis Kit (Fermentas) was used according to the manufacturer's protocol. For reverse transcription and cDNA production 1 – 2 µg of total RNA isolated from mammalian cells or mouse brain was used.

Quantitative *real-time* PCR

The quantitative *real-time* PCR (qRT-PCR) is a highly sensitive technique to simultaneously amplify and quantify a DNA target sequence, based on the principle of a normal PCR (Higuchi et al., 1992). The DNA quantification occurs by fluorescence measurement during the PCR-cycles. For fluorescence detection either the PCR products can be labelled with fluorescent dyes which unspecifically intercalate into DNA double-strands or a fluorescence probe is bound to the DNA template. The latter one, known as “TaqMan probe” is a sequence specific oligonucleotide, carrying a fluorophore (“reporter”) at their 5'-end and a quencher of fluorescence at the 3'-end of the probe. The close proximity of the reporter to the quencher prevents detection of its fluorescence; breakdown of the probe by the 5' to 3' exonuclease activity of the Taq polymerase breaks the reporter-quencher proximity and thus allows unquenched emission of fluorescence, which can be detected after excitation with a laser (Lee et al., 1993). The intensity of the fluorescence signal is direct proportional to the amount of amplified double stranded PCR product and therefore increases over time of the PCR reaction.

To perform a qRT-PCR, cDNA obtained from the reverse transcription of total RNA (see previous paragraph) was diluted 1:1000 in RNase-free H₂O and added to the PCR reaction as template. For detection of endogenous DDX24 mRNA purchased primer/probe mixes specific for either rat or mouse DDX24 were used (TaqMan Gene Expression Assay DDX24; FAM-labelled; Applied-Biosystems). As endogenous controls for normalization of the relative DDX24 mRNA levels to the amount of total RNA I used the TaqMan GAPD (GAPDH) Endogenous Control Assay (rat or mouse specific) and the TaqMan ACTB Endogenous Control Assay (rat specific), respectively. All used probes of the endogenous controls are VIC-labelled (AppliedBiosystems). For detection of Htt103Q-EGFP or Htt25Q-EGFP mRNA a self designed primer/probe set was used (FAM-labelled; Chapter 4.1.6, Table 4.1). All real-time PCR reactions were performed in triplicates as multiplexed samples detecting cDNA of both, target and endogenous control within the same well (possible because of their different fluorescence labelling). The composition of the real-time PCR reactions is shown below in Table 4.3a/b.

Materials and Methods

Table 4.3a: Components of a multiplexed real-time PCR reaction using purchased TaqMan Gene Expression Assays

Component	Volume (µl)
cDNA template	5
TaqMan Gene Expression Assay DDX24 (20X)	1
TaqMan Endogenous Control Assay (20X)	1
TaqMan Universal PCR Master Mix (2X)	10
Nuclease-free H ₂ O	3
Final volume	20

Table 4.3b: Components of a multiplexed real-time PCR reaction using self designed primer/probe set

Component	Volume (µl)
cDNA template	5
forward primer (10 pmol/µl)	0.5
Reverse primer (10 pmol/µl)	0.5
Fluorescent probe (10 pmol/µl)	0.5
TaqMan Endogenous Control Assay (20X)	1
TaqMan Universal PCR Master Mix (2X)	10
Nuclease-free H ₂ O	2.5
Final volume	20

All *real-time* PCR reactions were performed in the Applied Biosystems 7500 Real-Time PCR System using the standard amplification program:

50°C	15min	
95°C	2min	
95°C	15sec	}
60°C	45sec	

50 cycles

The quantification was done by analysis of the data collected during the run. The data was analyzed by the so called comparative *threshold cycle* method (C_T). The C_T -value corresponds with the PCR cycle in which the fluorescence intensity detected in the sample overcomes the background signal (threshold) for the first time. The more target cDNA is present in the sample the earlier the threshold will be exceeded, resulting in a small cycle number and a low C_T -value. The C_T -value of the sample is then normalized to the C_T -value of its endogenous control (calibrator) giving its ΔC_T -value, calculated as:

$$\Delta C_T = C_T \text{ target} - C_T \text{ calibrator}$$

Materials and Methods

To further compare the samples of interest with the corresponding negative controls a second comparison/calculation step is performed in which the ΔC_T -value of the sample is normalized to the ΔC_T -value of the corresponding control (for example induced PC12 cells vs. non induced PC12 cells) giving its $\Delta\Delta C_T$ -value, calculated as:

$$\Delta\Delta C_T = \Delta C_T \text{ sample} - \Delta C_T \text{ control}$$

On basis of the $\Delta\Delta C_T$ -value the x-fold change of target gene expression can be calculated using the formula:

$$\text{x-fold change} = 2^{-\Delta\Delta C_T}$$

4.2.2 Protein biochemistry

Protein isolation by acetone precipitation

To extract the content of total proteins from mouse striatal brain sections the organic phase and the interphase left over in the RNA isolation procedure (Chapter 4.2.1) were mixed with 4 volumes of ice cold (-20°C) acetone. The samples then were mixed by vortexing and incubated over night at -20°C. Precipitation samples then were centrifuged for 15 min at 15000 rpm in a pre-cooled centrifuge (4°C). The supernatant was removed and protein pellets were air-dried for 4 hours at room temperature. To resolve the proteins pellets were mixed with the standard lysis buffer supplemented with SDS to a final concentration of 2 % and vortexed for 1 hour. Since pellets did not resolve, properly samples were additionally heated for 30 min under shaking and the soluble fraction was used for further analysis. The total protein concentration was determined in supernatant by BCA method (see next paragraph).

Determination of the protein concentration

The concentration of proteins in aqueous solution was determined using BCA protein assay (Pierce). The bicinchoninic acid (BCA) method employs the reduction of Cu^{+2} to Cu^{+1} by protein in an alkaline medium. The combination of BCA and Cu^{+1} creates a purple-colored product that absorbs at 562 nm. The amount of product formed is dependent upon the amount of protein in the sample. The absorption of the protein solution was subsequently compared to a BSA standard dilution series to determine the exact concentration of the sample.

SDS-polyacrylamide gel electrophoresis (SDS-PAGE)

Separation of proteins according to their molecular mass was carried out according to Laemmli (Laemmli, 1970). Before loading onto the gel samples were mixed with 4x SDS-loading buffer and denatured by 98°C for 5 min. SDS-PAGE was performed following the instructions by Sambrook and Russell (Sambrook and Russell, 2001), with gels containing 12.5 % polyacrylamide. As protein standard Benchmark™ pre-stained protein ladder (Invitrogen) was used.

Western blotting

Following the separation by SDS-PAGE the proteins were transferred onto nitrocellulose membrane (Schleicher and Schuell) to immobilize the proteins and make them visible by immunostaining. The transfer was performed in the semi-dry Transblot Apparatus (Bio-Rad) at 20 V for 1.5 hours. Subsequently the membranes were blocked in 3 % skim milk solution for 1 hour at room temperature or at 4°C over night. The immunoblots then were incubated with the desired primary antibody overnight, washed several times with TBS-T and TBS and in a second step incubated with the corresponding secondary antibody conjugated to either alkaline phosphatase or peroxidase (POD) for 1 hour. Eventually, the proteins were detected by either fluorescence measurement under 460 nm UV-light (AttoPhos; Europa Bioproducts) or chemiluminescence (Western Lightning™; PerkinElmer) measurement in the LAS3000 Image reader (Fuji).

Detection of Htt aggregates by denatured and native filter retardation assay

To detect Htt aggregates a filter retardation assay was performed. After harvesting, PC12 cells were lysed in standard lysis buffer (Chapter 4.1.4) for 20 min on ice. The protein concentration was determined by BCA assay (Pierce) according to the manufacturer's protocol. For denatured filtration 2 % SDS and 50 mM DTT were added to the lysates and the samples were denatured at 98°C for 5 min. Two Whatman 3MM filter papers and one cellulose acetate membrane were soaked in 0.1% SDS, mounted on a filter unit and washed twice with 0.1 % SDS solution. The denatured protein samples were then filtered through the cellulose acetate membrane as described in the literature (Scherzinger et al., 1997). The membrane was washed twice with 100 µl of 0.1 % SDS-buffer and SDS resistant aggregates staying on the surface of the membrane were detected by the CAG53b antibody (1:5000, rabbit) recognizing Htt, as described for Western blotting.

To detect EGFP-labelled Htt103Q-EGFP aggregates samples were filtered under native conditions without addition of SDS/DTT to the lysis buffer or heat denaturation. For soaking of the filter papers and the cellulose acetate membrane SDS was substituted by 0.1 % NP-40 in the buffer. After filtration Htt103Q-EGFP aggregates were directly detected by exposure of the membrane to 460 nm UV-light in the LAS3000 Image reader (Fuji).

LUMIER (Luminescence-based Mammalian Interactome mapping technology)

The LUMIER assay which was established by M. Barrios-Rodiles in 2005 (Barrios-Rodiles et al., 2005) is a highly sensitive method to detect protein-protein interactions. In this assay two potential protein interaction partners are co-expressed in a mammalian cell culture system. Both of those are generated as fusion protein constructs whereby the one is a firefly-luciferase-fusion protein tagged to a V5-epitope tag (the *bait* protein) and the other a renilla-luciferase-fusion protein containing a PA-tag (serving as *prey* protein). After expression, the fusion proteins can be isolated from the cell extract by affinity purification using an PA (Protein A) -antibody. By several washing steps weakly bound endogenous cellular proteins are removed from the complex. In case of an interaction between *bait* and *prey* this can be detected by the luminescence of the firefly-luciferase substrate when added to the isolated protein complex. The *prey*-associated luminescence reveals the extent of *bait* interaction.

The clones used in the LUMIER assay were subcloned into the plasmids pPAREni-DM and pFireV5-DM, using the GATEWAY® technology creating the expression vectors pPAREni-FADD, pPAREni-DDX24, pFireV5-FADD and pFireV5-DDX24. The plasmids were co-transfected in HEK293 in combination of pPAREni-FADD/pFireV5-FADD and pPAREni-DDX24/pFireV5-FADD. In control cell combinations of all four plasmids and the contrary empty vector (pPAREni-DM or pFireV5-DM) were transfected. Double negative controls were treated with both empty vectors. The fusion proteins were co-expressed in HEK293 cells for 24 hours. Cell extracts were prepared and assessed for the expression of the fusion proteins by luciferase assays. Protein complexes were isolated from 80 µl cell extract using IgG-coated microtiter plates and washed with 100 µl PBS. The binding (Co-Immunoprecipitation) of the firefly-V5-tagged fusion protein to the PA-renilla-tagged protein was quantified by measuring the firefly-luciferase activity in a luminescence plate reader (Infinite M200, Tecan) using the Dual-Glo™ Luciferase Assay System (Promega). Renilla-luciferase activity was also measured as a control for PA-renilla-luciferase binding to the IgG-coated plates. Each experiment was performed as triplicate transfection.

Co-immunoprecipitation from cell lysates

For co-immunoprecipitation experiments of DDX24 and FADD in mammalian cells the same expression plasmids were used as for the LUMIER assay. HEK293 cells were co-transfected with pPAREni-FADD and pFireV5-DDX24 and incubated for 48 hours, followed by lysis under native conditions. Protein complexes were isolated from the crude lysate by incubation of the cell extracts with IgG-coated magnetic Dynal beads (Dynabeads M-280 Sheep anti-Rabbit IgG; Invitrogen) on a rotating wheel at 4°C over night. Following the binding, samples were washed twice with 1x TBS and twice with Co-IP wash buffer. Subsequently, 4x SDS-loading buffer was added to the beads and the samples were heat denatured by 98°C for 5 min, followed by SDS-PAGE and Western blotting.

4.2.3 Methods in cell biology

Cultivation of mammalian cells

Neuro2a cells were cultured in Dulbecco's modified Eagle medium (DMEM) with L-Glutamine, 1000 mg/L D-Glucose, Sodium Pyruvate supplemented with 10 % FCS, 5% non essential amino acids, 100 U/ml penicillin and 100 µg/ml streptomycin at 37°C and 5% CO₂. Cells were grown up to 90 % confluence and split down to 10 % confluence. To do so the culture medium was removed, cells were washed with 5 ml of pre-warmed D-PBS and detached from the flask by incubation with 0.5 % (w/v) trypsin/1 mM EDTA at room temperature. Cells were then resuspended in 10 ml pre-warmed culture medium and diluted into fresh 75 cm² culture flasks.

PC12 Htt103Q-EGFP & Htt25Q-EGFP cells were grown on collagen coated flasks in Dulbecco's modified Eagle medium (DMEM) with 4.5 g/L D-Glucose, Sodium Pyruvate, without L-Glutamine containing 5 % horse serum, 2.5 % FCS and 2 mM L-Glutamine. Antibiotics were added as described above. For selection 100 µg/ml zeocin and 50 µg/ml G418 were used. Cells were split down when they reached 80 % confluence as described for Neuro2a cells and diluted into a fresh cell culture flask. Induction of Htt103Q-EGFP or Htt25Q-EGFP protein expression was achieved by adding 2.5 µM muristerone to the medium. Controls were treated with corresponding volumes of solvent (ethanol).

HEK293 cells were cultured in Dulbecco's modified Eagle medium (DMEM) with L-Glutamine, 1000 mg/L D-Glucose, supplemented with 100 U/ml penicillin and 100 µg/ml streptomycin at 37°C and 5% CO₂. Cells were grown up to 90% confluence and split down to 10% confluence. As described for Neuro2a.

Long-term storage of mammalian cells

Cells were grown to 90% confluence in 75 cm² culture flasks. After removing of the medium cells were washed with pre-warmed D-PBS, detached by trypsinization and pelleted by centrifugation at 1000 x g for 10 min. Subsequently, cells were resuspended in 1 ml of culture medium supplemented with 20% FCS, DMSO was slowly added to a final concentration of 10 %. Cells were then slowly cooled down to -80°C in a cryo-tube placed in isopropanol over night. Finally, the tubes were transferred to the liquid nitrogen tank for long time storage at -180°C.

Determination of the cell number by TrypanBlue staining

TrypanBlue is an acidic dye, binding to cellular proteins. In dead cells the cell membrane is permeabilized which allows the dye to enter the cytosol resulting in a blue cell staining. Cells which are alive cannot be stained and appear bright under the microscope. Because of the dyeing it can be easily distinguished between living and dead cells. To determine numbers of living cells within a population a so called Neubauer counting chamber was used. 10 µl of cell suspension was mixed

Materials and Methods

in a 1:1 ratio with 0.4 % TrypanBlue staining solution (Sigma-Aldrich), applied to the counting chamber and the living cells were counted in each of the 4 counting squares. The number of viable cells is calculated according to the formula:

$$\text{Total cell number} = \frac{\text{Number of counted cells}}{4} \times 2 \times 10^4$$

Transient transfection of mammalian cells

Plasmid transfection: Mammalian cells were transfected with plasmid DNA using Lipofectamine 2000 transfection reagent (Invitrogen) according to the manufacturer's instructions. Depending on the format in which the transfection was performed, amounts of 0.2 µg (96 well format), 2 µg (6 well format) or 4 µg (6 cm dish) were used. The transfected cells were incubated for 24 – 72 hours, depending on the experimental setup at 37°C and 5% CO₂.

siRNA transfection and co-transfection with plasmid DNA: RNAi experiments were performed using pools of four synthetically produced siRNAs (siGENOME) purchased from Dharmacon. For the RNAi screen Neuro2a cells were seeded the day before transfection in 96well format (15000 cells/well) in medium without antibiotics to reach 30 – 50 % confluence the next day. For RNAi cells were treated with 2.5 pmol of gene specific siRNA (siGENOME smart pool) and additionally co-transfected with 0.2 µg of the Htt expression vector pcDNAI-HD320_Q68. The samples were incubated for 48 hours at 37°C and 5% CO₂.

Transfections of PC12 cells were performed in either 6 well cell culture plates or 6 cm Petri dishes. For RNAi experiments cells were seeded to reach 30 – 50% confluence on the day of transfection in medium without antibiotics or selection supplements. For endogenous protein silencing in 6 cm dishes samples were treated with 100 pmol of target specific siRNA. Non-targeting siRNA siGLOred transfection indicator in the corresponding amount was used as a control. For improvement of the transfection efficiency 4 µg denatured carrier DNA derived from herring sperm was co-transfected. The carrier DNA was substituted by plasmid DNA if overexpression of a specific protein was desired. Samples were transfected with 10 µl Lipofectamine 2000 in a total transfection volume of 6 ml. For transfections performed in 6 well format half of siRNA and DNA amounts were used. The volume of Lipofectamine 2000 was reduced to 4.2 µl in a transfection volume of 2.5 ml. After transfection the cells were incubated for 24 – 72 hours as described before. If expression of Htt103Q-EGFP or Htt25Q-EGFP was desired, cells were treated with 2.5 µM muristerone which was added with the transfection mix.

Determination of cell viability using resazurin

Resazurin is a non toxic oxidation-reduction indicator which is converted by viable cells to the fluorescent product resorufin (Ex560 nm/Em590 nm). Moreover, the turnover of resazurin to resorufin results in an absorption shift at 600 nm. The conversion of resazurin to resorufin is proportional to the number of metabolically active, viable cells and the fluorescence or the absorption at 600nm, respectively can be measured using a suitable plate reader. To determine the cell viability, resazurin was added to the cells in 96 well format to a final concentration of 0.01 $\mu\text{g}/\mu\text{l}$. Then the samples were incubated for 1 – 3 hours and the fluorescence signal or absorption was monitored in the plate reader (Infinite M200, Tecan).

Caspase activation assays

Detection of caspase activity was performed in 96 well format, using biochemical assays monitoring the activity of caspase-3/7, caspase-8 or caspase-9, respectively. Except of the RNA screen in which the cells were already grown and transfected in 96well format, cells growing in 6 well plates of Petri dishes were harvested after the appropriate incubation time by trypsinization to re-seed them in 96 well microtiter plates. To normalize the caspase signals to the cell number, the total number of living cells was determined by counting (see above), and 40,000 cells per well were re-seeded in triplicates in a plating volume of 50 μl . For detection of caspase-3/7 activity the Apo-ONE™ Homogenous Caspase-3/7 Assay (Promega) was used according to the manufacturer's instructions. The buffer of the assay rapidly lyses mammalian cells, and the caspase substrate Z-DEVD-R110 present in the solution can be cleaved by active caspase-3 and -7, revealing a fluorescent group whose emission at 521 nm can be detected after excitation at 499 nm in a fluorescent plate reader.

For detection of the signals in Neuro2a cells under screening conditions a volume of 100 μl Apo-ONE™ Homogenous Caspase-3/7 Assay was added to 100 μl cells in medium and the caspase activity signal was monitored over a time span of 1.5 hours measuring the fluorescence every 5 min.

The activity of caspase-8 and caspase-9 was determined using either the Caspase-Glo® 8 Assay or the Caspase-Glo® 9 Assay (both Promega). Both assays are based on the same system in which a pro-luminogenic luciferase substrate (caspase-8: Z-LETD-aminoluciferin; caspase-9: Z-LEHD-aminoluciferin) is added to the cells and incubated at room temperature in the dark. The active caspases proteolytically cleave their respective substrate resulting in the release of the luciferase substrate aminoluciferin. The substrate then is cleaved by the luciferase present in the buffer. The resulting luminescent signal can be measured in a suitable luminescence plate reader. The intensity of the luminescence signal is directly proportional to the amount of active caspase within the respective sample.

To detect activity of effector caspase-3/7 and one of the initiator caspases-8 or -9, so called “multiplex assays” were performed. These allow gathering of two data sets from the same sample.

Materials and Methods

In doing so the substrate from the caspase-3/7 assay is mixed with either Caspase-Glo® 8 or 9 assay and incubated in the dark. The activity of the caspases can then be detected by monitoring the fluorescence (Ex499/Em521) and luminescence signals (integration time luminescence: 500 msec).

All caspase activity assays performed with re-seeded cell samples were carried out in black polyesterol flat bottom microtiter plates with translucent bottom in a volume of 50 µl medium and 50 µl of the respective caspase assay mix. Incubation times were set to 3 hours with a kinetic measurement of fluorescence and/or luminescence signal every 5 min in the Infinite M200 plate reader (Tecan).

Combination of resazurin and caspase activation assays

In some experimental setups the number of different samples exceeded the capacity to be counted separately to normalize the caspase signal to the cell number. In these cases a combined resazurin conversion/caspase activity assay was performed in which the caspase activity is normalized to the metabolic activity of the cells (indicating their viability). Since the excitation and emission wavelength of resorufin does not interfere with the fluorescent caspase-3/7 activity signal, nor with the luminescence obtained in the Caspase-Glo® 8 or 9 assay, both signals can be measured within the same well.

To perform these assays cells were harvested by trypsinization and 50 µl of cell suspension was transferred to a black microtiter plate and supplemented with resazurin (10 µl) as described above. After read-out of the resorufin signal an equal volume (60 µl) of the desired caspase activity assay was directly added to the wells. Incubation and read-out of the respective caspase activity was carried out as described in the previous paragraph.

Immunofluorescence microscopy

To detect endogenous and/or overexpressed proteins directly in mammalian cells immunofluorescence staining experiments can be performed. For immunofluorescence stainings PC12 cells were grown on collagen coated sterile coverslips. Depending on the particular experimental approach cells were transfected with siRNA and/or plasmid DNA and/or induced for Htt25Q-EGFP or Htt103Q-EGFP expression. After the appropriate incubation time cells were washed carefully with D-PBS and fixed with 4% paraformaldehyde (PFA) in 1x PBS for 10 – 20 min at room temperature. Subsequently, cells were incubated with 50 mM NH₄Cl for 10 min to block free aldehyde groups of remaining PFA to reduce the background signal. Cells were then permeabilized with 0.2 % TritonX-100 for 2 min. Permeabilized cells were blocked in 1 % bovine serum albumin (BSA) in 1x PBS for 30 min, followed by incubation with a primary antibody recognizing the protein of interest diluted in 1% BSA/1x PBS. After several washing steps to remove unbound primary antibody the samples were incubated with a suitable fluorescence-labelled secondary antibody for 30 min at room temperature. After repetition of the washing steps coverslips carrying the stained cells were mounted upside down on glass plates using ProLong® Gold antifade reagent with DAPI (Invitrogen). The

Materials and Methods

mounted samples were stored over night at 4°C and subsequently examined using a fluorescence microscope (Zeiss) equipped with a CAM MR3 camera.

Filtersets:

DAPI:	Filterset 49	G 365	FT 395	BP 445/50
EGFP:	Filterset 38	BP 470/40	FT 495	BP 525/50
Cy3:	Filterset 43HE	BP 550/25	FT 570	BP 605/70
Cy 5:	Filterset 50	BP 640/30	FT 660	BP 690/50

All filtersets were purchased from Zeiss (https://www.micro-shop.zeiss.com/us/us_en/spektral.php?f=fi)

Cell-based FRET (Förster resonance energy transfer) assay

The FRET method was used to detect protein-protein interactions between two potential interaction partners which are co-expressed in mammalian cells. For monitoring the interaction one of the proteins is labeled with a ECFP-tag (donor) and the other with an EYFP-tag (acceptor). Therefore both proteins were generated as ECFP-/EYFP fusion proteins. The ECFP-flourescence can be excited with 436 nm UV-light and emits light at 485 nm, while EYFP is excited with 485 nm and fluorescence is detected at 530 nm. When they are dissociated, the ECFP emission is detected at 485 nm upon the excitation. When the donor (ECFP) and acceptor (EYFP) are in proximity (1-10 nm) due to the interaction between the fusion proteins, the emitted light from the donor at 485 nm can excite the acceptor which results in fluorescence at 530 nm. The emitted fluorescence of EYFP is observed because of the intermolecular FRET from the ECFP- to the EYFP-labeled protein.

HEK293 cells were seeded in 96well cell culture plates (45000 cells/well) and co-transfected with pdECFP-DDX24 and pdEYFP-FADD. As negative controls cells were treated either with pdECFP-DDX24 and pdEYFP-Amp (empty vector) or with pdEYFP-FADD and pdECFP-Amp. Moreover, other cells were transfected with pdECFP-DDX24/pcDNA3.1- β -Gal or pdEYFP-FADD/pcDNA3.1- β -Gal as controls for background fluorescence ("ECFP/EYFP correction"). For all reactions 2 x 0.1 μ g plasmid DNA was transfected. Samples were incubated for 24 hours at 37°C.

Protein combinations expressed in HEK293 cells:

ECFP-DDX24/EYFP-FADD	(FRET sample)
ECFP-DDX24/EYFP	(ECFP neg. control)
ECFP/EYFP-FADD	(EYFP neg. control)
ECFP-DDX24/ β -Gal	(ECFP correction)
EYFP-FADD/ β -Gal	(EYFP correction)

Materials and Methods

To prove the expression of the fusion proteins fluorescence signals were detected at Ex436nm/Em485nm (“ECFP_{485nm}”) and at Ex485nm/Em530nm (“EYFP_{530nm}”). For monitoring the interaction the FRET signal was detected at Ex436nm/Em530 nm (“FRET_{530nm}”) in a fluorescence plate reader (Infinite M200, Tecan). Background signals of non-transfected cells were subtracted in all samples.

Calculation of the FRET efficiency (netFRET)

1. calculation of ECFP-/EYFP correction factors:

$$\text{ECFP correction factor } a = \frac{\text{FRET}_{530\text{nm}} \text{ in ECFP correction}}{\text{ECFP}_{485\text{nm}} \text{ in ECFP correction}}$$

$$\text{EYFP correction factor } b = \frac{\text{FRET}_{530\text{nm}} \text{ in EYFP correction}}{\text{EYFP}_{530\text{nm}} \text{ in EYFP correction}}$$

2. calculation of the netFRET (for FRET sample and neg. controls):

$$\text{netFRET (RFU)} = (\text{FRET}_{530\text{nm}} - \text{ECFP}_{485\text{nm}}) \times a - \text{EYFP}_{530\text{nm}} \times b$$

3. calculation of the fold change in FRET samples:

$$\text{fold change ECFP} = \frac{\text{netFRET in FRET sample}}{\text{netFRET in ECFP neg. control}}$$

$$\text{fold change EYFP} = \frac{\text{netFRET in FRET sample}}{\text{netFRET in EYFP neg. control}}$$

Chapter 5

Literature

- Aiken C.T., Tobin A.J. and Schweitzer E.S. (2004) A cell-based screen for drugs to treat Huntington's disease. *Neurobiol Dis.* 16:546-555
- Akao Y., Seto M., Yamamoto K., Iida S., Nakazawa S., Inazawa J., Abe T., Takahashi T. and Ueda R. (1992) The RCK gene associated with t(1114) translocation is distinct from the MLL/ALL-1 gene with t(411) and t(1119) translocations. *Cancer Res.* 52:6083-6087
- Akao Y., Yoshida H., Matsumoto K., Matsui T., Hogetu K., Tanaka N. and Usukura J. (2003) A tumour-associated DEAD-box protein rck/p54 exhibits RNA unwinding activity toward c-mycRNAs in vitro. *Genes Cells.* 8:671-676
- Alnemri E.S., Livingston D.J., Nicholson D.W., Salvesen G., Thornberry N.A., Wong W.W. and Yuan J. (1996) Human ICE/CED-3 protease nomenclature. *Cell.* 87:171
- Andersen J.S., Lam Y.W., Leung A.K., Ong S.E., Lyon C.E., Lamond A.I. and Mann M. (2005) Nuclear proteome dynamics. *Nature.* 433:77-83
- Anderson A.N., Roncaroli F., Hodges A., Deprez M. and Turkheimer F.E. (2008) Chromosomal profiles of gene expression in Huntington's disease. *Brain.* 131:381-388
- Andrade M.A. and Bork P. (1995) Heat repeats in the huntington's disease protein. *Nat Genet.* 11:115-116
- Andrade M.A., Petosa C., O'Donoghue S.I., Muller C.W. and Bork P. (2001) Comparison of arm and heat protein repeats. *J Mol Biol.* 309:1-18
- Apostol B.L., Illes K., Pallos J., Bodai L., Wu J., Strand A., Schweitzer E.S., Olson J.M., Kazantsev A., Marsh J.L. and Thompson L.M. (2006) Mutant huntingtin alters MAPK signaling pathways in PC12 and striatal cells: ERK1/2 protects against mutant huntingtin-associated toxicity. *Hum Mol Genet.* 15:273-285
- Apostol B.L., Kazantsev A., Raffioni S., Illes K., Pallos J., Bodai L., Slepko N., Bear J.E., Gertler F.B., Hersch S., Housman D.E., Marsh J.L. and Thompson L.M. (2003) A cell-based assay for aggregation inhibitors as therapeutics of polyglutamine-repeat disease and validation in *Drosophila*. *Proc Natl Acad Sci USA.* 100:5950-5955
- Arrasate M., Mitra S., Schweitzer E.S., Segal M.R. and Finkbeiner S. (2004) Inclusion body formation reduces levels of mutant huntingtin and the risk of neuronal death. *Nature.* 431:805-810

Literature

- Arzberger T., Krampfl K., Leimgruber S. and Weindl A. (1997) Changes of NMDA receptor subunit (NR1, NR2B) and glutamate transporter (GLT1) mRNA expression in Huntington's disease - An in situ hybridization study. *J Neuropathol Exp Neurol.* 56:440-454
- Augood S.J., Faull R.L.M. and Emson P.C. (1997) Dopamine D1 and D2 receptor gene expression in the striatum in Huntington's disease. *Ann Neurol.* 42:215-221
- Bachoud-Levi A. C., Remy P., Nguyen J. P., Brugieres P., Lefaucheur J. P., Bourdet C., Baudic S., Gaura V., Maison P., Haddad B., Boisse M. F., Grandmougin T., Jeny R., Bartolomeo P., Dalla Barba G., Degos J. D., Lisovski F., Ergis A. M., Pailhous E., Cesaro P., Hantraye P. and Peschanski M. (2000) Motor and cognitive improvements in patients with huntington's disease after neural transplantation. *Lancet.* 356:1975-1979
- Bae B.I., Xu H., Igarashi S., Fujimuro M., Agrawal N., Taya Y., Hayward S.D., Moran T.H., Montell C., Ross C.A., Snyder S.H. and Sawa A. (2005) p53 mediates cellular dysfunction and behavioral abnormalities in Huntington's disease. *Neuron.* 47:29-41
- Bando Y., Onuki R., Katayama T., Manabe T., Kudo T., Taira K. and Tohyama M. (2005) Double-strand RNA dependent protein kinase (PKR) is involved in the extrastriatal degeneration in Parkinson's disease and Huntington's disease. *Neurochem Int.* 46:11-18
- Barrios-Rodiles M., Brown K.R., Ozdamar B., Bose R., Liu Z., Donovan R.S., Shinjo F., Liu Y., Dembowy J., Taylor I.W., Luga V., Przulj N., Robinson M., Suzuki H., Hayashizaki Y., Jurisica I. and Wrana J.L. (2005) High-throughput mapping of a dynamic signaling network in mammalian cells. *Science.* 307:1621-1625
- Bates G., Harper S.P. and Jones L. (2002) Huntington's Disease. *Oxford University Press*
- Bates G.J., Nicol S.M., Wilson B.J., Jacobs A.M., Bourdon J.C., Wardrop J., Gregory D.J., Lane D.P., Perkins N.D. and Fuller-Pace F.V. (2005) The DEAD box protein p68: a novel transcriptional coactivator of the p53 tumour suppressor. *EMBO J.* 24:543-553
- Becher M.W., Kotzok J.A., Sharp A.H., Davies S.W., Bates G.P., Price D.L. and Ross C.A. (1998) Intranuclear neuronal inclusions in Huntington's disease and dentatorubral and pallidoluysian atrophy: correlation between the density of inclusions and IT15 CAG triplet repeat length. *Neurobiol Dis.* 4:387-397
- Bence N.F., Sampat R.M. and Kopito R.R. (2001) Impairment of the ubiquitin-proteasome system by protein aggregation. *Science.* 292:1552-1555
- Berthelot K., Muldoon M., Rajkowitsch L., Hughes J. and McCarthy J.E. (2004) Dynamics and processivity of 40S ribosome scanning on mRNA in yeast. *Mol Microbiol.* 51:987-1001
- Besch R., Poeck H., Hohenauer T., Senft D., Häcker G., Berking C., Hornung V., Endres S., Ruzicka T., Rothenfusser S. and Hartmann G. (2009) Proapoptotic signaling induced by RIG-I and

Literature

- MDA-5 results in type I interferon-independent apoptosis in human melanoma cells. *J Clin Invest.* 119:2399-2411
- Bett J.S., Goellner G.M., Woodman B., Pratt G., Rechsteiner M. and Bates G.P. (2006) Proteasome impairment does not contribute to pathogenesis in R6/2Huntington's disease mice: exclusion of proteasome activator REGγ as a therapeutic target. *Hum Mol Genet.* 15:33-44
- Bilen J. and Bonini N.M. (2007) Genome-wide screen for modifiers of ataxin-3 neurodegeneration in *Drosophila*. *PLoS Genet.* 3:1950-1964
- Bilney B., Morris M.E. and Perry A. (2003) Effectiveness of physiotherapy, occupational therapy, and speech pathology for people with Huntington's disease: a systematic review. *Neurorehabil Neural Repair.* 17:12-24
- Birbes H., El Bawab S., Obeid L.M. and Hannun Y.A. (2002) Mitochondria and ceramide: intertwined roles in regulation of apoptosis. *Adv Enzyme Regul.* 42:113-129
- Block-Galarza J., Chase K.O., Sapp E., Vaughn K.T., Vallee R.B., Di-Figlia M. and Aronin N. (1997) Fast transport and retrograde movement of Huntingtin and hap 1 in axons. *Neuroreport.* 8:2247-2251
- Blum S., Schmid S.R., Pause A., Buser P., Linder P., Sonenberg N. and Trachsel H. (1992) ATP hydrolysis by initiation factor 4A is required for translation initiation in *Saccharomyces cerevisiae*. *Proc Natl Acad Sci USA.* 89:7664-7668
- Boatright K.M., Renatus M., Scott F.L., Sperandio S., Shin H., Pedersen I.M., Ricci J.E., Edris W.A., Sutherlin D.P., Green D.R. and Salvesen G.S. (2003) A unified model for apical caspase activation. *Mol Cell.* 11:529-541
- Bodner R.A., Outeiro T.F., Altmann S., Maxwell M.M., Cho S.H., Hyman B.T., McLean P.J., Young A.B., Housman D.E. and Kazantsev A.G. (2006) Pharmacological promotion of inclusion formation: a therapeutic approach for Huntington's and Parkinson's diseases. *Proc Natl Acad Sci USA.* 103:4246-4251
- Boldin M.P., Goncharov T.M., Goltsev Y.V. and Wallach D. (1996) Involvement of MACH a novel MORT1/FADD-Interacting Protease in Fas/APO-1- and TNF receptor induced cell death. *Cell.* 85:803-815
- Boldin M.P., Varfolomeev E.E., Pancer Z., Mett I.L., Camonis J.H. and Wallach D. (1995) A novel protein that interacts with the death domain of Fas/APO1 contains a sequence motif related to the death domain. *J Biol Chem.* 270:7795-7798
- Bonelli R.M., Niederwieser G., Diez J., Gruber A. and Költringer P. (2002) Pramipexole ameliorates neurologic and psychiatric symptoms in a Westphal variant of Huntington's disease. *Clin Neuropharmacol.* 25:58-60

Literature

- Borovecki F., Lovrecic L., Zhou J., Jeong H., Then F., Rosas H.D., Hersch S.M., Hogarth P., Bouzou B., Jensen R.V. and Krainc D. (2005) Genome-wide expression profiling of human blood reveals biomarkers for Huntington's disease. *Proc Natl Acad Sci USA*. 102:11023-11028
- Boutell J.M., Thomas P., Neal J.W., Weston V.J., Duce J., Harper P.S. and Jones A.L. (1999) Aberrant interactions of transcriptional repressor proteins with the Huntington's disease gene product huntingtin. *Hum Mol Genet*. 8:1647-1655
- Bowman A.B., Yoo S.Y., Dantuma N.P. and Zoghbi H.Y. (2005) Neuronal dysfunction in a polyglutamine disease model occurs in the absence of ubiquitin-proteasome system impairment and inversely correlates with the degree of nuclear inclusion formation. *Hum Mol Genet*. 14:679-691
- Branco J., A.I. Ramahi I., Ukani L., Perez A.M., Fernandez-Funez P., Rincon-Limas D. and Botas J. (2008) Comparative analysis of genetic modifiers in *Drosophila* points to common and distinct mechanisms of pathogenesis among polyglutamine diseases. *Hum Mol Genet*. 17:376-390
- Brandt J., Strauss M.E., Larus J., Jensen B., Folstein S.E. and Folstein M.F. (1984) Clinical correlates of dementia and disability in Huntington's disease. *J Clin Neuropsychol*. 6:401-412
- Bridge A.J., Pebernard S., Ducraux A., Nicoulaz A.-L and Iggo R. (2003) Induction of an interferon response by RNAi vectors in mammalian cells. *Nat Genet*. 34:263-264
- Brochier C., Gaillard M.C., Diguët E., Caudy N., Dossat C., Ségurens B., Wincker P., Roze E., Caboche J., Hantraye P., Brouillet E., Elalouf J.M. and de Chaldée M. (2008) Quantitative gene expression profiling of mouse brain regions reveals differential transcripts conserved in human and affected in disease models. *Physiol Genomics*. 33:170-179
- Browne S.E., Bowling A.C., MacGarvey U., Baik M.J., Berger S.C., Muqit MM, Bird E.D. and Beal M.F. (1997) Oxidative damage and metabolic dysfunction in Huntington's disease: Selective vulnerability of the basal ganglia. *Ann Neurol*. 41:646-653
- Bucciantini M., Calloni G., Chiti F., Formigli L., Nosi D., Dobson C.M. and Stefani M. (2004) Prefibrillar amyloid protein aggregates share common features of cytotoxicity. *J Biol Chem*. 279:31374-31382
- Bucciantini M., Giannoni E., Chiti F., Baroni F., Formigli L., Zurdo J., Taddei N., Ramponi G., Dobson C.M. and Stefani M. (2002) Inherent toxicity of aggregates implies a common mechanism for protein misfolding diseases. *Nature*. 416:507-511
- Castrillon D.H., Quade B.J., Wang T.Y., Quigley C. and Crum C.P. (2000) The human VASA gene is specifically expressed in the germ cell lineage. *Proc Natl Acad Sci USA*. 97:9585-9590
- Cattaneo E., Zuccato C. and Tartari M. (2005) Normal huntingtin function: an alternative approach to huntington's disease. *Nat Rev Neurosci*. 6:919-930
- Cha J.H. (2007) Transcriptional signatures in Huntington's disease. *Prog Neurobiol*. 83:228-248

Literature

- Chan C.C., Dostie J., Diem M.D., Feng W., Mann M., Rappsilber J. and Dreyfuss G. (2004) eIF4A3 is a novel component of the exonjunction complex. *RNA*. 10:200-209
- Chandra S., Shao J., Li J.X., Li M., Longo F.M. and Diamond M.I. (2008) A common motif targets huntingtin and the androgen receptor to the proteasome. *J Biol Chem*. 283:23950-23955
- Charroux B., Pellizzoni L., Perkinson R.A., Shevchenko A., Mann M. and Dreyfuss G. (1999) Gemin3: A novel DEAD box protein that interacts with SMN the spinal muscular atrophy gene product and is a component of gems. *J Cell Biol*. 147:1181-1194
- Chaurasia G., Iqbal Y., Hänig C., Herzel H., Wanker E.E. and Futschik M.E. (2007) UniHI: an entry gate to the human protein interactome. *Nucleic Acids Res*. 35:D590-D594
- Chaurasia G., Malhotra S., Russ J., Schnoegl S., Hänig C., Wanker E.E. and Futschik M.E. (2009) UniHI 4: new tools for query analysis and visualization of the human protein-protein interactome. *Nucleic Acids Res*. 37:D657-D660
- Chen J.Y.-F, Stands L., Staley J.P., Jackups R.R. Jr, Latus L.J. and Chang T.H. (2001) Specific alterations of U1-C protein or U1 small nuclear RNA can eliminate the requirement of Prp28p an essential DEAD box splicing factor. *Mol Cell*. 7:227-232
- Chen M., Ona V.O., Li M., Ferrante R.J., Fink K.B., Zhu S., Bian J., Guo L., Farrell L.A., Hersch S.M., Hobbs W., Vonsattel J.P., Cha J.H. and Friedlander R.M. (2000) Minocycline inhibits caspase-1 and caspase-3 expression and delays mortality in a transgenic mouse model of Huntington disease. *Nat Med*. 6:797-801
- Chinnaiyan A.M. (1999) The apoptosome: heart and soul of the cell death machine. *Neoplasia*. 1:5-15
- Chinnaiyan A.M., O'Rourke K., Tewari M. and Dixit V.M. (1995) FADD a novel death domain-containing protein interacts with the death domain of Fas and initiates apoptosis. *Cell*. 81:505-512
- Chiu E. and Alexander L. (1982) Causes of death in Huntington's disease. *Med J Aust*. 1:153
- Cho B., Lim Y., Lee D.Y., Park S.Y., Lee H., Kim W.H., Yang H., Bang Y.J. and Jeoung D.I. (2002) Identification and characterization of a novel cancer/testis antigen gene CAGE. *Biochem Biophys Res Commun*. 292:715-726
- Choi S.A., Kim S.J. and Chung K.C. (2006) Huntingtin-interacting protein 1-mediated neuronal cell death occurs through intrinsic apoptotic pathways and mitochondrial alterations. *FEBS Lett*. 580:5275-5282
- Choo Y.S., Johnson G.V., MacDonald M., Detloff P.J. and Lesort M. (2004) Mutant huntingtin directly increases susceptibility of mitochondria to the calcium-induced permeability transition and cytochrome c release. *Hum Mol Genet*. 13:1407-1420

Literature

- Chung J., Lee S.-G. and Song K. (1995) Identification of a human homologue of a putative RNA helicase gene (mDEAD3) expressed in mouse erythroid cells. *Korean J Biochem.* 27:193-197
- Ciechanover A. and Brundin P. (2003) The ubiquitin proteasome system in neurodegenerative diseases: sometimes the chicken sometimes the egg. *Neuron.* 40:427-446
- Colin E., Régulier E., Perrin V., Dürr A., Brice A., Aebischer P., Déglon N., Humbert S. and Saudou F. (2005) Akt is altered in an animal model of Huntington's disease and in patients. *Eur J Neurosci.* 21:1478-1488
- Cong S.Y., Pepers B.A., Evert B.O., Rubinsztein D.C., Roos R.A., van Ommen G.J. and Dorsman J.C. (2005) Mutant huntingtin represses CBP, but not p300, by binding and protein degradation. *Mol Cell Neurosci.* 30:560-571
- Cornwell G.G., Sletten K., Johansson B. and Westermark P. (1988) Evidence that the amyloid fibril protein in senile systemic amyloidosis is derived from normal prealbumin. *Biochem Biophys Res Commun.* 154:648-653
- Cory S. and Adams J.M. (2002) The Bcl2 family: regulators of the cellular life-or-death switch. *Nat Rev Cancer.* 2:647-656
- Coufal M., Maxwell M.M., Russel D.E., Amore A.M., Altmann S.M., Hollingsworth Z.R., Young A.B., Housman D.E. and Kazantsev A.G. (2007) Discovery of a novel small-molecule targeting selective clearance of mutant huntingtin fragments. *J Biomol Screen.* 12:351-360
- Crocker S.F., Costain W.J. and Robertson H.A. (2006) DNA microarray analysis of striatal gene expression in symptomatic transgenic Huntington's mice (R6/2) reveals neuroinflammation and insulin associations. *Brain Res.* 1088:176-186
- Cryns V. and Yuan J. (1998) Proteases to die for. *Genes Dev.* 12:1551-1570
- Cui L., Jeong H., Borovecki F., Parkhurst C.N., Tanese N. and Krainc D. (2006) Transcriptional repression of PGC-1alpha by mutant huntingtin leads to mitochondrial dysfunction and neurodegeneration. *Cell.* 127:59-69
- D'Amelio M., Cavallucci V. and Cecconi F. (2009) Neuronal caspase-3 signaling: not only cell death. *Cell Death Differ.* Epub ahead of print
- Davies S.W., Turmaine M., Cozens B.A., DiFiglia M., Sharp A.H., Ross C.A., Scherzinger E., Wanker E.E., Mangiarini L. and Bates G.P. (1997) Formation of neuronal intranuclear inclusions underlies the neurological dysfunction in mice transgenic for the HD mutation. *Cell.* 90:537-548
- de la Cruz J., Kressler D. and Linder P. (1999) Unwinding RNA in *Saccharomyces cerevisiae*: DEAD-box proteins and related families. *Trends Biochem.* 24:192-198
- de la Cruz J., Kressler D. and Linder P. (2003) Ribosomal subunit assembly. In: Olson, M.O.J. (Ed.), *The Nucleolus. Kluwer Academic/Plenum Publishers, New York.* 263-290.

Literature

- De Marchi N., Daniele F. and Ragone M.A. (2001) Fluoxetine in the treatment of Huntington's disease. *Psychopharmacology*. 153:264-266
- Desai U.A., Pallos J., Ma A.A., Stockwell B.R., Thompson L.M., Marsh J.L. and Diamond M.I. (2006) Biologically active molecules that reduce polyglutamine aggregation and toxicity. *Hum Mol Genet*. 15:2114-2124
- Dewhurst K., Oliver J.E. and McKnight A.L. (1970) Socio-psychiatric consequences of Huntington's disease. *Br J Psychiatry*. 116:255-258
- Diaz-Hernandez M., Hernandez F., Martin-Aparicio E., Gomez-Ramos P., Moran M.A., Castano J.G., Ferrer I., Avila J. and Lucas J.J. (2003) Neuronal induction of the immunoproteasome in Huntington's disease. *J Neurosci*. 23:11653-11661
- DiFiglia M., Sapp E., Chase K.O., Davies S.W., Bates G.P., Vonsattel J.P. and Aronin N. (1997) Aggregation of huntingtin in neuronal intranuclear inclusions and dystrophic neurites in brain. *Science*. 277:1990-1993
- DiFiglia M., Sapp E., Chase K., Schwarz C., Meloni A., Young C., Martin E., Vonsattel J.P., Carraway R., Reeves S.A. et al. (1995) Huntingtin is a cytoplasmic protein associated with vesicles in human and rat brain neurons. *Neuron*. 14:1075-1078
- Ding Q., Lewis J.J., Strum K.M., Dimayuga E., Bruce-Keller A.J., Dunn J.C. and Keller J.N. (2002) Polyglutamine expansion protein aggregation proteasome activity and neural survival. *J Biol Chem*. 277:13935-13942
- Ditton H.J., Zimmer J., Kamp C., Rajpert-De Meyts E. and Vogt P.H. (2004) The AZFa gene DBY (DDX3Y) is widely transcribed but the protein is limited to the male germ cells by translation control. *Hum Mol Genet*. 13:2333-2341
- Doumanis J., Wada K., Kino Y., Moore A.W. and Nukina N. (2009) RNAi screening in *Drosophila* cells identifies new modifiers of mutant huntingtin aggregation. *PLoS One*. 4:e7275
- Driscoll M. and Gerstbrein B. (2003) Dying for a cause: Invertebrate genetics takes on human neurodegeneration. *Nat Rev Genet*. 4:181-194
- Du C., Fang M., Li Y., Li L. and Wang X. (2000) Smac a mitochondrial protein that promotes cytochrome c-dependent caspase activation by eliminating IAP inhibition. *Cell*. 102:33-42
- Dumanchin-Njock C., Alves da Costa C.A, Mercken L., Pradier L. and Checler F. (2001) The caspase-derived C-terminal fragment of betaAPP induces caspase-independent toxicity and triggers selective increase of Abeta42 in mammalian cells. *J Neurochem*. 78:1153-1161
- Dunah A.W., Jeong H., Griffin A., Kim Y.M., Standaert D.G., Hersch S.M., Mouradian M.M., Young A.B., Tanese N. and Krainc D. (2002) Sp1 and TAFII130 transcriptional activity disrupted in early Huntington's disease. *Science*. 296:2238-2243

Literature

- Duyao M.P., Auerbach A.B., Ryan A., Persichetti F., Barnes G.T., McNeil S.M., Ge P., Vonsattel J.P., Gusella J.F., Joyner A.L. and MacDonald M.E. (1995) Inactivation of the mouse Huntington's disease gene homolog Hdh. *Science*. 269:407-410
- Earnshaw W.C., Martins L.M. and Kaufmann S.H. (1999) Mammalian caspases: structure activation substrates and functions during apoptosis. *Annu Rev Biochem*. 68:383-424
- Elmore S. (2007) Apoptosis: a review of programmed cell death. *Toxicol Pathol*. 35:495-516
- Emery E., Aldana P., Bunge M.B., Puckett W., Srinivasan A., Keane R.W., Bethea J. and Levi A.D. (1998) Apoptosis after traumatic human spinal cord injury. *J Neurosurg*. 89:911-920
- Enari M., Sakahira H., Yokoyama H., Okawa K., Iwamatsu A. and Nagata S. (1998) A caspase-activated DNase that degrades DNA during apoptosis and its inhibitor ICAD. *Nature*. 391:43-50
- Engelender S., Sharp A.H., Colomer V., Tokito M.K., Lanahan A., Worley P., Holzbaur E.L. and Ross C.A. (1997) Huntingtin-associated protein 1 (hap1) interacts with the p150glued subunit of dynactin. *Hum Mol Genet*. 6:2205-2212
- Eraly S.A. and Nigam S.K. (2002) Novel human cDNAs homologous to Drosophila Orct and mammalian carnitine transporters. *Biochem Biophys Res Commun*. 297:1159-1166
- Esposti M.D. (2002) The roles of Bid. *Apoptosis*. 7:433-440
- Fagni L., Lafon-Cazal M., Rondouin G., Manzoni O., Lerner-Natoli M. and Bockaert J. (1994) The role of free radicals in NMDA-dependent neurotoxicity. *Prog Brain Res*. 103:381-390
- Fan M.M. and Raymond L.A. (2007) N-methyl-D-aspartate (NMDA) receptor function and excitotoxicity in Huntington's disease. *Prog Neurobiol*. 81:272-293
- Fang J., Kubota S., Yang B., Zhou N., Zhang H., Godbout R. and Pomerantz R.J. (2004) A DEAD box protein facilitates HIV-1 replication as a cellular co-factor of Rev. *Virology*. 330:471-480
- Feng Z., Jin S., Zupnick A., Hoh J., de Stanchina E., Lowe S., Prives C. and Levine A.J. (2006) p53 tumor suppressor protein regulates the levels of huntingtin gene expression. *Oncogene*. 25:1-7
- Ferraiuolo M.A., Lee C.S., Ler L.W., Hsu J.L., Costa-Mattioli M., Luo M.J., Reed R. and Sonenberg N. (2004) A nuclear translation-like factor eIF4AIII is recruited to the mRNA during splicing and functions in nonsense-mediated decay. *Proc Natl Acad Sci USA*. 101:4118-4123
- Ferrer I., Blanco R., Cutillas B. and Ambrosio S. (2000) Fas and Fas-L expression in Huntington's disease and Parkinson's disease. *Neuropathol Appl Neurobiol*. 26:424-433
- Filiz G., Caragounis A., Bica L., Du T., Masters C.L., Crouch P.J. and White A.R. (2008) Clioquinol inhibits peroxide-mediated toxicity through up-regulation of phosphoinositol-3-kinase and inhibition of p53 activity. *Int J Biochem Cell Biol*. 40:1030-1042
- Fischer N. and Weis K. (2002) The DEAD box protein Dhh1 stimulates the decapping enzyme Dcp1. *EMBO J*. 21: 2788-2797

Literature

- Fleckner J., Zhang M., Valcarcel J. and Green M.R. (1997) U2AF65 recruits a novel human DEAD box protein required for the U2snRNP-branchpoint interaction. *Genes Dev.* 11:1864-1872
- Folstein S., Abbott M.H., Chase G.A., Jensen B.A. and Folstein M.F. (1983) The association of affective disorder with Huntington's disease in a case series and in families. *Psychol Med.* 3:537-542
- Folstein S.E., Chase G.A., Wahl W.E., McDonnell A.M. and Folstein M.F. (1987) Huntington disease in Maryland: clinical aspects of racial variation. *J Hum Genet.* 41:168-179
- Ford M.J., Anton I.A. and Lane D.P. (1988) Nuclear protein with sequence homology to translation initiation factor eIF-4A. *Nature.* 332:736-738
- Friedlander R.M. (2003) Apoptosis and caspases in neurodegenerative diseases. *N Engl J Med.* 348:1365-1375
- Gafni J. and Ellerby L.M. (2002) Calpain activation in Huntington's disease. *J Neurosci.* 22:4842-4849
- Gafni J., Hermel E., Young J.E., Wellington C.L., Hayden M.R. and Ellerby L.M. (2004) Inhibition of calpain cleavage of huntingtin reduces toxicity: accumulation of calpain/caspase fragments in the nucleus. *J Biol Chem.* 279:20211-20220
- Garcia E.P., Mehta S., Blair L.A., Wells D.G., Shang J., Fukushima T., Fallon J.R., Garner C.C. and Marshall J. (1998) SAP90 binds and clusters kainate receptors causing incomplete desensitization. *Neuron.* 21:727-739
- Garrido C., Galluzzi L., Brunet M., Puig P. E., Didelot C. and Kroemer G. (2006) Mechanisms of cytochrome c release from mitochondria. *Cell Death Differ.* 13:1423-1433
- Gatignol A., Buckler-White A.J., Berkhout B. and Jeang K.T. (1991) Characterization of a human TAR RNA-binding protein that activates the HIV-1 LTR. *Science.* 251:1597-1600
- Gauthier L.R., Charrin B.C., Borrell-Pages M., Dompierre J.P., Rangone H., Cordelieres F.P., De Mey J., MacDonald M.E., Lessmann V., Humbert S. and Saudou F. (2004) Huntingtin controls neurotrophic support and survival of neurons by enhancing BDNF vesicular transport along microtubules. *Cell.* 118:127-138
- Gerber H.P., Seipel K., Georgiev O., Hofferer M., Hug M., Rusconi S. and Schaffner W. (1994) Transcriptional activation modulated by homopolymeric glutamine and proline stretches. *Science.* 263:808-811
- Gervais F.G., Singaraja R., Xanthoudakis S., Gutekunst C.A., Leavitt B.R., Metzler M., Hackam A.S., Tam J., Vaillancourt J.P., Houtzager V., Rasper D.M., Roy S., Hayden M.R. and Nicholson D.W. (2002) Recruitment and activation of caspase-8 by the Huntingtin-interacting protein Hip-1 and a novel partner Hip1. *Nat Cell Biol.* 4:95-105

Literature

- Gevaert K., Goethals M., Martens L., Van Damme J., Staes A., Thomas G.R. and Vandekerckhove J. (2003) Exploring proteomes and analyzing protein processing by mass spectrometric identification of sorted N-terminal peptides. *Nat Biotechnol.* 21:566-569
- Gieselmann R., Kwiatkowski D.J., Janmey P.A. and Witke W. (1995) Distinct biochemical characteristics of the two human profilin isoforms. *Eur J Biochem.* 229:621-628
- Giorgini F., Guidetti P., Nguyen Q., Bennett S.C. and Muchowski P.J. (2005) A genomic screen in yeast implicates kynurenine 3-monooxygenase as a therapeutic target for Huntington disease. *Nat Genet.* 37:526-531
- Godbout R. and Squire J. (1993) Amplification of a DEAD box protein gene in retinoblastoma cell lines. *Proc Natl Acad Sci USA.* 90:7578-7582
- Goehler H., Lalowski M., Stelzl U., Waelter S., Stroedicke M., Worm U., Droege A., Lindenberg K.S., Knoblich M., Haenig C., Herbst M., Suopanki J., Scherzinger E., Abraham C., Bauer B., Hasenbank R., Fritzsche A., Ludewig A.H., Bussow K., Coleman S.H., Gutekunst C.A., Landwehrmeyer B.G., Lehrach H. and Wanker E.E. (2004) A protein interaction network links GIT1 an enhancer of huntingtin aggregation to Huntington's disease. *Mol Cell.* 15:853-865
- Goldberg Y.P., Nicholson D.W., Rasper D.M., Kalchman M.A, Koide H.B., Graham R.K., Bromm M., Kazemi-Esfarjani P., Thornberry N.A., Vaillancourt J.P. and Hayden M.R. (1996) Cleavage of huntingtin by apopain a proapoptotic cysteine protease is modulated by the polyglutamine tract. *Nat Genet.* 13:442-449
- Gorbalenya A.E., Koonin E.V., Donchenko A.P. and Blinov V.M. (1989) Two related superfamilies of putative helicases involved in replication recombination repair and expression of DNA and RNA genomes. *Nucleic Acids Res.* 17:4713-4730
- Graham R.K., Deng Y., Slow E.J., Haigh B., Bissada N., Lu G., Pearson J., Shehadeh J., Bertram L., Murphy Z., Warby S.C., Doty C.N., Roy S., Wellington C.L., Leavitt B.R., Raymond L.A., Nicholson D.W. and Hayden M.R. (2006) Cleavage at the caspase-6 site is required for neuronal dysfunction and degeneration due to mutant huntingtin. *Cell.* 125:1179-1191.
- Grandori C., Mac J., Siebelt F., Ayer D.E. and Eisenman R.N. (1996) Myc-Max heterodimers activate a DEAD box gene and interact with multiple E box-related sites in vivo. *EMBO J.* 15:4344-4357
- Green D.R. and Reed J.C. (1998) Mitochondria and apoptosis. *Science.* 281:1309-1312
- Greene L.A. and Tischler A.S. (1976) Establishment of a noradrenergic clonal line of rat adrenal pheochromocytoma cells which respond to nerve growth factor. *Proc Natl Acad Sci USA.* 73:2424-2428

Literature

- Gromley A., Jurczyk A., Sillibourne J., Halilovic E., Mogensen M., Groisman I., Blomberg M. and Doxsey S.J. (2003) A novel human protein of the maternal centriole is required for the final stages of cytokinesis and entry into S phase. *J Cell Biol.* 161:535-545
- Gromley A., Yeaman C., Rosa J., Redick S., Chen C.T., Mirabelle S., Guha M., Sillibourne J. and Doxsey S.J. (2005) Centriolin anchoring of exocyst and SNARE complexes at the midbody is required for secretory-vesicle-mediated abscission. *Cell.* 123:75-87
- Grundhoff A.T., Kremmer E., Tureci O., Glieden A., Gindorf C., Atz J., Mueller-Lantzsch N., Schubach W.H. and Grasser F.A. (1999) Characterization of DP103 a novel DEAD box protein that binds to the Epstein-Barr virus nuclear proteins EBNA2 and EBNA3C. *J Biol Chem.* 274:19136-19144
- Gunawardena S. and Goldstein L.S. (2005) Polyglutamine diseases and transport problems: deadly traffic jams on neuronal highways. *Arch Neurol.* 62:46-51
- Gunawardena S., Her L.S., Brusich R.G., Laymon R.A., Niesman I.R., Gordesky-Gold B., Sintasath L., Bonini N.M. and Goldstein L.S. (2003) Disruption of axonal transport by loss of huntingtin or expression of pathogenic polyQ proteins in *Drosophila*. *Neuron.* 40:25-40
- Gutekunst C.A., Levey A.I., Heilman C.J., Whaley W.L., Yi H., Nash N.R., Rees H.D., Madden J.J. and Hersch S.M. (1995) Identification and localization of huntingtin in brain and human lymphoblastoid cell lines with anti-fusion protein antibodies. *Proc Natl Acad Sci USA.* 92:8710-8714
- Gutekunst C.-A., Li S.-H., Yi H., Mulroy J.S., Kuemmerle S., Jones R., Rye D., Ferrante R.J., Hersch S.M. and Li X.-J. (1999) Nuclear and neuropil aggregates in Huntington's disease: relationship to neuropathology. *J Neurosci.* 19:2522-2534
- Gutti R.K., Tsai-Morris C.H. and Dufau M.L. (2008) Gonadotropin-regulated testicular helicase (DDX25) an essential regulator of spermatogenesis prevents testicular germ cell apoptosis. *J Biol Chem.* 283:17055-17064
- Haase A.D., Jaskiewicz L., Zhang H., Laine S., Sack R., Gatignol A. and Filipowicz W. (2005) TRBP, a regulator of cellular PKR and HIV-1 virus expression, interacts with Dicer and functions in RNA silencing. *EMBO Rep.* 6:961-967
- Hackam A.S., Yassa A.S., Singaraja R., Metzler M., Gutekunst C.A., Gan L., Warby S., Wellington C.L., Vaillancourt J., Chen N., Gervais F.G., Raymond L., Nicholson D.W. and Hayden M.R. (2000) Huntingtin interacting protein 1 induces apoptosis via a novel caspase-dependent death effector domain. *J Biol Chem.* 275:41299-41308
- Harjes P. and Wanker E.E. (2003) The hunt for huntingtin function: interaction partners tell many different stories. *Trends Biochem Sci.* 28:425-433.

Literature

- Hattula K. and Peranen J. (2000) Fip-2, a coiled-coil protein, links Huntingtin to rab8 and modulates cellular morphogenesis. *Curr Biol.* 10:1603-1606
- Hay D.G., Sathasivam K., Tobaben S., Stahl B., Marber M., Mestril R., Mahal A., Smith D.L., Woodman B. and Bates G.P. (2004) Progressive decrease in chaperone protein levels in a mouse model of Huntington's disease and induction of stress proteins as a therapeutic approach. *Hum Mol Genet.* 13:1389-1405
- HDCRG (1993) A novel gene containing a trinucleotide repeat that is unstable on Huntington's disease chromosomes. *Cell.* 72:971-983
- Hengartner M.O. (2000) The biochemistry of apoptosis. *Nature.* 407:770-776
- Henning D., So R.B., Jin R., Lau L.F. and Valdez B.C. (2003) Silencing of RNA helicase II/Galpha inhibits mammalian ribosomalRNA production. *J Biol Chem.* 278:52307-52314
- Hickey M.A. and Chesselet M.F. (2003) The use of transgenic and knock-in mice to study Huntington's disease. *Cytogenet Genome Res.* 100:276-286
- Higuchi R., Dollinger G., Walsh P.S. and Griffith R. (1992) Simultaneous amplification and detection of specific DNA sequences. *Biotechnology.* 10:413-417
- Hill M.M., Adrain C., Duriez P.J., Creagh E.M. and Martin S.J. (2004) Analysis of the composition assembly kinetics and activity of native Apaf-1 apoptosomes. *EMBO J.* 23:2134-2145
- Hloch P., Schiedner G. and Stahl H. (1990) Complete cDNA sequence of the human p68 protein. *Nucleic Acids Res.* 18:3045
- Hodges A., Strand A.D., Aragaki A.K., Kuhn A., Sengstag T., Hughes G., Elliston L.A., Hartog C., Goldstein D.R., Thu D., Hollingsworth Z.R., Collin F., Synek B., Holmans P.A., Young A.B., Wexler N.S., Delorenzi M., Kooperberg C., Augood S.J., Faull R.L., Olson J.M., Jones L. and Luthi-Carter R. (2006) Regional and cellular gene expression changes in human Huntington's disease brain. *Hum Mol Genet.* 15:965-977
- Holmberg C.I., Staniszewski K.E., Mensah K.N., Matouschek A. and Morimoto R.I. (2004) Inefficient degradation of truncated polyglutamine proteins by the proteasome. *Embo J.* 23:4307-4318
- Hoon R. (2006) Estrogen Regulation of Mitochondrial Transcription in HD. Boston University Medical Campus dept. Of neurology and National Institute of Neurological Disorders and Stroke. Available from: <http://researchresources.bumc.bu.edu/abstract/1R01NS052724-01.htm>
- Hsu H., Xiong J. and Goeddel D.V. (1995) The TNF receptor 1-associated protein TRADD signals cell death and NF-kappa B activation. *Cell.* 81:495-504
- Humbert S., Bryson E.A., Cordelieres F.P., Connors N.C., Datta S.R., Finkbeiner S., Greenberg M.E. and Saudou F. (2002) The igf-1/akt pathway is neuroprotective in huntington's disease and involves huntingtin phosphorylation by akt. *Dev Cell.* 2:831-837

Literature

- Huntington G. (1872) On chorea. *Medical and Surgical Reporter*. 26:320-321
- Irion U., Leptin M., Siller K., Fuerstenberg S., Cai Y., Doe C.Q., Chia W. and Yang X. (2004) Abstrakt, a DEAD box protein, regulates Insc levels and asymmetric division of neural and mesodermal progenitors. *Curr Biol*. 14:138-144
- Irion, U. and Leptin, M. (1999) Developmental and cell biological functions of the Drosophila DEAD-box protein abstrakt. *Curr Biol*. 9:1373-1381
- Irmeler M., Thome M., Hahne M., Schneider P., Hofmann K., Steiner V., Bodmer J.L., Schröter M., Burns K., Mattmann C., Rimoldi D., French L.E. and Tschopp J. (1997) Inhibition of death receptor signals by cellular FLIP. *Nature*. 388:190-195
- Iwata A., Riley B.E., Johnston J.A. and Kopito R.R. (2005) HDAC6 and microtubules are required for autophagic degradation of aggregated huntingtin. *J Biol Chem*. 280:40282-40292
- Jackson A.L., Bartz S.R., Schelter J., Kobayashi S.V., Burchard J., Mao M., Li B., Cavet G. and Linsley P.S. (2003) Expression profiling reveals off-target gene regulation by RNAi. *Nat Biotechnol*. 21:635-637
- Jackson A.L., Burchard J., Schelter J., Chau B.N., Cleary M., Lim L. and Linsley P.S. (2006) Widespread siRNA "off-target" transcript silencing mediated by seed region sequence complementarity. *RNA*. 12:1179-1187
- Jana N.R., Tanaka M., Wang G. and Nukina N. (2000) Polyglutamine length-dependent interaction of Hsp40 and Hsp70 family chaperones with truncated N-terminal huntingtin: their role in suppression of aggregation and cellular toxicity. *Hum Mol Genet*. 9:2009-2018
- Jana N.R., Zemskov E.A., Wang G.H. and Nukina N. (2001) Altered proteasomal function due to the expression of polyglutamine-expanded truncated N-terminal huntingtin induces apoptosis by caspase activation through mitochondrial cytochrome c release. *Hum Mol Genet*. 10:1049-1059
- Jänicke R.U., Walker P.A., Lin X.Y. and Porter A.G. (1996) Specific cleavage of the retinoblastoma protein by an ICE-like protease in apoptosis. *EMBO J*. 15:6969-6978
- Jensen P., Sorensen S.A., Fenger K. and Bolwig T.G. (1993) A study of psychiatric morbidity in patients with Huntington's disease their relatives and controls. Admissions to psychiatric hospitals in Denmark from 1969 to 1991. *Br J Psychiatry*. 163:790-797
- Jiang H., Poirier M.A., Liang Y., Pei Z., Weiskittel C.E., Smith W.W., DeFranco D.B. and Ross C.A. (2006) Depletion of CBP is directly linked with cellular toxicity caused by mutant huntingtin. *Neurobiol Dis*. 23:543-551
- Joel D. (2001) Open interconnected model of basal ganglia-thalamocortical circuitry and its relevance to the clinical syndrome of Huntington's disease. *Mov Disord*. 16:407-423

Literature

- Johnstone O. and Lasko P. (2004) Interaction with eIF5B is essential for Vasa function during development. *Development*. 131:4167-4178
- Joza N., Susin S.A., Daugas E., Stanford, W.L., Cho S.K., Li C.Y., Sasaki T., Elia A.J., Cheng H.Y., Ravagnan L., Ferri K.F., Zamzami N., Wakeham A., Hakem R., Yoshida H., Kong Y.Y., Mak T.W., Zuniga-Pflucker J.C., Kroemer G. and Penninger J.M. (2001) Essential role of the mitochondrial apoptosis-inducing factor in programmed cell death. *Nature*. 410:549-554
- Kahlem P., Green H. and Djian P. (1998) Transglutaminase action imitates Huntington's disease: selective polymerization of Huntingtin containing expanded polyglutamine. *Mol Cell*. 1:595-601
- Kalchman M.A., Graham R.K., Xia G., Koide H.B., Hodgson J.G., Graham K.C., Goldberg Y.P., Gitetz R.D., Pickart C.M. and Hayden M.R. (1996) Huntingtin is ubiquitinated and interacts with a specific ubiquitin-conjugating enzyme. *J Biol Chem*. 271:19385-19394
- Kalchman M.A., Koide H.B., McCutcheon K., Graham R.K., Nichol K., Nishiyama K., Kazemi-Esfarjani P., Lynn F.C., Wellington C., Metzler M., Goldberg Y.P., Kanazawa I., Gitetz R.D. and Hayden M.R. (1997) Hip1, a human homologue of *S. cerevisiae* sla2p, interacts with membrane-associated huntingtin in the brain. *Nat Genet*. 16:44-53
- Kaltenbach L.S., Romero E., Becklin R.R., Chettier R., Bell R., Phansalkar A., Strand A., Torcassi C., Savage J., Hurlburt A., Cha G.H., Ukani L., Chepanoske C.L., Zhen Y., Sahasrabudhe S., Olson J., Kurschner C., Ellerby L.M., Peltier J.M., Botas J. and Hughes R.E. (2007) e82. Huntingtin interacting proteins are genetic modifiers of neurodegeneration. *PLoS Genet*. 3:e82
- Karpuj M.V., Garren H., Slunt H., Price D.L., Gusella J., Becher M.W. and Steinman L. (1999) Transglutaminase aggregates huntingtin into nonamyloidogenic polymers, and its enzymatic activity increases in Huntington's disease brain nuclei. *Proc Natl Acad Sci USA*. 96:7388-7393
- Kazantsev A., Preisinger E., Dranovsky A., Goldgaber D. and Housman D. (1999) Insoluble detergent-resistant aggregates form between pathological and nonpathological lengths of polyglutamine in mammalian cells. *Proc Natl Acad Sci USA*. 96:11404-11409
- Kazemi-Esfarjani P. and Benzer S. (2000) Genetic suppression of polyglutamine toxicity in *Drosophila*. *Science*. 287:1837-1840
- Keene J.D. (2003) Organizing mRNA export. *Nat Genet*. 33:111-112
- Kegel K.B., Kim M., Sapp E., McIntyre C., Castaño J.G., Aronin N. and DiFiglia M. (2000) Huntingtin expression stimulates endosomal-lysosomal activity, endosome tubulation, and autophagy. *J Neurosci*. 20:7268-7278
- Kerr J.F., Wyllie A.H. and Currie A.R. (1972) Apoptosis: a basic biological phenomenon with wide-ranging implications in tissue kinetics. *Br J Cancer*. 26:239-257

Literature

- Kiechle T., Dedeoglu A., Kubilus J., Kowall N.W., Beal M.F., Friedlander R.M., Hersch S.M. and Ferrante R.J. (2002) Cytochrome C and caspase-9 expression in Huntington's disease. *Neuro-molecular Med.* 1:183-195
- Kim J.H., Liao D., Lau L.F. and Huganir R.L. (1998) SynGAP: a synaptic RasGAP that associates with the PSD-95/SAP90 protein family. *Neuron.* 20:683-691
- Kim Y.J., Yi Y., Sapp E., Wang Y., Cuiffo B., Kegel K.B., Qin Z.H., Aronin N. and DiFiglia M. (2001) Caspase 3-cleaved N-terminal fragments of wild-type and mutant huntingtin are present in normal and Huntington's disease brains associate with membranes and undergo calpain-dependent proteolysis. *Proc Natl Acad Sci USA.* 98:12784-12789
- Kischkel F.C., Hellbardt S., Behrmann I., Germer M., Pawlita M., Krammer P.H. and Peter M.E. (1995) Cytotoxicity-dependent APO-1 (Fas/CD95) - associated proteins form a death-inducing signaling complex (Dros. Inf. Serv.C) with the receptor. *EMBO J.* 14:5579-5588
- Kistler A.L. and Guthrie C. (2001) Deletion of MUD2 the yeast homolog of U2AF65 can bypass the requirement for Sub2 an essential spliceosomal ATPase. *Genes Dev.* 15:42-49
- Kita H., Carmichael J., Swartz J., Muro S., Wytenbach A., Matsubara K., Rubinsztein D.C. and Kato K. (2002) Modulation of polyglutamine-induced cell death by genes identified by expression profiling. *Hum Mol Genet.* 11:2279-2287
- Kothakota S., Azuma T., Reinhard C., Klippel A., Tang J., Chu K., McGarry T.J., Kirschner M.W., Koths K., Kwiatkowski D.J. and Williams L.T. (1997) Caspase-3-generated fragment of gelsolin: effector of morphological change in apoptosis. *Science.* 278:294-298
- Kressler D., Linder P. and de La Cruz J. (1999) Protein trans-acting factors involved in ribosome biogenesis in *Saccharomyces cerevisiae*. *Mol Cell Biol.* 19: 7897-7912
- Kuemmerle S., Gutekunst C.A., Klein A.M., Li X.J., Li S.H., Beal M.F., Hersch S.M. and Ferrante R.J. (1999) Huntington aggregates may not predict neuronal death in Huntington's disease. *Ann Neurol.* 46:842-849
- Kuhn A., Goldstein D.R., Hodges A., Strand A.D., Sengstag T., Kooperberg C., Becanovic K., Pouladi M.A., Sathasivam K., Cha J.H., Hannan A.J., Hayden M.R., Leavitt B.R., Dunnett S.B., Ferrante R.J., Albin R., Shelbourne P., Delorenzi M., Augood S.J., Faull R.L., Olson J.M., Bates G.P., Jones L. and Luthi-Carter R. (2007) Mutant huntingtin's effects on striatal gene expression in mice recapitulate changes observed in human Huntington's disease brain and do not differ with mutant huntingtin length or wild-type huntingtin dosage. *Hum Mol Genet.* 16:1845-1861
- Laemmli U.K. (1970) Cleavage of structural proteins during the assembly of the head of bacteriophage T4. *Nature.* 227:680-685
- Lafon-Cazal M., Pietri S., Culcasi M. and Bockaert J. (1993) NMDA-dependent superoxide production and neurotoxicity. *Nature.* 364:535-537

Literature

- Lamm G.M., Nicol S.M., Fuller-Pace F.V. and Lamond A.I. (1996) p72: a human nuclear DEAD box protein highly related to p68. *Nucleic Acids Res.* 24:3739-3747
- Landles C. and Bates G.P. (2004) Huntingtin and the molecular pathogenesis of Huntington's disease. *EMBO Rep.* 5:958-963
- Lee J.H., Rho S.B. and Chun T. (2005) GABAA receptor-associated protein (GABARAP) induces apoptosis by interacting with DEAD (Asp-Glu-Ala-Asp/His) box polypeptide 47 (DDX 47). *Bio-technol Lett.* 27:623-628
- Lee J.M., Ivanova E.V., Seong I.S., Cashorali T., Kohane I., Gusella J.F. and MacDonald M.E. (2007) Unbiased gene expression analysis implicates the huntingtin polyglutamine tract in extra-mitochondrial energy metabolism. *PLoS Genet.* 3:e135
- Lee L.G., Connell C.R. and Bloch W. (1993) Allelic discrimination by nick-translation PCR with fluorogenic probes. *Nucl Acids Res.* 21:3761-3766
- Lehner B. and Sanderson C.M. (2004) A protein interaction framework for human mRNA degradation. *Genome Res.* 14:1315-1323
- Lehner B., Semple J.I., Brown S.E., Counsell D., Campbell R.D. and Sanderson C.M. (2004) Analysis of a high-throughput yeasttwo-hybrid system and its use to predict the function of intracellular proteins encoded within the human MHC class III region. *Genomics.* 83:153-167
- Lennox G., Lowe J., Morrell K., Landon M. and Mayer R.J. (1988) Ubiquitin is a component of neurofibrillary tangles in a variety of neurodegenerative diseases. *Neurosci Lett.* 94:211-217
- Levine B. and Kroemer G. (2008) Autophagy in the pathogenesis of disease. *Cell.* 132:27-42
- Li H., Li S.H., Johnston H., Shelbourne P.F. and Li X.J. (2000) Amino-terminal fragments of mutant huntingtin show selective accumulation in striatal neurons and synaptic toxicity. *Nat Genet.* 25:385-389
- Li J.Y., Plomann M. and Brundin P. (2003) Huntington's disease: a synaptopathy? *Trends Mol Med.* 9:414-420
- Li L.Y., Luo X. and Wang X. (2001) Endonuclease G is an apoptotic DNase when released from mitochondria. *Nature.* 412:95-99
- Li S.H. and Li X.J. (2004) Huntingtin-protein interactions and the pathogenesis of Huntington's disease. *Trends Genet.* 20:146-154
- Li S.H., Li H., Torre E.R. and Li X.J. (2000) Expression of huntingtin-associated protein-1 in neuronal cells implicates a role in neuritic growth. *Mol Cell Neurosci.* 16:168-183
- Li Y. and Benezra R. (1996) Identification of a human mitotic checkpoint gene: hsMAD2. *Science.* 274:246-248

Literature

- Li Y., Wang H., Wang Z., Makhija S., Buchsbaum D., LoBuglio A., Kimberly R. and Zhou T. (2006) Inducible resistance of tumor cells to tumor necrosis factor-related apoptosis-inducing ligand receptor 2-mediated apoptosis by generation of a blockade at the death domain function. *Cancer Res.* 166:8520-8528
- Liévens J.C., Iché M., Laval M., Faivre-Sarrailh C. and Birman S. (2008) AKT-sensitive or insensitive pathways of toxicity in glial cells and neurons in *Drosophila* models of Huntington's disease. *Hum Mol Genet.* 17:882-894
- Linder P. (2003) Yeast RNA helicases of the DEAD-box family involved in translation initiation. *Biol Cell.* 95:157-167
- Linder P. and Stutz F. (2001) mRNA export: travelling with DEAD box proteins. *Curr Biol.* 11: R961-R963
- Linder P., Lasko P.F., Ashburner M., Leroy P., Nielsen P.J., Nishi K., Schnier J. and Slonimski P.P. (1989) Birth of the D-E-A-D box. *Nature.* 337:121-122
- Linnik M.D., Zobrist R.H. and Hatfield M.D. (1993) Evidence supporting a role for programmed cell death in focal cerebral ischemia in rats. *Stroke.* 24:2002-2009
- Liu X., Zou H., Slaughter C. and Wang X. (1997) DFF a heterodimeric protein that functions downstream of caspase-3 to trigger DNA fragmentation during apoptosis. *Cell.* 89:175-184
- Liu Y.F., Dorow D. and Marshall J. (2000) Activation of MLK2-mediated signaling cascades by polyglutamine-expanded huntingtin. *J Biol Chem.* 275:19035-19040
- Lorincz M.T. and Zawistowski V.A. (2009) Expanded CAG repeats in the murine Huntington's disease gene increases neuronal differentiation of embryonic and neural stem cells. *Mol Cell Neurosci.* 40:1-13
- Lovrecic L., Kastrin A., Kobal J., Pirtosek Z., Krainc D. and Peterlin B. (2009) Gene expression changes in blood as a putative biomarker for Huntington's disease. *Mov Disord.* 24:2277-2281
- Lowe J., Blanchard A., Morrell K., Lennox G., Reynolds L., Billett M., Landon M. and Mayer R.J. (1988) Ubiquitin is a common factor in intermediate filament inclusion bodies of diverse type in man including those of Parkinson's disease Pick's disease and Alzheimer's disease as well as Rosenthal fibres in cerebellar astrocytomas cytoplasmic bodies in muscle and mallory bodies in alcoholic liver disease. *J Pathol.* 155:9-15
- Lu D. and Yunis J.J. (1992) Cloning expression and localization of an RNA helicase gene from a human lymphoid cell line with chromosomal breakpoint 11q23.3. *Nucleic Acids Res.* 20:1967-1972
- Luking A., Stahl U. and Schmidt U. (1998) The protein family of RNA helicases. *Crit Rev Biochem Mol. Biol.* 33:259-296

Literature

- Luo S., Vacher C., Davies J.E. and Rubinsztein D.C. (2005) Cdk5 phosphorylation of huntingtin reduces its cleavage by caspases: implications for mutant huntingtin toxicity. *J Cell Biol.* 169:647-656
- Luthi-Carter R., Strand A., Peters N.L., Solano S.M., Hollingsworth Z.R., Menon A.S., Frey A.S., Spektor B.S., Penney E.B., Schilling G., Ross C.A., Borchelt D.R., Tapscott S.J., Young A.B., Cha J.-H.J. and Olson J.M. (2000) Decreased expression of striatal signaling genes in a mouse model of Huntington's disease. *Hum Mol Genet.* 9:1259-1271
- Ma J., Rong L., Zhou Y., Roy B.B., Lu J., Abrahamyan L., Mouland A.J., Pan Q. and Liang C. (2008) The requirement of the DEAD-box protein DDX24 for the packaging of human immunodeficiency virus type 1 RNA. *Virology.* 375:253-264
- Maiuri M.C., Zalckvar E., Kimchi A. and Kroemer G. (2007) Self-eating and self-killing: crosstalk between autophagy and apoptosis. *Nat Rev Mol Cell Biol.* 8:741-752
- Majumder P., Chattopadhyay B., Sukanya S., Ray T., Banerjee M., Mukhopadhyay D. and Bhattacharyya N.P. (2007a) Interaction of HIPPI with putative promoter sequence of caspase-1 in vitro and in vivo. *Biochem Biophys Res Commun.* 353:80-85
- Majumder P., Choudhury A., Banerjee M., Lahiri A. and Bhattacharyya N.P. (2007b) Interactions of HIPPI a molecular partner of Huntingtin interacting protein HIP1 with the specific motif present at the putative promoter sequence of the caspase-1 caspase-8 and caspase-10 genes. *FEBS J.* 274:3886-3899
- Martelange V., De Smet C., De Plaen E., Lurquin C. and Boon T. (2000) Identification on a human sarcoma of two new genes with tumor-specific expression. *Cancer Res.* 60:3848-3855
- Martin L.J. (2001) Neuronal cell death in nervous system development disease and injury. *J Mol Med.* 7:455-478
- Merienne K., Helmlinger D., Perkin G.R., Devys D. and Trottier Y. (2003) Polyglutamine expansion induces a protein-damaging stress connecting heat shock protein 70 to the JNK pathway. *J Biol Chem.* 278:16957-16967
- Metzler M., Legendre-Guillemain V., Gan L., Chopra V., Kwok A., McPherson P.S. and Hayden M.R. (2001) HIP1 functions in clathrin-mediated endocytosis through binding to clathrin and adaptor protein 2. *J Biol Chem.* 276:39271-39276
- Minshall N., Thom G. and Standart N. (2001) A conserved role of a DEAD box helicase in mRNA masking. *RNA.* 7:1728-1742
- Miyashita T. and Reed J.C. (1995) Tumor suppressor p53 is a direct transcriptional activator of the human bax gene. *Cell.* 80:293-299

Literature

- Modregger J., DiProspero N.A., Charles V., Tagle D.A. and Plomann M. (2002) Pascin 1 interacts with huntingtin and is absent from synaptic varicosities in presymptomatic huntington's disease brains. *Hum Mol Genet.* 11:2547-2558
- Mogi M., Harada M., Kondo T., Mizuno Y., Narabayashi H., Riederer P. and Nagatsu T. (1996) The soluble form of Fas molecule is elevated in parkinsonian brain tissues. *Neurosci Lett.* 220:195-198
- Morishima N., Nakanishi K., Takenouchi H., Shibata T. and Yasuhiko Y. (2002) An endoplasmic reticulum stress-specific caspase cascade in apoptosis. Cytochrome c-independent activation of caspase-9 by caspase-12. *J Biol Chem.* 277:34287-34294
- Morishima Y., Gotoh Y., Zieg J., Barrett T., Takano H., Flavell R., Davis R.J., Shirasaki Y. and Greenberg M.E. (2001) Beta-amyloid induces neuronal apoptosis via a mechanism that involves the c-Jun N-terminal kinase pathway and the induction of Fas ligand. *J Neurosci.* 21:7551-7560
- Morley J.F., Brignull H.R., Weyers J.J. and Morimoto R.I. (2002) The threshold for polyglutamine-expansion protein aggregation and cellular toxicity is dynamic and influenced by aging in *Caenorhabditis elegans*. *Proc Natl Acad Sci USA.* 99:10417-10422
- Mu T.W., Fowler D.M. and Kelly J.W. (2008) Partial restoration of mutant enzyme homeostasis in three distinct lysosomal storage disease cell lines by altering calcium homeostasis. *PLoS Biol.* 6:e26
- Muzio M., Chinnaiyan A.M., Kischkel F.C., O'Rourke K., Shevchenko A., Ni J., Scaffidi C., Bretz J.D., Zhang M., Gentz R., Mann M., Krammer P.J., Peter M.E. and Dixit V.M. (1996) FLICE a novel FADD homologous ICE/CED-3-like protease is recruited to the CD95 (Fas/Apo-1) death-inducing signaling complex. *Cell.* 85:817-827
- Nasir J., Floresco S.B., O'Kusky J.R., Diewert V.M., Richman J.M., Zeisler J., Borowski A., Marth J.D., Phillips A.G. and Hayden M.R. (1995) Targeted disruption of the Huntington's disease gene results in embryonic lethality and behavioral and morphological changes in heterozygotes. *Cell.* 81:811-823
- Nicholls D.G. and Budd S.L. (1998) Neuronal excitotoxicity: the role of mitochondria. *Biofactors.* 8:287-299
- Nollen E.A., Garcia S.M., van Haften G., Kim S., Chavez A., Morimoto R.I. and Plasterk R.H. (2004) Genome-wide RNA interference screen identifies previously undescribed regulators of polyglutamine aggregation. *Proc Natl Acad Sci USA.* 101:6403-6408
- Novelli A., Reilly J.A., Lysko P.G. and Henneberry R.C. (1988) Glutamate becomes neurotoxic via the N-methyl-D-aspartate receptor when intracellular energy levels are reduced. *Brain Res.* 451:205-212

Literature

- Nucifora Jr F.C., Sasaki M., Peters M.F., Huan H., Cooper J.K., Yamad M., Takahashi H., Tsuji S., Troncoso J., Dawson V.L., Dawson T.M. and Ross C.A. (2001) Interference by huntingtin and atrophin-1 with cbp-mediated transcription leading to cellular toxicity. *Science*. 291:2423-2428
- Omi K., Hachiya N.S., Tanaka M., Tokunaga K. and Kaneko K. (2008) 14-3-3zeta is indispensable for aggregate formation of polyglutamine-expanded huntingtin protein. *Neurosci Lett*. 431:45-50
- Ona V.O., Li M., Vonsattel J.P., Andrews L.J., Khan S.Q., Chung W.M., Frey A.S., Menon A.S., Li X.J., Stieg P.E., Yuan J., Penney J.B., Young A.B., Cha J.H. and Friedlander R.M. (1999) Inhibition of caspase-1 slows disease progression in a mouse model of Huntington's disease. *Nature*. 399:263-267
- Orr H.T. and Zoghbi H.Y. (2007) Trinucleotide repeat disorders. *Annu Rev Neurosci*. 30:575-621
- Palidwor G.A., Shcherbinin S., Huska M.R., Rasko T., Stelzl U., Arumughan A., Foulle R., Porras P., Sanchez-Pulido L., Wanker E.E. and Andrade-Navarro M.A. (2009) Detection of alpha-rod protein repeats using a neural network and application to huntingtin. *PLoS Comput Bio*. 5: e1000304
- Panov A.V., Gutekunst C.A., Leavitt B.R., Hayden M.R., Burke J.R., Strittmatter W.J. and Greenamyre J.T. (2002) Early mitochondrial calcium defects in Huntington's disease are a direct effect of polyglutamines. *Nature Neurosci*. 5:731-736
- Pause A. and Sonenberg N. (1992) Mutational analysis of a DEAD box RNA helicase: the mammalian translation initiation factor eIF-4A. *EMBO J*. 11:2643-2654
- Pause A., Me'oth N., Svitkin Y., Merrick W.C. and Sonenberg N. (1994) Dominant negative mutants of mammalian translation initiation factor eIF-4A define a critical role for eIF-4A in cap-dependent and cap-independent initiation of translation. *EMBO J*. 13:1205-1215
- Peel A.L. (2004) PKR activation in neurodegenerative disease. *J Neuropathol Exp Neurol*. 63:97-105
- Peel A.L., Rao R.V., Cottrell B.A., Hayden M.R., Ellerby L.M. and Bredesen D.E. (2001) Double-stranded RNA-dependent protein kinase, PKR, binds preferentially to Huntington's disease (HD) transcripts and is activated in HD tissue. *Hum Mol Genet*. 10:1531-1538
- Peelman L.J., Chardon P., Nunes M., Renard C., Geffrotin C., Vaiman M., Van-Zeveren A., Coppiepers W., van-de-Weghe A., Bouquet Y. et al (1995) The BAT1 gene in the MHC encodes an evolutionarily conserved putative nuclear RNA helicase of the DEAD family. *Genomics*. 26:210-218
- Penney Jr. J.B., Young A.B., Shoulson I., Starosta-Rubenstein S., Snodgrass, S.R., Sanchez-Ramos J., Ramos-Arroyo M., Gomez F., Penchaszadeh G., Alvir J., Esteves J., DeQuiroz I., Marsol N., Moreno H., Conneally P.M., Bonilla E. and Wexler N.S. (1990) Huntington's disease in Venezuela: 7 years of follow-up on symptomatic and asymptomatic individuals. *Mov Disord*. 5:93-99

Literature

- Perrin V., Dufour N., Raoul C., Hassig R., Brouillet E., Aebischer P., Luthi-Carter R. and Déglon N. (2009) Implication of the JNK pathway in a rat model of Huntington's disease. *Exp Neurol.* 215:191-200
- Perutz M.F., Johnson T., Suzuki M. and Finch J.T. (1994) Glutamine repeats as polar zippers: their possible role in inherited neurodegenerative diseases. *Proc Natl Acad Sci USA.* 91:5355-5358
- Pettus B.J., Chalfant C.E. and Hannun Y.A. (2002) Ceramide in apoptosis: an overview and current perspectives. *Biochim Biophys Acta.* 1585:114-125
- Poirier M.A., Li H., Macosko J., Cai S., Amzel M. and Ross C.A. (2002) Huntingtin spheroids and protofibrils as precursors in polyglutamine fibrilization. *J Biol Chem.* 277:41032-41037
- Polyak K., Xia Y., Zweier J.L., Kinzler K.W. and Vogelstein B. (1997) A model for p53-induced apoptosis. *Nature.* 389:300-305
- Prasad K.N., Zambemard J., Lasher R. and VanWoert M.H. (1970) Transmission of mouse neuroblastoma by a cell-free extract. *Nature.* 228:997-999
- Pryor A., Tung L., Yang Z., Kapadia F., Chang T.H. and Johnson L.F. (2004) Growth-regulated expression and G0-specific turnover of the mRNA that encodes URH49 a mammalian DExH/D box protein that is highly related to the mRNA export protein UAP56. *Nucleic Acids Res.* 32:1857-1865
- Puthalakath H., O'Reilly L.A., Gunn P., Lee L., Kelly P.N., Huntington N.D., Hughes P.D., Michalak E.M., McKimm-Breschkin J., Motoyama N., Gotoh T., Akira S., Bouillet P. and Strasser A. (2007) ER stress triggers apoptosis by activating BH3-only protein Bim. *Cell.* 129:1337-1349
- Qin Z.H., Wang Y., Sapp E., Cuiffo B., Wanker E., Hayden M.R., Kegel K.B., Aronin N. and DiFiglia M. (2004) Huntingtin bodies sequester vesicle-associated proteins by a polyproline-dependent interaction. *J Neurosci.* 24:269-281
- Raijmakers R., Schilders G. and Pruijn G.J. (2004) The exosome a molecular machine for controlled RNA degradation in both nucleus and cytoplasm. *Eur J Cell Biol.* 83:175-183
- Rajendran R.R., Nye A.C., Frasor J., Balsara R.D., Martini P.G. and Katzenellenbogen B.S. (2003) Regulation of nuclear receptor/transcriptional activity by a novel DEAD box RNA helicase (DP97). *J Biol Chem.* 278:4628-4638
- Ralser M., Nonhoff U., Albrecht M., Lengauer T., Wanker E.E., Lehrach H. and Krobitsch S. (2005) Ataxin-2 and huntingtin interact with endophilin-A complexes to function in plastin-associated pathways. *Hum Mol Genet.* 14:2893-2909
- Rao R.V., Castro-Obregon S., Frankowski H., Schuler M., Stoka V., del Rio G., Bredesen D.E. and Ellerby H.M. (2002) Coupling endoplasmic reticulum stress to the cell death program. An Apaf-1-independent intrinsic pathway. *J Biol Chem.* 277:21836-21842

Literature

- Reynolds I.J. and Hastings T.G. (1995) Glutamate induces the production of reactive oxygen species in cultured forebrain neurons following NMDA receptor activation. *J Neurosci.* 15:3318-3327
- Ribeiro F.M., Paquet M., Ferreira L.T., Cregan T., Swan P., Cregan S.P. and Ferguson S.S. (2010) Metabotropic glutamate receptor-mediated cell signaling pathways are altered in a mouse model of Huntington's disease. *J Neurosci.* 30:316-324
- Rigamonti D., Bauer J.H., De-Fraja C., Conti L., Sipione S., Sciorati C., Clementi E., Hackam A., Hayden M.R., Li Y., Cooper J.K., Ross C.A. Govoni S., Vincenz C. and Cattaneo E. (2000) Wild-type huntingtin protects from apoptosis upstream of caspase-3. *J Neurosci.* 20:3705-3713
- Rigamonti D., Sipione S., Goffredo D., Zuccato C., Fossale E. and Cattaneo E. (2001) Huntingtin's neuroprotective activity occurs via inhibition of procaspase-9 processing. *J Biol Chem.* 276:14545-14548
- Ringstad N., Nemoto Y. and Camilli P.D. (1997) The SH3p4/SH3p8/SH3p13 protein family: Binding partners for synaptojanin and dynamin via a Grb2-like Src homology 3 domain. *Proc Natl Acad Sci USA.* 94:8569-8574
- Rintahaka J., Wiik D., Kovanen P.E., Alenius H. and Matikainen S. (2008) Cytosolic antiviral RNA recognition pathway activates caspases 1 and 3. *J Immunol.* 180:1749-1757
- Rocak S. and Linder P. (2004) DEAD-box proteins: the driving forces behind RNA metabolism. *Nat Rev Mol Cell Biol.* 5:232-241
- Rogers Jr. G.W., Komar A.A. and Merrick W.C. (2002) eIF4A: the godfather of the DEAD box helicases. *Prog Nucleic Acid Res Mol Biol.* 72:307-331
- Ross C.A. (2002) Polyglutamine pathogenesis: emergence of unifying mechanisms for Huntington's disease and related disorders. *Neuron.* 35:819-822
- Ross, C.A. and Poirier, M.A. (2004) Protein aggregation and neurodegenerative disease. *Nat Med.* 10:S10-S17
- Rossow K. L. and Janknecht R. (2003) Synergism between p68 RNA helicase and the transcriptional coactivators CBP and p300. *Oncogene.* 22:151-156
- Rubinsztein D.C. (2002) Lessons from animal models of Huntington's disease. *Trends Genet.* 18:202-209
- Rubinsztein D.C., Leggo J., Coles R., Almqvist E., Biancalana V., Cassiman J.-J., Chotai K., Connarty M., Crauford D., Curtis A., Curtis D., Davidson M.J., Differ A.-M., Dode C., Dodge A., Frontali M., Ranen N.G., Stine O.C., Sherr M., Abbott M.H., Franz M.L., Graham C.A., Harper P.S., Hedreen J.C., Jackson A., Kaplan J.-C., Losekoot M., MacMillan J.C., Morrison P., Trottier Y., Novelletto A., Simpson S.A., Theilmann J., Whittaker J.L., Folstein S.E., Ross C.A. and Hayden M.R. (1996) Phenotypic characterisation of individuals with 30-40 CAG repeats in the Huntington's

Literature

- disease (HD) gene reveals HD cases with 36 repeats and apparently normal elderly individuals with 36-39 repeats. *Am J Hum Genet.* 59:16-22
- Runne H., Régulier E., Kuhn A., Zala D., Gokce O., Perrin V., Sick B., Aebischer P., Déglon N. and Luthi-Carter R.J. (2008) Dysregulation of gene expression in primary neuron models of Huntington's disease shows that polyglutamine-related effects on the striatal transcriptome may not be dependent on brain circuitry. *J Neurosci.* 28:9723-9731
- Saelens X., Festjens N., Vande Walle L., van Gorp M., van Loo G. and Vandenabeele P. (2004) Toxic proteins released from mitochondria in cell death. *Oncogene.* 23:2861-2874
- Sakahira H., Breuer P., Hayer-Hartl M.K. and Hartl F.U. (2002) Molecular chaperones as modulators of polyglutamine protein aggregation and toxicity. *Proc Natl Acad Sci USA.* 99:16412-16418
- Sakahira H., Enari M. and Nagata S. (1998) Cleavage of CAD inhibitor in CAD activation and DNA degradation during apoptosis. *Nature.* 391:96-99
- Sambrook J. and Russell D.W. (2001) Molecular Cloning. A Laboratory Manual. *Cold Spring Harbour Laboratory Press*
- Sanberg P.R., Fibiger H.C. and Mark R.F. (1981) Body weight and dietary factors in Huntington's disease patients compared with matched controls. *Med J Aust.* 1:407-409
- Sarkar S., Perlstein E.O., Imarisio S., Pineau S., Cordenier A., Maglathlin R.L., Webster J.A., Lewis T.A., O'Kane C.J., Schreiber S.L. and Rubinsztein D.C. (2007) Small molecules enhance autophagy and reduce toxicity in Huntington's disease models. *Nat Chem Biol.* 3:331-338
- Sathasivam K., Amaechi I., Mangiarini L. and Bates G. (1997) Identification of an HD patient with a (CAG)180 repeat expansion and the propagation of highly expanded CAG repeats in lambda phage. *Hum Genet.* 99:692-695
- Saudou F., Finkbeiner S., Devys D. and Greenberg M.E. (1998) Huntingtin acts in the nucleus to induce apoptosis but death does not correlate with the formation of intranuclear inclusions. *Cell.* 95:55-66
- Sawa A., Wiegand G.W., Cooper J., Margolis R.L., Sharp A.H., Lawler Jr J.F., Greenamyre J.T., Snyder S.H. and Ross C.A. (1999) Increased apoptosis of Huntington disease lymphoblasts associated with repeat lengthdependent mitochondrial depolarization. *Nature Med.* 5:1194-1198
- Schaffar G., Breuer P., Boteva R., Behrends C., Tzvetkov N., Strippel N., Sakahira H., Siegers K., Hayer-Hartl M. and Hartl F.U. (2004) Cellular toxicity of polyglutamine expansion proteins: mechanism of transcription factor deactivation. *Mol Cell.* 15:95-105
- Scherl A., Coute Y., Deon C., Calle A., Kindbeiter K., Sanchez J.C., Greco A., Hochstrasser D. and Diaz J.J. (2002) Functionalproteomic analysis of human nucleolus. *Mol Biol Cell.* 13:4100-4109

Literature

- Scherzinger E., Lurz R., Turmaine M., Mangiarini L., Hollenbach B., Hasenbank R., Bates G.P., Davies S.W., Lehrach H., and Wanker E.E. (1997) Huntingtin-encoded polyglutamine expansions form amyloid-like protein aggregates in vitro and in vivo. *Cell*. 90:549-558
- Scherzinger E., Sittler A., Schweiger K., Heiser V., Lurz R., Hasenbank R., Bates G.P., Lehrach H. and Wanker E.E. (1999) Self-assembly of polyglutamine-containing huntingtin fragments into amyloid-like fibrils: implications for huntington's disease pathology. *Proc Natl Acad Sci USA*. 96:4604-4609
- Schiffer N.W., C eraline J., Hartl F.U. and Broadley S.A. (2008) N-terminal polyglutamine-containing fragments inhibit androgen receptor transactivation function. *Biol Chem*. 389:1455-1466
- Schilling B., Gafni J., Torcassi C., Cong X., Row R.H., LaFevre-Bernt M.A., Cusack M.P., Ratovitski T., Hirschhorn R., Ross C.A., Gibson B.W. and Ellerby L.M. (2006) Huntingtin phosphorylation sites mapped by mass spectrometry. Modulation of cleavage and toxicity. *J Biol Chem*. 281:23686-23697
- Schilling G., Becher M.W., Sharp A.H., Jinnah H.A., Duan K., Kotzuk J.A., Slunt H.H., Ratovitski T., Cooper J.K., Jenkins N.A., Copeland N.G., Price D.L., Ross C.A. and Borchelt D.R. (1999) Intracellular inclusions and neuritic aggregates in transgenic mice expressing a mutant n-terminal fragment of huntingtin. *Hum Mol Genet*. 8:397-407
- Schilling G., Savonenko A.V., Klevytska A., Morton J.L., Tucker S.M., Poirier M., Gale A., Chan N., Gonzales V. and Slunt H.H. (2004) Nuclear-targeting of mutant huntingtin fragments produces Huntington's disease-like phenotypes in transgenic mice. *Hum Mol Genet*. 13:1599-1610
- Schimmer A.D. (2004) Inhibitor of apoptosis proteins: translating basic knowledge into clinical practice. *Cancer Res*. 64:7183-7190
- Schmitt C., von Kobbe C., Bach I.A., Pante N., Rodrigues J.P., Boscheron C., Rigaut G., Wilm M., Seraphin B., Carmo-Fonseca M. and Izaurralde E. (1999) Dbp5 a DEAD-box protein required for mRNA export, is recruited to the cytoplasmic fibrils of nuclear pore complex via a conserved interaction with CAN/Nup159p. *EMBO J*. 18:4332-4347
- Sekiguchi T., Iida H., Fukumura J. and Nishimoto T. (2004) Human DDX3Y the Y-encoded isoform of RNA helicase DDX3 rescues hamster temperature-sensitive ET24 mutant cell line with a DDX3X mutation. *Exp Cell Res*. 300:213-222
- Seong I.S., Ivanova E., Lee J.M., Choo Y.S., Fossale E., Anderson M., Gusella J.F., Laramie J.M., Myers R.H., Lesort M. and MacDonald M.E. (2005) HD CAG repeat implicates a dominant property of huntingtin in mitochondrial energy metabolism. *Hum Mol Genet*. 14:2871-2880
- Shao J., Welch W.J., Diprospero N.A. and Diamond M.I. (2008) Phosphorylation of profilin by ROCK1 regulates polyglutamine aggregation. *Mol Cell Biol*. 28:5196-5208

Literature

- Sieradzan K.A., Mehan A.O., Jones L., Wanker E.E., Nukina N. and Mann D.M. (1999) Huntington's disease intranuclear inclusions contain truncated ubiquitinated huntingtin protein. *Exp Neurol.* 156:92-99
- Sipione S., Rigamonti D., Valenza M., Zuccato C., Conti L., Pritchard J., Kooperberg C., Olson J.M. and Cattaneo E. (2002) Early transcriptional profiles in huntingtin-inducible striatal cells by microarray analyses. *Hum Mol Genet.* 11:1953-1965
- Sittler A., Walter S., Wedemeyer N., Hasenbank R., Scherzinger E., Eickhoff H., Bates G.P., Lehrach H. and Wanker E.E. (1998) Sh3gl3 associates with the huntingtin exon 1 protein and promotes the formation of polyglutamine-containing protein aggregates. *Mol Cell.* 2:427-436
- Sledz C.A., Holko M., de Veer M.J., Silverman R.H. and Williams B.R.G. (2003) Activation of the interferon system by short-interfering RNAs. *Nat Cell Biol.* 5:834-839
- Slee E.A., Adrain C. and Martin S.J. (2001) Executioner caspase-3 -6 and -7 perform distinct non-redundant roles during the demolition phase of apoptosis. *J Biol Chem.* 276:7320-7326
- Smale G., Nichols N.R., Brady D.R., Finch C.E. and Horton Jr. W.E. (1995) Evidence for apoptotic cell death in Alzheimer's disease. *Exp Neurol.* 133:225-230
- Smillie D.A. and Sommerville J. (2002) RNA helicase p54 (DDX6) is a shuttling protein involved in nuclear assembly of stored mRNP particles. *J Cell Sci.* 115:395-407
- Smith M.I. and Deshmukh M. (2007) Endoplasmic reticulum stress-induced apoptosis requires bax for commitment and Apaf-1 for execution in primary neurons. *Cell Death Differ.* 14:1011-1019
- Snyder B.R., Chiu A.M., Prockop D. J. and Chan A.W. (2010) Human multipotent stromal cells (MSCs) increase neurogenesis and decrease atrophy of the striatum in a transgenic mouse model for Huntington's disease. *PLoS One.* 5:e9347
- Steffan J.S., Agrawal N., Pallos J., Rockabrand E., Trotman L.C., Slepko N., Illes K., Lukacsovich T., Zhu Y.Z., Cattaneo E., Pandolfi P.P., Thompson L.M. and Marsh J.L. (2004) SUMO modification of Huntingtin and Huntington's disease pathology. *Science.* 304:100-104
- Steffan J.S., Kazantsev A., Spasic-Boskovic O., Greenwald M., Zhu Y.Z., Gohler H., Wanker E.E., Bates G.P., Housman D.E. and Thompson L.M. (2000) The Huntington's disease protein interacts with p53 and CREB binding protein and represses transcription. *Proc Natl Acad Sci USA.* 97:6763-6768
- Stott K., Blackburn J.M., Butler P.J. and Perutz M. (1995) Incorporation of glutamine repeats makes protein oligomerize: implications for neurodegenerative diseases. *Proc Natl Acad Sci USA.* 92:6509-6513

Literature

- Strong T. V., Tagle D. A., Valdes J. M., Elmer L. W., Boehm K., Swaroop M., Kaatz K. W., Collins F. S. and Albin R. L. (1993) Widespread expression of the human and rat huntington's disease gene in brain and nonneural tissues. *Nat Genet.* 5:259-265
- Su J.H., Anderson A.J., Cribbs D.H., Tu C., Tong L., Kesslack P. and Cotman C.W. (2003) Fas and Fas ligand are associated with neuritic degeneration in the AD brain and participate in beta-amyloid-induced neuronal death. *Neurobiol Dis.* 12:182-193
- Sugars K.L. and Rubinsztein D.C. (2003) Transcriptional abnormalities in Huntington disease. *Trends Genet.* 19:233-238
- Sun B., Fan W., Balciunas A., Cooper J.K., Bitan G., Steavenson S., Denis P.E., Young Y., Adler B., Daugherty L., Manoukian R., Elliott G., Shen W., Talvenheimo J., Teplow D.B., Haniu M., Haldankar R., Wypych J., Ross C.A., Citron M. and Richards W.G. (2002) Polyglutamine repeat length-dependent proteolysis of huntingtin. *Neurobiol Dis.* 11:111-122
- Sun M., Song L., Li Y., Zhou T. and Jope R.S. (2008) Identification of an antiapoptotic protein complex at death receptors. *Cell Death Differ.* 15:1887-1900
- Sun Y., Savanenin A., Reddy P.H. and Liu Y.F. (2001) Polyglutamine expanded huntingtin promotes sensitization of N-methyl-d-aspartate receptors via post-synaptic density 95. *J Biol Chem.* 276: 24713-24718
- Svitkin Y.V., Pause A., Haghighat A., Pyronnet S., Witherell G., Belsham G.J. and Sonenberg N. (2001) The requirement for eukaryotic initiation factor 4A (eIF4A) in translation is in direct proportion to the degree of mRNA 5' secondary structure. *RNA.* 7:382-394
- Tanese N. and Tjian R. (1993) Coactivators and TAFs: a new class of eukaryotic transcription factors that connect activators to the basal machinery. *Cold Spring Harbor Symp Quant Biol.* 58:179-185
- Tang P.Z., Tsai-Morris C.H. and Dufau M.L. (1999) A novel gonadotropin-regulated testicular RNA helicase. A new member of the dead-box family. *J Biol Chem.* 274:37932-37940
- Tanner N.K., Cordin O., Banroques J., Doe`re M. and Linder P. (2003) The Q motif. A newly identified motif in DEAD box helicases may regulate ATP binding and hydrolysis. *Mol Cell.* 11:127-138
- Teigelkamp S., Mundt C., Achsel T., Will C.L. and Luhrmann R. (1997) The human U5 snRNP-specific 100-kD protein is an RS domain-containing putative RNA helicase with significant homology to the yeast splicing factor Prp28p. *RNA.* 3:1313-1326
- Thomas L.B., Gates D.J., Richfield E.K., O'Brien T.F., Schweitzer J.B. and Steindler D.A. (1995) DNA end labeling (TUNEL) in Huntington's disease and other neuropathological conditions. *Exp Neurol.* 133:265-272

Literature

- Thompson P.D., Berardelli A., Rothwell J.C., Day B.L., Dick J.P., Benecke R., and Marsden C.D. (1988) The coexistence of bradykinesia and chorea in Huntington's disease and its implications for theories of basal ganglia control of movement. *Brain*. 111:223-244
- Thornberry N., Rano T., Peterson E., Rasper D., Timkey T., Garcia-Calvo M., Houtzager V., Nordstrom P., Roy S., Vaillancourt J., Chapman K. and Nicholson D. (1997) A combinatorial approach defines specificities of members of the caspase family and granzyme B. Functional relationships established for key mediators of apoptosis. *J Biol Chem*. 272:17907-17911
- Toulmond S., Tang K., Bureau Y., Ashdown H., Degen S., O'Donnell R., Tam J., Han Y., Colucci J., Giroux A., Zhu Y., Boucher M., Pikounis B., Xanthoudakis S., Roy S., Rigby M., Zamboni R., Robertson G.S., Ng G.Y., Nicholson D.W. and Flückiger J.P. (2004) Neuroprotective effects of M826 a reversible caspase-3 inhibitor in the rat malonate model of Huntington's disease. *Br J Pharmacol*. 141:689-697
- Troost D., Aten J., Morsink F. and de Jong J.M. (1995) Apoptosis in amyotrophic lateral sclerosis is not restricted to motor neurons. Bcl-2 expression is increased in unaffected post-central gyrus. *Neuropathol Appl Neurobiol*. 21:498-504
- Trottier Y., Devys D., Imbert G., Saudou F., An I., Lutz Y., Weber C., Agid Y., Hirsch E.C. and Mandel J.L. (1995) Cellular localization of the huntington's disease protein and discrimination of the normal and mutated form. *Nat Genet*. 10:104-110
- Tsai Y.C., Fishman P.S., Thakor N.V. and Oyler G.A. (2003) Parkin facilitates the elimination of expanded polyglutamine proteins and leads to preservation of proteasome function. *J Biol Chem*. 278:22044-22055
- Uney J.B., Anderton B.H. and Thomas S.M. (1993) Changes in heat shock protein 70 and ubiquitin mRNA levels in C1300 N2A mouse neuroblastoma cells following treatment with iron. *J Neurochem*. 60:659-665
- Valdez B.C., Henning D., Busch R.K., Woods K., Flores-Rozas H., Hurwitz J., Perlaky L. and Busch H. (1996) A nucleolar RNA helicase recognized by autoimmune antibodies from a patient with watermelon stomach disease. *Nucleic Acids Res*. 24:1220-1224
- Valdez B.C., Perlaky L. and Henning D. (2002a) Expression cellular localization and enzymatic activities of RNA helicase II/Gu(beta). *Exp Cell Res*. 276:249-263
- Valdez B.C., Yang H., Hong E. and Sequitin A.M. (2002b) Genomic structure of newly identified paralogue of RNA helicase II/Gu: detection of pseudogenes and multiple alternatively spliced mRNAs. *Gene*. 284:53-61
- Valgardsdottir R., Brede G., Eide L.G., Frengen E. and Prydz H. (2001) Cloning and characterization of MDDX28 a putative dead-boxhelicase with mitochondrial and nuclear localization. *J Biol Chem*. 276:32056-32063

Literature

- van Ham T.J., Breitling R., Swertz M.A. and Nollen E.A. (2009) Neurodegenerative diseases: Lessons from genome-wide screens in small model organisms. *EMBO Mol Med.* 1:360-370
- van Loo G., Saelens X., van Gurp M., MacFarlane M., Martin S.J. and Vandenabeele P. (2002a) The role of mitochondrial factors in apoptosis: a Russian roulette with more than one bullet. *Cell Death Differ.* 9:1031-1042
- van Loo G., van Gurp M., Depuydt B., Srinivasula S.M., Rodriguez I., Alnemri E.S., Gevaert K., Vandekerckhove J., Declercq W. and Vandenabeele P. (2002b) The serine protease Omi/HtrA2 is released from mitochondria during apoptosis. Omi interacts with caspase-inhibitor XIAP and induces enhanced caspase activity. *Cell Death Differ.* 9:20-26
- Vashisht A.A. and Tuteja N.J. (2006) Stress responsive DEAD-box helicases: a new pathway to engineer plant stress tolerance. *Photochem Photobiol B.* 84:150-160
- Velier J., Kim M., Schwarz C., Kim T.W., Sapp E., Chase K., Aronin N. and DiFiglia M. (1998) Wild-type and mutant huntingtins function in vesicle trafficking in the secretory and endocytic pathways. *Exp Neurol.* 152:34-40
- Venkatraman P., Wetzel R., Tanaka M., Nukina N. and Goldberg A.L. (2004) Eukaryotic proteasomes cannot digest polyglutamine sequences and release them during degradation of polyglutamine-containing proteins. *Mol Cell.* 14:95-104
- Vis J.C., Schipper E., de Boer-van Huizen R.T., Verbeek M.M., de Waal R.M., Wesseling P., ten Donkelaar H.J. and Kremer B. (2005) Expression pattern of apoptosis-related markers in Huntington's disease. *Acta Neuropathol.* 109:321-328
- Vogelstein B., Lane D., Levine A.J. (2000) Surfing the p53 network. *Nature.* 408:307-310
- von Rotz R.C., Kins S., Hipfel R., von der Kammer H. and Nitsch R.M. (2005) The novel cytosolic RING finger protein dactylidin is up-regulated in brains of patients with Alzheimer's disease. *Eur J Neurosci.* 21:1289-1298
- Vonsattel J.P. and DiFiglia M. (1998) Huntington disease. *J Neuropathol Exp Neurol.* 57:369-384
- Vonsattel J.P., Myers R.H., Stevens T.J., Ferrante R.J., Bird E.D. and Richardson Jr E.P. (1985) Neuropathological classification of Huntington's disease. *J Neuropathol Exp Neurol.* 44:559-577
- Waelter S., Boeddrich A., Lurz R., Scherzinger E., Lueder G., Lehrach H. and Wanker E.E. (2001b) Accumulation of mutant huntingtin fragments in aggresome-like inclusion bodies as a result of insufficient protein degradation. *Mol Biol Cell.* 12:1393-1407
- Waelter S., Scherzinger E., Hasenbank R., Nordhoff E., Lurz R., Goehler H., Gauss C., Sathasivam K., Bates G.P., Lehrach H. and Wanker E.E. (2001a) The huntingtin interacting protein HIP1 is a clathrin and alpha-adaptin binding protein involved in receptor-mediated endocytosis. *Hum Mol Genet.* 10:1807-1817
- Walker F.O. (2007) Huntington's disease. *Lancet.* 369:218-228

Literature

- Wang G.H., Mitsui K., Kotliarova S., Yamashita A., Nagao Y., Tokuhiko S., Iwatsubo T., Kanazawa I. and Nukina N. (1999) Caspase activation during apoptotic cell death induced by expanded polyglutamine in N2a cells. *Neuroreport*. 10:2435-2438
- Wanker E.E., Rovira C., Scherzinger E., Hasenbank R., Walter S., Tait D., Colicelli J. and Lehrach H. (1997) HIP-I: a huntingtin interacting protein isolated by the yeast two-hybrid system. *Hum Mol Genet*. 6:487-495
- Weirich C.S., Erzberger J.P., Berger J.M. and Weis K. (2004) The N-terminal domain of Nup159 forms a beta-propeller that functions in mRNA export by tethering the helicase Dbp5 to the nuclear pore. *Mol Cell*. 16:749-760
- Welch M.D., Depace A.H., Verma S., Iwamatsu A. and Mitchison T.J. (1997) The human Arp2/3 complex is composed of evolutionarily conserved subunits and is localized to cellular regions of dynamic actin filament assembly. *J Cell Biol*. 138:375-384
- Wellington C.L., Ellerby L. M., Hackam A.S., Margolis R.L., Trifiro M.A., Singaraja R., McCutcheon K., Salvesen G.S., Propp S.S., Bromm M., Rowland K.J., Zhang T., Rasper D., Roy S., Thornberry N., Pinsky L., Kakizuka A., Ross C.A., Nicholson D.W., Bredesen D.E. and Hayden M.R. (1998) Caspase cleavage of gene products associated with triplet expansion disorders generates truncated fragments containing the polyglutamine tract. *J Biol Chem*. 273:9158-9167
- Wellington C.L., Ellerby L.M., Gutekunst C.A., Rogers D., Warby S., Graham R.K., Loubser O., van Raamsdonk J., Singaraja R., Yang Y.Z., Gafni J., Bredesen D., Hersch S.M., Leavitt B.R., Roy S., Nicholson D.W. and Hayden M.R. (2002) Caspase cleavage of mutant huntingtin precedes neurodegeneration in huntington's disease. *J Neurosci*. 22:7862-7872
- Wellington C.L., Singaraja R., Ellerby L., Savill J., Roy S., Leavitt B., Cattaneo E., Hackam A., Sharp A., Thornberry N., Nicholson D.W., Bredesen D.E. and Hayden M.R. (2000) Inhibiting caspase cleavage of huntingtin reduces toxicity and aggregate formation in neuronal and nonneuronal cells. *J Biol Chem*. 275:19831-19838
- Westerheide S.D. and Morimoto R.I. (2005) Heat shock response modulators as therapeutic tools for diseases of protein conformation. *J Biol Chem*. 280:33097-33100
- Westermarck J., Weiss C., Saffrich R., Kast J., Musti A.M., Wessely M., Ansorge W., Seraphin B., Wilm M., Valdez B.C. and Bohmann D. (2002) The DEXD/H-box RNA helicase RHII/Gu is a co-factor for c-Jun-activated transcription. *EMBO J*. 21:451-460
- Will C.L., Urlaub H., Achsel T., Gentzel M., Wilm M. and Luhrmann R. (2002) Characterization of novel SF3b and 17S U2snRNP proteins including a human Prp5p homologue and an SF3b-DEAD-box protein. *EMBO J*. 21:4978-4988
- Willingham S., Outeiro T.F., DeVit M.J., Lindquist S.L. and Muchowski P.J. (2003) Yeast genes that enhance the toxicity of a mutant huntingtin fragment or α -synuclein. *Science*. 302:1769-1772

Literature

- Wilson B.J., Bates G.J., Nicol S.M., Gregory D.J., Perkins N.D. and Fuller-Pace F.V. (2004) The p68 and p72 DEAD box RNA helicases interact with HDAC1 and repress transcription in a promoter-specific manner. *BMC Mol Biol.* 5:11
- Wu-Baer F., Lane W.S. and Gaynor R.B. (1995) The cellular factor TRP-185 regulates RNA polymerase II binding to HIV-1 TAR RNA. *EMBO J.* 14:5995-6009
- Wyllie A.H. (1980) Glucocorticoid-induced thymocyte apoptosis is associated with endogenous endonuclease activation. *Nature.* 284:555-556
- Wyllie A.H., Kerr J.F. and Currie A.R. (1980) Cell death: the significance of apoptosis. *Int Rev Cytol.* 68:251-306
- Wyttenbach A., Carmichael J., Swartz J., Furlong R.A., Narain Y., Rankin J. and Rubinsztein D.C. (2000) Effects of heat shock protein 40 (HDJ-2) and proteasome inhibition on protein aggregation in cellular models of Huntington's disease. *Proc Natl Acad Sci USA.* 97:2898-2903
- Wyttenbach A., Swartz J., Kita H., Thykjaer T., Carmichael J., Bradley J., Brown R., Maxwell M., Schapira A., Orntoft T.F., Kato K. and Rubinsztein D.C. (2001) Polyglutamine expansions cause decreased CRE-mediated transcription and early gene expression changes prior to cell death in an inducible cell model of Huntington's disease. *Hum Mol Genet.* 10:1829-1845
- Xia J., Lee D.H., Taylor J., Vandelft M. and Truant R. (2003) Huntingtin contains a highly conserved nuclear export signal. *Hum Mol Genet.* 12:1393-1403
- Yamamoto A., Cremona M.L. and Rothman J.E. (2006) Autophagy-mediated clearance of huntingtin aggregates triggered by the insulin-signaling pathway. *J Cell Biol.* 172:719-731
- Yan X., Mouillet J. F., Ou Q. and Sadovsky Y. (2003) A novel domain within the DEAD-box protein DP103 is essential for transcriptional repression and helicase activity. *Mol Cell Biol.* 23:414-423
- Yanai A., Huang K., Kang R., Singaraja R.R., Arstikaitis P., Gan L., Orban P.C., Mullard A., Cowan C.M., Raymond L.A., Drisdell R.C., Green W.N., Ravikumar B., Rubinsztein D.C., El-Husseini A. and Hayden M.R. (2006) Palmitoylation of huntingtin by HIP14 is essential for its trafficking and function. *Nat Neurosci.* 9:824-831
- Yang H., Zhou J., Ochs R.L., Henning D., Jin R. and Valdez B.C. (2003) Down-regulation of RNA helicase II/Gu results in the depletion of 18 and 28 S rRNAs in *Xenopus* oocyte. *J Biol Chem.* 278:38847-38859
- Yedavalli V.S., Neuveut C., Chi Y.H., Kleiman L. and Jeang K.T. (2004) Requirement of DDX3 DEAD box RNA helicase for HIV-1 Rev-RRE export function. *Cell.* 119:381-392
- Yoshida H., Yoshizawa T., Shibasaki F., Shoji S. and Kanazawa I. (2002) Chemical chaperones reduce aggregate formation and cell death caused by the truncated Machado-Joseph disease gene product with an expanded polyglutamine stretch. *Neurobiol Dis.* 10:88-99

Literature

- Yu Z.X., Li S.H., Nguyen H.P. and Li X.J. (2002) Huntingtin inclusions do not deplete polyglutamine-containing transcription factors in HD mice. *Hum Mol Genet.* 11:905-914
- Yuan J. and Yankner B.A. (2000) Apoptosis in the nervous system. *Nature.* 407:802-809
- Zagulski M., Kressler D., Becam A.M., Rytka J. and Herbert C.J. (2003) Mak5p, which is required for the maintenance of the M1dsRNA virus, is encoded by the yeast ORF YBR142w and is involved in the biogenesis of the 60S subunit of the ribosome. *Mol Genet Genomics.* 270:216-224
- Zatloukal K., Stumptner C., Fuchsbichler A., Heid H., Schnoelzer M., Kenner L., Kleinert R., Prinz M., Aguzzi A. and Denk H. (2002) p62 Is a common component of cytoplasmic inclusions in protein aggregation diseases. *Am J Pathol.* 160:255-263
- Zeitlin S., Liu J.P., Chapman D.L., Papaioannou V.E. and Efstratiadis A. (1995) Increased apoptosis and early embryonic lethality in mice nullizygous for the Huntington's disease gene homologue. *Nat Genet.* 11:155-163
- Zeron M.M., Fernandes H.B., Krebs C., Shehadeh J., Wellington C.L., Leavitt B.R., Baimbridge K.G., Hayden M.R. and Raymond L.A. (2004) Potentiation of NMDA receptor-mediated excitotoxicity linked with intrinsic apoptotic pathway in YAC transgenic mouse model of Huntington's disease. *Mol Cell Neurosci.* 25:469-479
- Zeron M.M., Hansson O., Chen N., Wellington C.L., Leavitt B.R., Brundin P., Hayden M.R. and Raymond L.A. (2002) Increased sensitivity to N-methyl-D-aspartate receptor-mediated excitotoxicity in a mouse model of Huntington's disease. *Neuron.* 33:849-860
- Zhang H., Webb D J., Asmussen H. and Horwitz A.F. (2003) Synapse formation is regulated by the signaling adaptor git1. *J Cell Biol.* 161:131-142
- Zhang Y., Leavitt B.R., van Raamsdonk J.M., Dragatsis I., Goldowitz D., MacDonald M.E., Hayden M.R. and Friedlander R.M. (2006) Huntingtin inhibits caspase-3 activation. *EMBO J.* 25:5896-5906
- Zhao J., Jin S.B., Bjorkroth B., Wieslander L. and Daneholt B. (2002) The mRNA export factor Dbp5 is associated with Balbiani ring mRNP from gene to cytoplasm. *EMBO J.* 21:1177-1187
- Zhao Y., Yu L., Fu Q., Chen W., Jiang J., Gao J. and Zhao S. (2000) Cloning and characterization of human DDX24 and mouse Ddx24 two novel putative DEAD-Box proteins and mapping DDX24 to human chromosome 14q32. *Genomics.* 67:351-355
- Zhou H., Cao F., Wang Z., Yu Z.X., Nguyen H.P., Evans J., Li S.H. and Li X.J. (2003) Huntingtin forms toxic NH₂-terminal fragment complexes that are promoted by the age-dependent decrease in proteasome activity. *J Cell Biol.* 163:109-118
- Zhou Z., Kerk S. and Meng Lim T. (2008) Endogenous dopamine (DA) renders dopaminergic cells vulnerable to challenge of proteasome inhibitor MG132. *Free Radic Res.* 42:456-466

Literature

- Zirwes R.F., Eilbracht J., Kneissel S. and Schmidt-Zachmann M.S. (2000) A novel helicase-type protein in the nucleolus: proteinNOH61. *Mol Biol Cell.* 11:1153-1167
- Zoghbi H.Y. and Botas J. (2002) Mouse and fly models of neurodegeneration. *Trends Genet.* 18:463-471
- Zoghbi H.Y. and Orr H.T. (2000) Glutamine repeats and neurodegeneration. *Annu Rev Neurosci.* 23:217-247
- Zuccato C., Ciammola A., Rigamonti D., Leavitt B.R., Goffredo D., Conti L., MacDonald M.E., Friedlander R.M., Silani V., Hayden M.R., Timmusk T., Sipione S. and Cattaneo E. (2001) Loss of huntingtin-mediated BDNF gene transcription in Huntington's disease. *Science.* 293:493-498
- Zuccato C., Tartari M., Crotti A., Goffredo D., Valenza M., Conti L., Cataudella T., Leavitt B.R., Hayden M.R., Timmusk T., Rigamonti D. and Cattaneo E. (2003) Huntingtin interacts with REST/NRSF to modulate the transcription of NRSE-controlled neuronal genes. *Nat Genet.* 35:76-83

Abstract

Huntington's disease (HD) is an inherited progressive neurodegenerative disorder which manifests in progressive chorea, dementia and personality changes. The symptoms result from dysfunction and selective loss of neuronal cells in the striatal regions of the brain, caused by an expansion mutation in a polyglutamine sequence in the N-terminus of huntingtin protein (Htt). Proteolytical cleavage of Htt leads to accumulation of the N-terminal Htt fragments. These form cytoplasmatic and intranuclear inclusions which cause cellular dysfunction, cytotoxicity and eventually cell death. The mechanisms in which mutant Htt activates death signaling are still unclear, but key players of the extrinsic and intrinsic apoptosis pathways such as caspases-3/7, -8 and -9 have been found to be overexpressed and/or activated in the presence of mutant Htt. This study was performed to further elucidate the mechanism by which Htt induces cytotoxicity and apoptosis and to investigate proteins which modulate this mechanism.

In a Neuro2a cell system I performed an RNAi screen to identify proteins that modulate cytotoxicity of a transiently expressed N-terminal Htt fragment (HD320_Q68). 200 proteins were tested, selected based on literature information about biological processes that might influence HD pathogenesis. The screen revealed 13 highly reproducible modulators from which 7 were classified as toxicity suppressors and 6 as toxicity enhancers. A novel modulator of Htt-induced toxicity identified in this study is DDX24, a member of the DEAD-box protein family presumed to be an RNA helicase. RNAi experiments targeting DDX24 in a HD PC12 cell model demonstrated that DDX24 acts as a toxicity suppressor on Htt-induced caspase-3/7, -8 and -9 activity. Its silencing dramatically enhanced activity of the caspases in presence of mutant Htt (Htt103Q-EGFP). This effect could be rescued by overexpression of the human DDX24 protein. In addition, mRNA levels of DDX24 were upregulated in PC12 cells expressing Htt103Q-EGFP. In control cells expressing a wild-type like Htt25Q-EGFP protein no increase in DDX24 mRNA levels was observed. A similar result was obtained when mRNA levels in striatal tissue of a HD mouse were compared to the wild-type controls; in contrast, DDX24 protein levels were reduced in HD mice. Moreover, I could show that DDX24 does not impact caspase activity by exerting influence on Htt expression or aggregation, nor on the degradation of the mutant protein. Rather, an interaction of DDX24 with FADD, a key component of death receptor-mediated apoptosis signaling could be demonstrated. Additionally, I could show that DDX24 knock-down and FADD overexpression synergistically increase Htt-induced caspase-8 and -3 activity.

These findings suggest a protective role of DDX24 in Htt-induced cytotoxicity by modulating death receptor-mediated caspase-8 activation through its interaction with FADD.

Zusammenfassung

Chorea Huntington (HD) ist eine erbliche neurodegenerative Erkrankung, charakterisiert durch fortschreitende Chorea, Demenz und Persönlichkeitsveränderungen. Die Symptome werden durch einen selektiven Verlust an Neuronen im Striatum hervorgerufen, ausgelöst durch eine abnormale Verlängerung in der Polyglutaminsequenz des Huntingtin (Htt) Proteins. Durch proteolytische Spaltung von Htt entstehen N-terminale Proteinfragmente, die im Zytoplasma und im Nucleus akkumulieren und Einschlusskörper bilden, welche zu zellulärer Dysfunktion, Zytotoxizität und Zelltod führen. Es wurde jedoch gezeigt, dass Schlüsselproteine aus verschiedenen Apoptose Signalwegen, wie beispielsweise die Caspasen-3/7, -8 und -9, in Anwesenheit von mutiertem Htt verstärkt exprimiert und/oder aktiviert werden.

In einem Neuro2a Zellmodell wurde ein RNAi Screen durchgeführt um Proteine zu identifizieren, die die Zytotoxizität eines transient exprimierten N-terminalen Htt Proteins (HD320_Q68) modulieren. Getestet wurden 200 Proteine, selektiert anhand von Literaturinformationen über biologische Prozesse, die an der HD Pathogenese beteiligt sind. Im Rahmen des Screens wurden 13 gut reproduzierbare Toxizitätsmodulatoren identifiziert, von denen 7 als Toxizitätsunterdrücker und 6 als Toxizitätsverstärker klassifiziert wurden. Ein neu identifizierter Modulator der Htt-induzierten Toxizität ist DDX24, ein Mitglied der DEAD-box Proteinfamilie, für das eine Funktion als RNA Helikase vermutet wird. RNAi Experimente, durchgeführt in einem HD PC12 Zellmodell zeigten, dass DDX24 toxizitätsunterdrückend wirkt. Die Reduktion der DDX24 Expression durch RNAi führte zu einer drastischen Erhöhung der durch mutiertes Htt (Htt103Q-EGFP) hervorgerufenen Aktivität von Caspase-3, -8 und -9. Dieser Effekt konnte durch die zeitgleiche Überexpression des humanen DDX24 ausgeglichen werden. Darüber hinaus wurden erhöhte Mengen an DDX24 mRNA in PC12 Zellen gefunden, die toxisches Htt103Q-EGFP Protein exprimierten. In Zellen, in denen das dem Wildtyp (Wt) entsprechende Htt25Q-EGFP Protein exprimiert wurde, war hingegen keine Erhöhung der mRNA Menge festzustellen. Eine vergleichbare Erhöhung der DDX24 mRNA wurde beim Vergleich im Striatum von HD Mäusen gegenüber dem Wildtyp detektiert. Im Gegensatz zur mRNA von DDX24 waren die DDX24 Proteinmengen in den HD Mäusen gegenüber dem Wildtyp allerdings verringert. Es wurde außerdem gezeigt, dass der Einfluss von DDX24 auf die Caspaseaktivität nicht mit einer Modulierung der Expression, der Aggregation oder dem Proteinabbau von mutiertem Htt in Verbindung steht. Stattdessen konnte eine Interaktion von DDX24 mit FADD, einer Schlüsselkomponente des extrinsischen Apoptosesignalweges nachgewiesen werden. Eine Reduktion von DDX24 durch RNAi und die gleichzeitige Überexpression von FADD führten zu einer synergistischen Erhöhung der Caspase-8 und -3 Aktivität.

Anhand dieser Ergebnisse wird angenommen, dass DDX24 durch seine Interaktion mit FADD die rezeptorvermittelte Caspase-8 Aktivität moduliert und damit protektiv auf die Htt-induzierte Zytotoxizität wirkt.

Appendix A: List of abbreviations

°C	Degrees Celcius
µg	microgram
µl	microliter
µM	micor molar
µm	micrometer
aa	amino acid
Abk	Name
AD	Alzheimer's disease
ADP	adenosine diphosphate
ALS	amyotrophic lateral sclerosis
Amp	Ampicillin
APS	Ammonium persulfate
ATP	adenosine triphosphate
bp	base pair
BSA	Bovine serum albumin
cDNA	complementary Desoxiribonucleic acid
Co-IP	Co-immunoprecipitation
C-terminus	carboxy terminus
DD	Death domain
DEAD	Asp-Glu-Ala-Asp
DED	Death effector domain
DISC	death inducing signaling complex
DMEM	Dulbecco's Modified Eagle Medium
DMSO	Dimethylsulfoxide
DNA	Desoxiribonucleic acid
DSMZ	Deutsche Sammlung von Mikroorganismen und Zellkulturen GmbH
DTT	Dithiothreitol
E.coli	Escherichia coli
ECFP	enhanced cyan fluorescent protein
EDTA	ethylenediamine tetraacetic acid
EGFP	enhanced gree fluorescent protein
Em	emission wavelength
ER	endoplasmatic reticulum
Ex	excitation wavelength

Appendix

EYFP	enhanced yellow fluorescent protein
FCS	Fetal calf serum
FRET	Förster resonance energy transfer
g	earth's gravity
HA	haemagglutinin
HD	Huntington's disease
Htt	Huntingtin
IF	immuno fluorescence
kDa	Kilo Dalton
LB	Luria broth
LUMIER	luminescence-based mammalian interactome mapping
mg	milligram
min	minutes
ml	mililiter
mRNA	messenger ribonucleic acid
NGF	nerve growth factor
nm	nanometer
N-terminus	amino terminus
OD	optical density
PA	Protein A
PBS	phospho-buffered saline
PCR	polymerase chain reaction
PD	Parkinson's disease
PMSF	phenylmethylsulfonyl fluoride
PolyQ	polyglutamine
qRT-PCR	quantitative real-time polymerase chain reaction
RNA	ribonucleic acid
RNAi	RNA interference
rpm	rotations per minute
rRNA	ribosomal ribonucleic acid
SCA	spinocerebellar ataxias
SDS	sodium dodecyl sulphate
SDS-PAGE	sodium dodecyl sulphate polyacrylamide gel electrophoresis
siRNA	small interfering ribonucleic acid
TBS	tris buffered saline
TBS-T	tris buffered saline-tween20

Appendix

TEMED	N,N,N',N'-tetramethylethylenediamine, 1,2-bis(dimethylamino)-ethane
Tg	transgene
TNF	tumor necrosis factor
Tris	tris(hydroxymethyl)aminomethane
UPS	ubiquitin-proteasome system
UV	ultraviolet
WB	Western blotting
wt	wild-type
β -Gal	β -Galactosidase

Appendix B: “p200” onthology list

p200 #	Gene-ID	Gene Name	Description	apoptosis/cell death	cell communication	cell cycle/cell division	cellular comp./organelle organization	cytoskeleton organization/morphology	development	enzyme regulation	e-tracellular signal processing	metabolism	protein degradation	regulation cellular/biological processes	signal transduction	stress response	transport	other
1	1111	CHEK1	CHK1 checkpoint homolog (S. pombe)	•	•	•			•	•	•	•	•	•	•	•		•
2	11200	CHEK2	CHK2 checkpoint homolog (S. pombe)	•	•	•	•			•	•	•	•	•	•	•		•
3	207	AKT1	v-akt murine thymoma viral oncogene homolog 1	•	•	•	•	•	•	•	•	•	•	•	•	•	•	•
4	9212	AURKB	aurora kinase B			•	•					•	•	•				•
5	6795	AURKC	aurora kinase C			•	•		•			•	•	•				•
6	660	BMX	BMX non-receptor tyrosine kinase		•	•	•	•	•			•	•	•	•			•
7	699	BUB1	BUB1 budding uninhibited by benzimidazoles 1 homolog (yeast)			•	•					•	•	•				•
8	983	cdc2	cell division cycle 2, G1 to S and G2 to M	•		•	•		•			•	•	•				•
9	1020	CDK5	cyclin-dependent kinase 5	•	•	•	•	•	•	•	•	•	•	•	•	•	•	•
10	1026	CDKN1A	cyclin-dependent kinase inhibitor 1A (p21, Cip1)	•	•	•	•	•	•	•	•	•	•	•	•	•		
11	1027	CDKN1B	cyclin-dependent kinase inhibitor 1B (p27, Kip1)	•		•	•	•	•			•	•	•	•			
12	1263	PLK3	polo-like kinase 3 (Drosophila)			•	•					•	•	•				•
13	1445	CSK	c-src tyrosine kinase		•	•	•					•	•	•	•			•
14	1457	CSNK2A1	casein kinase 2, alpha 1 polypeptide		•	•	•					•	•	•	•			•
15	1846	DUSP4	dual specificity phosphatase 4		•		•			•		•	•	•	•			•
16	2534	FYN	FYN oncogene related to SRC, FGR, YES		•	•	•	•	•		•	•	•	•	•	•		•
17	2932	GSK3B	glycogen synthase kinase 3 beta	•	•	•	•				•	•	•	•	•	•	•	•
18	3611	ILK	integrin-linked kinase	•	•	•	•	•	•	•	•	•	•	•	•			•
19	3717	JAK2	Janus kinase 2 (a protein tyrosine kinase)	•	•	•	•	•	•	•	•	•	•	•	•	•	•	•

Appendix

p200 #	Gene-ID	Gene Name	Description	apoptosis/cell death	cell communication	cell cycle/cell division	cellular comp./organelle organization	cytoskeleton organization/morphology	development	enzyme regulation	e-tracellular signal processing	metabolism	protein degradation	regulation cellular/biological processes	signal transduction	stress response	transport	other
20	4067	LYN	v-yes-1 Yamaguchi sarcoma viral related oncogene homolog	•	•	•				•					•	•		
21	6416	MAP2K4	mitogen-activated protein kinase kinase 4	•		•				•	•	•	•	•	•	•		•
22	4296	MAP3K11	mitogen-activated protein kinase kinase kinase 11	•	•	•	•	•	•	•	•	•	•	•	•	•	•	•
23	4217	MAP3K5	mitogen-activated protein kinase kinase kinase 5	•	•		•		•	•	•	•	•	•	•	•		•
24	5594	MAPK1	mitogen-activated protein kinase 1	•	•	•	•	•	•	•	•	•	•	•	•	•	•	•
25	6300	MAPK12	mitogen-activated protein kinase 12		•	•	•	•	•	•	•	•	•	•	•	•		•
26	5595	MAPK3	mitogen-activated protein kinase 3		•	•	•					•	•	•	•			•
27	5599	MAPK8	mitogen-activated protein kinase 8	•	•	•	•	•	•	•	•	•	•	•	•	•		•
28	5601	MAPK9	mitogen-activated protein kinase 9	•	•	•	•	•	•	•	•	•	•	•	•	•		•
29	85366	MYLK2	myosin light chain kinase 2, skeletal muscle		•	•	•	•	•	•	•	•	•	•	•		•	•
30	4751	NEK2	NIMA (never in mitosis gene a)-related kinase 2			•	•	•				•	•	•			•	•
31	5058	PAK1	p21/Cdc42/Rac1-activated kinase 1 (STE20 homolog, yeast)	•	•		•	•	•	•	•	•	•	•	•			•
32	5062	PAK2	p21 (CDKN1A)-activated kinase 2	•	•	•	•		•		•	•	•	•	•			•
33	10298	PAK4	p21(CDKN1A)-activated kinase 4		•		•	•			•	•	•	•	•			•
34	5170	PDPK1	3-phosphoinositide dependent protein kinase-1		•	•	•	•	•	•	•	•	•	•	•	•		•
35	5291	PIK3CB	phosphoinositide-3-kinase, catalytic, beta polypeptide		•	•	•	•	•	•	•	•	•	•	•	•		•
36	5295	PIK3R1	phosphoinositide-3-kinase, regulatory subunit 1 (p85 alpha)		•		•			•	•	•		•	•	•		•
37	8503	PIK3R3	phosphoinositide-3-kinase, regulatory subunit 3 (p55, gamma)							•			•	•	•			•
38	65018	PINK1	PTEN induced putative kinase 1		•		•			•	•	•	•	•	•	•	•	•
39	5347	PLK1	polo-like kinase 1 (Drosophila)	•	•	•			•	•	•	•	•	•				•

Appendix

p200 #	Gene-ID	Gene Name	Description	apoptosis/cell death	cell communication	cell cycle/cell division	cellular comp./organelle organization	cytoskeleton organization/morphology	development	enzyme regulation	e-tracellular signal processing	metabolism	protein degradation	regulation cellular/biological processes	signal transduction	stress response	transport	other
40	5515	PPP2CA	protein phosphatase 2 (formerly 2A), catalytic subunit, alpha isoform	•	•	•	•	•	•	•	•	•	•	•	•			•
41	5566	PRKACA	protein kinase, cAMP-dependent, catalytic, alpha		•	•	•	•	•	•	•	•	•	•	•	•	•	•
42	5567	PRKACB	protein kinase, cAMP-dependent, catalytic, beta		•		•		•	•	•	•	•	•	•	•		•
43	5568	PRKACG	protein kinase, cAMP-dependent, catalytic, gamma		•	•	•	•	•	•	•	•	•	•	•	•		•
44	5578	PRKCA	protein kinase C, alpha	•	•	•	•	•	•	•	•	•	•	•	•	•	•	•
45	5579	PRKCB1	protein kinase C, beta 1		•		•					•	•	•	•			•
46	5582	PRKCG	protein kinase C, gamma	•	•		•	•		•	•	•	•	•	•			•
47	5590	PRKCZ	protein kinase C, zeta	•	•	•	•	•	•	•	•	•	•	•	•		•	•
48	5747	PTK2	PTK2 protein tyrosine kinase 2		•	•	•	•	•			•	•	•	•		•	•
49	5879	RAC1	ras-related C3 botulinum toxin substrate 1 (rho family, small GTP binding protein Rac1)	•	•	•	•	•	•	•	•	•	•	•	•	•	•	•
50	5894	RAF1	v-raf-1 murine leukemia viral oncogene homolog 1	•	•		•					•	•	•	•			•
51	10769	PLK2	polo-like kinase 2 (Drosophila)			•	•			•	•	•	•	•	•			•
52	8878	SQSTM1	sequestosome 1	•	•	•	•	•	•	•	•	•	•	•	•	•	•	•
53	10733	PLK4	polo-like kinase 4 (Drosophila)		•	•	•	•	•			•	•	•				•
54	333	APLP1	amyloid beta (A4) precursor-like protein 1	•	•	•	•	•	•	•	•		•				•	
55	572	BAD	BCL2-antagonist of cell death	•	•	•		•	•		•		•	•				
56	55755	CDK5RAP2	CDK5 regulatory subunit associated protein 2		•	•		•	•				•					
57	11190	CEP2	centrosomal protein 2			•	•	•					•				•	
58	1072	CFL1	cofilin 1 (non-muscle)	•	•	•	•	•		•	•	•	•	•	•	•		•
59	1822	ATN1	atrophin 1	•	•	•	•	•		•	•		•					

Appendix

p200 #	Gene-ID	Gene Name	Description	apoptosis/cell death	cell communication	cell cycle/cell division	cellular comp./organelle organization	cytoskeleton organization/morphology	development	enzyme regulation	e-tracellular signal processing	metabolism	protein degradation	regulation cellular/biological processes	signal transduction	stress response	transport	other
60	5217	PFN2	profilin 2				•	•				•	•					
61	5829	PXN	paxillin		•		•	•			•		•	•	•	•		•
62	6310	ATXN1	ataxin 1	•			•					•		•			•	•
63	6421	SFPQ	splicing factor proline/glutamine-rich (polypyrimidine tract binding protein associated)							•	•		•			•		
64	10580	SORBS1	sorbin and SH3 domain containing 1		•		•	•		•	•		•	•	•	•	•	•
65	6895	TARBP2	TAR (HIV) RNA binding protein 2		•	•	•	•		•	•		•	•	•			•
66	7429	VIL1	villin 1				•	•				•	•	•				•
67	7531	YWHAE	tyrosine 3-monooxygenase/tryptophan 5-monooxygenase activation protein, epsilon polypeptide	•	•	•	•	•	•			•	•	•	•		•	•
68	7534	YWHAZ	tyrosine 3-monooxygenase/tryptophan 5-monooxygenase activation protein, zeta polypeptide	•	•	•	•			•				•	•	•	•	•
69	7791	ZYX	zyxin		•									•	•			
70	351	APP	amyloid beta (A4) precursor protein (peptidase nexin-II, Alzheimer disease)	•	•	•	•	•	•	•	•	•	•	•	•	•	•	•
71	396	ARHGDI2	Rho GDP dissociation inhibitor (GDI) alpha	•	•	•	•	•	•					•	•			
72	2889	RAPGEF1	Rap guanine nucleotide exchange factor (GEF) 1		•		•			•			•	•				
73	3320	HSPCA	heat shock 90kDa protein 1, alpha		•		•	•		•	•	•	•	•	•	•	•	•
74	8976	WASL	Wiskott-Aldrich syndrome-like		•		•	•		•	•	•	•	•				•
75	9232	PTTG1	pituitary tumor-transforming 1		•	•	•			•	•		•			•		
76	1385	CREB1	cAMP responsive element binding protein 1	•	•	•	•	•	•	•	•	•	•	•	•		•	•
77	2002	ELK1	ELK1, member of ETS oncogene family									•		•				
78	2353	FOS	v-fos FBJ murine osteosarcoma viral oncogene homolog		•	•	•	•		•	•	•	•	•	•	•		•

Appendix

p200 #	Gene-ID	Gene Name	Description	apoptosis/cell death	cell communication	cell cycle/cell division	cellular comp./organelle organization	cytoskeleton organization/morphology	development	enzyme regulation	e-tracellular signal processing	metabolism	protein degradation	regulation cellular/biological processes	signal transduction	stress response	transport	other
79	3725	JUN	v-jun sarcoma virus 17 oncogene homolog (avian)	●	●	●	●	●	●	●	●	●	●	●	●	●	●	●
80	4790	NFKB1	nuclear factor of kappa light polypeptide gene enhancer in B-cells 1 (p105)	●	●	●	●	●	●	●	●	●	●	●	●	●	●	●
81	5201	PFDN1	prefoldin 1		●	●	●					●		●				
82	836	CASP3	caspase 3, apoptosis-related cysteine peptidase	●	●	●	●	●	●	●	●	●	●	●	●	●		
83	55585	UBE2Q1	ubiquitin-conjugating enzyme E2Q (putative) 1				●					●	●	●				●
84	7353	UFD1L	ubiquitin fusion degradation 1-like		●	●	●	●		●	●	●	●					●
85	6907	TBL1X	transducin (beta)-like 1X-linked		●		●					●	●	●	●			
86	10766	TOB2	transducer of ERBB2, 2		●	●		●				●		●				
87	10844	TUBGCP2	tubulin, gamma complex associated protein 2				●	●					●	●			●	●
88	29979	UBQLN1	ubiquilin 1	●									●		●			
89	1487	CTBP1	C-terminal binding protein 1		●		●	●				●	●	●				●
90	3265	HRAS	v-Ha-ras Harvey rat sarcoma viral oncogene homolog	●	●	●	●	●	●	●	●	●	●	●	●	●	●	●
91	3845	KRAS	v-Ki-ras2 Kirsten rat sarcoma viral oncogene homolog	●	●	●	●	●	●	●	●	●	●	●	●	●	●	●
92	4893	NRAS	neuroblastoma RAS viral (v-ras) oncogene homolog	●	●	●	●	●	●	●	●		●	●	●	●	●	●
93	5481	PPID	peptidylprolyl isomerase D (cyclophilin D)				●					●		●				
94	5901	RAN	RAN, member RAS oncogene family		●	●	●	●	●			●		●	●		●	●
95	6894	TARBP1	TAR (HIV) RNA binding protein 1									●		●				
96	10524	HTATIP	HIV-1 Tat interacting protein, 60kDa		●		●			●	●	●	●	●	●	●		●
97	9459	ARHGGEF6	Rac/Cdc42 guanine nucleotide exchange factor (GEF) 6	●	●					●			●	●	●			
98	7454	WAS	Wiskott-Aldrich syndrome (eczema-thrombocytopenia)	●	●	●	●	●		●		●	●	●	●	●	●	●

Appendix

p200 #	Gene-ID	Gene Name	Description	apoptosis/cell death	cell communication	cell cycle/cell division	cellular comp./organelle organization	cytoskeleton organization/morphology	development	enzyme regulation	e-tracellular signal processing	metabolism	protein degradation	regulation cellular/biological processes	signal transduction	stress response	transport	other
99	7345	UCHL1	ubiquitin carboxyl-terminal esterase L1 (ubiquitin thiolesterase)	•	•	•	•	•	•	•	•	•	•	•	•	•	•	•
100	5071	PARK2	Parkinson disease (autosomal recessive, juvenile) 2, parkin	•	•	•	•	•	•	•	•	•	•	•	•	•	•	•
101	10273	STUB1	STIP1 homology and U-box containing protein 1	•	•	•	•	•	•	•	•	•	•	•	•	•	•	•
102	10277	UBE4B	ubiquitination factor E4B (UFD2 homolog, yeast)	•	•	•	•	•	•	•	•	•	•	•	•	•	•	•
103	267	AMFR	autocrine motility factor receptor	•	•	•	•	•	•	•	•	•	•	•	•	•	•	•
104	5728	PTEN	phosphatase and tensin homolog (mutated in multiple advanced cancers 1)	•	•	•	•	•	•	•	•	•	•	•	•	•	•	•
105	5499	PPP1CA	protein phosphatase 1, catalytic subunit, alpha isoform	•	•	•	•	•	•	•	•	•	•	•	•	•	•	•
106	5770	PTPN1	protein tyrosine phosphatase, non-receptor type 1	•	•	•	•	•	•	•	•	•	•	•	•	•	•	•
107	5800	PTPRO	protein tyrosine phosphatase, receptor type, O	•	•	•	•	•	•	•	•	•	•	•	•	•	•	•
108	1398	CRK	v-crk sarcoma virus CT10 oncogene homolog (avian)	•	•	•	•	•	•	•	•	•	•	•	•	•	•	•
109	10163	WASF2	WAS protein family, member 2	•	•	•	•	•	•	•	•	•	•	•	•	•	•	•
110	10142	AKAP9	A kinase (PRKA) anchor protein (yotiao) 9	•	•	•	•	•	•	•	•	•	•	•	•	•	•	•
111	2885	GRB2	growth factor receptor-bound protein 2	•	•	•	•	•	•	•	•	•	•	•	•	•	•	•
112	8440	NCK2	NCK adaptor protein 2	•	•	•	•	•	•	•	•	•	•	•	•	•	•	•
113	10140	TOB1	transducer of ERBB2, 1	•	•	•	•	•	•	•	•	•	•	•	•	•	•	•
114	4035	LRP1	low density lipoprotein-related protein 1 (alpha-2-macroglobulin receptor)	•	•	•	•	•	•	•	•	•	•	•	•	•	•	•
115	3164	NR4A1	nuclear receptor subfamily 4, group A, member 1	•	•	•	•	•	•	•	•	•	•	•	•	•	•	•
116	6772	STAT1	signal transducer and activator of transcription 1, 91kDa	•	•	•	•	•	•	•	•	•	•	•	•	•	•	•
117	1499	CTNNB1	catenin (cadherin-associated protein), beta 1, 88kDa	•	•	•	•	•	•	•	•	•	•	•	•	•	•	•

Appendix

p200 #	Gene-ID	Gene Name	Description	apoptosis/cell death	cell communication	cell cycle/cell division	cellular comp./organelle organization	cytoskeleton organization/morphology	development	enzyme regulation	e-tracellular signal processing	metabolism	protein degradation	regulation cellular/biological processes	signal transduction	stress response	transport	other
118	27229	76P	gamma tubulin ring complex protein (76p gene)				•	•					•	•			•	•
119	10095	ARPC1B	actin related protein 2/3 complex, subunit 1B, 41kDa			•	•					•	•					•
120	857	CAV1	caveolin 1, caveolae protein, 22kDa	•	•	•	•	•	•	•	•	•	•	•	•	•	•	•
121	4771	NF2	neurofibromin 2 (bilateral acoustic neuroma)	•	•	•	•	•	•	•	•	•	•	•	•			
122	10426	TUBGCP3	tubulin, gamma complex associated protein 3			•	•						•				•	
123	6804	STX1A	syntaxin 1A (brain)	•		•				•			•	•			•	•
124	6857	SYT1	synaptotagmin I	•		•	•			•		•	•				•	•
125	387	RHOA	ras homolog gene family, member A	•	•	•	•	•	•	•	•		•	•	•	•	•	•
126	10092	ARPC5	actin related protein 2/3 complex, subunit 5, 16kDa			•	•					•	•					•
127	1386	ATF2	activating transcription factor 2				•					•	•					
128	546	ATRX	alpha thalassemia/mental retardation syndrome X-linked (RAD54 homolog, S. cerevisiae)	•	•		•	•		•		•	•			•		•
129	10950	BTG3	BTG family, member 3			•							•					
130	9184	BUB3	BUB3 budding uninhibited by benzimidazoles 3 homolog (yeast)			•	•		•		•	•	•	•				
131	991	cdc20	CDC20 cell division cycle 20 homolog (S. cerevisiae)			•	•		•		•	•	•	•				
132	998	CDC42	cell division cycle 42 (GTP binding protein, 25kDa)	•	•	•	•	•					•	•				•
133	11064	CEP1	centrosomal protein 1			•												
134	27185	DISC1	disrupted in schizophrenia 1	•	•	•	•	•					•	•				
135	595	CCND1	cyclin D1 (PRAD1: parathyroid adenomatosis 1)	•	•		•	•	•	•	•	•	•	•	•	•		
136	2059	EPS8	epidermal growth factor receptor pathway substrate 8	•		•	•	•		•			•	•				
137	9638	FEZ1	fasciculation and elongation protein zeta 1 (zygin I)	•	•	•	•	•					•					

Appendix

p200 #	Gene-ID	Gene Name	Description	apoptosis/cell death	cell communication	cell cycle/cell division	cellular comp./organelle organization	cytoskeleton organization/morphology	development	enzyme regulation	e-tracellular signal processing	metabolism	protein degradation	regulation cellular/biological processes	signal transduction	stress response	transport	other
138	9737	GPRASP1	G protein-coupled receptor associated sorting protein 1															
139	8379	MAD1L1	MAD1 mitotic arrest deficient-like 1 (yeast)			•	•							•				
140	4085	MAD2L1	MAD2 mitotic arrest deficient-like 1 (yeast)			•	•		•		•	•	•	•				
141	3303	HSPA1A	heat shock 70kDa protein 1A	•	•	•				•	•	•	•	•		•		
142	3315	HSPB1	heat shock 27kDa protein 1	•	•	•	•	•		•	•	•	•	•		•		
143	8481	OFD1	oral-facial-digital syndrome 1		•		•	•						•				•
144	11315	PARK7	Parkinson disease (autosomal recessive, early onset) 7		•		•	•	•	•	•	•	•	•	•	•		
145	5216	PFN1	profilin 1			•	•	•	•			•	•	•				
146	4478	MSN	moesin				•	•						•				
147	6203	RPS9	ribosomal protein S9			•	•					•	•	•				
148	6455	SH3GL1	SH3-domain GRB2-like 1		•	•	•	•	•	•	•		•	•	•			•
149	6622	SNCA	synuclein, alpha (non A4 component of amyloid precursor)	•	•	•	•	•	•	•	•	•	•	•	•	•	•	•
150	5881	RAC3	ras-related C3 botulinum toxin substrate 3 (rho family, small GTP binding protein Rac3)		•	•	•	•	•				•	•				
151	10048	RANBP9	RAN binding protein 9				•	•					•	•			•	•
152	160	AP2A1	adaptor-related protein complex 2, alpha 1 subunit				•			•			•	•			•	•
153	161	AP2A2	adaptor-related protein complex 2, alpha 2 subunit				•			•			•	•			•	•
154	166	AES	amino-terminal enhancer of split	•	•		•	•		•	•	•	•	•	•	•		
155	1400	CRMP1	collapsin response mediator protein 1		•	•	•	•			•		•	•				
156	1627	DBN1	drebrin 1		•	•	•	•	•	•			•	•				
157	1808	DPYSL2	dihydropyrimidinase-like 2	•	•		•	•			•		•	•				

Appendix

p200 #	Gene-ID	Gene Name	Description	apoptosis/cell death	cell communication	cell cycle/cell division	cellular comp./organelle organization	cytoskeleton organization/morphology	development	enzyme regulation	e-tracellular signal processing	metabolism	protein degradation	regulation cellular/biological processes	signal transduction	stress response	transport	other
158	3301	DNAJA1	DnaJ (Hsp40) homolog, subfamily A, member 1	•		•	•			•	•		•	•	•			
159	3337	DNAJB1	DnaJ (Hsp40) homolog, subfamily B, member 1	•		•				•	•		•		•			
160	4957	ODF2	outer dense fiber of sperm tails 2		•	•		•					•					
161	5121	PCP4	Purkinje cell protein 4		•	•	•	•										
162	84335	AKT1S1	AKT1 substrate 1 (proline-rich)	•	•	•	•	•	•	•	•	•	•	•	•			
163	6620	SNCB	synuclein, beta	•		•						•	•					
164	7408	VASP	vasodilator-stimulated phosphoprotein		•	•	•	•	•				•					
165	7415	VCP	valosin-containing protein	•	•		•	•	•	•	•	•	•	•	•	•	•	•
166	7802	DNALI1	dynein, axonemal, light intermediate polypeptide 1				•	•					•					
167	9627	SNCAIP	synuclein, alpha interacting protein (synphilin)		•		•			•	•		•	•				•
168	9637	FEZ2	fasciculation and elongation protein zeta 2 (zygin II)		•	•	•	•	•				•	•				
169	9788	MTSS1	metastasis suppressor 1		•		•	•					•	•				
170	10190	TXNDC9	thioredoxin domain containing 9															
171	10542	HBXIP	hepatitis B virus x interacting protein	•	•	•				•	•		•					
172	10989	IMMT	inner membrane protein, mitochondrial (mitofilin)										•					
173	23385	NCSTN	nicastrin	•	•		•		•		•		•	•				
174	23216	TBC1D1	TBC1 (tre-2/USP6, BUB2, cdc16) domain family, member 1						•	•			•	•				
175	29924	EPN1	epsin 1							•			•					
176	51003	MED31	mediator of RNA polymerase II transcription, subunit 31 homolog (yeast)								•		•					
177	55125	Cep192	centrosomal protein 192 kDa			•												

Appendix

p200 #	Gene-ID	Gene Name	Description	apoptosis/cell death	cell communication	cell cycle/cell division	cellular comp./organelle organization	cytoskeleton organization/morphology	development	enzyme regulation	e-tracellular signal processing	metabolism	protein degradation	regulation cellular/biological processes	signal transduction	stress response	transport	other
178	55211	DPPA4	developmental pluripotency associated 4															
179	55339	WDR33	WD repeat domain 33		●					●	●		●			●		
180	55666	NPL4	nuclear protein localization 4				●				●	●	●					
181	55722	Cep72	centrosomal protein 72 kDa			●	●	●					●				●	
182	55968	NSFL1C	NSFL1 (p97) cofactor (p47)															
183	56927	GPR108	G protein-coupled receptor 108															
184	57062	DDX24	DEAD (Asp-Glu-Ala-Asp) box polypeptide 24								●		●					
185	57562	KIAA1377	KIAA1377 protein															
186	65265	C8orf33	chromosome 8 open reading frame 33															
187	79902	PCNT1	pericentrin 1	●		●	●	●		●			●					
188	80254	Cep63	centrosome protein Cep63	●	●	●	●	●		●			●	●	●	●	●	
189	81847	RNF146	ring finger protein 146															
190	84289	ING5	inhibitor of growth family, member 5			●	●				●	●	●					●
191	85300	ATCAY	ataxia, cerebellar, Cayman type (caytaxin)				●											
192	85378	TUBGCP6	tubulin, gamma complex associated protein 6				●	●					●				●	
193	114928	GPRASP2	G protein-coupled receptor associated sorting protein 2															
194	116983	CENTB5	centaurin, beta 5						●	●			●	●				
195	120892	LRRK2	leucine-rich repeat kinase 2	●	●		●					●	●	●	●			●
196	207	AKT1	v-akt murine thymoma viral oncogene homolog 1	●	●	●	●	●	●	●	●	●	●	●	●	●	●	●
197	28964	GIT1	G protein-coupled receptor kinase interactor 1				●		●	●			●	●			●	
198	9815	GIT2	G protein-coupled receptor kinase interactor 2						●	●			●	●				

Appendix

p200 #	Gene-ID	Gene Name	Description	apoptosis/cell death	cell communication	cell cycle/cell division	cellular comp./organelle organization	cytoskeleton organization/morphology	development	enzyme regulation	e-tracellular signal processing	metabolism	protein degradation	regulation cellular/biological processes	signal transduction	stress response	transport	other
199	2861	GPR37	G protein-coupled receptor 37 (endothelin receptor type B-like)		●									●	●			
200	5291	PIK3CB	Phosphatidylinositol-4,5-bisphosphate 3-kinase catalytic subunit beta isoform	●	●	●	●	●	●	●			●	●	●	●		●

Appendix C: Result of “p200 screen”

Empty cells indicate that a target participated in screen, but was not identified as hit (x-fold change in toxicity below 0.8 or above 1.3, see Chapter 2.1.1).

*) target not included in subset screen

Number of Positives	p200 #	Gene-ID	Gene Name	x-fold change in toxicity				Average	Stdev
				Total Screen 1	Total Screen 2	Subset Screen 1	Subset Screen 2		
3	60	5217	PFN2	0,48	0,20	0,40	*)	0,36	0,12
3	95	6894	TARBP1	2,59	2,00	*)	3,15	2,58	0,47
3	133	11064	CEP1	0,67	0,58	0,55	*)	0,60	0,05
3	140	4085	MAD2L1	1,89	1,39	*)	1,49	1,59	0,22
3	172	10989	IMMT	2,08	1,63		1,42	1,71	0,27
3	184	57062	DDX24	0,75	0,79	0,62	*)	0,72	0,07
3	189	81847	RNF146	0,63	0,63	0,48	*)	0,58	0,07
2	13	1445	CSK	1,72	0,76		*)	1,24	0,48
2	22	4296	MAP3K11	0,66	0,56		*)	0,61	0,05
2	52	8878	SQSTM1	1,33	1,52		*)	1,43	0,09
2	65	6895	TARBP2	2,12	1,54	*)	*)	1,83	0,29
2	73	3320	HSPCA	1,48	0,72	*)	*)	1,10	0,38
2	76	1385	CREB1	1,32	0,64	*)	*)	0,98	0,34
2	115	3164	NR4A1	3,71	2,87	*)		3,29	0,42
2	119	10095	ARPC1B	2,24	2,12	*)		2,18	0,06
2	120	857	CAV1	0,75	1,50		*)	1,12	0,37
2	125	387	RHOA	1,54	0,74	*)	*)	1,14	0,40
2	148	6455	SH3GL1		0,74	0,67		0,70	0,03
1	1	1111	CHEK1	1,33		*)	*)	1,33	
1	2	11200	CHEK2	1,31		*)	*)	1,31	
1	3	207	AKT1		0,68	*)	*)	0,68	
1	6	660	BMX	2,42		*)	*)	2,42	
1	8	983	cdc2			0,51	*)	0,51	
1	10	1026	CDKN1A	1,60			*)	1,60	
1	11	1027	CDKN1B	1,93		*)	*)	1,93	
1	14	1457	CSNK2A1	2,72		*)	*)	2,72	
1	15	1846	DUSP4	1,40		*)	*)	1,40	
1	16	2534	FYN	0,33			*)	0,33	
1	18	3611	ILK	1,59			*)	1,59	
1	19	3717	JAK2	1,56		*)	*)	1,56	

Appendix

Number of Positives	p200 #	Gene-ID	Gene Name	x-fold change in toxicity				Average	Stdev
				Total Screen 1	Total Screen 2	Subset Screen 1	Subset Screen 2		
1	20	4067	LYN	1,93		*)	*)	1,93	
1	23	4217	MAP3K5		1,75	*)	*)	1,75	
1	25	6300	MAPK12		1,68	*)	*)	1,68	
1	26	5595	MAPK3		1,58	*)	*)	1,58	
1	28	5601	MAPK9	1,35		*)	*)	1,35	
1	29	85366	MYLK2		1,98	*)	*)	1,98	
1	31	5058	PAK1	1,69		*)	*)	1,69	
1	32	5062	PAK2	1,64		*)	*)	1,64	
1	38	65018	PINK1	1,35				1,35	
1	39	5347	PLK1	1,41			*)	1,41	
1	47	5590	PRKCZ			1,38	*)	1,38	
1	48	5747	PTK2		0,50	*)		0,50	
1	49	5879	RAC1			1,34		1,34	
1	50	5894	RAF1	1,37			*)	1,37	
1	51	10769	PLK2			0,79	*)	0,79	
1	57	11190	CEP2	1,50		*)	*)	1,50	
1	58	1072	CFL1			0,57	*)	0,57	
1	62	6310	ATXN1		0,47	*)	*)	0,47	
1	66	7429	VIL1			*)	0,69	0,69	
1	68	7534	YWHAZ		0,41	*)	*)	0,41	
1	71	396	ARHGDI1		0,58	*)	*)	0,58	
1	72	2889	RAPGEF1		0,51	*)		0,51	
1	74	8976	WASL	2,39		*)	*)	2,39	
1	77	2002	ELK1	1,56		*)	*)	1,56	
1	78	2353	FOS			0,63		0,63	
1	79	3725	JUN	1,93		*)	*)	1,93	
1	80	4790	NFKB1	0,28			*)	0,28	
1	81	5201	PFDN1	1,33		*)	*)	1,33	
1	86	10766	TOB2	3,00		*)	*)	3,00	
1	87	10844	TUBGCP2	1,45		*)	*)	1,45	
1	88	29979	UBQLN1	2,32		*)	*)	2,32	
1	89	1487	CTBP1	1,61		*)	*)	1,61	
1	90	3265	HRAS	2,65		*)	*)	2,65	
1	91	3845	KRAS	1,98		*)	*)	1,98	
1	100	5071	PARK2	1,57		*)	*)	1,57	
1	101	10273	STUB1		1,81	*)	*)	1,81	

Appendix

Number of Positives	p200 #	Gene-ID	Gene Name	x-fold change in toxicity				Average	Stdev
				Total Screen 1	Total Screen 2	Subset Screen 1	Subset Screen 2		
1	103	267	AMFR	1,59		*)	*)	1,59	
1	107	5800	PTPRO		1,87	*)	*)	1,87	
1	111	2885	GRB2		0,74	*)	*)	0,74	
1	112	8440	NCK2	2,59		*)	*)	2,59	
1	113	10140	TOB1	1,34			*)	1,34	
1	114	4035	LRP1	1,33			*)	1,33	
1	118	27229	76P		1,59	*)	*)	1,59	
1	121	4771	NF2		2,09		*)	2,09	
1	122	10426	TUBGCP3	0,63			*)	0,63	
1	124	6857	SYT1		0,59	*)		0,59	
1	127	1386	ATF2	1,82		*)	*)	1,82	
1	129	10950	BTG3	1,86		*)	*)	1,86	
1	130	9184	BUB3	1,78		*)	*)	1,78	
1	132	998	CDC42		1,49	*)	*)	1,49	
1	135	595	CCND1		0,74	*)	*)	0,74	
1	136	2059	EPS8		0,71	*)	*)	0,71	
1	137	9638	FEZ1		0,69	*)	*)	0,69	
1	138	9737	GPRASP1		0,61		*)	0,61	
1	139	8379	MAD1L1		0,78	*)		0,78	
1	141	3303	HSPA1A	2,31		*)	*)	2,31	
1	142	3315	HSPB1		2,78	*)	*)	2,78	
1	151	10048	RANBP9	1,41		*)	*)	1,41	
1	153	161	AP2A2	2,42		*)	*)	2,42	
1	154	166	AES	1,93		*)	*)	1,93	
1	156	1627	DBN1	1,92		*)	*)	1,92	
1	157	1808	DPYSL2	2,91		*)	*)	2,91	
1	158	3301	DNAJA1	1,33		*)	*)	1,33	
1	160	4957	ODF2	2,60		*)	*)	2,60	
1	161	5121	PCP4	1,70		*)	*)	1,70	
1	162	84335	AKT1S1		0,41		*)	0,41	
1	167	9627	SNCAIP	2,08		*)	*)	2,08	
1	169	9788	MTSS1	1,30		*)	*)	1,30	
1	170	10190	TXNDC9	2,55		*)	*)	2,55	
1	171	10542	HBXIP	2,43		*)	*)	2,43	
1	173	23385	NCSTN	1,74			*)	1,74	
1	174	23216	TBC1D1	1,36			*)	1,36	

Appendix

Number of Positives	p200 #	Gene-ID	Gene Name	x-fold change in toxicity				Average	Stdev
				Total Screen 1	Total Screen 2	Subset Screen 1	Subset Screen 2		
1	178	55211	DPPA4	1,57		*)	*)	1,57	
1	179	55339	WDR33	1,86		*)	*)	1,86	
1	181	55722	Cep72	1,34		*)	*)	1,34	
1	183	56927	GPR108	1,57		*)	*)	1,57	
1	187	79902	PCNT1			0,78	*)	0,78	
1	192	85378	TUBGCP6			*)	0,76	0,76	
1	193	114928	GPRASP2	2,25		*)	*)	2,25	
1	196	207	AKT1		0,67	*)		0,67	
0	4	9212	AURKB			*)	*)		
0	5	6795	AURKC			*)	*)		
0	7	699	BUB1			*)	*)		
0	9	1020	CDK5			*)	*)		
0	12	1263	PLK3				*)		
0	17	2932	GSK3B			*)	*)		
0	21	6416	MAP2K4				*)		
0	24	5594	MAPK1			*)	*)		
0	27	5599	MAPK8			*)	*)		
0	30	4751	NEK2			*)	*)		
0	33	10298	PAK4			*)	*)		
0	34	5170	PDPK1			*)	*)		
0	35	5291	PIK3CB			*)	*)		
0	36	5295	PIK3R1			*)	*)		
0	37	8503	PIK3R3			*)	*)		
0	40	5515	PPP2CA			*)	*)		
0	41	5566	PRKACA			*)	*)		
0	42	5567	PRKACB			*)	*)		
0	43	5568	PRKACG			*)	*)		
0	44	5578	PRKCA			*)	*)		
0	45	5579	PRKCB1			*)	*)		
0	46	5582	PRKCG			*)			
0	53	10733	PLK4				*)		
0	54	333	APLP1			*)			
0	55	572	BAD			*)	*)		
0	56	55755	CDK5RAP2			*)	*)		
0	59	1822	ATN1			*)	*)		
0	61	5829	PXN			*)	*)		

Appendix

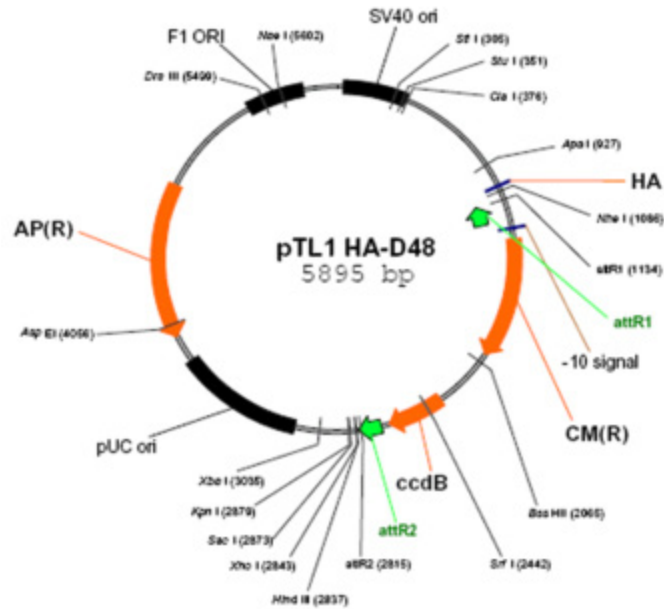
Number of Positives	p200 #	Gene-ID	Gene Name	x-fold change in toxicity				Average	Stdev
				Total Screen 1	Total Screen 2	Subset Screen 1	Subset Screen 2		
0	63	6421	SFPQ				*)		
0	64	10580	SORBS1			*)	*)		
0	67	7531	YWHAE			*)	*)		
0	69	7791	ZYX			*)	*)		
0	70	351	APP			*)	*)		
0	75	9232	PTTG1			*)	*)		
0	82	836	CASP3				*)		
0	83	55585	UBE2Q1			*)	*)		
0	84	7353	UFD1L			*)	*)		
0	85	6907	TBL1X			*)	*)		
0	92	4893	NRAS			*)	*)		
0	93	5481	PPID			*)	*)		
0	94	5901	RAN			*)	*)		
0	96	10524	HTATIP			*)	*)		
0	97	9459	ARHGEF6			*)	*)		
0	98	7454	WAS			*)	*)		
0	99	7345	UCHL1			*)	*)		
0	102	10277	UBE4B			*)	*)		
0	104	5728	PTEN			*)	*)		
0	105	5499	PPP1CA			*)	*)		
0	106	5770	PTPN1			*)			
0	108	1398	CRK				*)		
0	109	10163	WASF2			*)	*)		
0	110	10142	AKAP9			*)	*)		
0	116	6772	STAT1				*)		
0	117	1499	CTNNB1				*)		
0	123	6804	STX1A			*)	*)		
0	126	10092	ARPC5			*)			
0	128	546	ATRX			*)	*)		
0	131	991	cdc20				*)		
0	134	27185	DISC1			*)	*)		
0	143	8481	OFD1			*)			
0	144	11315	PARK7			*)	*)		
0	145	5216	PFN1				*)		
0	146	4478	MSN			*)	*)		
0	147	6203	RPS9			*)	*)		

Appendix

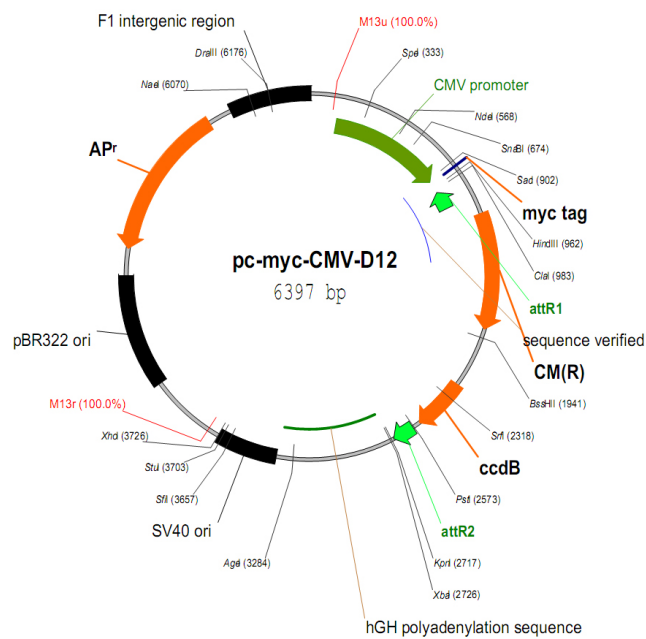
Number of Positives	p200 #	Gene-ID	Gene Name	x-fold change in toxicity				Average	Stdev
				Total Screen 1	Total Screen 2	Subset Screen 1	Subset Screen 2		
0	149	6622	SNCA			*)	*)		
0	150	5881	RAC3			*)	*)		
0	152	160	AP2A1			*)	*)		
0	155	1400	CRMP1				*)		
0	159	3337	DNAJB1			*)	*)		
0	163	6620	SNCB			*)	*)		
0	164	7408	VASP			*)	*)		
0	165	7415	VCP			*)	*)		
0	166	7802	DNALI1				*)		
0	168	9637	FEZ2			*)	*)		
0	175	29924	EPN1			*)	*)		
0	176	51003	MED31			*)	*)		
0	177	55125	Cep192			*)	*)		
0	180	55666	NPL4			*)			
0	182	55968	NSFL1C			*)	*)		
0	185	57562	KIAA1377			*)	*)		
0	186	65265	C8orf33			*)	*)		
0	188	80254	Cep63				*)		
0	190	84289	ING5			*)	*)		
0	191	85300	ATCAY			*)	*)		
0	194	116983	CENTB5			*)	*)		
0	195	120892	LRRK2			*)			
0	197	28964	GIT1			*)	*)		
0	198	9815	GIT2			*)	*)		
0	199	2861	GPR37			*)	*)		
0	200	5291	PIK3CB			*)	*)		

Appendix D: Plasmid maps

A.1 pTL1-HA-D48

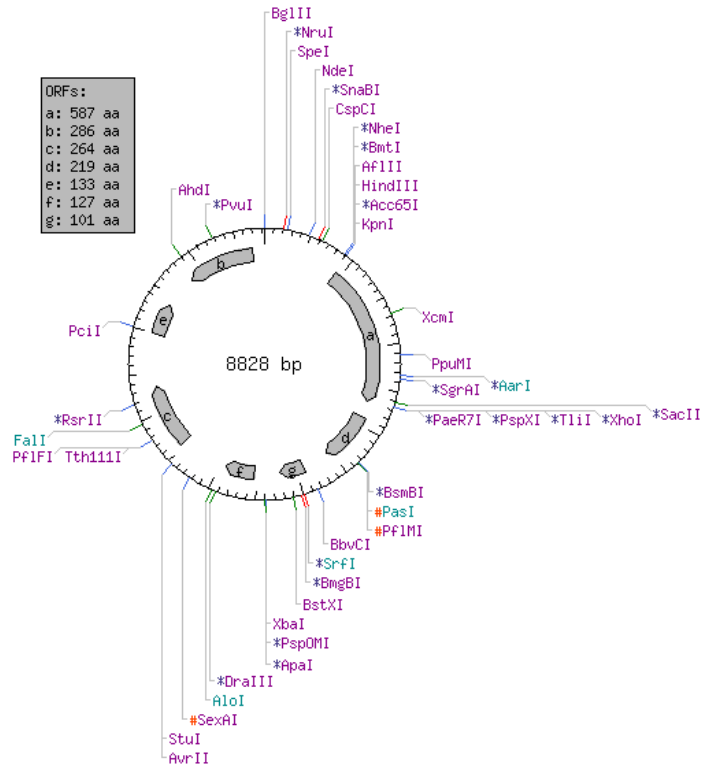


A.2 pc-myc-CMV-D12

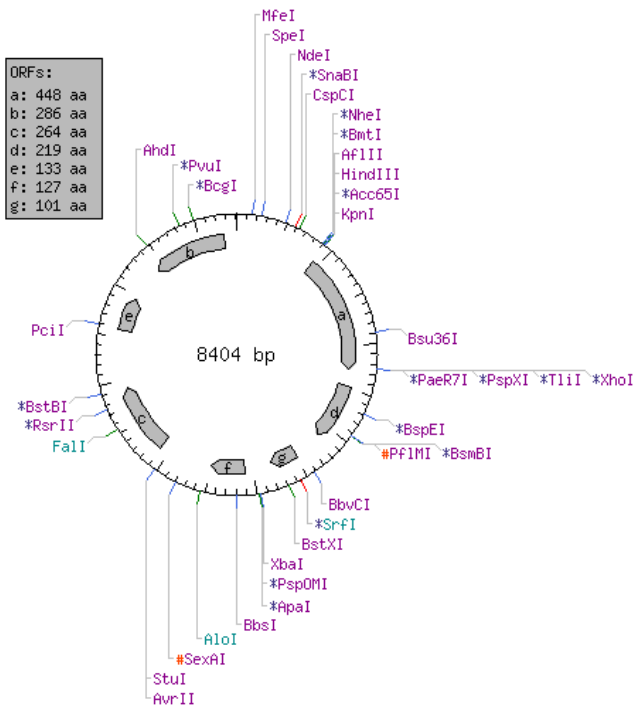


Appendix

A.4 pFire-V5-DM

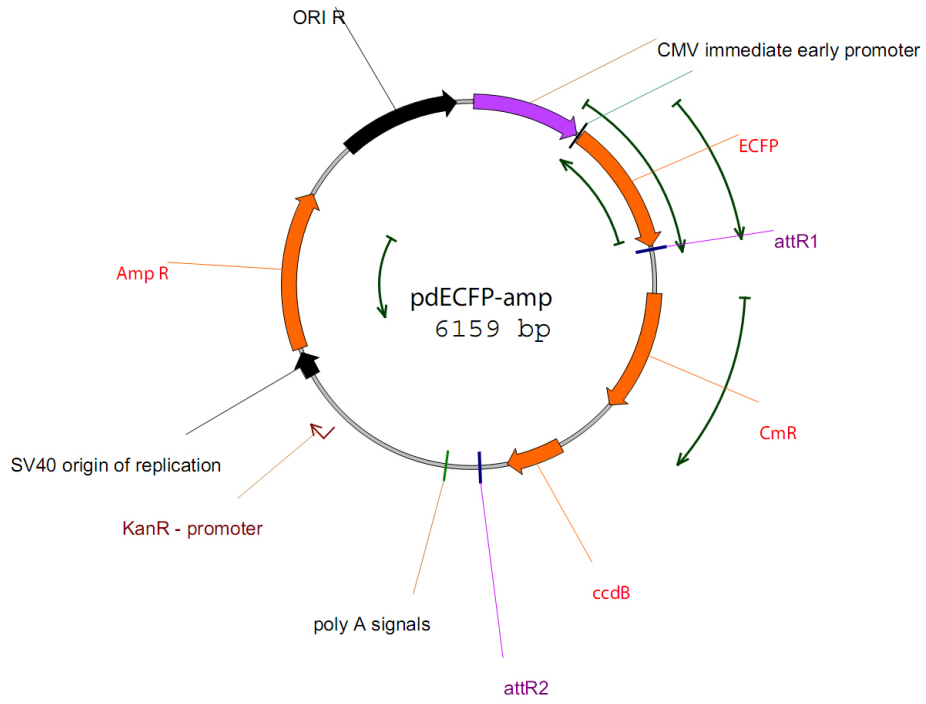


A.5 pPA-Reni-DM

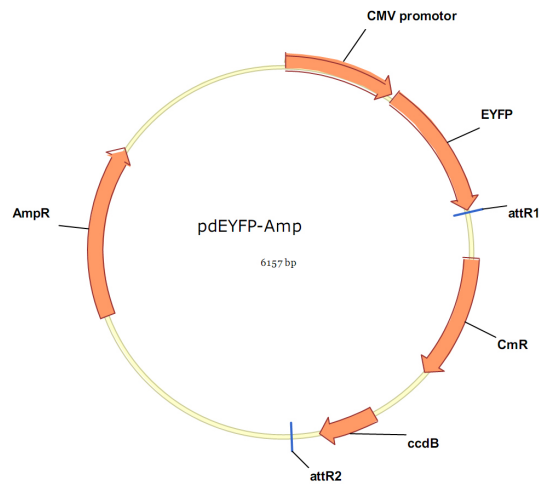


Appendix

A.5 pdECFP-amp



A.6 pdEYFP-Amp



Selbständigkeitserklärung

Hiermit erkläre ich, die vorliegende Arbeit selbständig ohne fremde Hilfe verfasst und nur die angegebene Literatur und Hilfsmittel verwendet zu haben.

Katja Dorothea Welsch

31. März 2010